TGFβ Signaling as a Modulator of Epithelial Inflammation and Barrier Function in the Mouse Colon

By

Paula Marincola Smith, M.D.

Dissertation

Submitted to the Faculty of the

Graduate School of Vanderbilt University

In partial fulfillment of the requirements

For the degree of

DOCTOR OF PHILOSOPHY

in

Cancer Biology

May 31, 2021

Nashville, Tennessee

Approved:

Christopher S. Williams, M.D., Ph.D., Chair

Barbara M. Fingleton, Ph.D.

Sergey V. Novitskiy, M.D., Ph.D.

Ken Lau, Ph.D.

James R. Goldenring, M.D., Ph.D.

To my son, James, the most curious person in the world

And

To my daughter, Naomi, whom I can't wait to know

And

To my husband, Peyton, whose love and support is everything

ACKNOWLEDGEMENTS

This work would not have been possible without the financial support of the National Cancer Institute and the Burroughs Wellcome Foundation. I would like to acknowledge the multiple Vanderbilt University and Vanderbilt University Medical Center Core Services who made this work possible, including Vanderbilt University Cell Imaging Shared Resource (VU-CISR), Vanderbilt Technologies for Advanced Genomics (VANTAGE), Vanderbilt University Medical Center Translational Pathology Shared Resource (TPSR), the Vanderbilt University Molecular Cell Biology Resource Core, the Vanderbilt University Medical Center Division of Animal Care (DAC), and the Vanderbilt Flow Cytometry Shared Resource.

I am especially grateful to the Vanderbilt University Medical Center Section of Surgical Sciences, Department of Surgery, and General Surgery Residency Program including Drs R. Daniel Beauchamp, Seth Karp, Carmen Solórzano, Kyla Terhune, and Christina Bailey, for supporting my career goals and providing me with the protected academic time to pursue those goals.

I am grateful for the people whom I have had the opportunity to work with and learn from throughout my time in graduate school on my dissertation and related projects. A special thanks to lab mates and friends Jenny Zi, Connie Weaver, Keeli Lewis, Jalal Hamaamen, and David Hanna who taught me so much. Collaborators Kay Washington, Sergey Novitskiy, Ken Lau, Izumi Kaji, Yash Choksi, Nick Markham, Qi Liu, and Jing Yang each opened my eyes to a different but critical element of scientific inquiry that shaped the way I think about problem solving. Each member of my Dissertation Committee, including Drs. Christopher Williams, Jim Goldenring, Barbara Fingleton, Sergey Novitskiy, and Ken Lau, has provided me unparalleled scientific and professional mentorship for which I am endlessly grateful.

My thesis advisor, Dr. R. Daniel Beauchamp, deserves a special thank you. There were moments along the way where I felt I couldn't go on. I will be forever indebted to you for telling me not to quit on my worst day. And to Dr. Anna Means, who provided the day-to-day guidance that was invaluable for this surgery resident-turned-scientist. Without your help and oversight, I could have never accomplished this.

Most significantly, no one is more important to me or has been more supportive of my dreams than my family. To all four of my loving grandparents who built our family a robust foundation, but in particular my maternal grandfather, James B.D. Mark, M.D. ("Gonger"), whose professional achievements fill me with pride and motivate me daily. To my mom, who demonstrated with grace what a powerful woman and working mother looks like. To my dad, who always pushed me to be better (on the soccer field and in the classroom) and whose intellectual curiosity is second to none. To my big brother, Jamie, whose achievements have always kept me on my toes and are a constant reminder that I should do better. To my little sister, Rachel, who is as smart as she is loyal and kind, and who I hope I can be like when I grow up. To my in-laws, who have welcomed me with open arms and made me feel loved like one of their own. And last but far from least, I want to thank the world's most amazing husband, Peyton, our perfect son, James, and our soon-to-be daughter, Naomi. Without you three, none of this would have been possible or worthwhile.

TABLE OF CONTENTS

LIST OF TABLES

Table Page

LIST OF FIGURES

Figure Page

LIST OF ABBREVIATIONS/NOMENCLATURE/SYMBOLS

Abbreviation	Definition
ActD	Actinomycin D
AJ	Adherens Junction
ALI	Air-Liquid Interface
ANOVA	Analysis of Variance
ARDS	Acute Respiratory Distress Syndrome
BMP	Bone Morphogenic Protein
BPAECs	Bovine Pulmonary Artery Endothelial Cells
BRECs	Bovine Retinal Endothelial Cells
IBD	Inflammatory Bowel Disease
Colonoids	Colon Organoids
CAC	Colitis-Associated Cancer
CAMs	Cell Adhesion Molecules
CCL	Chemokine (C-C motif) Ligand
CCR	C-C Chemokine Receptor
CD	Crohn's Disease
ChIP-seq	Chromatin Immunoprecipitation Sequencing
CHX	Cycloheximide
CMS	Consensus Molecular Subtype of Colorectal Cancer
CRC	Colorectal Cancer
CTL	Cytotoxic T Cell
DC	Dendritic Cell
DMSO	Dimethyl Sulfoxide
DSS	Dextran Sulfate Sodium
ECM	Extracellular Matrix
EDTA	Ethylenediaminetetraacetic Acid
EEC	Enteroendocrine Cells
EGFP	Enhanced Green Fluorescent Protein
EJC	Epithelial Junctional Complex

EMT ..... Epithelial to Mesenchymal Transition

EMT-TFs ..... EMT-Transcription Factors

EpCAM ..... Epithelial cell adhesion molecule

FD4 ..... 4-kilodalton FITC-Dextran

FDR ..... False discovery Rate

FFPE ..... Formalin Fixed and Paraffin Embedded

FISH ..... Fluorescence *In Situ* Hybridization

FITC ..... Fluorescein isothiocyanate

FITC-D ..... Fluorescein isothiocyanate-Dextran

GALT ..... Gut-Associated Lymphoid Tissue

GFP ..... Green Fluorescent Protein

GFR ..... Growth Factor Reduced

H&E ..... Hematoxylin and Eosin

HBSS ..... Hank's Balanced Salt Solution

HNSCC ..... Head and Neck Squamous Cell Carcinoma

I-SMADs ..... Inhibitory SMADs

IBD ..... Inflammatory Bowel Disease

IF ..... Immunofluorescence

IFN ..... Interferon

IHC ..... Immunohistochemistry

IL ..... Interleukin

JAM ..... Junction Adhesion Molecule

JPS ..... Juvenile Polyposis Syndrome

KO ..... Knockout

LPS ..... Lipopolysaccharide

MMP ..... Matrix Metalloproteinase

MSI-high ..... Microsatellite Instability-high colorectal cancer

MSS ..... Microsatellite stable colorectal cancer

mRNA ..... messenger RNA

NK ..... Natural Killer Cell

OCT ..... Optimal Cutting Temperature

PBS ..... Phosphate-Buffered Saline

PC ..... Principal Component

PFA ..... Paraformaldehyde

PGDH ..... Hydroxyprostaglandin Dehydrogenase

qPCR ..... Quantitative Polymerase Chain Reaction

R-SMADs ..... Receptor-Associated SMADs

RNA-seq ..... RNA-sequencing

SBE ..... SMAD-Binding Element

scRNA-seq..... Single Cell RNA-sequencing

TA ..... Transient Amplifying

TCGA ..... The Cancer Genome Atlas

TER ..... Transepithelial Resistance

TGFβ ..... Transforming Growth Factor Beta

Th17 ..... T helper 17 Cell

TJ ..... Tight Junction

TLR ..... Toll-like Receptor

TNFα ..... Tissue Necrosis Factor-α

Treg ..... Regulatory T Cell

UC ..... Ulcerative Colitis

UMAP ..... Uniform Manifold Approximation and Projection

UMI ..... Unique Molecular Identifier

WB ..... Western Blot

ZO ..... Zona Occludens

CHAPTER I

This chapter is adapted from "Immunomodulatory Effects of TGFβ Family Signaling within Intestinal Epithelial Cells and Carcinomas" published in Gastrointestinal Disorders and has been reproduced with the permission of the publisher and my co-authors, Anna L. Means and R. Daniel Beauchamp.
Reference: P Marincola Smith, et al. Immunomodulatory effects of TGFβ Family Signaling within Intestinal Epithelial Cells and Carcinomas. *Gastrointestinal Disorders*. 2019:1(2);290-300.

INTRODUCTION 1 – TGFβ SIGNALING AND INFLAMMATION

TGFβ Signaling Pathway

The TGF-β superfamily is comprised of over thirty distinct, secreted cytokines (including TGF-βs, BMPs, Nodal, and Activin) (Weiss and Attisano, 2013) that perform many cellular functions including control of cell growth, cell proliferation, cell differentiation, and apoptosis (Moses and Serra, 1996; Samanta and Datta, 2012; Shi and Massagué, 2003; Weiss and Attisano, 2013). TGF-β family signaling is critical for gastrulation, embryonic development, and morphogenesis, and it has pleiotropic roles in many adult tissues and cell types. The impact of TGF-β family pathway signaling is highly cell type- and context-dependent.

TGF-β ligands bind to a family of TGF-β cell surface receptors, which are present on most cell types in the body, and include TGF-βRII, TGF-βRI, BMPR2, BMPR1A/1B, ACVR2A/2B, and ACVR1A/1B (Weiss and Attisano, 2013). Upon TGF-β ligand binding, the TGF-βRII receptors activate the type I receptors via transphosphorylation and form a hetero-tetrameric complex composed of two TGF-βRIIs and two TGF-βRIs (Shi and Massagué, 2003). Upon TGF-βR activation and complex formation, downstream signaling is perpetuated via two major routes: SMAD-dependent (canonical) and SMAD-independent (non-canonical) signaling (Moustakas and Heldin, 2005). The canonical signaling pathway is the more well-characterized pathway whereas the non-canonical pathway is less well understood, and its biological relevance remains less clear. In canonical signaling, TGF-βR activation leads to phosphorylation of the receptor-regulated SMADs (R-SMADs), which includes SMADs 2/3 in the case of TGF-βRs and ACVRs, and SMADs 1/5/9 in the case of BMPRs. After phosphorylation/activation, the R-SMADs associate with the common partner SMAD (co-SMAD), SMAD4, before translocation to the nucleus (Shi and Massagué, 2003). Once in the nucleus, the SMAD complexes bind directly to DNA via their MH1 domain and regulate transcription via their MH2 domain (Morikawa et al., 2013; Samanta and Datta, 2012; Shi and Massagué, 2003). The inhibitory SMADs (I-SMADs), SMADs 6 and 7, are induced by canonical TGF-β pathway signaling and function to block R-SMAD phosphorylation and R-SMAD/SMAD4 complex formation, thus negatively regulating TGF-β pathway signaling (Hayashi et al., 1997; Moustakas and Heldin, 2005). A visual representation of the canonical TGF-β signaling pathway is depicted in **Figure 1.1**, as was first published by Marincola Smith and colleagues (Marincola-Smith et al., 2019). Of note, there is some evidence to suggest R-SMADs may function independently of SMAD4 in some circumstances (Aloysius et al., 2018), although these pathways remain incompletely investigated.

Through canonical TGF-β family member signaling, SMAD complexes interact with a wide variety of distinct DNA binding sites and target genes. Importantly, once in the nucleus, SMAD complexes require the cooperation of cofactors (coactivators and corepressors) to successfully bind DNA and regulate transcriptional programs. The transcriptional program induced by the TGF-β family signaling pathway via SMAD proteins is thus highly cell type- and context-specific, as the presence or absence of various cofactors can have a dramatic impact on SMAD-target gene interactions (Morikawa et al., 2013). Recent research suggests that SMAD complexes determine their target sites along with other DNA-binding cofactors by two distinct mechanisms. First, cell type- or lineage-specific transcriptional cofactors open chromatin at specific SMAD Binding Elements (SBEs), making certain SBEs accessible to nuclear SMAD complexes. Second, DNA-binding cofactors, induced and activated in a context-dependent manner, can directly strengthen the interaction between

SMAD complexes and DNA. The result of this cofactor dependence is that the downstream effects of TGF-β superfamily canonical signaling may differ based on the cell type and context in which it is delivered, thus causing significant heterogeneity in TGF-β superfamily signaling responses between different tissues and within tissues at different stages of development or differentiation. This also means that TGF-β response data from cell culture experiments should be interpreted with caution.

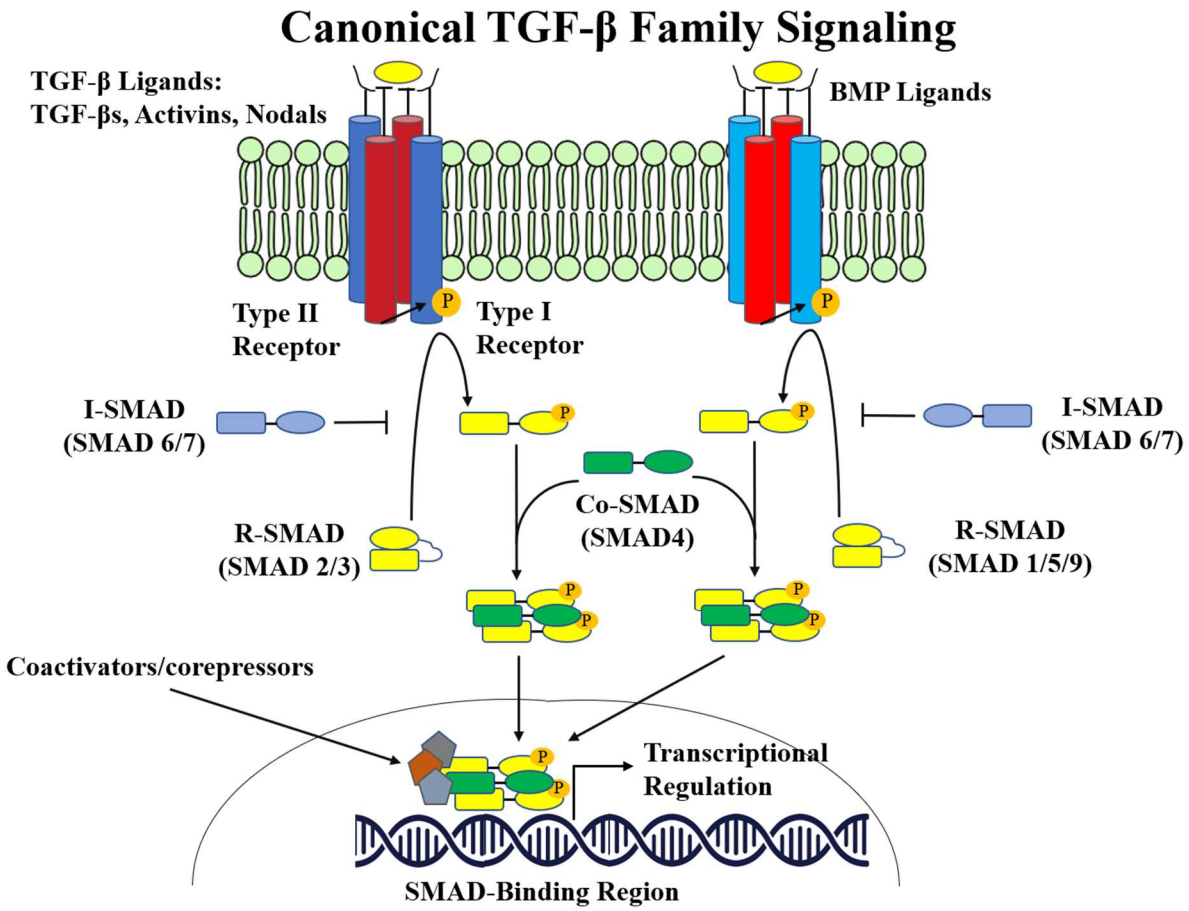

Figure 1.1 - Visual representation of the Canonical TGF-β signaling pathway.

The non-canonical TGF-β signaling pathways are less well-characterized but may play important roles in regulating many TGF-β pathway functions through three distinct mechanisms: Non-SMAD signaling pathways that directly modify SMAD function, non-SMAD proteins whose function is directly modulated by SMADs and which transmit signals to other pathways, and non-SMAD proteins that directly interact with or become phosphorylated by TGF-β receptors and do not necessary affect SMAD function. Some signaling molecules that have been implicated in non-SMAD TGF-β signaling include various elements of the MAP kinase pathway (including Erk and JNK/p38 activation) (Bhowmick et al., 2001a; Engel et al., 1999; Hanafusa et al., 1999; Hocevar et al., 1999), Rho-like GTPase signaling pathway (Bhowmick et al., 2001b; Sofia et al., 2002), and phosphatidylinositol-3-kinase/AKT pathway (Bakin et al., 2000; Shin et al., 2001; Wilkes et al., 2005; Yi et al., 2005). These collective SMAD-independent pathways appear to affect target cells by promoting apoptosis and cellular differentiation, impinging on cell proliferation, contributing to epithelial to mesenchymal transition (EMT), and modulating matrix regulation (Zhang, 2009). These non-canonical TGF-β signaling activities,

especially those that are involved with cytoskeletal remodeling and EMT, are of particular importance in understanding TGF-β's duality of function between tumor prevention and tumor promotion (described in more detail in the following section: TGF-β Pathway Dysregulation in Cancer). A complete review of the SMAD-independent pathways is beyond the scope of this dissertation, and this topic has been previously reviewed by Moustakas and colleagues (Moustakas and Heldin, 2005) as well as Zhang (Zhang, 2009). Nonetheless, it is important to acknowledge that the SMAD-independent pathways likely impinge on the highly context-specific responses to TGF-β signaling, and that these pathways are deserving of further investigation.

TGFβ in Cancer

Various components of the TGF-β signaling pathway are frequently reported lost or dysregulated in multiple types of cancer. Functional loss of TGF-βRII is frequently reported in colorectal cancer (CRC), including bi-allelic mutations in >80% of microsatellite instability-high (MSI-High) (Markowitz et al., 1995; Parsons et al., 1995) and roughly 15% of microsatellite stable (MSS) CRCs (Grady et al., 1999). TGF-βRII loss is also frequently reported in tumors of biliary, gastric, brain, and lung tissues (Levy and Hill, 2006). SMAD4 is the most common SMAD family protein disrupted in cancers, and its functional loss or repression has been reported at high frequencies in pancreatic cancer, head and neck squamous cell carcinoma (HNSCC), and CRC, as well as in biliary, bladder, breast, liver, lung, and esophageal cancers (Zhao et al., 2018). Though point mutations and genetic loss of TGF-β family genes exist with variable frequencies in different cancers, epigenetics also appear to play a significant role in the dysregulation of TGF-β pathway components in cancer. For example, silencing of the TGF-βRII and TGF-βRI genes through hypermethylation has been reported in human mammary carcinomas, and SMAD4 promoter methylation has been reported in advanced prostate cancers (Aitchison et al., 2008; Hinshelwood et al., 2007). Similarly, functional loss of TGF-β family signaling can occur through up-regulation of the I-SMADs (particularly SMAD7) (Hayashi et al., 1997; Monteleone et al., 2001), increased ubiquitination of the SMAD proteins by SMURF1/2 (Samanta and Datta, 2012), or increased cytosolic attenuation of SMAD activity by the Ras/Raf/ERK pathway (Zhao et al., 2018).

Inherited mutations in TGF-β pathway components have also been associated with heredity cancer syndromes. Most notably is Juvenile Polyposis Syndrome (JPS), which is characterized by the development of juvenile polyps of the stomach, small bowel, and large bowel, and increased risk of cancers of the gastrointestinal tract. JPS patients with inherited SMAD4 mutations develop a more severe gastric phenotype and worse prognosis compared to those with inherited mutations in BMPR1A (Aytac et al., 2015). Additionally, germline mutations in TGF-βRs have been associated with increased risk of colon, breast, and ovarian cancers (Liao et al., 2010; Pasche et al., 1999, 2004).

Interestingly, the TGF-β pathway appears to have a duality of function between tumor prevention and tumor promotion (Ikushima and Miyazono, 2010; Miyazono et al., 2011; Principe et al., 2014; Roberts and Wakefield, 2003). In benign epithelia and early-stage tumors, TGF-β is a potent inducer of growth arrest and apoptosis. This is corroborated by the fact that loss of TGF-β family components is often associated with the development of malignant tumors in multiple tissue types. This association has been validated in multiple *in vivo* mouse models that demonstrate clearly that loss of TGF-β family signaling elements leads to increased rates of tumor formation in multiple tissues including the pancreas, stomach, liver, skin, and colon (Bardeesy et al., 2006; Freeman et al., 2012; Izeradjene et al., 2007; Li et al., 2003; Means et al., 2018; Qiao et al., 2006; Takaku et al., 1998; Teng et al., 2006; Xu et al., 2000, 2006; Yang et al., 2005). On the other hand, in advanced tumors, TGF-β signaling appears to promote tumor growth, progression, and metastasis, likely reflecting the severe dysregulation at TGF-β family signaling elements (Bardeesy et al., 2006; Izeradjene et al., 2007; Teng et al., 2006; Xu et al., 2000). The mechanism behind this functional switch from tumor suppressor to tumor promoter remains incompletely understood but may be related to relative contributions of the canonical and non-canonical TGF-β signaling pathways, differences in intracellular coactivators and corepressors that alter SMAD complex DNA binding activity, or alterations in the tumor microenvironment (Principe et al., 2014).

This functional switch from tumor suppressor to tumor promoter is known as the TGF-β paradox and is comprehensively reviewed by Principe and colleagues (Principe et al., 2014).

TGFβ in Inflammation and Immune Cell Recruitment

Importantly, TGF-β ligand remains in the extracellular matrix (ECM) of carcinomas, regardless of the cancer cell's intrinsic ability to respond to TGF-β signaling. In fact, multiple studies have suggested that stromal TGF-β ligand levels are higher in ECM of tumors with defective TGF-β signaling (Hahm et al., 2001; Lu et al., 2006b; Principe et al., 2017; Yang et al., 2008). Thus, even in tumors with inability to respond to TGF-β, abundant TGF-β ligand remains in the ECM to impinge upon the behavior of adjacent cell populations, including immune cells, fibroblasts, and endothelial cells. The impact of TGF-β signaling on the immune system is significant and well-documented.

It was demonstrated in early murine studies that TGF-β plays a central role in immunomodulation (Bierie and Moses, 2010). In whole-body knockout of TGF-β1 expression, mice develop multifocal autoimmune disease, acute wasting, and early death (Li et al., 2003; Qiao et al., 2006). Subsequent studies demonstrated that T cell specific attenuation of TGF-β signaling also results in autoimmune disease and spontaneous effector T cell differentiation (Gorelik and Flavell, 2000). We now know that TGF-β functionally regulates differentiation of effector and helper T cell sub-populations, inhibiting Th1 and Th2 T cell differentiation while promoting regulatory T cell (Treg) differentiation and suppressing cytotoxic T cell (CTL) activity (Gorelik and Flavell, 2002; Li et al., 2006; Wrzesinski et al., 2007). Importantly, Tregs have a known immuno-inhibitory function and themselves secrete high levels of TGF-β ligand, further perpetuating TGF-β's negative regulation of effector T-cells. Additionally, it has been demonstrated that inhibition of TGF-β signaling results in increased tumor cytotoxicity and clearance *in vivo*, owing in part to the enhanced effector functions of CTLs (Kontani et al., 2006; Thomas and Massagué, 2005).

Like the immunomodulatory effects of TGF-β on T cells, the TGF-β immuno-inhibitory role is furthered through its impact on other leukocyte subsets including natural killer (NK) cells (Viel et al., 2016), neutrophils (Brandes et al., 1991; Chen et al., 1998), and macrophages (Yang et al., 2010a). It has been demonstrated that TGF-β inhibits metabolic activity and interferon-responsiveness of NK cells (via repression of the mTOR pathway) (Viel et al., 2016). Perhaps not surprisingly, it has been additionally demonstrated the inhibiting the TGF-β receptor enhances the cytotoxic ability of NK cells in the context of adoptive cell transfer in pre-clinical models (Otegbeye et al., 2018). TGF-β has also been implicated in polarization of neutrophils (Fridlender et al., 2009) and macrophages (Zhang et al., 2015), particularly in the tumor microenvironment. TGF-β blockade also increases influx of tumor-associated neutrophils with increased cytotoxic/anti-tumor activities whereas, conversely, TGF-β ligand within the tumor microenvironment induces a population of neutrophils with a pro-tumor phenotype (Fridlender et al., 2009). Similarly, TGF-β induces a pro-tumor phenotype in macrophages characterized by up-regulation of anti-inflammation cytokine IL-10 and down-regulation of pro-inflammatory cytokines TNF-α and IL-12 (Zhang et al., 2015).

Taken together, TGF-β is a major negative modulator of the immune system. This suggests a potentially parallel immunosuppressive role in other cell types, including epithelial cells. Additionally, it is perhaps highly relevant that carcinomas with abrogated TGF-β signaling seem to have increased levels of TGF-β ligand in their tumor-associated stroma (Hahm et al., 2001; Lu et al., 2006b; Principe et al., 2017). Elevated TGF-β ligand, while having limited epithelial cell-specific effects in the context of TGF-β desensitization, can impinge on the surrounding immune microenvironment to suppress cytotoxicity and promote immune-tolerance. This may be a major mechanism of immuno-evasion of epithelial tumors with defective TGF-β signaling.

TGFβ in Epithelial Homeostasis

TGF-β's most well-established role in the epithelial compartment relates to its direct anti-proliferative effects. TGF-β signaling is well known to induces epithelial cell growth arrest through several mechanisms, including direct control over various cyclin-dependent kinase inhibitors, as well as promoting apoptosis and

cellular differentiation (Biswas et al., 2004; Gottfried et al., 2004; Hofmann et al., 2003; Moses and Serra, 1996; Moustakas and Heldin, 2005; Principe et al., 2014; Samanta and Datta, 2012; Takaku et al., 1998). While epithelial cell-intrinsic growth control by TGF-β is relatively well characterized, the epithelial cell-intrinsic immunomodulatory control on the surrounding microenvironment by TGF-β and how such modulation may impinge on tumorigenesis or tumor progression is less well understood.

The immunomodulatory role of TGFβ in epithelial cells and epithelial cancers

Several studies have pointed to an immunomodulatory role for TGF-β signaling within the epithelial compartment. For instance, cultured colon epithelial cells continuously exposed to TGF-β ligand were shown to significantly upregulate 15-hydroxyprostaglandin dehydrogenase (PGDH), a protein known to metabolize and decrease the levels of pro-inflammatory prostaglandins. Interestingly, normal colon epithelial cells appear to express relatively high levels of 15-PGDH, whereas 15-PGDH is nearly undetectable in CRC samples. This discrepancy has been attributed to the fact that TGF-β family signaling is disrupted in nearly 80% of CRCs, and suggests an anti-inflammatory role for TGF-β family signaling in colon epithelium (Grady et al., 1999; Yan et al., 2004).

Prior work from our lab adds to the evidence that TGF-β plays an important immunomodulatory role in colon epithelium (Means et al., 2018). Using mice with intestinal epithelium-specific SMAD4 knockout which have impaired canonical TGF-β signaling within the epithelial compartment but intact TGF-β family signaling in the surrounding stroma and immune cells, our lab demonstrated increased intestinal epithelial cell expression of genes encoding a variety of pro-inflammatory chemokines and cytokines, including *Cxcl5, Ccl20, Ccl8, Il34*, and *Il18*, and this upregulated pro-inflammatory response appears to be at least partially cell-autonomous (Means et al., 2018). Additionally, mouse and human Smad4/SMAD4-deficient intestinal tumors have been associated with increased immune cell accumulation compared to SMAD4-expressing controls (Inamoto et al., 2016; Itatani et al., 2013; Kitamura et al., 2007). Invasive intestinal tumors of *cis-*$Apc^{+/716}$*;*$Smad4^{+/-}$ mice that exhibited bi-allelic loss of heterozygosity were observed to have marked increased expression of CCL9 and resultant accumulation of immature myeloid cells compared to tumors arising from $Apc^{+/716}$*;*$Smad4^{+/+}$ controls (Kitamura et al., 2007). Interestingly, in human CRC samples, CCL15 (the human orthologue to murine CCL9) expression appears to be inversely correlated with SMAD4 expression, and increased tumor CCL15 expression is associated with a three-fold increase in $CCR1^+$ immune cell infiltration (Itatani et al., 2013).

In humans, low SMAD4 expression in CRC tumors has similarly been associated with increased $CD11b^+$ myeloid cell infiltration (Izeradjene et al., 2007; Li et al., 2006). Interestingly, a recently published retrospective analysis of human colorectal tumors demonstrated that loss of SMAD4 expression was associated with lower levels of tumor infiltrating lymphocytes and a trend towards decreased peritumoral lymphocyte aggregates (Wasserman et al., 2018). These experiments collectively suggest that canonical TGF-β pathway signaling within intestinal epithelial cells and intestinal carcinoma cells has an important role in modulation of surrounding immune cells.

Two additional high-profile papers deserved to be discussed. In 2015, an international consortium focused on large-scale data sharing and analytics published four consensus molecular subtypes (CMSs) of CRC with distinguishing features (Guinney et al., 2015). CMS4 is known as the “mesenchymal” subtype and is distinguished by TGFβ activation, stromal infiltration, and angiogenesis, and is demonstrated to have shorter relapse-free survival and survival after relapse when compared to the other three CMS subtypes (Guinney et al., 2015). The second paper relied on a powerful mouse model which leveraged a quadruple-mutant mouse which developed metastatic intestinal tumors that displayed features highly similar to human microsatellite stable (MSS) CRC (including a low mutational burden, T cell exclusion, and TGFβ-activated stroma) (Tauriello et al., 2018). They found that inhibiting PD-1/PD-L1 (a strategy frequently used in MSI-high CRC and other immunogenic tumors) had limited ability to invoke a response in this model system but that TGFβ inhibition resulted in a potent and enduring cytotoxic T cell response, prevented metastatic spread of intestinal tumors, and increased tumor susceptibility to anti-PD-1/PD-L1 therapy (Tauriello et al., 2018). These two papers provide

powerful evidence that TGFβ plays an important role in immune evasion in CRC and has implications for potential therapeutic strategies, particularly in MSS CRC.

Altered immune cell recruitment due to abrogated TGF-β pathway signaling has additionally been demonstrated in models of HNSCC. In a murine model with epithelial-specific deletion of *Smad4* within the oral mucosa, numerous infiltrating leukocytes (including macrophages, granulocytes, and T cells) were observed in the sub-epithelial stroma of $Smad4^{-/-}$ mucosa compared to controls with $Smad4^{+/+}$ mucosa. Additionally, $Smad4^{-/-}$ mucosa had markedly increased expression of several cytokines including *MCP-1*, *Cxcr7, Csf3,* and *Ppdp*. Of note, mice with $Smad4^{-/-}$ mucosa spontaneously developed invasive oral tumors whereas $Smad4^{+/+}$ and $Smad4^{+/-}$ controls did not (Bornstein et al., 2009). In a parallel experiment, investigators deleted *Tgfbr2* (which encodes TGF-βRII) from the head-and-neck epithelium of *Kras* mutant mice and found a significant increase in leukocyte infiltration in the buccal mucosa and HNSCCs of mice with $Tgfbr2^{-/-}$ mucosa compared to control mice. In this case, leukocytic infiltrate had a predominance of macrophages and granulocytes (Lu et al., 2006b).

Similar immunomodulatory effects of TGF-β pathway signaling have been observed in human mammary cells and in models of mammary carcinoma. In established mammary epithelial cell lines, TGF-β1 suppressed basal and OSM-induced *Cxcl1, Cxcl5,* and *Ccl20* expression (Bierie et al., 2009). In mouse models of mammary carcinoma, carcinoma-specific deletion of TGF-βRII resulted in increased Gr-1^{+}CD$11b^{+}$ myeloid cell recruitment to the tumor invasion front, and such recruitment was attributed to upregulation of two chemokine axes: CXCL5/CXCR2 and CXCL12/CXCR4 (Yang et al., 2008).

These data together suggest an important immunomodulatory role for TGF-β family signaling within epithelial cells. Dysregulation of TGF-β signaling, frequently occurring in pre-malignant and malignant lesions of the gastrointestinal tract, appears to have a substantial impact on the immune microenvironment that may in turn impact tumorigenesis and tumor progression through altered immune cell recruitment. In several of the above-discussed experiments, tumor progression and metastasis were directly attributed to myeloid cell recruitment to TGF-β signaling-deficient tumors due to myeloid production of MMPs (Inamoto et al., 2016; Itatani et al., 2013; Kitamura et al., 2007; Yang et al., 2008). This suggests a novel mechanism of TGF-β's tumor suppressor role in epithelial tissues beyond the well-characterized effects on cell cycle control, although the full impact of immunomodulation by epithelial TGF-β signaling remains incompletely understood.

TGFβ dysregulation in inflammatory bowel disease

A careful balance of pro- and anti-inflammatory signals in the intestinal epithelium is critical for maintaining intestinal homeostasis. The intestine is home to thousands of microbial species (Qin et al., 2010), and the intestinal mucosa must extinguish invading pathogens quickly to prevent organismal infection due to minor mucosal injuries. At the same time, the inflammatory response to resident bacteria must be tempered and self-limited to prevent pathologic intestinal inflammation. Dysregulation of this equilibrium between pro- and anti-inflammatory signals in the intestine is thought to be a major contributing factor to inflammatory bowel disease (IBD), and the dysregulated pathways that contribute to the development of IBD is an active area of research (Zhang and Li, 2014).

TGF-β pathway signaling may play a critical role in extinguishing pro-inflammatory signals in response to resident microbes in the intestine. In an intestine-specific dominant-negative *Tgfbr2* (dnR2) transgenic mouse model, dnR2 mice were healthy when housed under specific pathogen-free conditions but quickly developed spontaneous colitis, weight loss, severe diarrhea, and hematochezia when housed in normal rodent housing in the presence of standard microbes. The intestinal mucosa of dnR2 mice was found to have significantly increased expression of *Il-2, Il1-β, IFN-γ, IL-10,* and *TGF-β1*, and dnR2 mice appeared to be highly susceptible to Dextran Sulfate Sodium (DSS)-induced colitis compared to wild type mice (Hahm et al., 2001).

Interestingly, inhibitory-SMAD (SMAD7) protein levels have been found to be increased in mucosal biopsy samples of patients with Crohn's Disease as compared to healthy controls (Monteleone et al., 2001, 2005). Accordingly, SMAD3 phosphorylation levels, a marker of canonical TGF-β pathway activity, was markedly reduced in mucosal samples of Crohn's patients compared to mucosal samples from healthy controls

(Monteleone et al., 2001). Importantly, it was demonstrated that *SMAD7* antisense therapy reduced SMAD7 protein levels, increased levels of phosphorylated SMAD3, and decreased levels of mucosal pro-inflammatory cytokines including TNF-α and IFN-γ (Monteleone et al., 2001). Phase 1 clinical trials of oral *SMAD7* knockdown therapy demonstrated clinical safety (Monteleone et al., 2012a) and a double-blind phase 2 trial found that patients with Crohn's Disease who received *SMAD7* knockdown therapy had significantly higher rates of remission and clinical response than those who received placebo (Monteleone et al., 2015), however this therapy failed to demonstrate efficacy versus placebo in a blinded phase 3 trial published five years later (Sands et al., 2020).

Conclusions and Unanswered Questions

While TGF-β's roles in modulating epithelial cell proliferation and immune cell activation have been well characterized, the role of TGF-β signaling within epithelial cells as it impinges on immunomodulation is less well understood. Several murine experiments have recently drawn attention to the immunomodulatory role of TGF-β family signaling in epithelial cells and epithelial cancers (Bierie et al., 2009; Bornstein et al., 2009; Grady et al., 1999; Hahm et al., 2001; Inamoto et al., 2016; Itatani et al., 2013; Kitamura et al., 2007; Lu et al., 2006b; Means et al., 2018; Monteleone et al., 2001, 2005, 2012a, 2015; Principe et al., 2017; Yan et al., 2004; Yang et al., 2008). It appears that canonical TGF-β signaling within epithelial cells plays a role in suppressing pro-inflammatory chemokine and cytokine expression, and that loss of functional TGF-β signaling results in up-regulation of multiple pro-inflammatory chemokines and cytokines, resulting in altered immune cell recruitment (**Figure 1.2**). Though in some contexts this altered leukocyte recruitment may directly impinge on epithelial cancer progression, such as through increased immature myeloid recruitment and subsequent MMP secretion, exactly how this altered chemokine/cytokine expression profile impinges on the immune system and its implications for tumorigenesis and tumor progression remains largely unexplored. Furthermore, whether the altered landscape of chemokine/cytokine production that occurs because of aberrant epithelial TGF-β signaling has implications for leukocyte activation, differentiation, or behavior in the epithelial microenvironment remains unknown.

Furthering the intricacy of this scenario of altered immune cell recruitment towards TGF-β signaling-deficient epithelium and epithelial cancers is the observation that tumors with altered TGF-β signaling appear to have increased TGF-β ligand in their tumor-associated stroma (Hahm et al., 2001; Lu et al., 2006b; Principe et al., 2017; Yang et al., 2008). While increased TGF-β ligand abundance is generally felt to be an important mediator of immune-evasion in tumors with defective TGF-β signaling (Guinney et al., 2015; Tauriello et al., 2018), how altered epithelial cell chemokine/cytokine expression in this context may further impinge on leukocyte recruitment, differentiation, cytotoxicity, and behavior beyond the known immunomodulatory-effects of TGF-β ligand on leukocytes is largely unknown.

Developing a more sophisticated understanding of the immunomodulatory role of TGF-β family signaling within epithelial cells has the potential to greatly improve our understanding of TGF-β's tumor suppressive role beyond its well-known anti-proliferative effects. Additionally, such investigation may allow us to understand how loss of functional TGF-β signaling in epithelial tumors, a relatively frequent event, may lead to targetable alterations in the immune microenvironment. Such insight could have therapeutic implication for IBD patients and for patients with TGF-β-deficient epithelial tumors.

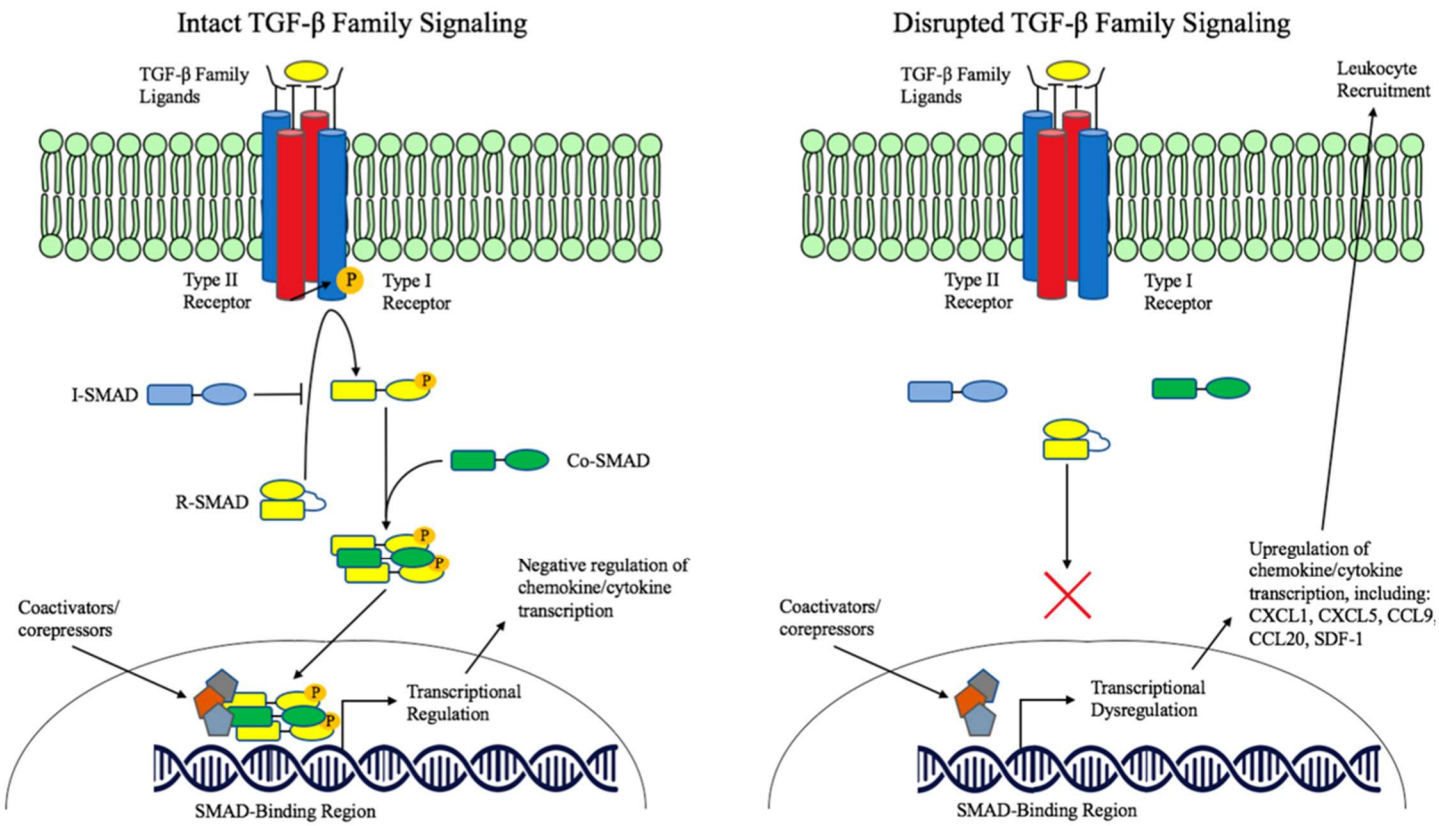

Figure 1.2 – Summary figure taken from Marincola Smith, et al. *(Marincola-Smith et al., 2019)*. Canonical TGFβ signaling within epithelial cells plays negative regulates the expression of multiple pro-inflammatory chemokines and cytokines. Loss of canonical TGFβ signaling (though TGFβ-R mutations, loss of SMAD protein expression, or otherwise) leads to dysregulation of chemokine/cytokine expression and altered leukocyte recruitment/activation.

CHAPTER II

Part of this chapter is adapted from "Epithelial Smad4 Deletion Up-Regulates Inflammation and Promotes Inflammation-Associated Cancer" published in *Cell and Molecular Gastroenterology and Hepatology (CMGH)* and has been reproduced with the permission of the publisher and my co-authors, Anna L. Means, Tanner J Freeman, Jing Zhu, Luke G Woodbury, Chao Wu, Anne R Meyer, Connie J Weaver, Chandrasekhar Padmanabhan, Hanbing An, Jinghuan Zi, Bronson C Wessinger, Rupesh Chaturvedi, Tasia D Brown, Natasha G Deane, Robert J Coffey, Keith T Wilson, J Joshua Smith, Charles L Sawyers, James R Goldenring, Sergey Novitskiy, M Kay Washington, Chanjuan Shi, and R. Daniel Beauchamp.
Reference: AL Means, et al. Epithelial Smad4 Deletion Up-Regulates Inflammation and Promotes Inflammation-Associated Cancer. *CMGH*. 2018;24(3):257-276.

TGFβ/SMAD4 MODULATES INFLAMMATION AND CCL20 EXPRESSION IN MOUSE COLONOCYTES

Abstract:
Background & Aims: We previously reported that Dextran sodium sulfate (DSS) induced colitis initiates development of invasive colon adenocarcinomas in mice with intestine-specific *Smad4* knockout, but not in mice expressing SMAD4 in the intestinal epithelium, and that intestinal SMAD4 loss results in increased expression of CCL20, a chemokine implicated in both inflammatory bowel disease (IBD) and colon cancer. Here we investigate whether the CCL20/CCR6 signaling axis plays a causative role in colitis-associated tumorigenesis due to SMAD4 loss.
Methods: Transgenic mice with Cre-recombinase expression under the control of an intestine-specific promoter (*Lrig1*) and LoxP sites inserted around critical exons of the *Smad4* gene locus are administered tamoxifen to induce intestine-specific *Smad4* loss ($Smad4^{\Delta Lrig1}$). Four weeks after recombination, sub-epithelial stroma is isolated for RNA-sequencing (RNA-seq). $Smad4^{\Delta Lrig1}$ are additionally crossed with mice that have GFP knocked into the *Ccr6* gene. $Smad4^{\Delta Lrig1}$; $Ccr6^{+/-}$ and $Smad4^{\Delta Lrig1}$; $Ccr6^{-/-}$ mice were subjected to DSS in drinking water to induce chronic colitis and dissection 9 weeks later for histological examination.
Results: Loss of intestinal epithelial *Smad4* expression was associated with a 3-fold increase in *Ccl20* expression in the epithelium and 2.75-fold increase in *Ccr6* expression in the sub-epithelial stroma of mouse colons (both $p<0.01$). Nine weeks after colitis induction, 100% of *Ccr6*-expressing ($Smad4^{\Delta Lrig1}$; $Ccr6^{+/-}$) mice had one or more invasive adenocarcinomas of the colon compared to 16.7% of *Ccr6*-null mice ($Smad4^{\Delta Lrig1}$; $Ccr6^{-/-}$; $p<0.05$). *Ccr6*-expressing mice additionally developed a significantly higher number of invasive tumors compared to *Ccr6*-null mice (1.7 vs 0.2 tumors per mouse, $p<0.03$).
Conclusion: Loss of intestinal TGFβ signaling is associated with an increase in epithelial *Ccl20* expression and a corresponding increase in stromal *Ccr6* expression in mice, both of which have been observed in humans with IBD and colitis associated cancer (CAC). Blocking the *Ccl20/Ccr6* axis through *Ccr6* knockout significantly diminishes the susceptibility to CAC in *Smad4*-null mice. These results support the hypothesis that the tumor suppressor role of SMAD4 involves regulation of inflammatory pathways, including the CCL20/CCR6 axis.

Background:

Chronic inflammation is a predisposing condition for many cancers including colorectal cancer (CRC) (Elinav et al., 2013). There is compelling evidence that colorectal carcinogenesis is promoted by a combination of microbiota-dependent and host-dependent mechanisms that trigger intestinal epithelial cell inflammatory signaling (Arthur et al., 2012; Fukata et al., 2007; Grivennikov et al., 2012; Rakoff-Nahoum and Medzhitov, 2007). This is particularly true in colitis-associated cancer (CAC) with longstanding ulcerative colitis (UC)

predisposing to CAC (Elinav et al., 2013). TGFβ pathway signaling has a known role in regulating immune cell responses through its direct regulation of lymphoid and myeloid cell proliferation, differentiation, and survival (Yang et al., 2010a). Preclinical studies have implicated defective TGFβ pathway signaling due to increased stability of SMAD7 (a protein that inhibits the TGFβ signaling pathway (Meng et al., 2013)) as an important contributory factor in inflammatory bowel disease (IBD) (Monteleone et al., 2001, 2012b, 2015).

SMAD4 is a highly conserved protein in metazoans and is a critical mediator of the TGFβ signaling pathway (Höfler et al., 1993; Massagué, 2012; Yang et al., 2010a). Previous work in our lab has demonstrated that TGFβ signaling via SMAD4 plays a central inhibitory role in intrinsic colon epithelial cell inflammatory signaling and that TGFβ signaling is able to block or repress effects of pro-inflammatory cytokines in colonic epithelial tissue. Additionally, we found that conditionally and selectively knocking out *Smad4* in murine intestinal epithelial cells leads to strikingly increased inflammatory signaling within the epithelial compartment and that these mice demonstrated a significant and robust increase in immune ($CD45^+$) cell infiltration in *Smad4* knock-out versus control mouse colon under homeostatic conditions. Furthermore, after Dextran Sulfate Sodium (DSS)-induced colitis, these mice are susceptible to the development of invasive mucinous adenocarcinomas of the distal colon that are morphologically similar to those seen in human CACs (Means et al., 2018). Additionally, we observed loss of SMAD4 protein in 48% of human CAC samples as compared with 19% of sporadic CRCs (Means et al., 2018), and several prior studies identified SMAD4 loss as an independent risk factor for worse recurrence free survival in CRC patients (Alazzouzi et al., 2005; Roth et al., 2012; Yan et al., 2016).

A key chemokine regulated by the SMAD4 pathway is CCL20. CCL20 is induced by pro-inflammatory cytokines including TNF-α and IL-1β, and by Toll-like receptor signaling (Wang et al., 2008). CCL20 is the exclusive ligand for the CCR6 receptor which is expressed on multiple immune cell subtypes including Th17 cells (T_h17), regulatory T cells (Tregs), B cells, multiple dendritic cell (DC) subsets, and others (Comerford et al., 2010). The role of CCL20 in immune response is complex with both pro-inflammatory and anti-inflammatory functions. In humans, CCL20 is upregulated in both UC and CD (Comerford et al., 2010; Skovdahl et al., 2015; Zhang et al., 2012), and the gene encoding CCR6 is in a locus associated with CD (Khor et al., 2011). Furthermore, CCL20 is elevated in colorectal adenomas and in CRC, suggesting that it may influence cancer susceptibility (Frick et al., 2013; McLean et al., 2011).

Through the following experiments, we demonstrate that *Ccl20* expression is regulated by SMAD4 in mouse colonocytes, that intestinal SMAD4 loss is associated with increased expression of *Ccr6* in the sub-epithelial stroma, and that the *Ccl20/Ccr6* axis plays a significant role in colitis-associated tumorigenesis due to intestinal SMAD4 loss in mice.

Methods:

Mouse model

Animal work was performed with approval from the Vanderbilt University Institutional Animal Care and Use Committee and followed ARRIVE guidelines. Mouse alleles $Lrig1^{CreERT2}$ and $Smad4^{fl/fl}$ have been previously published (Bardeesy et al., 2006; Means et al., 2008, 2018; Powell et al., 2012) and were bred into the C57BL/6J background for at least 10 generations. Mice were given tamoxifen (2mg in 0.1mL corn oil) intraperitoneally two times on alternating days after 8 weeks of age to ensure that *Smad4* gene deletion occurred during adulthood and not during development. Mice with $Lrig1^{CreERT2}$ $Smad4^{fl/fl}$ genotype that received tamoxifen injections and who were confirmed by immunohistochemistry (IHC) to have undergone recombination with loss of SMAD4 protein in the intestinal crypts are referred to as $Smad4^{\Delta Lrig1}$. $Smad4^{\Delta Lrig1}$ mice demonstrate loss of SMAD4 protein in 90% or more of colon crypts (Means et al., 2018).

Mice with *Lrig1*^{CreERT2} and *Smad4*$^{fl/fl}$ alleles were bred with mice from Jackson Laboratory that have *EGFP* knocked into the *Ccr6* coding region (Kucharzik et al., 2002; Lügering et al., 2010) such that cells transcribing from the *Ccr6* promoter can be tracked by *EGFP* expression in heterozygous *Ccr6*$^{+/EGFP}$ mice and in *Ccr6*$^{EGFP/EGFP}$ null mice. Crossing these lines with our previously described *Smad4*$^{\Delta Lrig1}$ lines yielded pups with bi-allelic loss of *Ccr6* and conditional intestinal epithelial loss of *Smad4* as well as necessary controls including *Ccr6*$^{+/EGFP}$ mice with and without conditional loss of *Smad4*.

Controls were sibling littermates and cage mates, and male/female mice were split evenly between experimental arms. After tamoxifen treatment, bedding was mixed among cages within an experiment once per week. SMAD4-expressing control mice (mice with *Smad4*$^{fl/fl}$ genotype + tamoxifen injection) are referred to as *Smad4*$^{fl/fl}$, SMAD4+, or simply "control" mice for simplicity.

Tissue Preparation, Staining, and Imaging

For hematoxylin and eosin (H&E) and IHC, mouse colons were fixed in 4% paraformaldehyde (PFA) overnight and embedded in paraffin as previously described(Blaine et al., 2010; Means et al., 2003; Ray et al., 2014). SMAD4 and GFP antibodies are listed in **Table 2.1** and immunostaining was performed as published (Means et al., 2003, 2018; Ray et al., 2014). Brightfield images were captured on an Axioskop 40 microscope using Axiovision software (Carl Zeiss Microimaging, Thornwood, NY) through the Vanderbilt University Digital Histology Shared Resource.

Antibodies				
Target Protein	**Company**	**Product Number**	**Dilution**	**References**
SMAD4	Abcam	40759	1:1000 (IHC [FFPE])	(Means et al., 2018)
GFP	Novus Biologicals	600-308	1:5000 (IHC [FFPE])	(Corbet et al., 2020)

qPCR Primers		
Target Gene	**Forward (5' to 3')**	**Reverse (5' to 3')**
Tnfa	tgaggaaggctgtgcattg	ggccttcctaccttcagacc
Cxcl5	tgccctacggtggaagtcat	agctttctttttgtcactgccc
Ccl20	ggtactgctggctcacctct	tgtacgagaggcaacagtcg
Il18	caaaccttccaaatcacttcct	tccttgaagttgacgcaaga
Il18bp	agctattcggggcttaggag	tgcaagcaagtctggtgtct
Il34	ccacccgtcctggaagtat	ggccaatctccacatccat
Ccl8	ttctttgcctgctgctcata	gcaggtgactggagccttat
Il1rn	ctccttctcatccttctgtttca	ggtcttctggttagtatcccagatt
Smad7	acccccatcaccttagtcg	gaaaatccattgggtatctgga
Pmm1 (Reference Gene)	gggtggctctgactactctaagat	acacgtagtcaaacttctcaatgact

Table 2.1: Antibodies and qPCR primers utilized in Chapter III. IHC = immunohistochemistry. FFPE = Formalin fixed and paraffin embedded.

Bulk RNA-sequencing (RNA-seq)

Three *Smad4*$^{\Delta Lrig1}$ and three SMAD4+ control mice were dissected 1 month after administration of tamoxifen. Colon crypts were chelated using Ethylenediaminetetraacetic acid (EDTA). Following crypt chelation, the sub-epithelial stroma was removed from the underlying muscle layer by scraping. RNA was then made from the sub-epithelial stroma using RNeasy kit (Qiagen, Germantown, MD) and RNA-seq performed by the Vanderbilt Technologies for Advanced Genomics (VANTAGE) core facility. 32–37 million 51–base pair,

single-end reads were generated per sample. Reads were mapped to the mouse genome mm10 using TopHat-2.1.0, uniquely mapping 86%–95% single-end reads to the genome, depending on the study. The number of reads that fell into annotated genes were counted using samtools-1.3.1 and HTSeq-0.5.4p5. Count-based differential expression analysis was performed using edgeR_3.4.2.

Pathways and upstream regulators were analyzed using IPA software (Qiagen, Inc, https://www.qiagenbioinformatics.com/products/ingenuity-pathway-analysis). Immune cell composition was predicted using ImmuCC software (http://218.4.234.74:3200/immune/) as previously described (Chen et al., 2018).

Flow Cytometry

After euthanasia, the colon distal to the ascending colon was removed, measured, washed with phosphate-buffered saline (PBS), cut longitudinally, then cut into 1-cm lengths. Tissue then was incubated in cold 30 mL Hank's balanced salt solution (HBSS) + 0.3 mmol/L dithiothreitol and rocked at 4°C for 20 minutes, washed with PBS, and moved to 30 mL HBSS + 1 mmol/L EDTA and again rocked at 4°C for 20 minutes. Tissue then was minced rapidly with scissors, added to prewarmed collagenase solution (1 mg/mL Collagenase I [Sigma Aldrich] + 1 mg/mL Dispase II [Sigma Aldrich] in 10 mL HBSS), and digested for 40 minutes at 37°C shaking at 350 rpm. After a brief vortex to ensure adequate dissociation of tissue, suspension was filtered through 500-µm mesh and then through 70-µm mesh. Thirty milliliters of DNase solution (30 mL HBSS + 5% fetal bovine serum [FBS; Atlanta Biologicals, Atlanta, GA] + 25 U DNase I [Sigma Aldrich]) was added and cells were incubated at room temperature for 5 minutes and then centrifuged at 1500 rpm for 10 minutes at 4°C. The pellet then was resuspended in fluorescence-activated cell sorting buffer and aliquoted for staining 2 different panels. Antibodies (all from Biolegend, San Diego, CA) for the lymphoid panel included fluorescein isothiocyanate–anti-CD45, AF700–anti-CD3, phycoerythrin (PE)–C7–anti-CD4, PE–anti-CD8, and APC–Cy7–CD19. Antibodies for the myeloid panel included fluorescein isothiocyanate–anti-CD45, AF700–anti-CD11b, PE–Cy7–anti-CD11c, PE–anti-CD103, APC–Gr1 (anti-Ly6G/Ly6C), and PerCP5.5–anti-F4/80. 4′,6-Diamidino-2-phenylindole was used to distinguish live from dead cells. Fluorescence minus one controls were performed in parallel on separate mice to compensate for spectral overlap.

Data were collected on a 5-laser BD Biosciences LSRII Flow Cytometer (San Jose, CA) in the Vanderbilt University Medical Center Flow Cytometry Shared Resource (FCSR) Core. Fluorescence-activated cell sorter gating and analysis were performed using FlowJo 10 software (FlowJo, Ashland, OR).

Gut-Associated Lymphoid Tissue (GALT) Analysis

Five $Smad4^{\Delta Lrig1}$ and five SMAD4+ control mice were used for histologic analysis for Gut-Associated Lymphoid Tissue (GALT) aggregates. Four weeks after tamoxifen-induced recombination, mice were dissected, and their colons removed/fixed in 4% PFA prior to embedding in paraffin. Three 5-micron sections were cut and examined per mouse, each 1000 microns apart. Sections were stained by H&E and examined for the presence of GALTs. Number of GALTs per swiss roll section as well as cross-sectional GALT area was quantified and normalized to amount of tissue present using VU-DHSR Digital Histology Hub (Leica Biosystems, Buffalo Grove, IL).

Colon Organoid ("Colonoid") Experiments

Mouse colonoids were generated from $Lrig1^{CreERT2}$; $Smad4^{fl/fl}$ mice and cultured as previously described (Means et al., 2018). Colonoids were suspended and plated in 50-µL beads of Growth Factor Reduced Matrigel (GFR; Corning, Tewksbury, MA). Complete colonoid medium was composed of 40% basal medium (advanced DMEM/F12 [Gibco] supplemented with penicillin/streptomycin [Gibco], N2 [Gibco], B27 [Gibco], Glutamax

[Gibco], HEPES [Sigma Aldrich], 50 ng/mL epidermal growth factor [R&D Systems]), 40% Wnt3a-conditioned medium, 10% R-Spondin–conditioned medium, and 10% Noggin-conditioned medium. Colonoids were grown at 37°C in 5% CO_2, media was changed every 2-3 days, and colonoids were passaged every 5-7 days.

After establishing colonoids in culture, colonoids were incubated at 37°C with 20μg/mL 4-OH-Tamoxifen or methanol vehicle control for 24 hours to create a SMAD4 knockout (KO) line or a matched SMAD4+ control line, respectively. SMAD4 KO and control colonoid lines were maintained in culture under the same conditions.

Colonoids at density of 70-100 per well were treated three days after passage with TGFβ1 (3ng/mL), BMP2 (100ng/mL), TGFβ1/BMP2 (3ng and 100ng/mL, respectively), and/or vehicle control at designated time points for qPCR experiments. Vehicle for TGFβ1 and BMP2 was 4mM HCl + 0.1% BSA in PBS. Wells treated with BMP2 had the BMP-inhibitor, Noggin, withheld from the media.

Quantitative Reverse-Transcription Polymerase Chain Reaction (qPCR)

RNA was extracted from colonoids from at least 3 experimental replicates performed on different days and purified as described (Freeman et al., 2012). Samples were run using a standard SYBR Green qPCR protocol (Green and Sambrook, 2018). All samples were run in triplicate with a negative control on a CFX96 Thermal Cycler (Bio-Rad, Hercules, CA). A well-known TGFβ/SMAD-response gene (Zhao et al., 2000), *Smad7*, was used for a positive control to confirm TGFβ pathway stimulation in all experimental replicates. mRNA levels were normalized to the level of *Pmm1*. All qPCR primer sequences are listed in Table 2.1. Each point on each qPCR graph represents a single experimental replicate (each done on a separate day), and each experimental replicate reflects the mean value of three technical replicates.

Colitis and Tumorigenesis Experiment

$Smad4^{fl/fl}$ mice with/without $Lrig1^{CreERT}$ expression and with/without CCR6 expression ($Ccr6^{EGFP/+}$ or $Ccr6^{EGFP/EGFP}$) were given tamoxifen to induce Cre-recombinase activation and SMAD4 loss, as described above. A total of two SMAD4+; $Ccr6^{EGFP/+}$, eight $Smad4^{\Delta Lrig1}$; $Ccr6^{EGFP/+}$, six SMAD4+; $Ccr6^{EGFP/EGFP}$, and eleven $Smad4^{\Delta Lrig1}$; $Ccr6^{+/+}$ were included in this experiment. Mice were littermates and genotypes were split evenly among male/female mice. Bedding was mixed weekly between cages.

One month after tamoxifen-induced recombination, mice were subjected to three rounds of 2.2% DSS in drinking water (five days on, five days off) to induce chronic colitis (Freeman et al., 2012; Means et al., 2018). Following induction of chronic colitis, mice were allowed to recover and were observed for up to 3 months or until a humane endpoint was reached. By 3 months post-DSS, mice were dissected, their colons fixed, sectioned, and stained with H&E. A collaborating pathologist with expertise in murine gastrointestinal tumors who was blinded to mouse genotype examined 6 sections per mouse, each 200μm apart, and scored the sections for inflammation, crypt damage, and number/type of invasive tumors (Dieleman et al., 1988).

Statistical Analysis

Mann-Whitney U test was used to compare GALT area, inflammation score, and mean number of tumors between groups *in vivo* following DSS treatment. Fisher's Exact test was used to compare proportion of animals in each group who develop tumors following DSS treatment. Flow cytometry results were analyzed by 2-tailed T test with Holm-Sidak multiple test correction. Two-way ANOVA was used to compare gene expression levels between groups in qPCR experiments with post-hoc Welch's T test. Statistical analyses were performed using GraphPad Prism 9 Software (San Diego, CA). Throughout the chapter, statistical significance is designated as: ns ($p \geq 0.05$), * ($p < 0.05$), ** ($p < 0.01$), or *** ($p < 0.001$).

Results:

The sub-epithelial stroma of Smad4$^{\Delta Lrig1}$ *mice demonstrates increased expression of multiple immune-related genes*

In order to investigate whether the increased inflammatory signaling in the colonic epithelium due to intestinal SMAD4 loss was associated with a reciprocal increase in sub-epithelial inflammatory signaling, the lab previously performed RNAseq on the sub-epithelial stromal layer from three *Smad4$^{\Delta Lrig1}$* and three littermate SMAD4+ control mice. One month after tamoxifen injection, mice were dissected, their colons isolated, and the epithelial crypts were removed by EDTA chelation. A scraping of the sub-epithelial stroma was subsequently taken and RNAseq performed.

A comparison of gene expression within the sub-epithelial stroma of *Smad4$^{\Delta Lrig1}$* mice relative to SMAD4+ control mice demonstrated a marked increase in inflammatory gene signaling. Of the 95 genes that were upregulated by at least 2.5-fold ($\geq$1.32 Log_2 Fold Change) and a false discovery rate <0.05, 51 genes are known to be expressed on immune cells or have immune-related functions. The 51 upregulated immune-related genes are list in **Table 2.2** along with a brief description of their known functions.

Gene Symbol	Protein Function	Log_2 Fold Change	P-value	FDR	Base Mean
Fcrl1	Fc immunoglobulin receptor, may function as activating co-receptor in B cells	2.05	$4.2x10^{-13}$	$2.0x10^{-9}$	91.4
Faim3	Fc immunoglobulin receptor	1.81	$4.2x10^{-12}$	$8.7x10^{-9}$	119.5
Cr2	Complement receptor, expressed on B cells, plays role in B cell activation and maturation	1.79	$5.5x10^{-11}$	$1.0x10^{-7}$	173.6
Btla	Induced during T cell activation, expressed on Th1 but not Th2 cells, inhibits activation of CD8+ cancer-specific T cells	1.77	$2.9x10^{-13}$	$2.0x10^{-9}$	123.6
Sell	Selectin L, cell adhesin molecules expressed on leukocytes, important in lymphocyte-endothelial cell interaction	1.73	$2.0x10^{-8}$	$6.3x10^{-6}$	76.8
Tlr9	Toll-like receptor, innate immune response, expressed on APCs, preferentially binds bacterial/viral DNA and trigger pro-inflammatory cytokine response	1.72	$3.9x10^{-9}$	$2.0x10^{-6}$	39.4
Cxcr4	Binds SDF-1/CXCL12, lymphocyte chemotactic activity	1.71	$3.4x10^{-10}$	$2.9x10^{-7}$	174.1
Cd22	Expressed on mature B cells, involved with B cell trafficking to Peyer's Patches	1.70	$1.1x10^{-9}$	$7.3x10^{-7}$	337.9
Treml2	Interaction with CD276 on T-cells, enhances T-cell activation	1.69	$4.4x10^{-9}$	$2.0x10^{-6}$	53.8
Gp2	Expressed on apical surface of M-cells in Peyer's Patches, receptor for subset of mucosal commensal & pathogenic bacteria	1.69	$3.7x10^{-7}$	$6.7x10^{-5}$	46.3
Ms4a1	B lymphocyte antigen	1.68	$4.0x10^{-10}$	$3.0x10^{-7}$	278.6
Pyhin1	Interferon-inducible transcription factor, involved in defense against infection through recognition of foreign/microbial DNA	1.67	$2.5x10^{-10}$	$2.7x10^{-7}$	79.4
Tnfrsf13c	Membrane receptor of TNF superfamily, recognizes BAFF (essential factor for B cell maturation/survival)	1.67	$7.8x10^{-11}$	$1.0x10^{-7}$	136.3
Cd79a	Together with CD79b forms dimer with membrane-bound immunoglobulin in B cells, forming B cell antigen receptor	1.66	$6.8x10^{-9}$	$2.8x10^{-6}$	201.5
Cd79b	Together with CD79a forms dimer with membrane-bound immunoglobulin in B cells, forming B cell antigen receptor	1.66	$7.2x10^{-11}$	$1.0x10^{-7}$	258.2

H2-Oa	Histocompatibility	1.66	$2.0x10^{-9}$	$1.2x10^{-6}$	56.5
Fcrla	Fc immunoglobulin receptor, mediate phagocytosis of IgG-coated pathogens	1.65	$7.1x10^{-10}$	$5.2x10^{-7}$	100.0
Irf4	Interferon regulatory factor 4, key regulator of lymphoid-, myeloid-, and dendritic-cell differentiation	1.63	$6.5x10^{-9}$	$2.8x10^{-6}$	103.1
Ly6d	Marks early B cell specification	1.63	$3.8x10^{-12}$	$8.7x10^{-9}$	132.0
H2-Ob	Histocompatibility	1.62	$2.6x10^{-10}$	$2.7x10^{-7}$	242.1
Ebf1	Controls expression of proteins involved with B cell differentiation, signal transduction, and function	1.62	$2.2x10^{-7}$	$4.5x10^{-5}$	61.2
Blk	B lymphocyte kinase, non-receptor tyrosine kinase, B cell proliferation/development	1.59	$1.3x10^{-9}$	$8.8x10^{-7}$	85.1
Bank1	Involved with B cell receptor induced Ca^{2+} mobilization from intracellular stores	1.58	$3.0x10^{-7}$	$5.5x10^{-5}$	141.8
Iglc2	Constant region of immunoglobulin light chain	1.57	$7.1x10^{-7}$	$1.2x10^{-4}$	108.5
Cxcl13	Binds to CXCR5, selectively chemotactic to B cells, together with CXCR5 controls organization of B cells within follicles and lymphoid tissues	1.56	$1.6x10^{-6}$	$2.1x10^{-4}$	90.4
H2-Eb2	Histocompatibility	1.55	$2.2x10^{-9}$	$1.2x10^{-6}$	90.2
Cxcr5	Receptor for CXCL13, role in B cell migration and together with CXCL13 causes development of lymph nodes and Peyer's Patches	1.54	$1.2x10^{-8}$	$4.5x10^{-6}$	169.3
Pou2af1	Transcriptional coactivator, expressed by B cells, controls expression of immunoglobulin and other B cell critical genes	1.54	$1.4x10^{-8}$	$4.9x10^{-6}$	285.0
Gpr183	Expressed in B cells, assists with B cell homing in lymph nodes	1.53	$2.1x10^{-8}$	$6.5x10^{-6}$	53.7
Ifi203	Interferon activated gene	1.52	$1.9x10^{-9}$	$1.1x10^{-6}$	70.2
Pax5	B cell lineage specific activator protein, expressed at early (but not late) stages of B cell differentiation	1.52	$2.9x10^{-7}$	$5.5x10^{-5}$	52.1
Cd19	B cell surface antigen, expressed on all B lineage cells	1.50	$2.1x10^{-8}$	$6.3x10^{-6}$	310.9
Ly9	T lymphocyte surface antigen, involved in regulation/interaction between innate and adaptive immune response	1.49	$1.1x10^{-6}$	$1.6x10^{-4}$	50.0
Ighm	Constant region of immunoglobulin heavy chains	1.48	$1.8x10^{-8}$	$5.8x10^{-6}$	800.2
Ikzf1	Transcription factor, regulates B cell/CD4+ T cell development	1.48	$1.8x10^{-8}$	$5.8x10^{-6}$	221.4
Sfpi1	Transcription factor, regulates myeloid/B cell development	1.46	$7.7x10^{-7}$	$1.2x10^{-4}$	42.4
Ccr6	Receptor for CCL20/MIP3A, expressed on B cells, immature dendritic cells, T cells (Th1, Th2, Th17, Treg), NK cells, and neutrophils, involved with leukocyte migration/recruitment and B cell maturation/differentiation	1.46	$1.6x10^{-6}$	$2.1x10^{-4}$	73.5
Igkv2-137	Variable region of immunoglobulin kappa chain	1.45	$1.2x10^{-5}$	0.0011	23.7
Igkv17-121	Variable region of immunoglobulin kappa chain	1.44	$1.2x10^{-5}$	0.0011	44.4
Ikzf3	Transcription factor, regulates B cell proliferation/differentiation	1.44	$1.5x10^{-8}$	$5.2x10^{-6}$	225.4
Cd37	Surface antigen on B cells > T cells and myeloid cells, involved in both humoral and cellular immune response	1.42	$5.9x10^{-9}$	$2.7x10^{-6}$	293.8
Ly86	Together with CD180/TLR4, coordinates innate immune response to LPS	1.40	$2.0x10^{-6}$	$2.5x10^{-4}$	57.3
Iglv3	Variable region of immunoglobulin lambda chain	1.40	$2.5x10^{-5}$	0.0020	42.7

Lax1	Negatively regulates the T cell receptor and B cell receptor in T and B cells, respectively	1.39	$1.4x10^{-7}$	$3.2x10^{-5}$	102.0
Tnfsf8	Cytokine, ligand for CD30, engagement of ligand with CD30 on B cells plays inhibitory role in Ig class switch, induced lymphocyte proliferation	1.37	$9.3x10^{-6}$	$9.1x10^{-4}$	21.1
Il9r	Cytokine receptor for IL9, ligand binding causes activation of JAK/STAT pathway	1.36	$2.0x10^{-5}$	0.0017	13.6
Ccr7	Receptor for CCL19 and CCL21, expressed on T cells, B cells, and activated dendritic cells, involved with T cell homing to secondary lymphoid organs	1.35	$2.2x10^{-5}$	0.0018	52.2
Cd72	Expressed on B cells, mediates B/T cell interaction, negative regulator of B cell activation/response	1.34	$7.4x10^{-8}$	$1.9x10^{-5}$	129.2
Zeb1	Transcription factor, suppresses IL2 secretion by T cells, induces expression of BMP inhibitors	1.33	$4.7x10^{-5}$	0.0033	25.8
Cd53	Expressed on T cells and NK cells, role in growth regulation	1.32	$5.3x10^{-7}$	$8.9x10^{-5}$	229.2
Ighv3-6	Variable region of immunoglobulin heavy chain	1.32	$2.9x10^{-5}$	0.0022	82.4

Table 2.2: Inflammation-related genes that are significantly upregulated (with at least 2.5-fold change/1.32 Log_2 Fold change, $q<0.05$) in the sub-epithelial stroma of *Smad4*$^{\Delta Lrig1}$ versus SMAD4+ control mice. Genes listed in descending order of most to least upregulated. FDR = False discovery rate (q-value). Data generated from RNA-sequencing of the sub-epithelial stroma of three *Smad4*$^{\Delta Lrig1}$ and three SMAD4+ control mice. Mice were littermates and cage mates. Genotypes were split evenly between sexes.

An examination of Table 2.2 demonstrates a significant representation of B cell-related genes including B cell antigens (*Cd22, Ms4a1, CD79a, CD79b, Ly6d, Blk, Bank1, Cxcr5, Gpr183, Pax5, Cd19, Ikzf1, Ccr6, Cd37, Lax1, Tnfsf8, Ccr7, Cd72*), B cell transcription factors/transcriptional coactivators (*Ebf1, Pou2af1, Sfpi1. Ikzf3*), and immunoglobulins/immunoglobulin receptors (*Fcrl1, Faim3, Fcrla, Iglc2, Ighm, Igkv2-137, Igkv17-121, Iglv3, Ighv3-6*). There are also several upregulated genes that are known to play a role in recognition of microbes and pathogens (*Tlr9, Gp2, Pyhin1, Fcrla, Ly86*) as well as several genes with known roles in formation, function, and trafficking of lymphoid aggregates including intestinal Peyer's Patches (*Cd22, Gp2, Cxcl13, Cxcr5, Gpr183, Ccr6, Ccr7*).

For an unbiased approach, IPA analysis of our RNA-seq data was done to assess the gene expression changes in the sub-epithelial stroma in *Smad4*$^{\Delta Lrig1}$ mice versus control in the context of the biological system. This analysis demonstrated a significant increase in signaling pathways that relate to T cell activation/differentiation, B cell development/signaling, myeloid cell differentiation/proliferation/chemotaxis, and communication between the innate and adaptive immune systems. The top 15 most significantly changed canonical signaling pathways, as predicted by IPA analysis, are immune-related, including pathways related to Th1/Th2 signaling and activation, B cell development and signaling, leukocyte extravasation signaling, dendritic cell maturation, and more (**Figure 2.1**).

In order to predict how differences in immune cell composition may partially or fully explain these differences in bulk gene expression in the sub-epithelial stroma due to epithelial SMAD4 loss, we performed ImmuCC analysis using the above RNAseq data set. ImmuCC is an open access platform specialized in deconvolution of gene expression data to estimate the immune cell composition of a given mouse tissue sample (Chen et al., 2018). This analysis of our sub-epithelial stroma samples from three *Smad4*$^{\Delta Lrig1}$ and three SMAD4+ control mice is demonstrated in **Figure 2.2**. This analysis suggests a relative increase in B cells and $CD4^+$ T cells, and a relative decrease in $CD8^+$ T cells and monocytes in our *Smad4*$^{\Delta Lrig1}$ mice relative to controls.

Collectively, gene expression data from the sub-epithelial stroma of *Smad4*$^{\Delta Lrig1}$ and control mice suggest increased gene expression related to immune cell activation and signaling. Additionally, it appears that mice lacking intestinal epithelial SMAD4 expression have an increase in stromal B cell gene signature as well as increased expression of genes related to GALT trafficking and microbe recognition in the sub-epithelial colonic stroma, with deconvolution analysis predicting an increase in B cell/CD4^{+} T cell infiltration and decreased CD8^{+} T cell/monocyte infiltration in mice lacking epithelial SMAD4 expression.

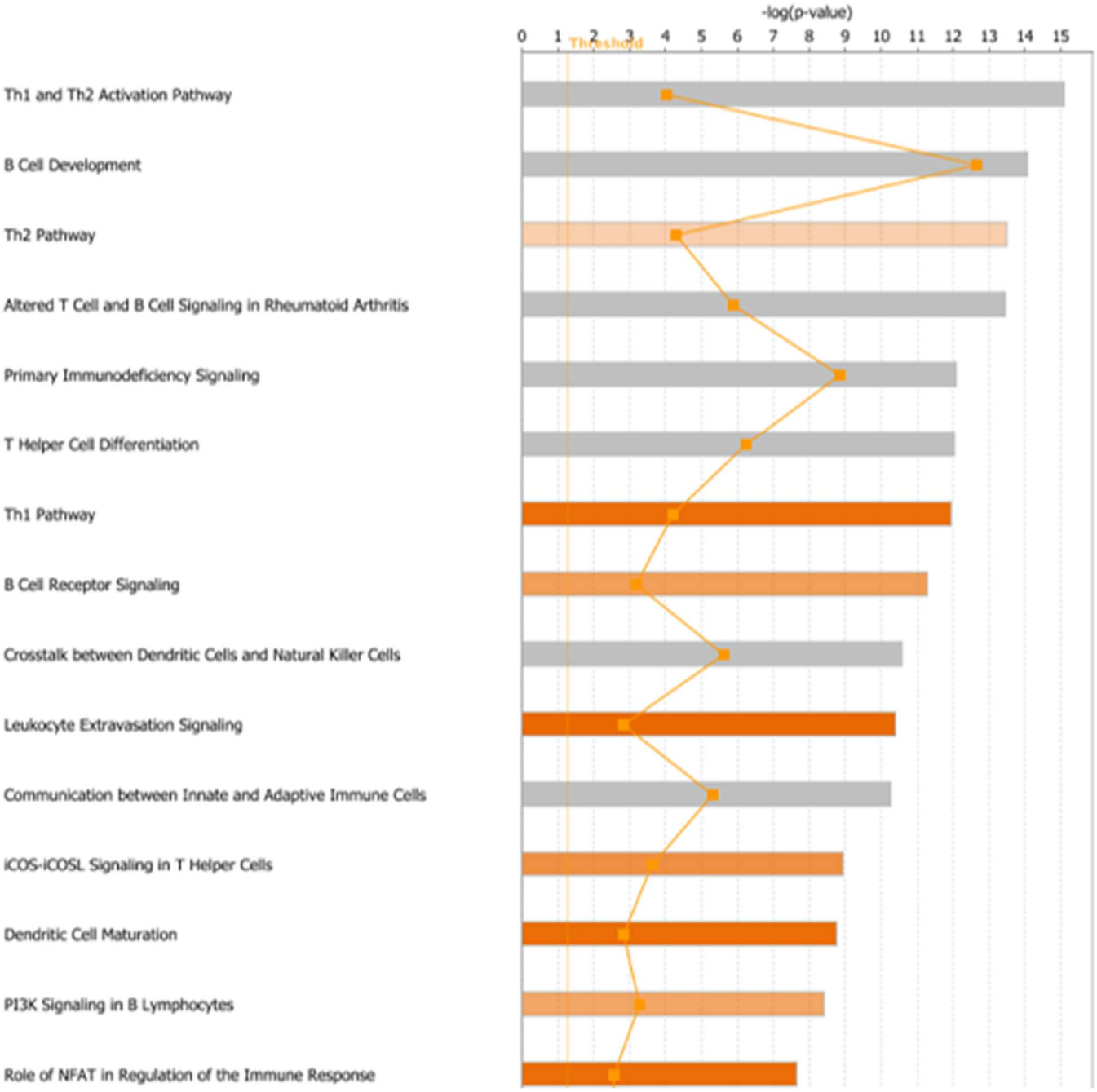

Figure 2.1 - Examination of the most differentially expression canonical signaling pathways in the sub-epithelial stroma of *Smad4*$^{\Delta Lrig1}$ mice relative to control by Ingenuity Pathway Analysis

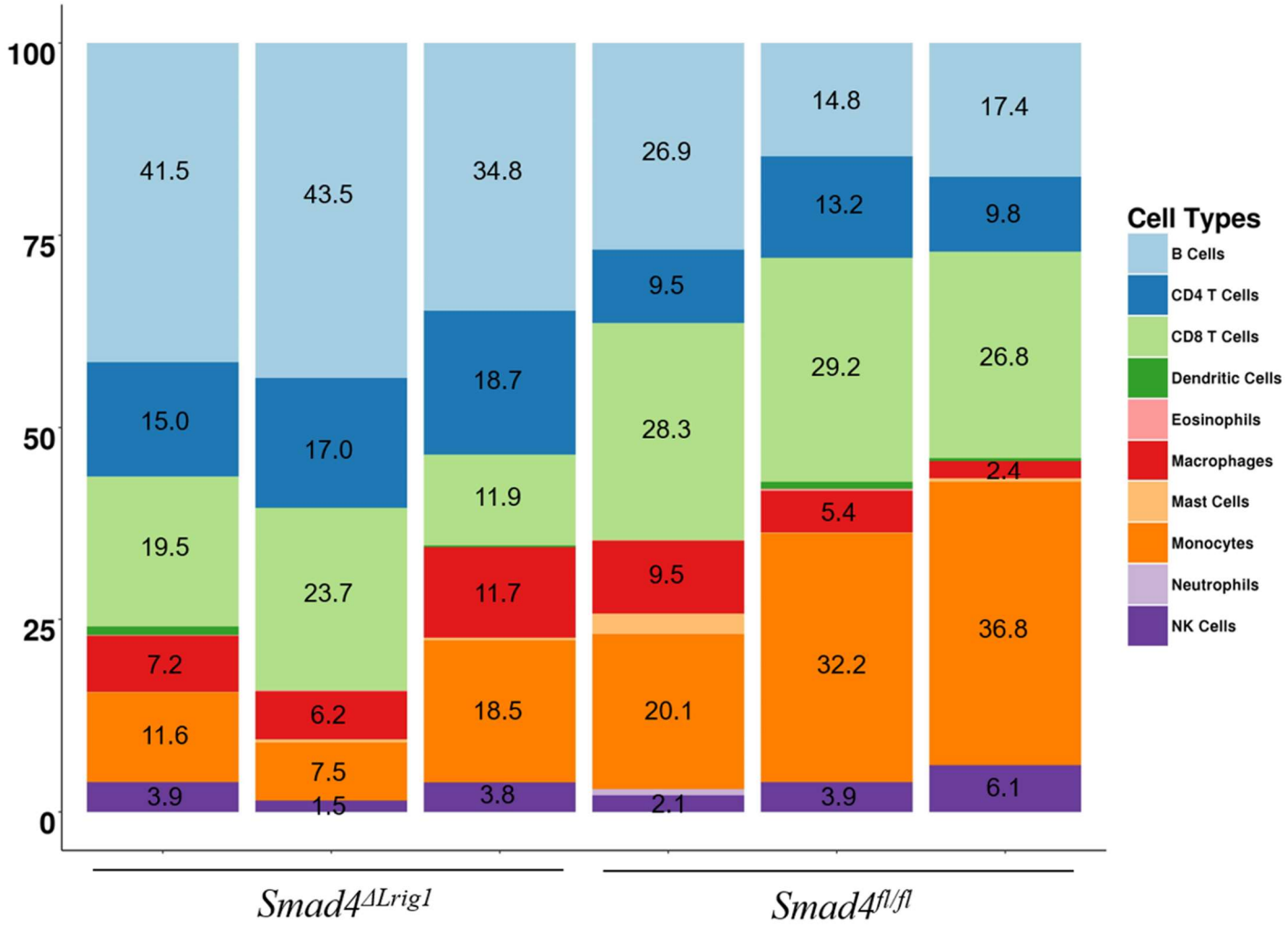

Figure 2.2 – Prediction of immune cell composition in the sub-epithelial stroma of three *Smad4*$^{\Delta Lrig1}$ mice versus three SMAD4+ control mice based on RNAseq data, analyzed using ImmuCC software. Numbers represent predicted proportion of each immune cell type.

The sub-epithelial stroma of Smad4$^{\Delta Lrig1}$ *mice demonstrate increased immune cell infiltration relative to SMAD4+ control mice*

To confirm our findings from the bulk RNAseq analysis just described, we performed flow cytometry of the lamina propria. This analysis enabled us to examine whether there is an alteration in immune cell infiltrate into the colonic lamina propria when epithelial SMAD4 is lost. We found that loss of epithelial SMAD4 in the intestinal epithelium led to an overall increase in leukocytes (CD45$^+$ cells) in the underlying stroma (**Figure 2.3a-b**). This overall 4-fold increase in leukocytes was reflected in significant increases in CD19$^+$ B cells, Gr-1^{high}/CD11b$^+$ neutrophils, Gr-1^{low}/CD11b$^+$ monocytes, GR-1$^-$/CD11b$^+$/F4/80$^-$ dendritic cells, and GR-1$^-$/CD11b$^+$/F4/80$^+$ macrophages (**Figure 2.3c**). When these cell populations were normalized to the total number of CD45$^+$ leukocytes, however, no disproportionate alteration in any one cell type was observed (**Figure 2.3d**), suggesting that the array of chemokines regulated by intestinal SMAD4 act broadly on many components of the immune microenvironment.

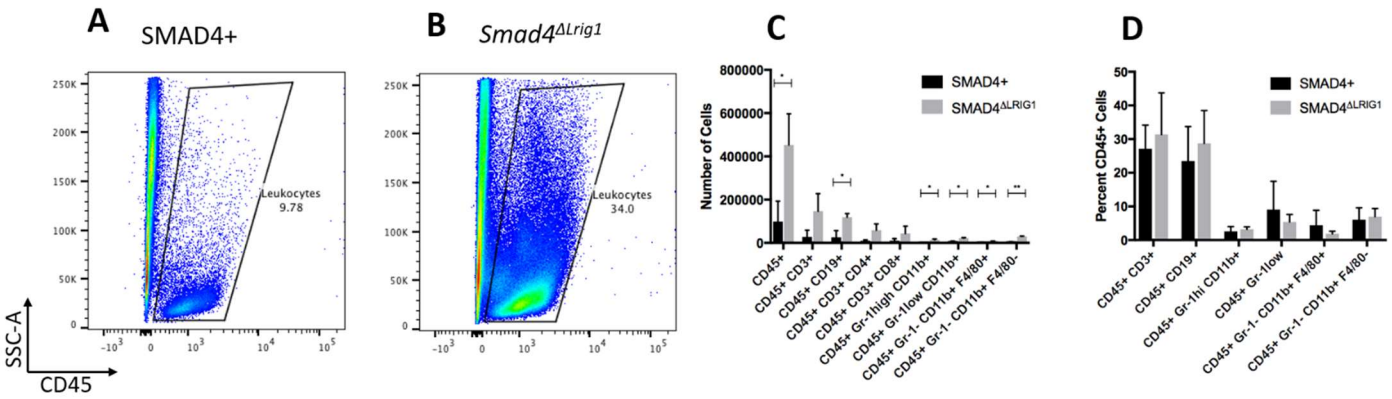

Figure 2.3 – Flow cytometry analysis comparing immune cell infiltration into the lamina propria of three *Smad4$^{\Delta Lrig1}$* mice to three SMAD4+ control mice. A) Representative flow graph for CD45+ cells (leukocytes) in SMAD4+ control mice. B) Representative flow graph for CD45+ cells in *Smad4$^{\Delta Lrig1}$* mice. C) Quantitative comparison of number of cells detected in each immune cell subset (identifying markers listed below graph on X axis) from three *Smad4$^{\Delta Lrig1}$* mice and three SMAD4+ control mice. D) Quantitative comparison of proportion of CD45+ cells detected from each immune cell subset (identifying markers listed below graph on X axis). Black bars represent mean/standard deviation of SMAD4+ control mice. Gray bars represent mean/standard deviation of *Smad4$^{\Delta Lrig1}$* mice.

Gut-associated lymphoid tissues (GALTs) are larger, but not more frequent, in Smad4$^{\Delta Lrig1}$ *versus SMAD4+ control mice*

The gut-associate lymphoid tissue aggregates (GALTs) of the colon are known to play an important role in immune cell trafficking and protection from microbial invasion (Rhee et al., 2005). In order to determine whether the increased inflammatory signaling and immune cell infiltration identified by RNA expression and immunophenotyping might be partially explained by alterations in number or size of GALTs, we performed H&E staining of formalin-fixed paraffin embedded (FFPE) colon sections from *Smad4$^{\Delta Lrig1}$* and *Smad4$^{+/+}$* mice (representative image, **Figure 2.4a**). Three sections were examined per mouse, each >1000µm apart. GALTs were counted and cross-sectional area was measured and normalized to whole tissue area. This analysis demonstrated no significant difference in number of GALTs in *Smad4$^{\Delta Lrig1}$* versus *Smad4$^{+/+}$* mouse colon

sections (17.2 vs 14.7, p=0.353 by Mann-Whitney test, **Figure 2.4b**). However, *Smad4*$^{\Delta Lrig1}$ mice did appear to have larger GALTs (as measured by normalized GALT area) compared to SMAD4+ control mice (1.22 vs 0.97, p=0.042 by Mann-Whitney test, **Figure 2.4c**).

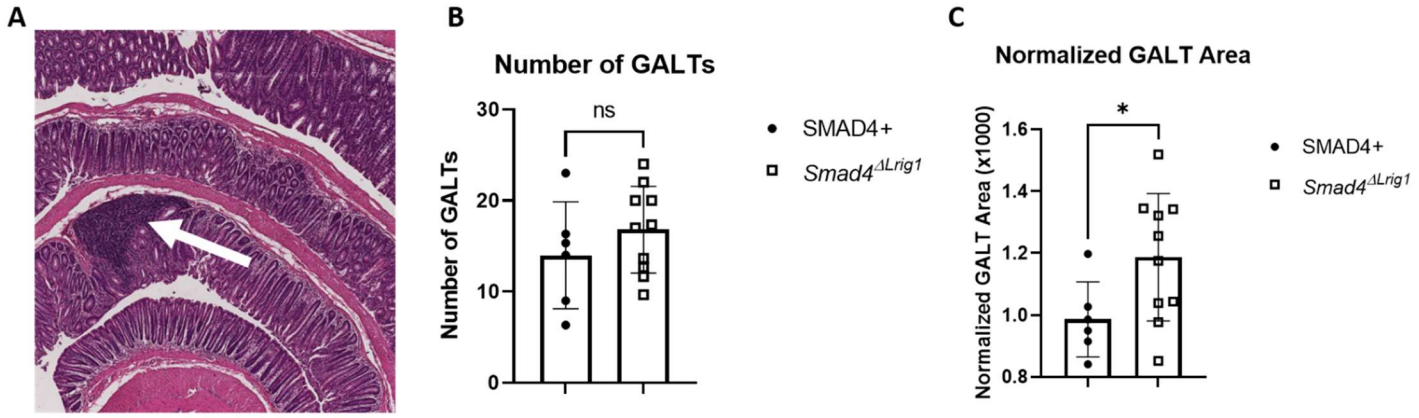

Figure 2.4 – Comparison of Gut-Associated Lymphoid Tissue (GALT) aggregates in *Smad4*$^{\Delta Lrig1}$ vs SMAD4+ control mice. A) Representative image of an H&E stain of mouse colon. White arrow indicates a GALT. B) Quantitative comparison of number of GALTs per mouse identified in *Smad4*$^{\Delta Lrig1}$ vs SMAD4+ control mice. C) Quantitative comparison of normalized GALT area (as calculated by measured surface area of GALT divided by measured total area of tissue visible on the examined section of mouse colon) in *Smad4*$^{\Delta Lrig1}$ vs SMAD4+ control mice.

Loss of SMAD4 from mouse colonoids in vitro *associated with increased expression of multiple chemokines and cytokines*

Our lab previously demonstrated that mouse intestinal SMAD4 loss (*Smad4*$^{\Delta Lrig1}$) had a significant up-regulation in multiple chemokines and cytokines in their colonic epithelium and that some of these cytokines (particularly *Ccl20*) were differentially regulated with TGFβ treatment and SMAD4 knockout in immortalized cell lines *in vivo*. To determine if these changes in chemokine/cytokine production occur in a cell-autonomous manner in a more relevant biological system, colon organoids (colonoids) were utilized. As described in detail in the methods section, above, colonic crypts from mice with genotype *Lrig*^{CreERT}*;Smad4*$^{fl/fl}$ were isolated and established as three-dimensional colonoids grown in Matrigel (Means et al., 2018). After a single, SMAD4-expressing, colonoid line was established, parallel colonoid lines were generated by other lab members by treatment with either 4OH-tamoxifen to stimulate Cre-recombinase activity and establish a SMAD4 knockout (KO) line or vehicle to maintain a SMAD4+ control line. SMAD4 KO and SMAD4+ control lines were then maintained in parallel and subsequently treated with TGFβ1/BMP2 or vehicle for 24 hours and RNA isolated for qPCR analysis.

As is consistent with previous work from our lab in 2-dimensional cell lines (Means et al., 2018), this analysis demonstrated a subset of the chemokines/cytokines that were upregulated with intestinal SMAD4 loss *in vivo* were also regulated by canonical TGFβ signaling *in vitro*. In particular, *Ccl20* expression was markedly suppressed with TGFβ/BMP treatment of SMAD4+ colonoids (Fold Change 0.07) relative to vehicle-treated controls ($p<0.001$). This TGFβ-responsiveness was lost with SMAD4 loss, as SMAD4 KO colonoids were unresponsive to TGFβ/BMP co-treatment. However, SMAD4 KO colonoids had significantly higher levels of *Ccl20* expression than SMAD4+ control colonoids following TGFβ pathway stimulation (p=0.03) (**Figure 2.5**).

The remainder of the chemokines/cytokines examined had mixed results. Unlike previously published results from our lab in 2-dimensional cell lines (Means et al., 2018), *Cxcl5* mRNA levels were not significantly changed with TGFβ pathway stimulation of SMAD4+ colonoids and SMAD4 KO did not significantly alter *Cxcl5* gene expression levels in the setting of TGFβ pathway stimulation. While *Il18* demonstrated some suppression in SMAD4+ control colonoids in response to TGFβ pathway stimulation, *Il18* mRNA expression levels did not significantly increase with SMAD4 loss *in vitro*, a finding that is consistent with previous findings from our lab using 2-dimensional cell lines (Means et al., 2018). Interestingly, *Il34* expression was significantly increased with TGFβ/BMP co-treatment relative of SMAD4+ colonoids relative to vehicle-treated controls, and *Il34* levels were decreased with SMAD4 KO. *Il1rn* was similarly decreased with SMAD4 KO *in vitro.* TGFβ-dependent regulation of *Il34* and *Il1rn* mRNA expression, therefore, appears to be the opposite of that observed with intestinal SMAD4 loss *in vivo*.

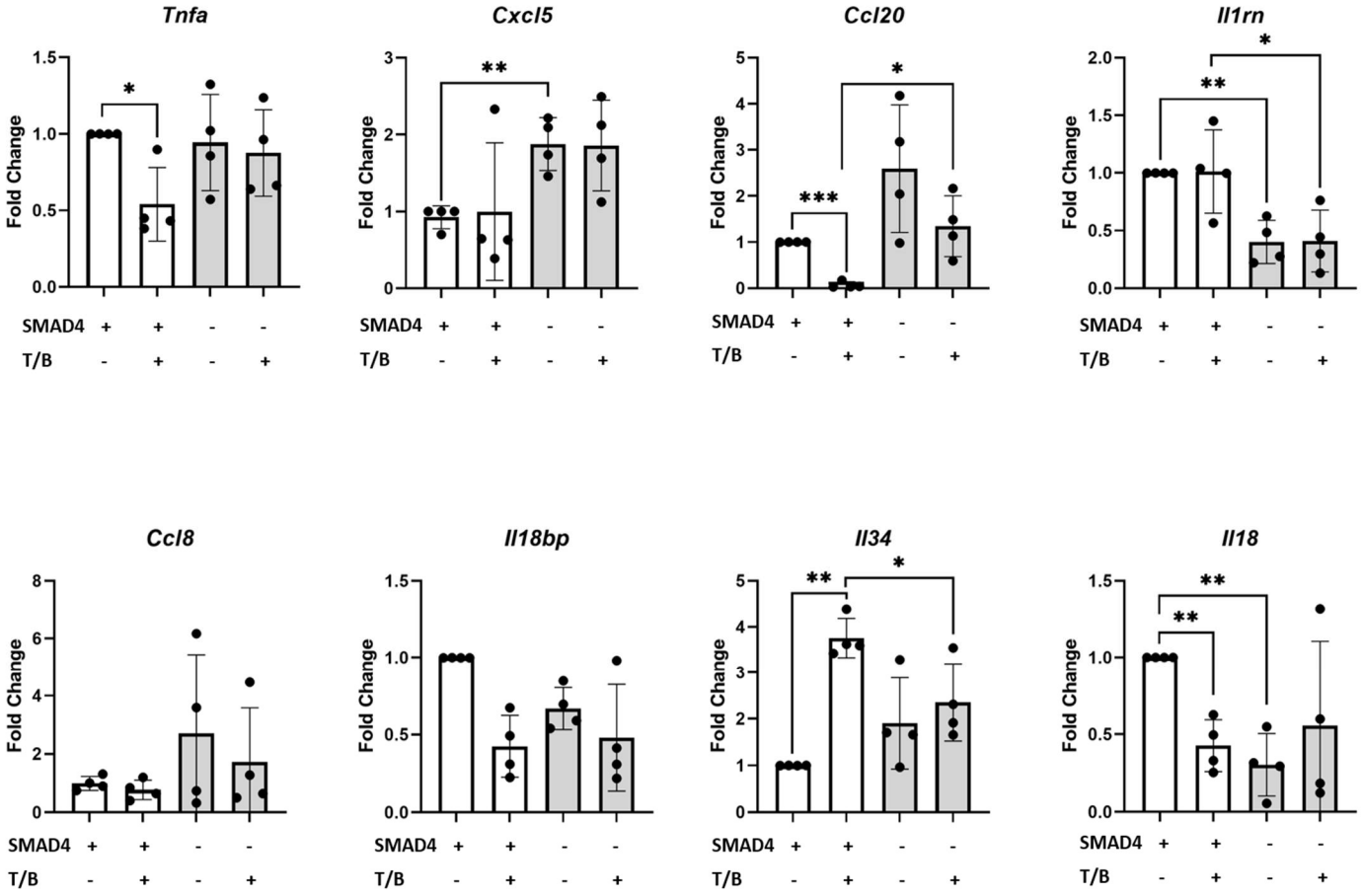

Figure 2.5 – qPCR examining gene expression from SMAD4 KO and SMAD4+ control colonoids treated with TGFβ1/BMP2 or vehicle control for 24 hours. White bars represent SMAD4+ control colonoids. Gray bars represent SMAD4 KO colonoids. Labels below X axis denote SMAD4 expression status and TGFβ/BMP treatment status. Gene expression is expressed as fold change relative to vehicle-treated SMAD4+ control colonoids. Expression levels compared 2-way ANOVA with post-hoc Welch's t test.

Collectively, these colonoid experiments are consistent with the cell culture experiments previously published by our lab (Means et al., 2018) and suggest that many of the chemokines/cytokines upregulated with epithelial SMAD4 loss *in vivo* are similarly upregulated with SMAD4 loss *in vitro*. *Ccl20* stands out as unique amongst the chemokines/cytokines examined as having been significantly changed with both TGFβ pathway stimulation and inhibition (SMAD4 loss) *in vitro*, indicating that the increased *Ccl20* mRNA expression associated with intestinal *Smad4* loss detected *in vivo* is likely the result of a cell-autonomous process.

The Ccl20/Ccr6 axis does not modulate the degree of DSS-induced chronic inflammation in the mouse colon by histologic examination

The above data demonstrate increased epithelial *Ccl20* expression (both *in vivo* and *in vitro*), increased stromal *Ccr6* gene expression, increased stromal immune cell infiltration, and increased GALT size in the colons of $Smad4^{\Delta Lrig1}$ mice relative to SMAD4+ control. We thus hypothesized that alterations in chemokine/cytokine signaling and immune cell recruitment/activation could be playing a role in SMAD4-dependent colitis-associated carcinogenesis. In particular, the *Ccl20/Ccr6* axis is of particular interest given our experimental findings together with the knowledge that *Ccl20/Ccr6* are known to be dysregulated in CRC and IBD (Comerford et al., 2010; Frick et al., 2013; Khor et al., 2011; McLean et al., 2011; Skovdahl et al., 2015; Zhang et al., 2012). To examine this possibility, we performed the following *in vivo* experiment.

$Smad4^{\Delta Lrig1}$ mice were crossed with mice that had *EGFP* knocked into the *Ccr6* gene. Representative images demonstrating confirmatory immunostaining for SMAD4 in SMAD4+/$Smad4^{\Delta Lrig1}$ mice and for GFP in $Ccr6^{+/+}$/$Ccr6^{EGFP/EGFP}$ mice (IHC staining for GPF performed by Dr. David Hanna) are shown in **Figure 2.6**. Importantly, $Ccr6^{EGFP/+}$ heterozygotes express CCR6 similarly to $Ccr6^{+/+}$ wild type control mice, while $Ccr6^{EGFP/EGFP}$ mice are null for CCR6 expression. Eight (8) $Smad4^{\Delta Lrig1}$ $Ccr6^{EGFP/+}$ mice, eleven (11) $Smad4^{\Delta Lrig1}$ $Ccr6^{EGFP/EGFP}$ mice, two (2) SMAD4+ $Ccr6^{EGFP/+}$ mice, and six (6) SMAD4+ $Ccr6^{EGFP/EGFP}$ mice were subjected to three rounds of DSS in drinking water to induce chronic colitis. Nine weeks following completion of DSS treatment, mice were dissected, and their colons preserved. Mouse colons were subsequently stained by H&E and examined histologically by Dr. Kay Washington, a consulting expert pathologist who was blinded to the mouse genotypes.

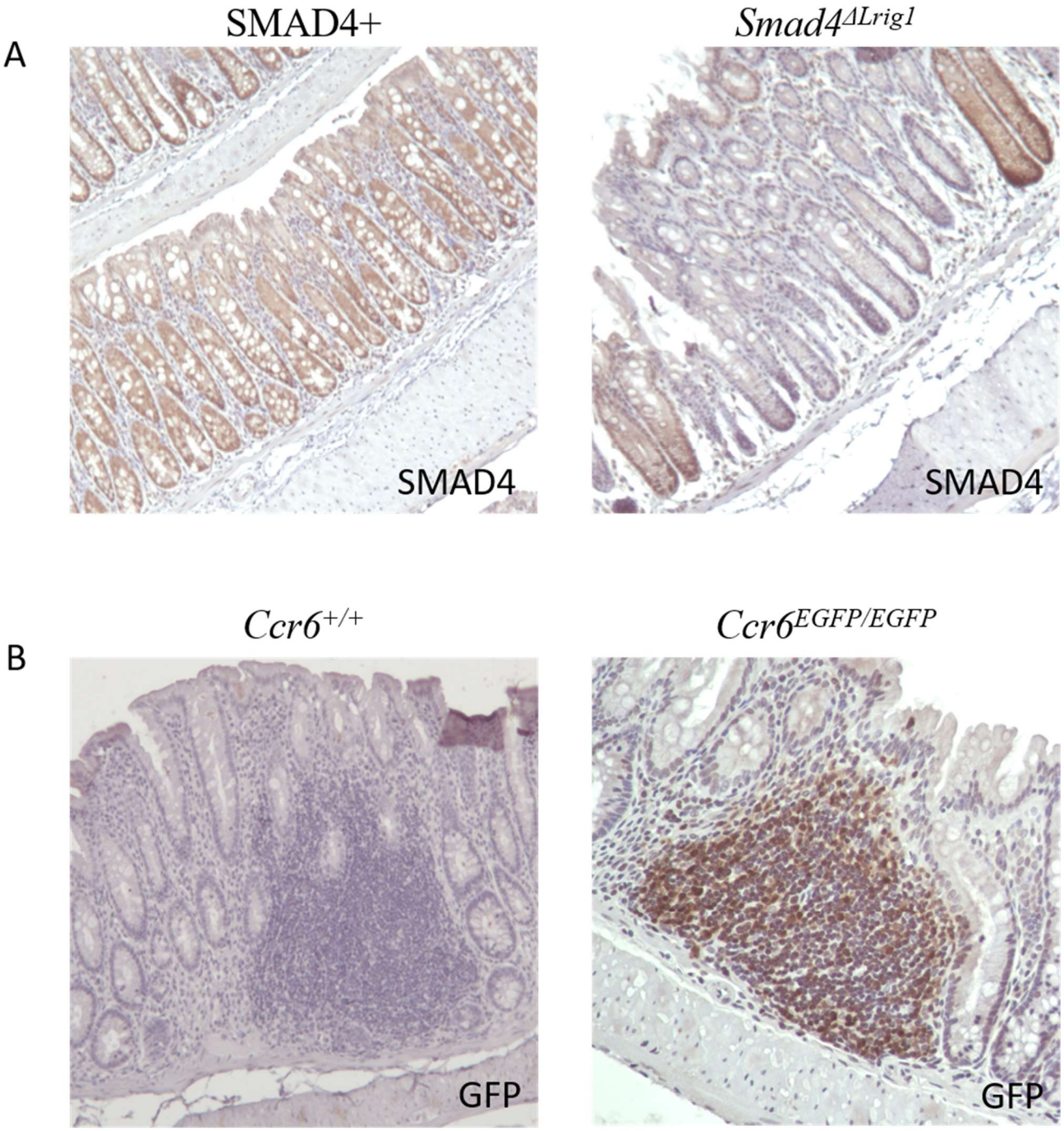

Figure 2.6 – Representative images of confirmatory immunostaining for SMAD4 (A) and GFP (B). (A) SMAD4 staining (brown) is evident in 100% of colon crypts in SMAD4+ control mice while SMAD4 staining is absent in >90% of colon crypts in *Smad4*$^{\Delta Lrig1}$ mice. (B) GFP staining (brown) is present in the lymphoid aggregates and in occasional intraepithelial cells of *Ccr6*$^{EGFP/EGFP}$ mice and absent from *Ccr6*$^{+/+}$ control mice.

Colon inflammation was scored by Dr. Washington in a manner previously published by Dieleman and colleagues (Dieleman et al., 1988). Briefly, each of the examined sections was given a numerical score in each of five categories: Inflammation (0-3), % involved by inflammation (0-4), depth of inflammation (0-3), crypt damage (1-4), and % involved by crypt damage (0-4). Amongst the *Smad4*$^{\Delta Lrig1}$ mice, there was no significant difference between *Ccr6* expressing and *Ccr6* null mice in any of these five categories. Among SMAD4+ control mice, *Ccr6* expression status similarly had minimal effect on degree of inflammation (**Table 2.3**). Interestingly, SMAD4+ mice (regardless of *Ccr6* expression) had higher average crypt damage scores than *Smad4*$^{\Delta Lrig1}$ mice (1.75 vs 0.47, $p<0.01$), but a trend towards smaller % of crypts involved by crypt damage (% Crypt Damage Score 0.00 vs 0.26, $p=0.285$).

Genotype	n	Inflammation (0-3)	% Inflammation (0-4)	Depth of Inflammation (0-3)	Crypt Damage (1-4)	% Crypt Damage (0-4)
Smad4$^{\Delta Lrig1}$ *Ccr6*$^{EGFP/+}$	8	1.38	2.25	1.63	0.5	1.5
Smad4$^{\Delta Lrig1}$ *Ccr6*$^{EGFP/EGFP}$	11	1.18	2.09	1.46	0.46	0.25
SMAD4+ *Ccr6*$^{EGFP/+}$	2	1.50	2.00	1.50	2.00	0.00
SMAD4+ *Ccr6*$^{EGFP/EGFP}$	6	1.50	1.17	1.67	1.67	0.00

Table 2.3: Numerical scoring for histologic grading of colitis. Eight (8) *Smad4*$^{\Delta Lrig1}$ *Ccr6*$^{EGFP/+}$ mice and eleven (11) *Smad4*$^{\Delta Lrig1}$ *Ccr6*$^{EGFP/EGFP}$ mice, two (2) SMAD4+ *Ccr6*$^{EGFP/+}$ mice, and six (6) SMAD4+ *Ccr6*$^{EGFP/EGFP}$ mice were subjected to three rounds of DSS in drinking water to induce chronic colitis. Three months following completion of DSS treatment, mice were dissected, and their colons preserved and examined by a consulting pathologist who was blinded to mouse genotype. Inflammation scoring(Dieleman et al., 1988) is as follows: Inflammation (0=none, 1=mild, 2=moderate, 3=severe); % involved by inflammation (0=focal/<10%, 1=10-25%, 2=>25-30%, 3=>50-75%, 4=>75%); Depth of inflammation (0=none, 1=mucosa, 2=submucosa, 3=transmural); Crypt damage (1=basal 1/3 damaged, 2=basal 2/3 damaged, 3=only surface intact, 4=entire crypt and surface lost); % involved by crypt damage (0=focal/<10%, 1=10-25%, 2=>25-30%, 3=>50-75%, 4=>75%). Numbers in the table represent mean scores for all mice of that genotype.

The Ccl20/Ccr6 axis plays a critical role in colitis-associated cancer due to intestinal SMAD4 loss

The same mice described above were examined from the presence/absence of invasive tumors by Dr. Washington who was blinded to the mouse genotypes. Eight of eight (100%) of *Smad4*$^{\Delta Lrig1}$ *Ccr6*$^{EGFP/+}$ mice have developed one or more invasive adenocarcinoma of the colon, consistent with prior observations from our group in *Smad4*$^{\Delta Lrig1}$ *Ccr6*$^{+/+}$ mice (Means et al., 2018). Representative images of invasive adenocarcinomas observed in *Smad4*$^{\Delta Lrig1}$ *Ccr6*$^{EGFP/+}$ mice are shown in **Figure 2.7**. Importantly, only two of eleven (18.2%) *Smad4*$^{\Delta Lrig1}$ *Ccr6*$^{EGFP/EGFP}$ mice developed invasive adenocarcinomas of the colon, demonstrating that loss of *Ccr6* expression is associated with a significant decrease in colitis-associated tumor development in *Smad4* null mice (100.0 vs 18.2%, $p<0.001$ by Fisher's Exact test). Loss of *Ccr6* expression was similarly associated with fewer invasive tumors, with *Smad4*$^{\Delta Lrig1}$ *Ccr6*$^{EGFP/+}$ mice developing an average of 1.50 invasive adenocarcinomas per mouse colon compared to 0.27 invasive adenocarcinomas per mouse colon in *Smad4*$^{\Delta Lrig1}$ *Ccr6*$^{EGFP/EGFP}$ mice ($p<0.001$ by Mann-Whitney test) (**Table 2.4**).

SMAD4+ control mice, by and large did not develop evidence of significant invasive cancers of the colon, as has been observed in previous experiments in our lab (Means et al., 2018). We did note, however, that

there was evidence of a single invasive crypt on a single section of one SMAD4+ *Ccr6*$^{EGFP/EGFP}$ mouse. This is consistent with prior observations from our group and others (Means et al., 2018; Okayasu et al., 2002), indicating that DSS-induced chronic colitis alone can occasionally induce colon tumorigenesis even in the presence of intact SMAD4 expression/TGFβ signaling and despite disruption of the *Ccl20/Ccr6.*

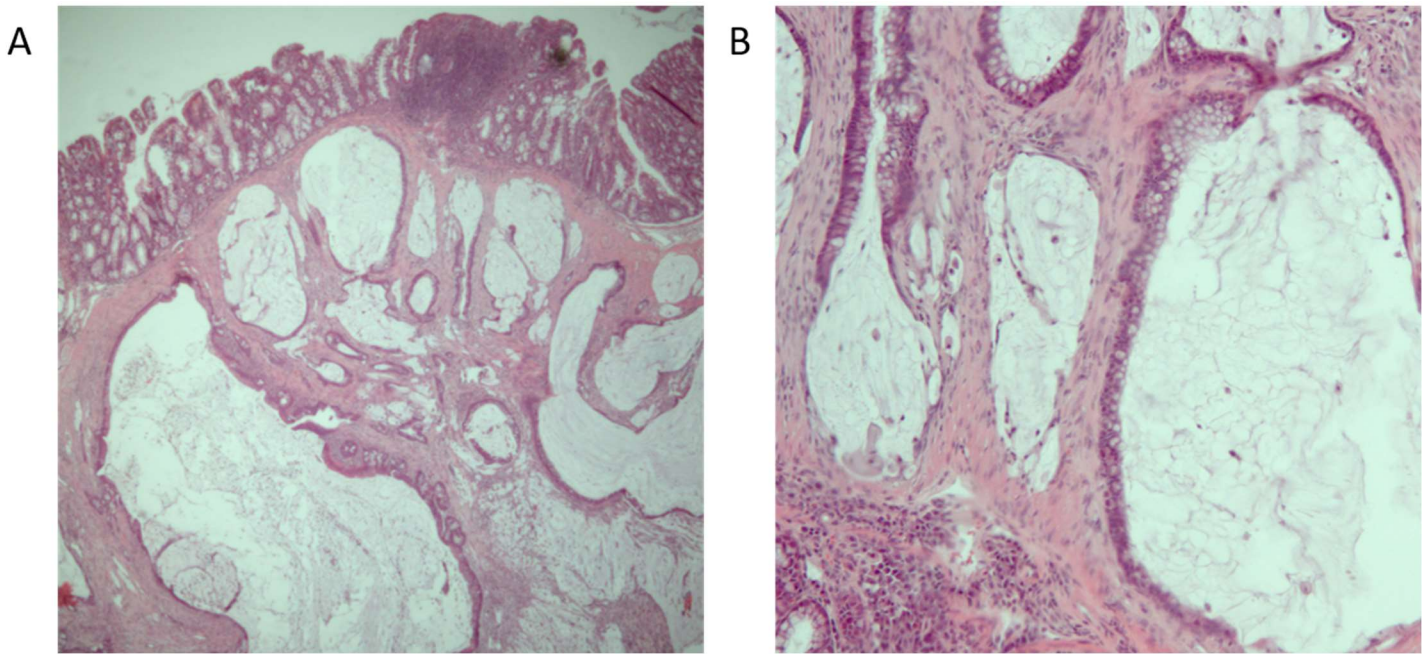

Figure 2.7 – Representative images demonstrating invasive, mucinous, adenocarcinoma of the distal colon in *Smad4*$^{\Delta Lrig1}$*Ccr6*$^{EGFP/+}$ mice 9 weeks after induction of DSS colitis. Images depict the same tumor imaged at 2.5x (A) and 10x (B).

Genotype	Total # of mice with invasive tumors	% mice with invasive tumors	Average # of invasive tumors per mouse
Smad4$^{\Delta Lrig1}$ *Ccr6*$^{EGFP/+}$	8 of 8	100%	1.50
Smad4$^{\Delta Lrig1}$ *Ccr6*$^{EGFP/EGFP}$	2 of 11	18.2%	0.27
SMAD4+ *Ccr6*$^{EGFP/+}$	0 of 2	0.0%	0.00
SMAD4+ *Ccr6*$^{EGFP/EGFP}$	1 of 6	16.7%	0.17

Table 2.4: Quantification of invasive adenocarcinomas in mice. Eight (8) *Smad4*$^{\Delta Lrig1}$ *Ccr6*$^{EGFP/+}$ mice, eleven (11) *Smad4*$^{\Delta Lrig1}$ *Ccr6*$^{EGFP/EGFP}$ mice, two (2) SMAD4+ *Ccr6*$^{EGFP/+}$ mice, and six (6) SMAD4+ *Ccr6*$^{EGFP/EGFP}$ mice were subjected to three rounds of DSS in drinking water to induce chronic colitis. 9 weeks following completion of DSS treatment, mice were dissected, and their colons preserved and examined by a consulting pathologist who was blinded to mouse genotype.

Discussion:

Multiple elements of the TGFβ pathway, including receptor mutations and loss of SMAD4 expression, have been previously implicated in multiple gastrointestinal pathologies including CRC and IBD. Previous attention has primarily focused on TGFβ's critical functions in maintenance of cell homeostasis including regulation of cell growth, cell cycle regulation, differentiation, and apoptosis, all of which are likely to play an important part in SMAD4's role as a tumor suppressor (Bardeesy et al., 2006; Freeman et al., 2012; Ikushima and Miyazono, 2010; Izeradjene et al., 2007; Li et al., 2003; Means et al., 2018; Principe et al., 2014; Qiao et al., 2006; Roberts and Wakefield, 2003; Takaku et al., 1998; Teng et al., 2006; Xu et al., 2000; Yang et al., 2005). Previous work from our lab and others, however, additionally demonstrates that canonical TGFβ signaling via SMAD4 in epithelial tissues plays a critical role in regulation of chemokine/cytokine expression (Grady et al., 1999; Inamoto et al., 2016; Itatani et al., 2013; Izeradjene et al., 2007; Kitamura et al., 2007; Li et al., 2006; Means et al., 2018; Yan et al., 2004). Thus, the immunoregulatory role of TGFβ/SMAD4 together with the findings presented in this chapter strongly suggest that SMAD4-dependent immunoregulation may be an important element of TGFβ's well-known function as a tumor suppressor.

However, we observed that not all chemokines/cytokines upregulated with SMAD4 loss *in vivo* are significantly modulated with TGFβ pathway stimulation or SMAD4 loss *in vitro.* Of the top chemokines/cytokines examined by qPCR *in vitro*, only *Ccl20* appears to be significantly regulated by canonical TGFβ signaling in a cell-autonomous manner. Interestingly, the CCL20/CCR6 chemokine/chemokine receptor axis is of particular clinical interest as it has been previously implicated in CRC and IBD (Frick et al., 2013; Khor et al., 2011; McLean et al., 2011).

Despite its association with IBD/CRC, until now, the CCL20/CCR6 axis had not been intimately connected to the tumor suppressor function of the TGFβ signaling pathway. Our findings suggest that, among other tumor-suppressing functions, canonical TGFβ signaling directly modulates the expression *Ccl20*, and that intestinal SMAD4 loss is associated with increased epithelial *Ccl20* expression, increased stromal immune cell infiltration, stromal inflammatory signaling, and stromal *Ccr6* expression. Further, we demonstrate that the *Ccl20/Ccr6* axis plays a significant role in susceptibility to colitis-associated carcinoma due to intestinal SMAD4 loss, as blocking the *Ccl20/Ccr6* axis greatly reduces colitis-associated tumor development in mice with intestinal SMAD4 loss. Taken together, these findings suggest that the tumor suppressor role of TGFβ via SMAD4 involves regulation of inflammatory pathways, including the *Ccl20/Ccr6* axis.

There are many elements of this work that remains to be explored. First and foremost, the entirety of function of the CCL20/CCR6 axis in the context of intestinal SMAD4 loss remains to be discovered. A well-known chemokine, CCL20 is likely to significantly alter immune cell recruitment into the sub-epithelial stroma. While we have evidence for increased leukocyte infiltration generally (as evidenced by increased CD45+ leukocyte infiltration into the sub-epithelial stroma by flow cytometry), our flow cytometry analysis has thus far not been sufficiently comprehensive to examine all of the immune cell subsets of interest (including Th17 cells, Tregs, and dendritic cell subsets). Several immunophenotyping experiments remain ongoing in our lab and will shed light on which cell types are disproportionally recruited to the sub-epithelial stroma in mice lacking intestinal SMAD4 expression. Such analyses are likely to provide clues as to how the *Ccl20/Ccr6* axis is contributing to colitis-associated tumorigenesis.

We additionally observed that *Smad4*$^{\Delta Lrig1}$ mice have larger GALTs than their SMAD4+ counterparts. This is supported by our flow cytometry and RNA-seq data, which demonstrate evidence of increased B cell infiltration and increased gene expression related to B cell signaling in our *Smad4*$^{\Delta Lrig1}$ mice compared to control. This is consistent with increased GALT size, as GALTs are heavily composed of B cells (Mörbe et al., 2021). Additionally, several of the upregulated genes in the stroma of *Smad4*$^{\Delta Lrig1}$ mice (including *Cd22, Cxcl13, Cxcr5, Gpr183, Ccr7,* and others) have a known role in homing to secondary lymphoid aggregates,

such as GALTs in the colon and Peyer's Patches in the small intestine. Interestingly, GALTs have a critical role in mucosal immunity, serving as major trafficking centers for bacterial sampling and pathogen-directed immune response. In addition, several of the stromal genes up-regulated with intestinal SMAD4 loss have a role in pathogen sampling and M cell function. M cells are specialized cells of the small and large intestine that overly GALTs/Peyer's Patches and play a critical role in initiating mucosal immune response by transporting pathogens and bacterial antigens to the underlying lymphoid tissue aggregate (GALT). Collectively, these data suggest that in addition to a global increase in immune activation and signaling, there appears to be a B cell/GALT/M cell-specific signature that may suggest increased exposure to luminal antigens. This possibility will be explored further in Chapter IV.

Overall, these data indicate that loss of canonical TGFβ signaling within the intestinal epithelium, something that occurs frequently in IBD and CRC, results in increased chemokine/cytokine expression in the colonic epithelial compartment as well as increased inflammation (increased inflammatory signaling and increased immune cell infiltration) in the sub-epithelial stroma. Amongst the various chemokine/cytokines upregulated with SMAD4 loss is *Ccl20*, and the CCL20/CCR6 appears to play a significant role in colitis-associated tumorigenesis due to SMAD4 loss. Additionally, increased GALT size and increased gene expression related to pathogen recognition and sampling, paired with the finding that several of the chemokines/cytokines upregulated with SMAD4 loss *in vivo* are not significantly altered with TGFβ treatment or SMAD4 loss *in vitro*, suggests that increased luminal antigen exposure, perhaps through a mucosal barrier defect, could be contributing to the inflammatory phenotype observed in $Smad4^{\Delta Lrig1}$ mice.

CHAPTER III

INTRODUCTION 2 – JUNCTIONAL COMPLEXES, BARRIER FUNCTION, and TGFβ SIGNALING

Junctional Protein Complexes in Epithelial Tissues

Epithelial tissues form the outer layer of the body as well as line the internal surface of the alimentary (gastrointestinal) tract and other hollow cavities including the respiratory tract. Epithelia play a critical role in protecting the body from the hostile external environment while simultaneously playing an important role in both secretion and absorption of physiologically critical materials. The protein complexes that make up the cell-cell junctions in epithelial tissues and their role in governing epithelial barrier function and in disease are well established and have been reviewed many times previously (Bhat et al., 2019; France and Turner, 2017; Krug et al., 2014; McGuckin et al., 2009; Shen et al., 2011; Singh et al., 2010; Zeisel et al., 2019). A brief description of the salient points critical to understanding the implications of this dissertation are included herein.

Epithelial cells are tethered together into functional sheets by the epithelial junctional complex (EJC) which is made up of three primary components: tight junctions (TJ), adherens junctions (AJ), and desmosomes (**Figure 3.1**). TJs are the apical-most junctions of the EJC, occurring on the most apical aspect of the lateral cell membrane. TJs are protein complexes made up of multiple transmembrane proteins, including Claudins, Occludin, Tricellulin, and Junction Adhesion Molecules (JAMs). Tethered to the cytoplasmic domain of these transmembrane proteins are additional TJ-associated proteins which including Zonula Occludens (ZO)-1, -2, and -3, which assist in anchoring the transmembrane components to the underlying actin cytoskeleton. The transmembrane components of the TJ interact directly with similar molecules on neighboring cells, creating a tight seal of the intercellular space and allowing TJs to perform their primary function of regulating paracellular permeability (France and Turner, 2017; Krug et al., 2014; Shen et al., 2011; Tsukita et al., 2018).

Importantly, while TJs exist in all epithelial tissues, level of paracellular permeability governed by these junctional complexes is highly variable between tissue types. For instance, while the proximal tubule of the kidney is highly permeable to multiple anions and cations, the collecting duct is nearly impermeable to solutes and allows passage of H_20 only. This variability in permeability between tissue types is, in large part, dependent upon the expression patterns of Claudin proteins (Günzel and Yu, 2013; Shen et al., 2011). The Claudin family of proteins (including at least 26 members in humans) are tetra-spanning membrane proteins with two extracellular loops (Günzel and Yu, 2013). Most Claudin proteins can be categorized as either “closed” or “selectively permeable” based on their structure. While the Claudins share a common motif in their C-terminal region, the first extracellular loop contains variable amino acid sequences, and it is this region that confers the various Claudin proteins unique characteristics that determine their paracellular tightness as well as selectivity for ion permeability. For instance, Claudin 2 is a well-known “pore forming” claudin that supports permeability to both anions and water. As a result, high Claudin 2 protein expression is associated with increased paracellular permeability (Luettig et al., 2015; Raju et al., 2020; Randall et al., 2016; Rosenthal et al., 2010). On the other hand, Claudin 7 is a “closed” or “barrier forming” Claudin that is responsible for more tightly sealing the intercellular space and protection from paracellular solute and ion flux (Xu et al., 2019). As a result of their unique characteristics, the expression pattern and combination of various Claudin proteins within the TJs of different tissues has a large impact on tissue permeability. Partially as a result of variable Claudin protein expression, different epithelial types have unique functional characteristics (Günzel and Yu, 2013). In addition to modulating permeability, TJs have the additional important role of modulating cell polarity, as the TJ marks the border separating the apical and basolateral cell surfaces (Balda and Matter, 2014; Farkas et al., 2012; Singh et al., 2017; Zihni et al., 2014).

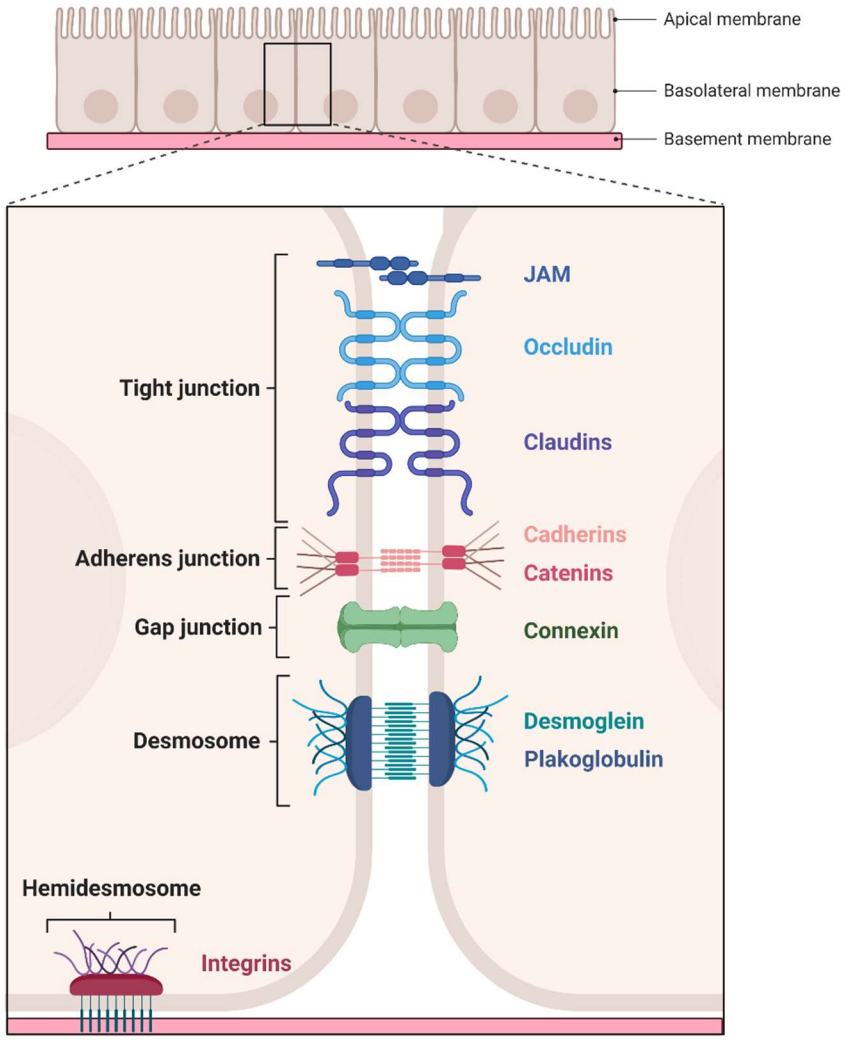

Figure 3.1 – Graphical depiction of major junctional complexes in epithelial tissues with their predominant protein components. Figure generated using Biorender.com.

Just basal to the TJs are the AJs. AJs are composed of transmembrane Cadherins as well as cytosolic components vinculin, p120/catenin, α-, β-, and γ-catenin. The AJ is responsible for anchoring neighboring epithelial cells to one another while conferring mechanical strength to the tissue. In epithelial tissues, AJs form a continuous adhesion belt (also known as the Zonula Adherens) just below the level of the TJs, where each interacting cell in the epithelial sheet is completely encircled by the adhesion belt. In these AJs, transmembrane Cadherin proteins from adjacent cells form homodimers while maintaining anchorage, via the Catenin proteins and Vinculin, to a contractile bundle of intracellular actin filaments that lies within the cytoplasm just parallel to the plasma membrane. The result is that the underlying intracellular actin bundles are linked to an extensive multi-cellular network, giving epithelial tissues rigidity and, with the assistance of myosin motor proteins, allowing epithelia to form physiologically critical secondary structures (Harris and Tepass, 2010). Importantly, there is additionally ample evidence to suggest that most Cadherin-binding proteins can translocate to the nucleus and regulate transcription, suggesting that AJs have an important role not only in regulating tissue rigidity but also in intracellular signaling cascades (McEwen et al., 2012).

Desmosomes, like AJs, play an important role in providing mechanical strength to epithelial layers. Rather than being organized into bands, desmosomes form "button-like" intercellular connections, serving as an anchor for intermediate filaments which are critical for providing organized tissues with tensile strength. Via their desmosomal connections, the intermediate filaments run from membrane to membrane, linking adjacent cells into a net-like complex. Desmosomes are composed of a dense intracellular plaque, which includes intracellular proteins (plakoglobulin and desmoplakin) that anchor the adhesion proteins to the cytoplasmic intermediate filaments, as well as a transmembrane component composed of Cadherin adhesion proteins (desmoglein and desmocollin), which interact with their counterparts on adjacent cells to form homodimers and hold the intercellular complex together. The type of intermediate filaments is variable between tissue types, but in most epithelial tissues they are made of keratin filaments (Garrod and Chidgey, 2008; Johnson et al., 2014).

Additional junction protein complexes, including gap junctions (which directly connect the cytoplasm of two cells, allowing rapid propagation of inter-cellular signaling), focal adhesion hemidesmosomes (which function to attach epithelial cells to their extracellular matrix), and non-classical junctions (including selectins, Ig-superfamily Cell Adhesion Molecules [CAMs], and integrins) play important roles in cell-cell adhesion but are beyond the scope of this introductory review chapter.

Junctional Protein Complexes in Endothelial Tissues

While epithelial tissues line body cavities and surfaces, endothelium is the single layer of cells that line the interior surface of blood and lymph vessels. Of mesodermal origin, the endothelium plays an important role in forming a semi-permeable barrier between vessels and tissues, controlling the flow of fluid, nutrients, and other molecules into and out of our vital organs.

While epithelial cells are critically tethered with the three components of the EJC, endothelial cells lack desmosomes. Junctional complexes that mediate cell-to-cell adhesion in endothelial cells include TJs and AJs only. Endothelial cells additionally contain gap junctions that support cell-to-cell communication. Another critical difference between epithelial and endothelial tissues is that, while epithelial cells maintain a well-organized system of junctional protein expression and localization (with TJs concentrated at the apical rim and AJs occur below), the junctional organization of endothelial cells is less well defined, and TJs and AJs are intermingled along the lateral cell membrane (Bazzoni and Dejana, 2004; Morita et al., 1999; Sukriti et al., 2014).

Despite slight differences in their expression patterns, localization, and organization, the endothelial junctional complexes, like their counterparts in epithelial tissues, also play important roles in mediating tissue rigidity, permeability, and homeostasis. While epithelial tissues are tasked with protecting our bodies from external pathogens, endothelial cells have the important job of regulating the permeability of plasma solutes and mediating leukocyte extravasation at sites of inflammation. Like epithelial tissues, the character and function of endothelial tissues varies dramatically depending on its location and function (Komarova et al., 2017). For example, in the brain where strict control of solute and fluid permeability is required to maintain constant intracranial pressures and neural signaling, endothelial cells are "well sealed" with relatively high expression of TJs. On the other hand, the endothelium of the glomerulus of the kidney is highly specialized in fluid filtration and junctional protein expression supports "leakiness" to fluids and solutes. As with epithelial tissues, the heterogeneity in junctional protein expression patterns enables endothelium to support the unique needs of their associated organ system (Bazzoni and Dejana, 2004; Hernandez et al., 2012; Morita et al., 1999; Sukriti et al., 2014).

Barrier Dysfunction in Human Disease

Epithelial barriers are tasked with separating self from non-self. As such, epithelial barrier dysfunction can lead to increased exposure to foreign antigens, stimulating an inflammatory host response. As a result, and not surprisingly, epithelial barrier dysfunction is linked to multiple human pathologies including Acute Respiratory Distress Syndrome (ARDS) and inflammatory bowel disease (IBD).

ARDS is a syndrome of acute respiratory failure due to noncardiac pulmonary edema (fluid filling the terminal air spaces of the lungs, known as alveoli) and is believed to be the result, in part, of dysregulated pulmonary inflammation as well as epithelial and endothelial permeability (Huppert et al., 2019; Thompson et al., 2017). The pathophysiology of ARDS and its relationship to barrier dysfunction have been reviewed previously (Huppert et al., 2019; Matthay et al., 2019; Thompson et al., 2017). In brief, ARDS is believed to be initiated by an acute insult such as infection, trauma, or otherwise. Foreign antigens (including microbial byproducts) or cell injury-associated endogenous molecules bind to Toll-like receptors (TLRs) on lung epithelium or alveolar macrophages, activating the innate immune response and generating reactive oxygen species, chemokines, and cytokines, and resulting in inflammation and causing tissue injury. This inflammation leads to disruption of the endothelial junctional complexes (through destabilization of Vascular Endothelial Cadherin [VE-cadherin], among other things) (Broermann et al., 2011; Corada et al., 1999; Huppert et al., 2019; Schulte et al., 2011; Vestweber, 2007), leading to leakage of protein-rich fluid, leukocytes, and inflammatory mediators across the alveolar wall into the terminal air spaces. In turn, the epithelial lining, which is classically much less permeable than the previously mentioned endothelial layer, can undergo apoptosis and subsequently erosion/sloughing (Thompson et al., 2017), leading to the formation of large gaps in the epithelial lining and further breakdown of alveolar barrier function (Ginzberg et al., 2004; Huppert et al., 2019; Zemans and Matthay, 2004). In addition to alveolar cell death and tissue sloughing, dysfunction of intercellular TJs, including due to dysregulated levels of Claudin proteins, has been linked to increased paracellular permeability and pulmonary edema in human disease specimens and in animal models (Overgaard et al., 2012). In this way, dysregulated inflammation causes barrier dysfunction and barrier dysfunction perpetuates inflammation, leading to a dire respiratory pathology that is unfortunately lethal in many cases (McNicholas et al., 2018).

Like ARDS in the lungs, IBD is an inflammatory condition of the intestine that has been intimately associated with epithelial barrier dysfunction. While the pathophysiology of IBD is very complex with multiple genetic, environmental, and microbial factors likely contributing, its primary manifestation is chronic relapsing inflammation of the gastrointestinal tract, resulting in abdominal pain, diarrhea with or without blood, malabsorption, as well as abscesses, fistulas, and strictures (Glassner et al., 2020; Guan, 2019; Martini et al., 2017; McGuckin et al., 2009; Munkholm et al., 1994; Vancamelbeke et al., 2017). There has long been recognition, however, that barrier dysfunction is likely to play a central role in the pathophysiology of IBD. One of the first studies pointing to diminished barrier integrity as an important risk factor for the development of IBD was published by Hollander and colleagues in 1986. This group administered polyethylene glycol-400 by ingestion with a standard meal to 11 Crohn's Disease (CD) patients along with 32 of their healthy (clinically unaffected) first-degree relatives and 17 normal healthy volunteer controls and found that both CD patients and their healthy relatives had a roughly 2-fold increase in permeability to polyethylene glycol-400 compared to healthy non-relative controls (Hollander et al., 1986). Several other studies subsequently had similar findings suggesting abnormal barrier function in first-degree relatives in CD patients relative to healthy unrelated controls (Fries et al., 2005; May et al., 1993; Peeters et al., 1997). While the previously mentioned studies failed to follow these relatives with abnormal intestinal permeability over time, one case report observed that a woman who had been enrolled in a cross-sectional cohort study of intestinal permeability at age 13 (while she was asymptomatic with no macroscopic or microscopic evidence of IBD but was found to have elevated gut permeability) was subsequently diagnosed with ileocolic CD at age 21, suggesting that at least in one case, an intestinal permeability defect preceded onset of IBD (Irvine and Marshall, 2000). Additional evidence by Vivinus-Nebot and colleagues found that patients with quiescent IBD had significantly higher intestinal permeability (along with lower expression level of ZO-1 and α-catenin and increased levels of intraepithelial lymphocytes and TNFα) relative to healthy controls in colonic mucosal biopsy samples, suggesting subclinical inflammation and barrier dysfunction persist between clinical relapses in IBD patients (Vivinus-Nébot et al.,

2014). Collectively, these data suggest that intestinal barrier dysfunction may precede inflammatory symptoms in at least a subset of IBD patients. Additional evidence in both humans and animals specifically points towards junctional protein dysregulation as a contributing factor in IBD. For example, *in vivo* studies have demonstrated that intestinal Claudin 7 deletion initiates colonic inflammation, destruction of the mucosal barrier, and even early death in mice (Tanaka et al., 2015; Xu et al., 2019). A similar study examining the intestinal mucosa of JAM-A knockout mice showed that loss of JAM-A expression led to increased intestinal inflammation (including increased polymorphonuclear leukocyte infiltrate and larger lymphoid aggregates), increased mucosal permeability to macromolecules *in vivo*, and decreased transepithelial resistance (TER) *ex vivo* (Laukoetter et al., 2007). Collectively, these data and others suggest that dysregulation of critical TJ-related proteins directly contributes to intestinal inflammation in animal models, supporting a causative role of barrier function in IBD. Studies of intestinal biopsy specimens in humans have additionally tied Claudin expression level changes and/or distribution to IBD (Lameris et al., 2012; Zeissig et al., 2007), further supporting this hypothesis.

Both ARDS and IBD are examples of human pathologies that result, at least in part, from the deleterious effects of epithelial and endothelial barrier dysfunction. In both cases, inflammatory processes are intimately associated with barrier dysregulation which in turn appears to contribute to increased inflammation. Inflammation and barrier dysfunction are intimately related and likely act synergistically to contribute to human disease.

TGFβ and Barrier Function

Several studies have examined the effect of TGFβ family signaling on barrier function over the past 20-30 years, as summarized in **Table 3.1**. The most well-studied organ systems include the pulmonary endothelium, the ocular vasculature, and the intestinal tract (primarily the jejunum). The findings from these published studies are diverse and are generally supportive of the notion that the effects of TGFβ signaling are highly tissue- and context-dependent.

In the pulmonary vascular endothelium and alveolar epithelium, TGFβ signaling is felt to be largely deleterious for barrier integrity. Evidence for this comes from several studies. In the early 2000s, a small number of early observational studies from human patients suggested a relationship between TGFβ and ARDS, a pathology characterized by leakiness of the lining of the lungs, causing impaired gas exchange and respiratory failure. Fahy and colleagues, for instance, detected elevated levels of TGFβ1 in the broncho-alveolar lavage samples of patients with ARDS compared to healthy controls, suggesting an association between TGFβ1 and pulmonary barrier dysfunction and inflammation (Fahy et al., 2003). Laun and colleagues similarly observed that higher serum TGFβ1 levels were associated with sepsis and ARDS in patients hospitalized following severe trauma (Laun et al., 2003). Several studies followed which leveraged human and bovine cell lines to examine the impact of TGFβ signaling on barrier function *in vitro*. In one study, TGFβ treatment of bovine pulmonary artery endothelial cells (BPAECs) decreased TER, induced paracellular gap formation, and loss of cell-cell contact (Birukova et al., 2005a). A second study confirmed that TGFβ treatment of BPAECs *in vitro* decreased TER and implicated Alk5/Smad4 signaling (Birukova et al., 2005b). Additional experiments examined the effects of TGFβ1 on calf pulmonary artery endothelial cell (CCL-209) monolayers and found that TGFβ1 caused increased permeability, increased stress fiber formation, formation of intracellular gaps, and AJ disassembly and implicated non-canonical (SMAD-independent) pathways (Clements et al., 2005; Goldberg et al., 2002; Hurst et al., 1999). Another group also performed primary culture of rat alveolar epithelial type II (ATII) monolayers and found that TGFβ decreased TER of ATII cells *in vitro* (Pittet et al., 2001).

In the ocular vasculature, we see mixed evidence suggesting that TGFβ signaling has both pro- and anti-barrier functions. In one *in vivo* study, mice were subjected to systemic TGFβ inhibition which demonstrated

increased retinal permeability to macromolecular FITC-dextran, decreased TJ protein (Occludin and ZO-1) association, and decreased TJ formation between retinal microvascular endothelial cells, and that *in vivo* treatment with TGFβ of primary endothelial cells enhanced cell-cell association and increased Occludin/ZO-1 interaction (Walshe et al., 2009). However, a study examining bovine retinal endothelial cells (BRECs) demonstrated increased MMP9 expression with TGFβ treatment, that either MMP9 or TGFβ treatment increased BREC permeability, decreased Occludin expression, and that anti-TGFβ and anti-MMP9 antibodies could block these effects (Behzadian et al., 2001).

In the small intestine, TGFβ appears to contribute to a barrier preservation phenotype. In one *in vivo* study, pigs were treated with either Lipopolysaccharide (LPS), LPS + Anemonin, or vehicle control. Anemonin was found to increase the expression of TGFβ1 expression levels as well as the expression of multiple TGFβ-response genes, and was also observed to increased jejunal villus height, decrease crypt depth, increase TER, and decrease permeability to 4kD FITC-Dextran compared to the LPS-alone group. The LPS + Aneomonin-treated group was additionally observed to have increased Claudin 1, Occludin, and ZO-1 expression compared to the LPS treated group (Xiao et al., 2016). Subsequent *in vitro* experiments in jejunal (IEC-6) and colon cancer (T84, HT29) cell lines demonstrated that TGFβ signaling enhances wound restitution (Dignass and Podolsky, 1993), blocked cytokine- and pathogen-induced barrier dysfunction (McKay and Singh, 1997; Planchon et al., 1994, 1999; Roche et al., 2000), increased TER (Hering et al., 2011; Howe et al., 2002, 2005; Planchon et al., 1994), and augmented the expression of TJ-related proteins (Hering et al., 2011; Howe et al., 2005) in a manner both dependent on- and independent of-SMAD proteins (Hering et al., 2011; Howe et al., 2002, 2005).

TGFβ and Epithelial-to-Mesenchymal Transition (EMT)

EMT in epithelial cancers is another domain of human pathology where dysregulation of junctional proteins plays a critical role. EMT has been reviewed extensively in the past by multiple authors (Dongre and Weinberg, 2019; Ribatti et al., 2020), and thus we will discuss only briefly the most salient points here as they relate to junctional protein dysregulation. EMT is the process by which epithelial cells lose their epithelial character through a series of programmed gene expression changes in favor of acquiring cell characteristics more consistent with a mesenchymal phenotype, including loss of polarity/expression of epithelial-specific markers (such as E-Cadherin) and acquisition of a spindle-shape/expression of mesenchymal markers (such as N-Cadherin)/ability to migrate. This transcriptional program is often reversible, is the result of EMT-inducing transcription factors (EMT-TFs, including SNAIL, SLUG, ZEB1, ZEB2, and TWIST), and is a critical physiologic process in embryogenesis/tissue morphogenesis as well as in adults during wound healing. In addition to these physiologic settings, however, EMT is felt to be a central process in the invasion-metastasis cascade in human epithelial cancers (carcinomas). In essence, the process by which a primary tumor cell is able to migrate to a distant site and spawn a macroscopic metastasis requires the activation of EMT programs, and thus EMT is a necessary step for progression to metastatic carcinoma. While the EMT-TFs regulate the transcription of hundreds of genes simultaneously and thus impart many biological traits that are essential to the malignant progression of cancer, there is ample evidence that these EMT-TFs negatively regulate the expression of multiple epithelial junctional proteins including E-Cadherin, Epithelial cell adhesion molecules (EpCAM), Occludin, Claudins, αβ integrins, and more. SNAIL and ZEB1, for example, directly repress the expression of *Chd1* (which encodes the protein for E-Cadherin) as well as multiple proteins involved in regulating TJ formation. Loss of junctional protein expression and the concomitant loss of apical-basal polarity due to loss of TJ assembly subsequently plays a central role in the malignant progression of carcinoma (Aigner et al., 2007; Batlle et al., 2000; Cano et al., 2000; Dongre and Weinberg, 2019; Kojima et al., 2007; Ribatti et al., 2020; Sánchez-Tilló et al., 2010; Spaderna et al., 2008; Yang et al., 2010b).

TGFβ has been widely implicated in the process of EMT, both in health and disease (Xu et al., 2009). TGFβ has been demonstrated to induce the transcription of multiple EMT-TFs, including SNAIL, SLUG, ZEB1, and TWIST, which in turn suppress critical epithelial adhesion molecules including E-Cadherin. Interestingly, EMT-TFs subsequently upregulate TGFβ family ligand expression, establishing a positive feedback loop via autocrine signaling, enabling cells to maintain expression of EMT transcriptional programs once these programs have been initiated (Dhasarathy et al., 2011; Dongre and Weinberg, 2019; Grande et al., 2015). TGFβ controls the expression of EMT-TFs via several mechanisms, including direct SMAD complex binding to promoter/enhancer regions (Dhasarathy et al., 2011; Grande et al., 2015), post-translational modifications (Gudey et al., 2017; Ye and Weinberg, 2017), and regulation of non-coding RNA expression (Grelet et al., 2017a, 2017b; Richards et al., 2015; Schmitz et al., 2016). The propensity of the data suggests that TGFβ signaling thus negatively regulates epithelial cell adhesion through dysregulation of junctional complexes and initiation of other pro-EMT cell processes, thus pushing epithelial cells towards an invasive, mesenchymal phenotype, in certain physiologic and pathologic settings.

Tissue Type	**Effect of TGFβ on Barrier Function**	**Model System**	**Primary Assay(s) & Pertinent Findings**	**Implicated Pathways or Pathway Components**	**Reference**
Pulmonary	↓	Human umbilical vein endothelial cells	TGFβ1 treatment decreases TER *in vitro*	p38 induction/RhoA activation via Smad2	(Lu et al., 2006a)
	↓	Human BAL samples	TGFβ1 elevated in ARDS patients BAL samples compared to controls	-	(Fahy et al., 2003)
	=	Mice transfected with human IL-1β transgene	IL-1β expressing mice had increased inflammation, increased BAL cellularity, and increased TGFβ in BAL fluid	-	(Kolb et al., 2001)
	=	β6 KO mice	β6 KO and control mice treated with bleomycin, 53 TGFβ-inducible genes up-regulated in the lung tissue of control mice (who get fibrosis) compared to β6 KO mice (who are protected)	-	(Kaminski et al., 2000)
	↓	Integrin αvβ6 KO mice, primary culture of rat alveolar epithelial type II (ATII) cell monolayers *in vitro*	KO mice protected from bleomycin-induced lung injury (permeability and extra-vascular water content); inhibition of TGFβ protects WT mice from bleomycin or E Coli-induced pulmonary edema; TGFβ decreased TER of ATII cells *in vitro*	-	(Pittet et al., 2001)
	↓	Bovine pulmonary artery endothelial cells (BPAECs)	TGFβ treatment: decreases TER, induces paracellular gap formation, disappearance of F-actin cortical ring, increased actin stress fiber formation, loss of cell-call contacts, dissolution of microtubules	Crosstalk between microtubule dynamics and TGFβ-dependent Rho activity	(Birukova et al., 2005a)
	↓	Bovine pulmonary artery endothelial cells (BPAECs)	TGFβ treatment: decreases TER, induces stress fiber formation and phosphorylation of myosin light chains and myosin-specific phosphatase. Can all be blocked by inhibition of Alk5/Smad4 (but not Alk1)	Alk5/Smad4 signaling	(Birukova et al., 2005b)

	↓	Bovine pulmonary artery endothelial cells (BPAECs)		RhoA/Rho-kinase pathway & RhoA-independent pathways	(Clements et al., 2005)
	↓	Calf pulmonary artery endothelial cells (CCL-209)	TGFβ1-induced permeability of CCL-209 cells, myosin light chain phosphorylation, peripheral band of actin, increased stress fiber formation, and formation of intercellular gaps all blocked by p38 MAPK inhibition	p38 MAPK activation by TGFβ1 increased myosin light chain phosphorylation	(Goldberg et al., 2002)
	↓	Calf pulmonary artery endothelial cells (CCL-209)	Immunofluorescence staining for adherens junction proteins after TGFβ treatment of CPAECs demonstrates that adherens junction disassembly occurs after cell separation during TGFβ1-induced pulmonary endothelial monolayer dysfunction	Myosin light chain kinase-dependent signaling cascade	(Hurst et al., 1999)
	↓	Serum samples from human trauma patients	Higher serum TGFβ1 levels associated sepsis and possibly ARDS	-	(Laun et al., 2003)
Ocular Vasculature	↑	*In Vivo*: systemic inhibition of TGFβ in mice; *In vitro*: primary endothelial cells (ECs) and 10T1/2 cells (murine embryonic mesenchymal cell line)	TGFβ inhibition *in vivo* decreases retinal perfusion, impairs peripheral vascular autoregulation, increased retinal permeability to FITC-D, decreased Occludin and ZO-1 association, and structural alteration in tight junctions between microvascular cells; TGFβ treatment *in vitro* enhanced association between adjacent ECs and increased Occludin and ZO-1 interaction	Tight junction protein (Occludin & ZO-1) association	(Walshe et al., 2009)
	↑	Corneal Endothelial Cells (CECs)	TGFβ1 treatment improved endothelial phenotype of confluent CECs; improved localization of ZO-1 and increased expression of N-Cadherin	ZO-1 localization and N-Cadherin expression	(Leclerc et al., 2018)
	↓	Bovine retinal endothelial cells (BRECs)	BRECs express MMP9 when treated with TGFβ or co-cultured with TGFβ-expressing glial cells; both MMP9 and TGFβ increase BREC permeability and reduce occluding expression; TGFβ-induced permeability effect blocked by anti-TGFβ and anti-MMP9 antibodies	TGFβ-induced MMP9 expression; reduced Occludin expression	(Behzadian et al., 2001)
Vas Deferens	↓	Porcine vas deferens epithelial (VDE) cells	TGFβ1 treatment of VDE cell *in vitro* causes 70-99% decrease in TER and decrease in anion secretory response to Forskolin	Re-distribution of Occludin and Claudin 7	(Pierucci-Alves et al., 2012)
Nasal Epithelium	=	Human nasal epithelial cells transfected with hTERT	TGFβ treatment *in vitro* led to increased Claudin 4 expression (no change in Claudin 1, Claudin 7, Occludin, JAM-A, or E-Cadherin). No change in TER.	Increased Claudin 4 expression	(Kurose et al., 2007)
Liver	↓	Rat hepatocytes	TGFβ treatment *in vitro* caused increased Occludin and Claudin 2 expression, decreased Claudin 1 expression, decreased tight junction strands by freeze fracture microscopy, F-actin disorganization	Increased Occludin and Claudin 2, decreased Claudin 1	(Kojima et al., 2007)
Intestinal Tract	↑	IPEC-J2 (jejunal)	Pre-treatment with TGFβ1 blocked decrease in TER/increased permeability to 4kD FITC-D due to TNFα treatment	ZO-1 and Occludin	(Xiao et al., 2017)

	↑	*In vivo:* 18 pigs treated with LPS, LPS + anemonin, or control	Anemonin increased villus height, increased TER, decreased crypt depth, and decreased 4kD FITC-D permeability compared to LPA alone group; increased Claudin 1, Occludin, and ZO-1 expression compared to LPS-only group	Claudin 1,Occludin, and ZO-1	(Xiao et al., 2016)
	↑	*In vivo*: piglets killed at 0-, 3-, 7-, and 14-days post-weaning	Occludin, Claudin 1, and ZO-1 levels were decreased in jejunum of piglets post-weaning (compared to pre-weaning); Increased TGFβ1 levels post-weaning as well (but normal levels of TGFβRs, Smads)	-	(Xiao et al., 2014)
	↑	IEC-6 cells	TGFα, EGF, IL1β, and IFNγ all enhanced wound restitution *in vitro* and increased production of TGFβ1 ligand. Clocking TGFβ1 with neutralizing antibody blocked promotion of restitution by these cytokines	TGFα, EGF, IL1β, and IFNγ promote intestinal restitution after injury via increasing TGFβ1 production	(Dignass and Podolsky, 1993)
	↑	T84 cells	Co-culture of T84 cells with immune cells demonstrated 70% drop in TER and increased permeability to mannitol; addition of specific cytokine-blocking antibodies (anti- IFNγ, TNFα) blocked these effects; Addition of TGFβ2 partially prevented barrier dysfunction due to immune cell co-culture in a dose-dependent manner	-	(McKay and Singh, 1997)
	↑	T84 cells	Pre-treatment or co-treatment with TGFβ1 diminished capacity of co-cultured LPMCs to disrupt epithelial barrier (measured by TER)	-	(Planchon et al., 1999)
	↑	T84 cells	Pre-treatment with TGFβ1 blocked cryptosporidium parvum-induced barrier dysfunction (measured by TER)	-	(Roche et al., 2000)
	↑	T84 cells	TGFβ1 treatment increases TER of T84 cell monolayer; increased Claudin 1 expression by qPCR (no change by IF); Pre-treatment with TGFβ1 blocked decrease in TER and increase in permeability to tagged mannitol due to EHEC infection	Claudin 1 expression, ERK/MAPK and SMAD2/3 signaling	(Howe et al., 2005)
	↑	T84 cells; HT29 cells	TGFβ treatment has no impact on *Isc* in Ussing chambers but caused decreased Cl^- secretion due to Forskolin, VIP, and cholera toxin; Pre-treatment with p38 MAPK inhibitor decreased effect of TGFβ on Cl^- secretion; TGFβ treatment caused 3x increase in TER *in vitro*	p38 MAPK pathway	(Howe et al., 2002)
	↑	T84 cells	TGFβ treatment increases TER and barrier integrity to macromolecules, and significantly reduces capacity of IFNγ and cryptosporidium parvum infection to disrupt epithelial barrier	-	(Planchon et al., 1994)
	↑	HT-29/B6 cells	TGFβ and TGFβ-containing whey protein treatment of HT-20/B6 cells leads to increased Claudin 4 promoter activity and increased Claudin 4 expression; TGFβ or	Claudin 4 regulation, both SMAD4 dependent and	(Hering et al., 2011)

			whey protein treatment could block IFNγ-induced barrier dysfunction (measured by TER and permeability)	SMAD4 independent pathways	
Fibroblasts	=	WI-38 human lung fibroblasts	TGFβ1 treatment causes increased expression of the α1, α2, α5, and β1 integrin subunits as well as increased assembly into their αβ complexes and exposure on cell surface	Induction of integrin subunits involved with mediating cell adhesion to ECM	(Heino et al., 1989)
	=	Multiple cell lines	TGFβ increases expression of fibronectin and collagen and incorporation of fibronectin/collagen into the ECM	-	(Ignotz and Massague, 1986)
EMT	↓	MCF-7 breast cancer cell line	Inhibition of TGFβ signaling pathway following SNAIL or SLUG addition to MCF-7 cells resulted in decreased cell migration with no impact on cell junction complex (Claudin) repression by SNAIL/SLUG	SNAIL/SLUG expression causes increased histone acetylation at promoter region of *TGFBR2)*	(Dhasarathy et al., 2011)
	↓	Prostate, Lung, and Breast cancer cell lines	TGFβ activates EMT by SNAIL1 activation	TGFβ stimulates SNAIL1 sumoylation lysine residue 234, which confers it transcriptionally active	(Gudey et al., 2017)
	↓	NMuMG epithelial cell line	TGFβ increases expression of multiple long noncoding RNAs (LncRNAs), and a subset of these LncRNAs mediate TGFβ induced cell migration, invasion, and EMT (including tight junction dissolution). Elevation of this subset of LncRNAs associated with increased invasiveness of human breast cancer cell lines	E-cadherin identified as major target of LncRNAs	(Richards et al., 2015)
	↓	Primary culture of adult rat hepatocytes	TGFβ induced EMT, increased expression of SNAIL, down-regulated E-cadherin and Claudin 1, and disruption of "fence function" as measured by fluorescent molecule diffusion. TGFβ-dependent "Fence function" disruption blocks by TGFβ inhibitors	-	(Kojima et al., 2007)

Table 3.1 – Table summarizing previously published literature examining the effect of TGFβ signaling on barrier function. EMT = Epithelial-to-mesenchymal transition.

Conclusions and Unanswered Questions

From the data reviewed here, it is clear that tightly controlled junctional protein expression is critical for maintaining tissue homeostasis and that alterations in junctional complex expression or localization can have deleterious effects on tissue function and, ultimately, health. What is furthermore becoming apparent is that TGFβ signaling, well-established to play a central role in cell growth, proliferation, differentiation, and apoptosis, additionally appears to modulate the expression of critical junctional protein-related genes.

Due to the tissue- and context-dependent nature of TGFβ signaling, as well as the diverse impact of TGFβ signaling on multiple critical cellular processes, much remains to be discovered about TGFβ signaling, barrier function, and how TGFβ dysregulation impinges on barrier function in the context of human disease. One particular challenge in regard to more completely understanding the relationship between TGFβ signaling and barrier dysfunction in human disease lies in the highly context-dependent nature of TGFβ signaling and the need for more biologically relevant model systems. While many areas of basic science rely on cancer or

transformed/immortalized cell lines to study gene regulation *in vitro*, these model systems are highly flawed, particularly when examining cell adhesion processes. Specifically, few cell lines that grow on plastic form normal tight junction/cell adhesion complexes or polarize as normal tissues do *in vivo*, making it difficult to study the regulation of cell adhesion complexes in these model systems. For this reason, there is a significant need for more biologically relevant model systems when examining epithelial barrier function. This could take the form of carefully designed *in vivo* and *ex vivo* studies that utilize macromolecular permeability assays or Ussing chambers to examine the impact of targeted genetic changes on epithelial permeability and ion transport. Alternatively, more modern *in vitro* assays, including three dimensional organoids, whereby epithelial cells are grown in a three-dimensional matrix and form normal cell adhesion complexes and secondary structures, can be leveraged. A combination of these *in vivo* and *in vitro* strategies may provide more biologically relevant information in regard to junctional protein regulation in epithelial tissues.

Another important area for future research includes the interplay between inflammation and barrier function. As was reviewed in Chapter I, there is ample evidence that TGFβ signaling directly regulates the expression of multiple pro-inflammatory chemokines and cytokines (Marincola-Smith et al., 2019; Means et al., 2018). At the same time, cytokines are known to have a profound effect on junctional protein expression and epithelial integrity (Amoozadeh et al., 2015; Capaldo and Nusrat, 2009; Mazzon and Cuzzocrea, 2007; Watson et al., 2005). However, impaired epithelial integrity may in and of itself predispose to inflammation by allowing increased flux of bacterial organisms or bacterial-derived antigens across mucosal linings, exposing epithelial and stromal cells to foreign antigens which in turn stimulate inflammation. Evidence for this exists in the fact that impaired barrier function has been observed in healthy first-degree relatives of patients with IBD, and increased permeability has been detected in the intestines of IBD patients prior to clinical flares (Lameris et al., 2012; Martini et al., 2017; Munkholm et al., 1994; Vivinus-Nébot et al., 2014). While the truth is likely complex (with inflammation leading to barrier dysfunction and barrier dysfunction reciprocally perpetuating inflammation), future studies should leverage *in vitro* assays to tease out cause and effect. Such insight will enable improved understanding of the root cause of inflammatory disorders and potentially direct translational research in the field.

Much remains to be discovered as it relates to TGFβ signaling and epithelial barrier function. As presented in this chapter, the effect of TGFβ signaling on barrier integrity appears to be highly tissue- and context-dependent, with TGFβ diminishing barrier function/promoting dissolution of epithelial adhesion and polarization in some contexts while enhancing barrier function in others. In order to gain a better understanding of how TGFβ signaling contributes to barrier function (or dysfunction) in any given tissue or in the context of human disease process, investigators must leverage biologically relevant model systems. Barrier dysfunction and TGFβ pathway signaling defects have both been separately implicated in the pathophysiology of IBD separately, but little research has been done to investigate a causal link between the two. Studies that have relied on 2-dimensional jejunal and colon cancer cell lines may or may not be representative of TGFβ's true effect on junctional protein expression or barrier function *in vivo*, and further investigation is required to understand this relationship in the context of human disease.

CHAPTER IV

This chapter is adapted from "Colon epithelial cell TGFβ signaling modulates the expression of tight junction proteins and barrier function in mice" published in *American Journal of Physiology – Gastrointestinal and Liver Physiology* and has been reproduced with the permission of the publisher and my co-authors, Yash A Choksi, Nicholas O Markham, David N. Hanna, Jinghuan Zi, Connie J Weaver, Jalal A Hamaamen, Keeli B Lewis, Jing Yang, Qi Liu, Izumi Kaji, Anna L. Means, and R. Daniel Beauchamp.
Reference: P Marincola Smith, et al. Colon epithelial cell TGFβ signaling modulates the expression of tight junction proteins and barrier function in mice. *American Journal of Physiology – Gastrointestinal and Liver Physiology*. 2021. Online ahead of print.

TGFβ/SMAD4 MODULATES THE EXPRESSION OF CRITICAL JUNCTIONAL PROTEINS AND BARRIER FUNCTION IN MOUSE COLON

Abstract:
Background: Defective barrier function is a predisposing factor in inflammatory bowel disease (IBD) and colitis-associated cancer (CAC). While TGFβ signaling defects have been associated with IBD and CAC, few studies have examined the relationship between TGFβ and intestinal barrier function. Here, we examine the role of TGFβ signaling via SMAD4 in modulation of colon barrier function.
Methods: The *Smad4* gene was conditionally deleted in the intestines of adult mice and intestinal permeability assessed using an *in vivo* 4kD FITC-Dextran (FD4) permeability assay. Mouse colon was isolated for gene expression (RNA-sequencing), western blot, and immunofluorescence analysis. *In vitro* colon organoid culture was utilized to assess junction-related gene expression by qPCR and trans-epithelial resistance (TER). *In silico* analyses of human IBD and colon cancer databases were performed.
Results: Mice lacking intestinal expression of *Smad4* demonstrate increased colonic permeability to FD4 without gross mucosal damage. mRNA/protein expression analyses demonstrate significant increases in *Cldn2*/Claudin 2 and *Cldn8*/Claudin 8, and decreases in *Cldn3*, *Cldn4*, and *Cldn7*/Claudin 7 with intestinal SMAD4 loss *in vivo* without changes in Claudin protein localization. TGFβ1/BMP2 treatment of polarized SMAD4+ colonoids increases TER. *Cldn2, Cldn4, Cldn7,* and *Cldn8* are regulated by canonical TGFβ signaling, and TGFβ-dependent regulation of these genes is dependent on nascent RNA transcription (*Cldn2, Cldn4, Cldn8*) but not nascent protein translation (*Cldn4*, *Cldn8*). Human IBD/colon cancer specimens demonstrate decreased *SMAD4, CLDN4, CLDN7,* and *CLDN8* and increased *CLDN2* compared to healthy controls.
Conclusion: Canonical TGFβ signaling modulates the expression of tight junction proteins and barrier function in mouse colon.

Background:

While the pathophysiology of Inflammatory Bowel Disease (IBD) and Colitis-Associated Cancer (CAC) is multifactorial, there is increasing evidence that defective intestinal barrier function plays a role (Allaire et al., 2011; Laukoetter et al., 2007; Martini et al., 2017; McGuckin et al., 2009; Sluis et al., 2006; Söderholm et al., 1999; Vancamelbeke et al., 2017; Wehkamp et al., 2008). At the same time, the TGFβ signaling pathway is known to be frequently altered in IBD (Allaire et al., 2011; Babyatsky et al., 1996; Monteleone et al., 2001, 2015; Sedda et al., 2015), sporadic colorectal cancer (CRC) (Alazzouzi et al., 2005), and CAC (Allaire et al., 2011; Means et al., 2018). Although the TGFβ signaling pathway has been implicated in the modulation of endothelial and epithelial barrier function previously, the impact of this signaling on maintaining or, conversely, degrading barrier integrity is widely variable between tissue types and contexts. For example, TGFβ is a potent inhibitor of barrier integrity in pulmonary endothelium (Birukova et al., 2005a; Goldberg et al., 2002; Hurst et

al., 1999; Pittet et al., 2001) and esophageal epithelium (Nguyen et al., 2018). On the other hand, TGFβ signaling has been demonstrated to increase trans-epithelial resistance (TER) and preserve barrier function in two-dimensional immortalized jejunal and colon cancer cell lines (Hering et al., 2011; Howe et al., 2005; McKay and Singh, 1997; Planchon et al., 1994, 1999; Roche et al., 2000; Toyonaga et al., 2020; Xiao et al., 2017). However, it remains unclear whether canonical TGFβ signaling affects colon barrier integrity *in vivo* or whether TGFβ signaling defects could lead to impaired intestinal barrier function and/or IBD and CAC.

Importantly, the TGFβ signaling pathway has both canonical and non-canonical components. In the canonical pathway, binding of the TGFβ family of extracellular ligands (including TGFβs, BMPs, Activins, and Nodals) to cell surface receptors activates intracellular, receptor-associated SMAD (R-SMAD) proteins (Shi and Massagué, 2003). TGFβ-1, -2, and -3 bind to TGFβ-type serine/threonine kinase receptors, causing phosphorylation of R-SMADs-2 and -3 (SMAD2/3). BMPs (including BMPs 2-15) bind to BMP-type receptors and cause phosphorylation of R-SMADs-1, -5, and -9 (SMAD1/5/9). Once phosphorylated, R-SMADs from either side of the pathway must interact with the common SMAD, SMAD4, to translocate to the nucleus and regulate transcription. The canonical signaling activity downstream of all TGFβ ligands and receptors is therefore dependent on SMAD4, and loss of SMAD4 abrogates all canonical signaling by TGFβ family members (Massagué, 2012). Importantly, the TGFβ signaling pathway is also postulated to have non-canonical (SMAD-independent) components wherein receptors interact directly with and activate non-SMAD protein kinases (Moustakas and Heldin, 2005; Zhang, 2009).

Previous work from our group demonstrated that loss of canonical TGFβ signaling through conditional intestine-specific deletion of SMAD4 results in a profound increase in colon epithelial inflammatory gene expression, a concomitant increase in colon immune cell infiltration, and significant susceptibility to CAC development (Means et al., 2018). While the canonical TGFβ signaling pathway was observed to directly modulate the expression of selected inflammatory genes in a cell-autonomous manner, expression of numerous other inflammatory genes that were significantly altered with intestinal SMAD4 loss *in vivo* were not significantly changed with SMAD4 loss or TGFβ pathway stimulation in cultured colon epithelial cells (Means et al., 2018). These findings led us to postulate that there may be other mechanisms triggered by loss of epithelial TGFβ signaling *in vivo* – aside from direct regulation of inflammatory gene expression – that contribute to inflammation and CAC susceptibility. One such possibility is a role for TGFβ in preservation of intestinal barrier function.

We hypothesized that TGFβ signaling via SMAD4 preserves colon mucosal barrier integrity through direct modulation of critical junctional protein expression. Through the following experiments, we demonstrate that loss of intestinal SMAD4 expression is associated with impaired colon mucosal barrier function *in vivo*, and that TGFβ signaling via SMAD4 modulates the expression of critical junctional proteins. Furthermore, we show that altered expression levels of both *SMAD4* and critical junction-related genes are observed in human IBD and colon cancer specimens and that *SMAD4* expression is significantly correlated with junction-related gene expression, suggesting that alterations in critical junctional proteins may play an important role in intestinal barrier dysfunction and/or inflammation due to SMAD4 loss or in the pathogenesis of human IBD, CRC, and/or CAC.

Methods:

Mouse model

Animal work was performed with approval from the Vanderbilt University Institutional Animal Care and Use Committee and followed ARRIVE guidelines. Mouse alleles *Lrig1*^{CreERT2} and *Smad4*$^{fl/fl}$ have been previously published (Bardeesy et al., 2006; Means et al., 2008, 2018; Powell et al., 2012) and were bred into the C57BL/6J background for at least 10 generations. Controls were sibling littermates and cage mates, and

male/female mice were split evenly between experimental arms. Mice were given tamoxifen (2mg in 0.1mL corn oil) intraperitoneally two times on alternating days after 8 weeks of age to ensure that *Smad4* gene deletion occurred during adulthood and not during development. After tamoxifen treatment, bedding was mixed among cages within an experiment once per week.

Mice with *Lrig1*^{CreERT2} *Smad4*$^{fl/fl}$ genotype that received tamoxifen injections and who were confirmed by immunohistochemistry (IHC) to have undergone recombination with loss of SMAD4 protein in the intestinal crypts are referred to as *Smad4*$^{\Delta Lrig1}$. *Smad4*$^{\Delta Lrig1}$ mice demonstrate loss of SMAD4 protein in 90% or more of colon crypts (Means et al., 2018). SMAD4-expressing control mice (mice with *Smad4*$^{fl/fl}$ genotype + tamoxifen injection) are referred to as *Smad4*$^{fl/fl}$, SMAD4+, or simply "control" mice for simplicity.

RNA-Sequencing (RNA-seq) Data Analysis

Previously published RNA-seq data sets generated in our lab (Means et al., 2018) were utilized for *in silico* analysis of differentially expressed junctional protein-encoding genes. Data files are publicly available on the National Institute of Health Gene Expression Omnibus (GEO) database (Barrett et al., 2013; Edgar et al., 2002), accession number GSE100082.

Tissue Preparation and Imaging

For hematoxylin and eosin (H&E), IHC, and immunofluorescence (IF), mouse colons were fixed in 4% paraformaldehyde and embedded in paraffin or preserved fresh in Optimal Cutting Temperature (OCT) compound as previously described (Blaine et al., 2010; Means et al., 2003; Ray et al., 2014). For Fluorescence *In Situ* Hybridization (FISH) and mucous staining, colons were fixed in poloxamer solution as previously published (Macedonia et al., 2020). All antibodies have been previously validated and published (Amoozadeh et al., 2015; Ashikari et al., 2017; Cheng et al., 2019; Healing et al., 2019; Means et al., 2018; Otani et al., 2019; Zhou et al., 2019), and antibody catalogue numbers and dilutions for all staining are listed in **Table 4.1**.

Brightfield images were captured on an Axioskop 40 microscope using Axiovision software (Carl Zeiss Microimaging, Thornwood, NY) through the Vanderbilt University Digital Histology Shared Resource. Fluorescent images were captured with the Zeiss LSM 510 Meta Inverted Confocal Microscope through the Vanderbilt University Cell Imaging Shared Resource.

In Vivo Permeability Assay

Mice (eight *Smad4*$^{\Delta Lrig1}$ and eight control) were administered 484 mg/kg body weight of 4kD Fluorescein isothiocyanate-Dextran (FITC-D, Sigma Aldrich, 46944) in Phosphate-buffered saline (PBS) by oral gavage. Four hours later, mice were anesthetized in isoflurane until unresponsive. Once unresponsive, a midline abdominal incision was made, and the inferior vena cava was exposed. One mL of blood was drawn from the vena cava using a 22G needle and blood was immediately put in Eppendorf tubes containing 15µL 1M EDTA and placed on ice. Eppendorf tubes were spun down at 3000 RPM for 20 minutes. 200µL of plasma was transferred into a new Eppendorf tube and diluted 1 to 1 with PBS. 120µL of diluted plasma was transferred into a fluorimeter tray in triplicate. Samples were subsequently analyzed by spectrophotofluorometer (Promega, San Luis Obispo, CA) with excitation/emission wavelength 485nm/530nm (FITC). Signal intensity across the three measurements per mouse were averaged, and plasma Dextran concentration for each mouse was then calculated using a standard curve. Of note, blood from one *Smad4*$^{\Delta Lrig1}$ mouse clotted during collection and thus we were unable to isolate plasma for fluorescent analysis from this mouse. This left the final experiment cohort for this element of the experiment to be 15 mice (*Smad4*$^{\Delta Lrig1}$ mice, n = 7; Control mice, n = 8).

Following blood collection, mice were euthanized by cervical dislocation and the colon was removed. Mouse colon specimens were preserved in OCT and were cut and stained with an HRP conjugated anti-FITC

antibody (Table 4.1). Signal was amplified using a Cy3-Tyramide amplification kit (Perkin Elmer, Boston, MA) diluted 1:1000 for 10 minutes at room temperature and counterstained with TOTO-3 (1:3000) in 50mM HEPES, pH 7.7. Of note, all eight mice from each arm, regardless of ability to measure plasma FITC concentration, had their colons preserved in OCT and were included in this element of the experiment (total n=16; n=8 in each cohort).

Antibodies				
Target Protein	**Company**	**Product Number**	**Dilution**	**References**
SMAD4	Abcam	40759	1:1000 (IHC [FFPE/Cryo]) 1:500 (WB)	(Means et al., 2018)
Claudin 2	Invitrogen	51-6100	1:125 (IF [Cryo]) 1:1000 (WB)	(Amoozadeh et al., 2015)
Claudin 3	Invitrogen	34-1700	1:150 (IF [FFPE]) 1:500 (WB)	(Otani et al., 2019)
Claudin 7	Invitrogen	34-9100	1:250 (IF [Cryo]) 1:20,000 (WB)	(Otani et al., 2019)
Claudin 8	Abcam	183738	1:1000 (IF [FFPE]) 1:1000 (WB)	(Ashikari et al., 2017; Cheng et al., 2019; Zhou et al., 2019)
FITC	Abcam	ab6656	1:1000 (IF [Cryo])	(Healing et al., 2019)

qPCR Primers		
Target Gene	**Forward (5' to 3')**	**Reverse (5' to 3')**
Cldn2	tgaacacggaccactgaaag	ttagcaggaagctgggtcag
Cldn3	gtggccactgcagctactt	gtttcatggtttgcctgtctc
Cldn4	ttttgtggtcaccgactttg	tgtagtcccatagacgccatc
Cldn7	tgtcttgtggagggcttga	caagcatggccattgaaa
Cldn8	gggcctggggataaaagag	aatccttaagctgtttttaggcaat
Smad7	acccccatcaccttagtcg	gaaaatccattgggtatctgga
Pmm1 (Reference Gene)	gggtggctctgactactctaagat	acacgtagtcaaacttctcaatgact

Fluorescence *in situ* Hybridization (FISH) Probes	
Eub338	5' – Cy3 – GCTGCCTCCCGTAGGAGT – 3'
Non-Eub (Negative Control)	5' – Cy3 – CGACGGAGGGCATCCTCA – 3'

Table 4.1: Antibodies, qPCR primers, and Fluorescence *in situ* Hybridization (FISH) probes utilized in Chapter IV. IHC = immunohistochemistry. IF = Immunofluorescence. FFPE = Formalin fixed and paraffin embedded. Cryo = cryopreserved (fresh frozen) tissue. WB = Western Blot.

Fluorescent In Situ Hybridization (FISH)

Custom oligonucleotides were generated by the Vanderbilt University Molecular Cell Biology Resource Core in partnership with Sigma/Genosys (Woodlands, TX). The pan-bacterial probe (Eub338) and negative control probe (Non-Eub) sequences are listed in Table 4.1.

Five *Smad4*$^{\Delta Lrig1}$ and five littermate control mice were used for this analysis. All female mice (three *Smad4*$^{\Delta Lrig1}$ and two control mice) were housed together while all male mice (two *Smad4*$^{\Delta Lrig1}$ and three control mice) were housed together. Bedding was mixed weekly between the two cages. Two centimeters of distal colon was collected and poloxamer-preserved (Macedonia et al., 2020) four weeks after tamoxifen injection. Poloxamer-preserved colon sections were cut and placed in a hybridization oven at 50° C for 10 minutes to melt paraffin and then de-paraffinized in Histoclear® (National Diagnostics) and re-hydrated by ethanol gradient before being placed in 20 mM Tris buffer. Bacterial probes were diluted to 2 μM in pre-warmed hybridization buffer (20 mM Tris-HCl [pH 8.0] + 0.9 M NaCl + 0.01% sodium dodecyl sulfate). Approximately 150 μL probe solution was then placed on each slide until sample was completely covered and slides were incubated for 1.5 hours at 46° C in humidity chamber. Slides were then washed in FISH wash buffer (225 mM NaCl + 20 mM Tris + 5 mM EDTA) for 5 minutes, three times followed by Hoechst 33342 (1:10,000 diluted in PBS) for 5 minutes. Slides were then washed again in FISH wash buffer for five minutes, twice, and the slides were cover slipped with prolong gold and allowed to cure in the dark for 48 hours prior to sealing.

16S Targeted Sequencing of Mouse Colon Microbiome

The same ten mice used in the FISH experiment described above were used for this analysis. Stool pellets were collected from mice prior to dissection and colon mucosal scrapings were taken from 5cm of middle and distal colon (proximal to the 2cm used for poloxamer preservation, above). Following collection, microbiota samples were processed and analyzed by the ZymoBIOMICS® Service: Targeted Metagenomic Sequencing (Zymo Research, Irvine, CA). DNA was extracted using the ZymoBIOMICS®-96 MagBead DNA Kit (Zymo Research, Irvine, CA). DNA samples were prepared for targeted sequencing using the *Quick*-16S™ NGS Library Prep Kit (Zymo Research, Irvine, CA). DNA library was sequenced on Illumina® MiSeq™ with a v3 reagent kit (600 cycles). The sequencing was performed with >10% PhiX spike-in. Unique amplicon sequences were inferred from raw reads and chimeric sequences removed using the Dada2 pipeline (Callahan et al., 2016). Taxonomy assignment and composition visualization, alpha-diversity, and beta-diversity analyses were performed using Uclust from Qiime v.1.9.1 (Caporaso et al., 2010). Taxonomy was assigned using the Zymo Research Database.

Mucin Staining

The ten sections of poloxamer-preserved (Macedonia et al., 2020) distal colon (as described above) were cut, deparaffinized, and rehydrated with an ethanol gradient. Slides were placed in 3% acetic acid for 3 minutes followed by Alcian Blue solution (5g Alcian Blue-8GX, 500mL Acetic Acid 3%, pH 2.5) for 30 minutes at room temperature. Slides were then rinsed in 3% acetic acid and washed in running tap water for 10 minutes before being dehydrated, counterstained with eosin, and cover slipped.

Western Blotting

Five *Smad4*$^{\Delta Lrig1}$ and five littermate control mice were dissected and their colon isolated. Genotypes were split evenly between male/female mice, and mice of the same sex were housed together with bedding mixed between cages weekly. Colon crypts were isolated by removing and flushing the colon, opening it longitudinally, rinsing, and incubating at 4°C in 1.5 mmol/L EDTA in PBS followed by shaking for 1 minute.

Following EDTA chelation, protein lysates were generated, Western blots performed as published (Shiou et al., 2006), and density quantified using ImageJ software (Schneider et al., 2012). Antibodies are listed in Table 4.1.

Colon Organoid ("Colonoid") Experiments

Mouse colonoids were generated and cultured as previously described (Means et al., 2018). Colonoids were suspended and plated in 50-µL beads of Growth Factor Reduced Matrigel (GFR; Corning, Tewksbury, MA). Complete colonoid medium was composed of 40% basal medium (advanced DMEM/F12 [Gibco] supplemented with penicillin/streptomycin [Gibco], N2 [Gibco], B27 [Gibco], Glutamax [Gibco], HEPES [Sigma Aldrich], 50 ng/mL epidermal growth factor [R&D Systems]), 40% Wnt3a-conditioned medium, 10% R-Spondin–conditioned medium, and 10% Noggin-conditioned medium. Colonoids were grown at 37°C in 5% CO_2, media was changed every 2-3 days, and colonoids were passaged every 5-7 days.

After establishing colonoids in culture, colonoids were incubated at 37°C with 20µg/mL 4-OH-Tamoxifen or methanol vehicle control for 24 hours to create a SMAD4 knockout (KO) line or a matched SMAD4+ control line, respectively. SMAD4 KO and control colonoid lines were maintained in culture under the same conditions.

Colonoids at density of 70-100 per well were treated three days after passage with TGFβ1 (3ng/mL), BMP2 (100ng/mL), TGFβ1/BMP2 (3ng/mL and 100ng/mL, respectively), Actinomycin D (5µg/mL), Cycloheximide (100µM), and/or vehicle control at designated time points for qPCR and RNA-seq experiments. Vehicle for TGFβ1 and BMP2 was 4mM HCl + 0.1% BSA in PBS. Vehicle for Actinomycin D and Cycloheximide was dimethyl sulfoxide (DMSO). Wells treated with BMP2 had the BMP-inhibitor, Noggin, withheld from the media.

Quantitative Reverse-Transcription Polymerase Chain Reaction (qPCR)

RNA was extracted from colonoids from at least 3 experimental replicates and purified as described (Freeman et al., 2012). Samples were run using a standard SYBR Green qPCR protocol (Green and Sambrook, 2018). All samples were run in triplicate with a negative control on a CFX96 Thermal Cycler (Bio-Rad, Hercules, CA). A well-known TGFβ/SMAD-response gene (Zhao et al., 2000), *Smad7*, was used for a positive control to confirm TGFβ pathway stimulation in all experimental replicates. mRNA levels were normalized to the level of *Pmm1*. All qPCR primer sequences are listed in Table 4.1. Each point on each qPCR graph represents a single experimental replicate (each done on a separate day), and each experimental replicate reflects the mean value of three technical replicates.

In vitro measures of permeability

Colonoids were grown on transwell membranes and TER measurements were taken on colonoids as previously described (Choksi et al., 2018). Briefly, colonoids were collected and dissociated using 0.25% Trypsin. Following dissociation, cells were washed and resuspended in complete media + ROCK Inhibitor (Y27632, R&D Systems, 1:1000) and plated on Collagen (Collagen I, Gibco)-coated 0.4µm transwell filters (Corning) with 75,000 cells plated per transwell. After one day, ROCK inhibitor was removed from culture media. TER was measured by Ohm meter daily after plating. Following polarization on day 2-3 after plating, media was removed from the apical chamber to create an air-liquid interface (ALI) and to induce 3-dimensional differentiation, and transwells were treated with 3ng/mL TGFβ1 and 100ng/mL BMP2 or equivalent volume vehicle control in the basolateral chamber. TER was subsequently measured at 24- and 48-hours following treatment.

Graphs provided represent the mean and standard deviation of three biological replicates, each representing separate experiments performed on different days. Each experiment included 3-6 wells per arm, depending on cell number availability.

In silico Analysis of Microarray Data and The Cancer Genome Atlas (TCGA)

We queried a previously published (Vancamelbeke et al., 2017) database consisting of transcriptomic data from IBD patients and healthy controls generated from endoscopic biopsy samples and analyzed by Microarray (data accessible at NCBI GEO database (Barrett et al., 2013; Edgar et al., 2002), accession number GSE75214). This database included colon mucosal biopsies from 74 patients with active UC (UCa), 23 patients with inactive UC (UCi), 8 patients with active Crohn's Disease (CDa), and 11 healthy controls (HC). Data represented in Log2 scale.

We additionally queried The Cancer Genome Atlas (TCGA) database (https://www.cancer.gov/tcga) utilizing the Firehose web browser from the Broad Institute (https://gdac.broadinstitute.org/). mRNA-seq expression data for 282 colon cancer (CC) specimens and 41 healthy control colon (HCc) specimens were available and downloaded for *in silico* comparison of gene expression. Data represented in Log2 scale. The authors recognize the contribution of the specimen donors and research groups who made this analysis from the TCGA possible.

Statistical Analysis

Results from *in vivo* assays including FITC-D permeability assays and Western blots were compared using non-parametric Mann-Whitney test. Results from *in vivo* and *in vitro* RNA-seq assays were compared as described (Means et al., 2018). For the 16S targeted sequencing microbiome analysis, species detection levels and Simpson Diversity scores (Simpson, 1949) were compared using the nonparametric Wilcoxon test. *In vitro* colonoid qPCR assays were compared using non-parametric Kruskal-Wallis test and post hoc Welch's *t* test. *In vitro* colonoid TER assays were compared using Repeated Measured ANOVA/Mixed-Effects model. *In silico* analysis of gene expression in human biopsy samples were compared using the non-parametric Kruskal-Wallis test with post hoc Welch's *t* test (IBD specimens), non-parametric Mann-Whitney test (TCGA specimens), or non-parametric Spearman's correlation (IBD and TCGA specimens), as appropriate. Statistical analyses were performed using GraphPad Prism 9 Software (San Diego, CA). Throughout the chapter, statistical significance is designated as: ns ($p \geq 0.05$), * ($p < 0.05$), ** ($p < 0.01$), or *** ($p < 0.001$).

Results:

Loss of SMAD4 expression within the intestinal epithelium is associated with increased intestinal permeability in vivo

We previously demonstrated that $Lrig1^{CreERT2}$ $Smad4^{fl/fl}$ ($Smad4^{\Delta Lrig1}$) adult mice lose expression of SMAD4 protein in >90% of their colonic crypts by one month after tamoxifen treatment and that $Smad4^{\Delta Lrig1}$ mice demonstrate increased colon epithelial inflammatory signaling and increased immune cell infiltration into the subepithelial colonic stroma compared to their SMAD4+ (either vehicle-treated $Lrig1^{CreERT2}$ $Smad4^{fl/fl}$ or tamoxifen-treated $Smad4^{fl/fl}$ mice) counterparts (Means et al., 2018). We sought to determine whether an alteration in intestinal permeability in $Smad4^{\Delta Lrig1}$ mice existed and could at least partially explain the observed inflammatory phenotype in mice with intestinal SMAD4 deletion. In order to assess this, we performed an *in vivo* FITC-Dextran permeability assay (Volynets et al., 2016), whereby mice were given 4kD FITC-Dextran (FD4) by oral gavage and then blood was extracted by IVC puncture 4 hours later for measurement of plasma FD4 concentration (**Figure 4.1a**). This analysis demonstrated a 2.5-fold increase in gastrointestinal permeability

to FD4 in *Smad4*$^{\Delta Lrig1}$ versus SMAD4+ mice (**Figure 4.1b**). Colon frozen sections from these mice were stained with an anti-FITC antibody. This demonstrated increased translocation of the FD4 molecule across the colon epithelium in *Smad4*$^{\Delta Lrig1}$ mice compared to control (**Figure 4.1c**), supporting the notion that a colon mucosal barrier defect exists in mice with conditional intestinal *Smad4* deletion.

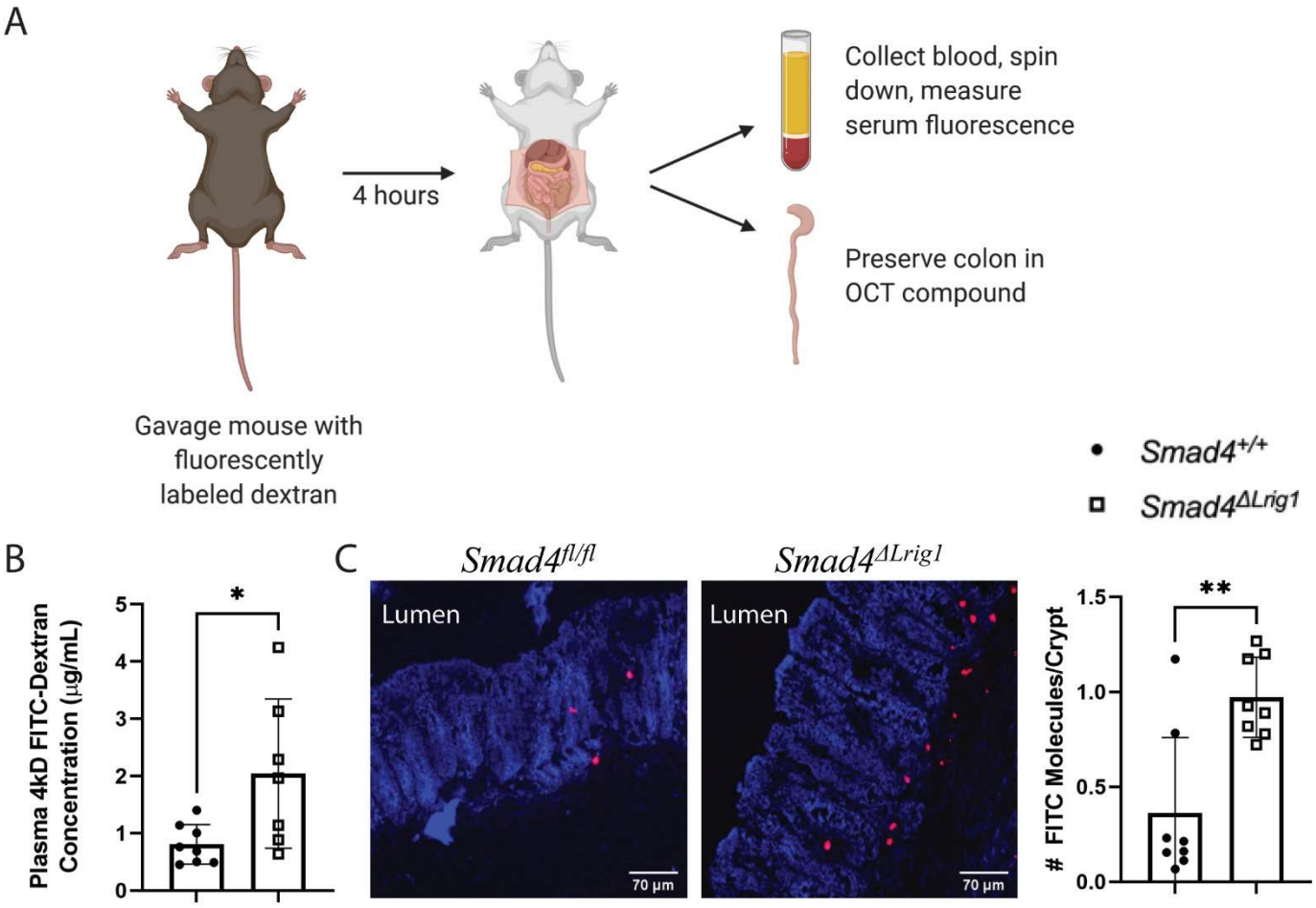

Figure 4.1 - Intestinal *Smad4* loss associated with impaired barrier function in mice. (A) Seven *Smad4*$^{\Delta Lrig1}$ mice and eight control mice were administered 4kD FITC-D (FD4) by oral gavage. Blood was collected and colon was fresh frozen 4 hours later. Image created with BioRender.com. (B) *Smad4*$^{\Delta Lrig1}$ mice demonstrated a 2.5-fold increase in plasma concentration of FD4 compared to control mice, suggesting an intestinal barrier defect (p=0.029 by Mann-Whitney test). (C) FITC molecules in preserved colon sections from eight *Smad4*$^{\Delta Lrig1}$ mice and eight control mice were detected using an anti-FITC antibody (red), demonstrating more FITC molecules per crypt in *Smad4*$^{\Delta Lrig1}$ mice compared to control (0.187 vs 0.908, p=0.007 by Mann-Whitney test).

Three distinct pathways of trans-epithelial permeability have been described. The “pore” and “leak” pathways both govern tight junction-mediated flux via the paracellular route without associated evidence of gross epithelial damage/ulceration and are distinguished by their size and charge selectivity (Anderson and Itallie, 2009; Itallie et al., 2008, 2009; Shen et al., 2011; Weber et al., 2010; Zuo et al., 2020). A third tight junction-independent “damage” pathway is characterized by gross tissue damage, ulceration, and epithelial cell

death (France and Turner, 2017; Zuo et al., 2020). While the "pore" pathway is typically permeable only to very small molecules (diameter <4-6 Å), both the "leak" and "damage" pathways allow for passage of larger uncharged solutes, including FD4 (diameter 28 Å). And while the "leak" pathway allows passage of molecules with diameters up to 100Å, the "damage" pathway allows unrestricted movement of macromolecules and even bacterial organisms. Given that the above experiments demonstrated a 2.5-fold increase in permeability to FD4, it is unlikely that the permeability defect observed is due solely to a defect in the "pore" pathway (which would show no increase in permeability to a FD4 (Shen et al., 2011)) or the "damage" pathway (which would show a much larger increase in permeability to FD4 (Kim et al., 2017; Panpetch et al., 2018)).

To validate our hypothesis that intestinal SMAD4 loss is associated with a barrier defect via the tight junction-dependent "leak" pathway rather than a more extensive "damage" phenotype, we examined the colon mucosa of *Smad4*$^{\Delta Lrig1}$ mice both grossly and histologically and saw no evidence of widespread mucosal damage, ulceration, or tissue breakdown compared to control mice (**Figure 4.2a**). To further explore whether intestinal SMAD4 loss is associated with a widespread epithelial "damage" phenotype wherein luminal bacteria are able to cross the epithelial barrier and invade the colon wall, we performed FISH for bacterial organisms on poloxamer-preserved sections of distal colon. FISH was performed using the pan-bacterial probe, Eub338, which demonstrated no difference in bacterial translocation across the colon epithelium of *Smad4*$^{\Delta Lrig1}$ compared to SMAD4+ mice (**Figure 4.2b**).

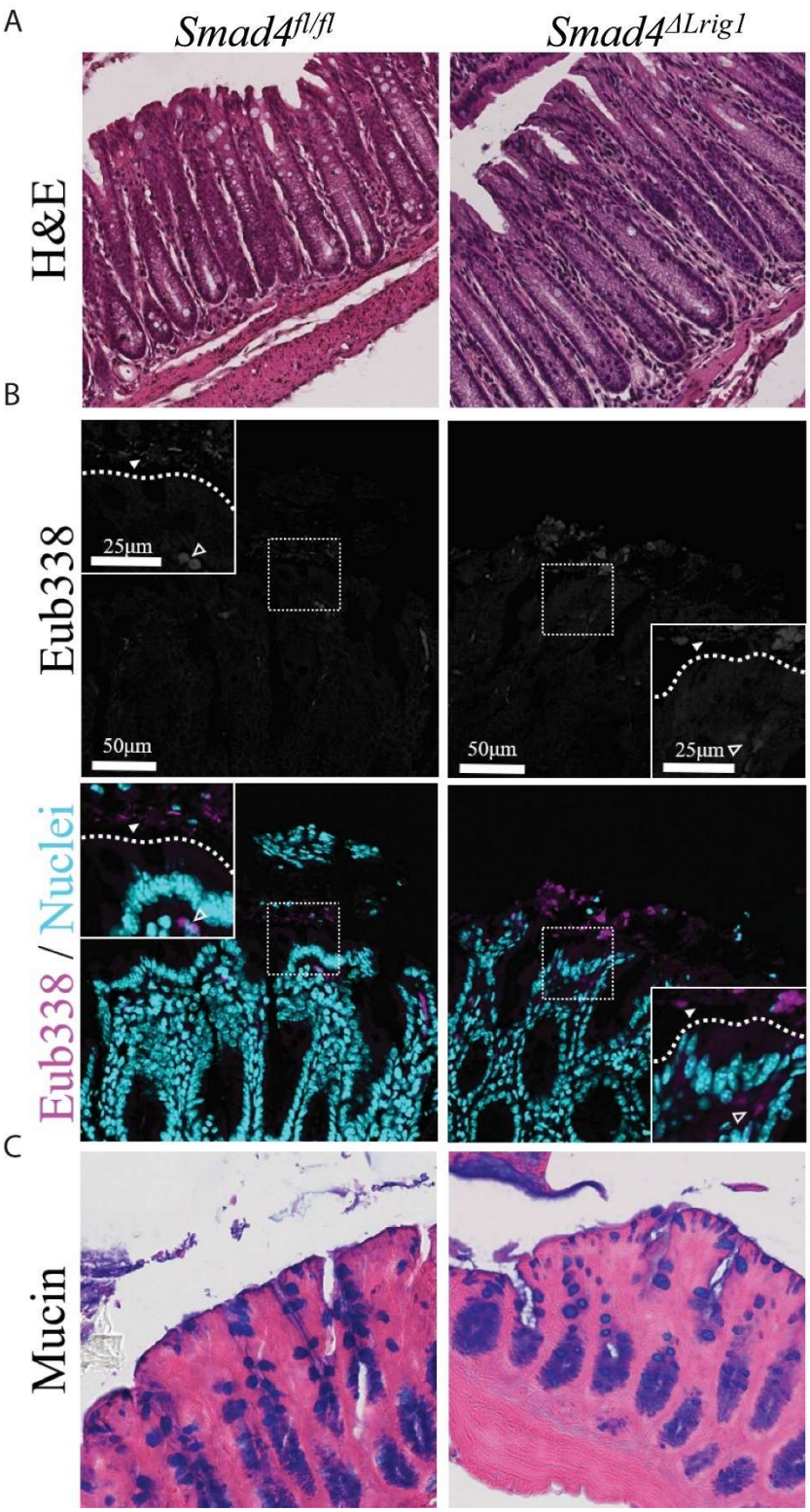

Figure 4.2 - Colons from *Smad4*$^{\Delta Lrig1}$ mice show no evidence of gross mucosal damage. (A) Representative H&E stains from *Smad4*$^{\Delta Lrig1}$ and control mice showing epithelial integrity. (B) Fluorescence *in situ* hybridization (FISH) staining with the pan-bacterial probe, Eub338 (red). Nuclei in light blue. Bacterial species indicated by solid arrowhead. Autofluorescent red blood cells indicated by open arrowhead. Border between lumen and epithelium demarcated with dashed line. (C) Alcian Blue (pH 2.5) stain for mucins (blue).

Loss of intestinal SMAD4 expression is not associated with major changes in mucin accumulation or microbiome composition

As mucins play a very important role in barrier function and mucosal protection in the gastrointestinal tract and colon (Sluis et al., 2006), major alterations in mucin expression, accumulation, or localization have the potential to be a confounding variable in the inflammatory and permeability phenotypes we've observed with intestinal SMAD4 loss *in vivo*. In order to examine this possibility, we performed an Alcian blue (pH 2.5) stain, which is known to stain all sulfated and carboxylated acid mucopolysaccharides and sialomucins (glycoproteins) (Myers et al., 2018) and thus represents a reliable indicator of general mucin accumulation and distribution, on poloxamer-preserved colon sections from mice with and without intestinal SMAD4 expression. We observed no change in mucin localization or accumulation in $Smad4^{\Delta Lrig1}$ compared to SMAD4+ mice (**Figure 4.2c**).

As the microbiome is also known to regulate gastrointestinal inflammation and pathology (Glassner et al., 2020; Song et al., 2019), we examined matched stool pellets and colonic mucosal scrapings with 16S targeted sequencing to characterize the microbiome in mice with intestinal SMAD4 loss. 16S sequencing data for all samples (stool pellets and mucosal scrapings) at all taxonomic levels (phylum, class, order, family, genus, and species) are available in **Supplemental Table 1** (https://github.com/JingYangSciBio/Supplemental-Table-1). Comparison of species detection levels demonstrated that, when comparing the microbiome composition between five $Smad4^{\Delta Lrig1}$ and five SMAD4+ control mice, there was significant mouse-to-mouse variability with some similarities between mice of the same sex that were housed together (**Figure 4.3a-b**). Additionally, when unsupervised hierarchical clustering was performed, minimal clustering between mouse genotypes occurred for either the stool pellets or colon mucosal scrapings, and mice of the same sex/housed together appeared to cluster more closely together (**Figure 4.3c-d**).

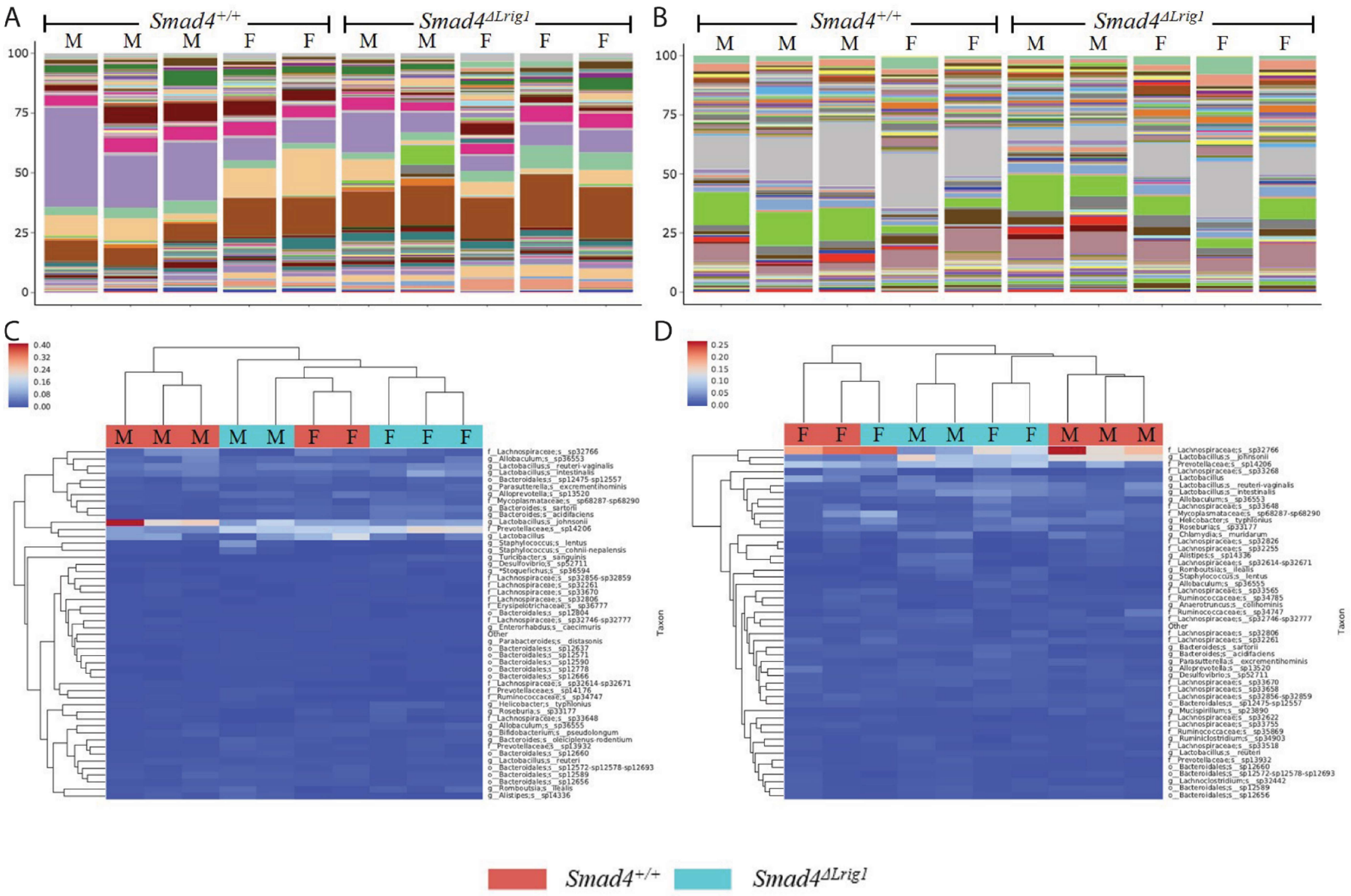
A
Smad4+/+
Smad4ΔLrig1
M M M F F M M F F F
100
75
50
25
0
B
Smad4+/+
Smad4ΔLrig1
M M M F F M M F F F
100
75
50
25
0
C
0.40
0.32
0.24
0.16
0.08
0.00
M M M M M F F F F F
f__Lachnospiraceae;s__sp32766
g__Allobaculum;s__sp36553
g__Lactobacillus;s__reuteri-vaginalis
g__Lactobacillus;s__intestinalis
o__Bacteroidales;s__sp12475-sp12557
g__Parasutterella;s__excrementihominis
g__Allogrevotella;s__sp13520
f__Mycoplasmataceae;s__sp68287-sp68290
g__Bacteroides;s__sartorii
g__Bacteroides;s__acidifaciens
g__Lactobacillus;s__johnsonii
f__Prevotellaceae;s__sp14206
g__Lactobacillus
g__Staphylococcus;s__lentus
g__Staphylococcus;s__cohnii-nepalensis
g__Turicibacter;s__sanguinis
g__Desulfovibrio;s__sp52711
g__*Stoquefichus;s__sp36594
f__Lachnospiraceae;s__sp32856-sp32859
f__Lachnospiraceae;s__sp32261
f__Lachnospiraceae;s__sp33670
f__Lachnospiraceae;s__sp32806
f__Erysipelotrichaceae;s__sp36777
o__Bacteroidales;s__sp12804
f__Lachnospiraceae;s__sp32746-sp32777
g__Enterorhabdus;s__caecimuris
Other
g__Parabacteroides;s__distasonis
o__Bacteroidales;s__sp12637
o__Bacteroidales;s__sp12571
o__Bacteroidales;s__sp12590
o__Bacteroidales;s__sp12778
o__Bacteroidales;s__sp12666
f__Lachnospiraceae;s__sp32614-sp32671
f__Prevotellaceae;s__sp14176
f__Ruminococcaceae;s__sp34747
g__Helicobacter;s__typhlonius
g__Roseburia;s__sp33177
f__Lachnospiraceae;s__sp33648
g__Allobaculum;s__sp36555
g__Bifidobacterium;s__pseudolongum
g__Bacteroides;s__oleiciplenus-rodentium
f__Prevotellaceae;s__sp13932
o__Bacteroidales;s__sp12660
g__Lactobacillus;s__reuteri
o__Bacteroidales;s__sp12572-sp12578-sp12693
o__Bacteroidales;s__sp12589
o__Bacteroidales;s__sp12656
g__Romboutsia;s__ilealis
g__Alistipes;s__sp14336
Taxon
D
0.25
0.20
0.15
0.10
0.05
0.00
F F F M M F F M M M
f__Lachnospiraceae;s__sp32766
g__Lactobacillus;s__johnsonii
f__Prevotellaceae;s__sp14206
f__Lachnospiraceae;s__sp33268
g__Lactobacillus
g__Lactobacillus;s__reuteri-vaginalis
g__Lactobacillus;s__intestinalis
g__Allobaculum;s__sp36553
f__Lachnospiraceae;s__sp33648
f__Mycoplasmataceae;s__sp68287-sp68290
g__Helicobacter;s__typhlonius
g__Roseburia;s__sp33177
g__Chlamydia;s__muridarum
f__Lachnospiraceae;s__sp32826
f__Lachnospiraceae;s__sp32255
g__Alistipes;s__sp14336
f__Lachnospiraceae;s__sp32614-sp32671
g__Romboutsia;s__ilealis
g__Staphylococcus;s__lentus
g__Allobaculum;s__sp36555
f__Lachnospiraceae;s__sp33565
f__Ruminococcaceae;s__sp34785
g__Anaerotruncus;s__colihominis
f__Ruminococcaceae;s__sp34747
f__Lachnospiraceae;s__sp32746-sp32777
Other
f__Lachnospiraceae;s__sp32806
f__Lachnospiraceae;s__sp32261
g__Bacteroides;s__sartorii
g__Bacteroides;s__acidifaciens
g__Parasutterella;s__excrementihominis
g__Allogrevotella;s__sp13520
g__Desulfovibrio;s__sp52711
f__Lachnospiraceae;s__sp33670
f__Lachnospiraceae;s__sp33658
f__Lachnospiraceae;s__sp32856-sp32859
o__Bacteroidales;s__sp12475-sp12557
g__Mucispirillum;s__sp23890
f__Lachnospiraceae;s__sp32622
f__Lachnospiraceae;s__sp33755
f__Ruminococcaceae;s__sp35869
g__Ruminiclostridium;s__sp34903
f__Lachnospiraceae;s__sp33518
g__Lactobacillus;s__reuteri
f__Prevotellaceae;s__sp13932
o__Bacteroidales;s__sp12660
o__Bacteroidales;s__sp12572-sp12578-sp12693
g__Lachnoclostridium;s__sp32442
o__Bacteroidales;s__sp12589
o__Bacteroidales;s__sp12656
Taxon
Smad4+/+
Smad4ΔLrig1

Figure 4.3 - Colonic microbiome composition in five *Smad4*$^{\Delta Lrig1}$ and five control mice. Composition bar plots from stool pellets (A) and colon mucosal scrapings (B) of five *Smad4*$^{\Delta Lrig1}$ and five control mice. Each color represents a unique bacterial species. Heatmaps with unsupervised hierarchical clustering of stool pellets (C) and colon mucosal scrapings (D) from five *Smad4*$^{\Delta Lrig1}$ and five control mice. All mice were littermates. "F" indicates female mice who were housed together, and "M" indicates male mice who were housed together (bedding mixed between the one male and one female cage weekly).

Importantly, over the 232 unique bacterial species identified in all 20 samples, 25 species were present in a significantly different proportion (increased or decreased) in *Smad4*$^{\Delta Lrig1}$ compared to SMAD4+ control mice in either the stool pellet or colon mucosal scraping samples (**Table 4.2**). Of those 25 species, 22 species were significantly different in the stool pellets of *Smad4*$^{\Delta Lrig1}$ relative to SMAD4+ control mice, 7 were significantly different in the colon mucosal scrapings of *Smad4*$^{\Delta Lrig1}$ relative to control, and 4 species were significantly different in both stool pellets and colon mucosal scrapings from *Smad4*$^{\Delta Lrig1}$ mice relative to control. All four of these species were detected at significantly lower levels in *Smad4*$^{\Delta Lrig1}$ mice compared to control and all four species belong to the phylum Firmicutes. These four species were: *Firmicutes Bacilli Lactobacillales Streptococcaceae Streptococcus danieliae*; *Firmicutes Clostridia Clostridiales Lachnospiraceae sp33625*; *Firmicutes Clostridia Clostridiales Ruminococcaceae sp35382-sp35403-sp35432*; and *Firmicutes Clostridia Clostridiales Lachnospiraceae sp32758*. Of these four species, all were detected in *Smad4*$^{\Delta Lrig1}$ mice at levels at least 2-fold lower than control mice in both stool pellets and mucosal scrapings.

When microbiome alterations were examined at the family level, small but statistically significant differences in *Bacteroidetes Bacteroidia Bacteroidales Bacteroidaceae* (stool pellet fold change -1.6, p=0.03; mucosal scraping fold change -1.05, p=0.01) and *Firmicutes Bacilli Lactobacillales Streptococcaceae* (stool pellet fold change 0.87, p=0.04; mucosal scraping fold change 0.75, p=0.02) were observed in *Smad4*$^{\Delta Lrig1}$ mice relative to control. At the genus level, small but significant differences in *Bacteroidetes Bacteroidia Bacteroidales Bacteroidaceae Bacteroides* (stool pellet fold change -1.6, p=0.03; mucosal scraping fold change -1.05, p=0.01) and *Firmicutes Bacilli Lactobacillales Streptococcaceae Streptococcus* (stool pellet fold change 0.87, p=0.05; mucosal scraping fold change 0.75, p=0.02) were again detected.

We additionally examined microbial diversity between samples. Comparison of the Simpson Diversity Index (Simpson, 1949) demonstrated an increase in diversity in stool pellets from *Smad4*$^{\Delta Lrig1}$ mice compared to control mice at the family (0.84 vs 0.76, p=0.02) and genus (0.85 vs 0.77, p=0.02) levels but not the species level (0.93 vs 0.90, p=0.15*).* There was no significant difference in Simpson Diversity Index score in colon mucosal scraping samples between *Smad4*$^{\Delta Lrig1}$ and control mice at the family (0.82 vs 0.76, p=0.10), genus (0.85 vs 0.80, p=0.10), or species (0.95 vs 0.93, p=0.10) levels.

While some statistically significant differences in microbiome composition and diversity were detected, the implications for their influence on inflammatory, tumorigenic, and barrier phenotypes seen in *Smad4*$^{\Delta Lrig1}$ mice are unclear.

These data relating to histologic architecture, mucin distribution, bacterial translocation, and microbiota composition/diversity collectively suggest that while mice with intestine-specific deletion of SMAD4 exhibit increased intestinal permeability, neither a global mucosal "damage" pathway nor major changes in mucin accumulation or microbiome composition are likely to singularly explain this phenotype. Rather, a tight junction-dependent "leak" pathway is most likely to explain the barrier defect detected in *Smad4*$^{\Delta Lrig1}$ mice.

Species Name	Stool Pellets			Colon Mucosal Scrapings		
	% detected species (*SMAD4+*)	% detected species (*Smad4*$^{\Delta Lrig1}$)	p-value	% detected species (*SMAD4+*)	% detected species (*Smad4*$^{\Delta Lrig1}$)	p-value
Firmicutes; Clostridia; Clostridiales; Peptostreptococcaceae; Romboutsia; ilealis	0.8379	2.0481	0.095	0.1991	1.0541	0.016
Bacteroidetes; Bacteroidia; Bacteroidales; Bacteroidaceae; Bacteroides; oleiciplenus-rodentium	0.5212	1.2221	0.032	0.2307	0.6080	0.095
Firmicutes; Clostridia; Clostridiales; Family XIII; NA; sp31521	0.0135	0.0462	0.036	0.0076	0.0188	0.265
Bacteroidetes; Bacteroidia; Bacteroidales; Porphyromonadaceae; Parabacteroides; sp13265	0.1112	0.2483	0.016	0.0485	0.1046	0.151
Bacteroidetes; Bacteroidia; Bacteroidales; Bacteroidaceae; Bacteroides; sartorii	1.3250	3.8431	0.016	0.6562	1.3833	0.095
Bacteroidetes; Bacteroidia; Bacteroidales; NA; NA; sp12520	0.1155	0.2571	0.008	0.0662	0.1035	0.056
Bacteroidetes; Bacteroidia; Bacteroidales; Prevotellaceae; NA; sp14206	10.8367	18.3292	0.032	6.0529	8.0463	0.222
Firmicutes; Bacilli; Lactobacillales; Lactobacillaceae; Lactobacillus; johnsonii	21.3527	9.8224	0.032	9.6831	8.9486	1.000
Firmicutes; Clostridia; Clostridiales; Lachnospiraceae; NA; sp32746-sp32777	0.4938	0.2613	0.008	1.2803	1.0871	0.691
Firmicutes; Clostridia; Clostridiales; Lachnospiraceae; NA; sp32655	0.1455	0.0452	0.016	0.2828	0.2337	0.691
Firmicutes; Clostridia; Clostridiales; Lachnospiraceae; Roseburia; sp33136	0.0388	0.0050	0.011	0.1075	0.0883	0.548
Actinobacteria; Coriobacteriia; Coriobacteriales; Coriobacteriaceae; Enterorhabdus; caecimuris	0.3641	0.2244	0.008	0.4050	0.2743	0.095
Firmicutes; Clostridia; Clostridiales; Lachnospiraceae; NA; sp33577	0.1223	0.0576	0.095	0.3545	0.2342	0.016
Firmicutes; Clostridia; Clostridiales; Lachnospiraceae; Tyzzerella; sp33289-sp33291	0.0167	0.0000	0.025	0.0289	0.0186	0.672
Firmicutes; Clostridia; Clostridiales; Lachnospiraceae; NA; sp33451-sp33593	0.1123	0.0221	0.036	0.2692	0.1586	0.151
Bacteroidetes; Bacteroidia; Bacteroidales; NA; NA; sp12597-sp12621	0.2880	0.2173	0.421	0.2329	0.1312	0.008
Firmicutes; Erysipelotrichia; Erysipelotrichales; Erysipelotrichaceae; NA; sp36777	0.4539	0.1368	0.032	0.3133	0.1547	0.222
Actinobacteria; Coriobacteriia; Coriobacteriales; Coriobacteriaceae; Paraeggerthella; hongkongensis	0.0872	0.0235	0.008	0.1238	0.0595	0.095
Firmicutes; Clostridia; Clostridiales; Lachnospiraceae; Roseburia; sp33168	0.2563	0.0244	0.012	0.5081	0.2373	0.095
Firmicutes; Clostridia; Clostridiales; Lachnospiraceae; NA; sp32623	0.0563	0.0040	0.045	0.0862	0.0321	0.094

Firmicutes; Bacilli; Lactobacillales; Streptococcaceae; Streptococcus; danieliae	**0.0394**	**0.0053**	**0.045**	**0.0392**	**0.0098**	**0.020**
Firmicutes; Clostridia; Clostridiales; Lachnospiraceae; NA; sp33625	**0.0490**	**0.0000**	**0.008**	**0.1880**	**0.0426**	**0.020**
Firmicutes; Clostridia; Clostridiales; Ruminococcaceae; NA; sp35382-sp35403-sp35432	**0.0966**	**0.0105**	**0.045**	**0.0643**	**0.0120**	**0.045**
Firmicutes; Clostridia; Clostridiales; Lachnospiraceae; NA; sp32758	**0.0698**	**0.0000**	**0.026**	**0.1215**	**0.0044**	**0.045**
Firmicutes; Erysipelotrichia; Erysipelotrichales; Erysipelotrichaceae; *Stoquefichus; sp36592-sp36804	0.0178	0.0028	0.045	0.0047	0.000	0.424

Table 4.2: Bacterial species that are significantly increased or decreased as a proportion of all detected bacteria in *Smad4*$^{\Delta Lrig1}$ vs control mice. Bolded/greyed species are bacterial species that are significantly altered (p<0.05) in both stool pellet and colon mucosal scraping samples. All species listed are from the kingdom Bacteria. Species name are listed as Phylum; Class; Order; Family; Genus; Species. NA = Not Applicable. Data represents five *Smad4*$^{\Delta Lrig1}$ and five control mice. Genotypes were split evenly between male and female male. All mice were littermates. All female mice were housed together while all male mice were housed together. Bedding was mixed between male/female cages weekly.

Loss of Smad4 expression within intestinal epithelium is associated with altered gene expression levels for multiple junctional proteins in vivo

To begin understanding how the regulation of intestinal barrier function is altered with SMAD4 loss *in vivo*, colon epithelial cells from *Smad4*$^{\Delta Lrig1}$ and SMAD4+ mice were analyzed by RNA-seq (Means et al., 2018). An exhaustive survey of differential junction-related gene expression identified at least 30 genes related to barrier function (including junctional complexes, cell adhesion, and mucin production) that were significantly altered in *Smad4*$^{\Delta Lrig1}$ compared to SMAD4+ control mice (**Table 4.3, left columns**).

TGFβ pathway stimulation results in junctional protein gene expression changes in vitro

Using an unbiased approach to determine whether the barrier function-related genes altered in *Smad4*$^{\Delta Lrig1}$ mice are due to a cell-intrinsic process of TGFβ-dependent gene expression versus other downstream functions of SMAD4 *in vivo*, a complimentary RNA-seq experiment was conducted *in vitro*. Importantly, because many transformed and immortalized 2-dimensional cell lines either fail to polarize or exhibit abnormal expression of tight junction proteins *in vitro*, these experiments were performed using 3-dimensional colon organoids (hereafter referred to as "colonoids") which are known to form tight junctions (McClintock et al., 2020). Colonoids generated from wild type mice were incubated *in vitro* with TGFβ1 and BMP2 or vehicle for 24 hours and RNA-seq analysis was again performed (Means et al., 2018). An exhaustive survey of the RNA-seq results for barrier function-related genes was performed (**Table 4.3, right columns**). This analysis revealed 40 differentially expressed barrier function-related genes.

A comparison of the differentially expressed genes due to SMAD4 loss *in vivo* and TGFβ pathway stimulation *in vitro* revealed 11 candidate genes that could potentially be directly regulated by canonical TGFβ family signaling as evidenced by significant (p<0.05) but opposite gene expression changes in the two described experimental systems. These 11 genes included *Cldn2, Cldn3, Cldn4, Cldn7, Cldn8*, *Pkp3*, *Gjb3*, *Gja1*, *Ceacam10*, *Ceacam18*, and *Muc13* (bolded in Table 4.3).

Five of the above listed genes are of particular interest in the context of our observed tight junction-dependent barrier defect: *Cldn2* (encoding Claudin 2), *Cldn3* (Claudin 3), *Cldn4* (Claudin 4), *Cldn7* (Claudin

7), and *Cldn8* (Claudin 8). The Claudin proteins are an integral part of the tight junction complex (Tsukita et al., 2018), and altered Claudin protein levels are associated with tight junction disassembly and impaired barrier integrity (France and Turner, 2017; Shen et al., 2011). Because intestine-specific SMAD4 loss appears to be related to a tight junction-dependent "leak" pathway phenotype *in vivo*, we chose to focus our subsequent experiments primarily on the above implicated Claudins.

		SMAD4 KO *in vivo*				**TGFβ1/BMP2 Treatment *in vitro***			
	***Gene Symbol* (Protein Name)**	**Fold Change**	**Log_2 Fold Change**	**p-value**	**FDR**	**Fold Change**	**Log_2 Fold Change**	**p-value**	**FDR**
Tight Junction	*Tjp1* (ZO-1)	1.64	0.71	<0.001	<0.001	1.71	0.78	<0.001	<0.001
	Tjp2 (ZO-2)	1.30	0.38	0.005	0.016	1.85	0.89	<0.001	<0.001
	Ocln (Occludin)	0.85	-0.24	0.109	0.198	1.35	0.43	0.023	0.051
	***Cldn2* (Claudin 2)**	**1.22**	**0.28**	**0.045**	**0.098**	**0.06**	**-4.14**	**<0.001**	**<0.001**
	***Cldn3* (Claudin 3)**	**0.56**	**-0.85**	**<0.001**	**<0.001**	**1.29**	**0.37**	**0.040**	**0.081**
	***Cldn4* (Claudin 4)**	**0.64**	**-0.64**	**0.002**	**0.007**	**5.79**	**2.53**	**<0.001**	**<0.001**
	***Cldn7* (Claudin 7)**	**0.82**	**-0.29**	**0.041**	**0.092**	**1.49**	**0.58**	**0.002**	**0.004**
	***Cldn8* (Claudin 8)**	**2.13**	**1.09**	**<0.001**	**<0.001**	**0.06**	**-4.10**	**<0.001**	**<0.001**
	Cldn10 (Claudin 10)	10.45	3.39	<0.001	<0.001				
	Cldn12 (Claudin 12)	1.11	0.15	0.323	0.454	0.81	-0.31	0.112	0.188
	Cldn14 (Claudin 14)	1.04	0.06	0.821	0.882	0.12	-3.02	<0.001	<0.001
	Cldn15 (Claudin 15)	0.53	-0.91	<0.001	<0.001	0.06	-4.09	<0.001	<0.001
	Cldn23 (Claudin 23)	1.03	0.04	0.796	0.865	3.66	1.87	<0.001	<0.001
	Cldn25 (Claudin 25)	0.91	-0.13	0.316	0.447	1.45	0.54	0.013	0.033
	Marveld2 (Tricellulin)	1.04	0.06	0.642	0.747	1.51	0.59	0.009	0.023
AJ	*Cdh1* (E-Cadherin)	1.27	0.35	0.012	0.033	2.54	1.35	<0.001	<0.001
	Ctnna1 (Alpha-1-Catenin)	1.15	0.20	0.142	0.242	2.31	1.21	<0.001	<0.001
	Ctnnb1 (Beta-Catenin)	0.99	-0.01	0.929	0.958	2.11	1.08	<0.001	<0.001
	Ctnnd1 (P120 Catenin)	1.47	0.56	<0.001	<0.001	3.20	1.68	<0.001	<0.001
	Vcl (Vinculin)	1.27	0.34	0.012	0.032	1.79	0.84	<0.001	<0.001
	Actn1 (Actinin Alpha 1)	1.74	0.80	<0.001	<0.001	2.93	1.55	<0.001	<0.001
	Actn4 (Actinin Alpha 4)	1.09	0.13	0.405	0.539	2.50	1.32	<0.001	<0.001
Desmosome	*Dsc2* (Desmocollin 2)	1.40	0.49	0.001	0.005	2.89	1.53	<0.001	<0.001
	Dsg2 (Desmoglein 2)	1.51	0.59	<0.001	<0.001	2.25	1.17	<0.001	<0.001
	Dsg3 (Desmoglein 3)					9.13	3.19	<0.001	<0.001
	Jup (Plakoglobulin)	0.93	-0.11	0.495	0.622	3.39	1.76	<0.001	<0.001
	Pkp1 (Plakophilin 1)	1.03	0.04	0.771	0.845	2.70	1.43	<0.001	<0.001
	Pkp2 (Plakophilin 2)	1.36	0.44	<0.001	0.002	1.65	0.72	<0.001	0.001
	***Pkp3* (Plakophilin 3)**	**0.66**	**-0.59**	**<0.001**	**<0.001**	**2.85**	**1.51**	**<0.001**	**<0.001**
Gap Junction	*Gjb4* (Connexin 30.3)					14.1	3.82	<0.001	<0.001
	***Gjb3* (Connexin 31)**	**0.75**	**-0.42**	**0.003**	**0.010**	**3.20**	**1.68**	**<0.001**	**<0.001**
	Gjb5 (Connexin 31.1)					9.19	3.20	<0.001	<0.001
	Gjb1 (Connexin 32)	0.80	-0.32	0.010	0.028	0.35	-1.51	<0.001	<0.001
	Gja5 (Connexin 40)					29.0	4.86	<0.001	<0.001
	***Gja1* (Connexin 43)**	**2.19**	**1.13**	**0.012**	**0.032**	**0.46**	**-1.12**	**0.002**	**0.005**
CAMs	*Ceacam1* (Carcinoembryonic Antigen-related Cell Adhesion Molecule 1)	1.54	0.63	<0.001	<0.001	2.33	1.22	<0.001	<0.001
	***Ceacam10* (Carcinoembryonic Antigen-related Cell Adhesion Molecule 10)**	**1.35**	**0.43**	**0.007**	**0.022**	**0.17**	**-2.57**	**<0.001**	**<0.001**
	***Ceacam18* (Carcinoembryonic Antigen-related Cell Adhesion Molecule 18)**	**0.58**	**-0.79**	**<0.001**	**<0.001**	**2.12**	**1.09**	**0.030**	**0.070**

	Ceacam20 (Carcinoembryonic Antigen/CEA)	1.47	0.56	<0.001	0.001	2.01	1.01	<0.001	0.002
Mucins	*Muc1* (Mucin 1)	2.36	1.24	<0.001	<0.001	0.49	-1.02	0.066	0.123
	Muc2 (Mucin 2)	0.76	-0.39	0.015	0.041	0.20	-2.34	<0.001	<0.001
	Muc3 (Mucin 3)	0.98	-0.03	0.864	0.913				
	Muc4 (Mucin 4)	2.01	1.01	<0.001	<0.001	2.19	1.13	<0.001	<0.001
	***Muc13* (Mucin 13)**	**1.31**	**0.39**	**0.008**	**0.023**	**0.65**	**-0.62**	**0.001**	**0.002**
	Muc20 (Mucin 20)	2.07	1.05	0.006	0.019				

Table 4.3: Junctional protein-related genes are altered with loss of epithelial *Smad4* expression *in vivo* and with TGFβ pathway stimulation *in vitro*. Comparison of two RNA-sequencing (RNA-seq) data sets. Left columns titled "SMAD4 KO *in vivo*" represents RNA-seq data comparing gene expression in the colon epithelium of three $Smad4^{\Delta Lrig1}$ and three control mice. Right columns titled "TGFβ1/BMP2 Treatment *in vitro*" represents RNA-seq data comparing gene expression in wild type colonoids treated with TGFβ1 + BMP2 or vehicle x24 hours (three biological replicates). Rows bolded and shaded in grey represent genes that are significantly changed ($p<0.05$) in opposite directions with SMAD4 knock out *in vivo* and TGFβ/BMP treatment *in vitro*, suggesting a possible role for direct regulation by canonical TGFβ signaling. KO = knock out; FDR = false discover rate. AJ = Adherens Junction. CAMs = Cell Adhesion Molecules.

Loss of SMAD4 within intestinal epithelium of mice is associated with altered levels of Claudin protein but normal cellular localization

In order to determine if alterations in *Cldn* mRNA levels were reflected in altered protein levels, we isolated the colon epithelium from five $Smad4^{\Delta Lrig1}$ and five SMAD4+ control mice and created protein lysates which we used to perform Western Blots (WB). WB analysis demonstrated an increase in Claudin 2 and Claudin 8 protein levels in the colon epithelium of $Smad4^{\Delta Lrig1}$ mice compared to control. Conversely, a significant decrease in Claudin 7 protein was observed in the colon epithelium of mice with intestinal deletion of SMAD4, consistent with the changes in RNA expression observed by RNA-seq. Claudin 3 protein levels were not significantly changed in $Smad4^{\Delta Lrig1}$ mice compared to control (**Figure 4.4a-b**).

To determine if there were any alterations in junctional protein localization in $Smad4^{\Delta Lrig1}$ mice compared to control, we performed immunostaining of mouse colons with and without SMAD4 expression. Immunostaining confirmed >90% SMAD4 loss in the colons of $Smad4^{\Delta Lrig1}$ mice (**Figure 4.4c**). For both $Smad4^{\Delta Lrig1}$ and SMAD4+ mice, immunofluorescence staining demonstrated Claudin 2 subapical localization largely concentrated in cells at the crypt base (**Figure 4.4d**). Claudins 3 and 7 were localized to the subapical and basolateral membranes and were uniformly present along the crypt axis in both $Smad4^{\Delta Lrig1}$ and SMAD4+ mice. Similar to Claudins 3 and 7, Claudin 8 was expressed subapically and basolaterally, however unlike Claudins 3 and 7, Claudin 8 was predominantly localized in the middle and tops of crypts with very low levels observed at the crypt base. Protein localization for each of the above described Claudin proteins was consistent with previously published reports (Darsigny et al., 2009; Raju et al., 2020; Tanaka et al., 2015).

These data suggest that epithelial TGFβ signaling via SMAD4 modulates the levels, but not the localization, of Claudin 2, Claudin 7, and Claudin 8 protein and that epithelial TGFβ signaling does not impact Claudin 3 production or localization *in vivo*. Unfortunately, we were unable to reliably detect Claudin 4 by immunostaining or Western Blot and thus were unable to assess Claudin 4 production or localization *in vivo*.

A

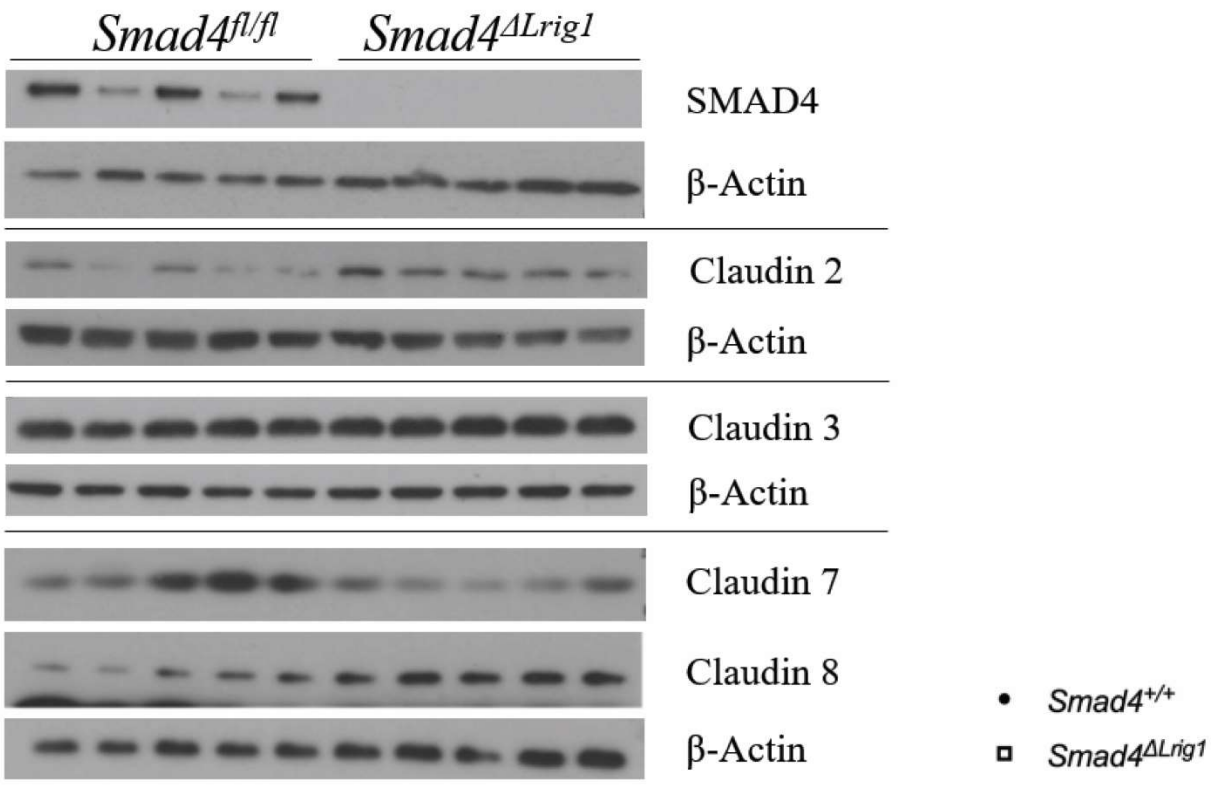
Smad4fl/fl
Smad4ΔLrig1
SMAD4
β-Actin
Claudin 2
β-Actin
Claudin 3
β-Actin
Claudin 7
Claudin 8
β-Actin
Smad4+/+
Smad4ΔLrig1

B

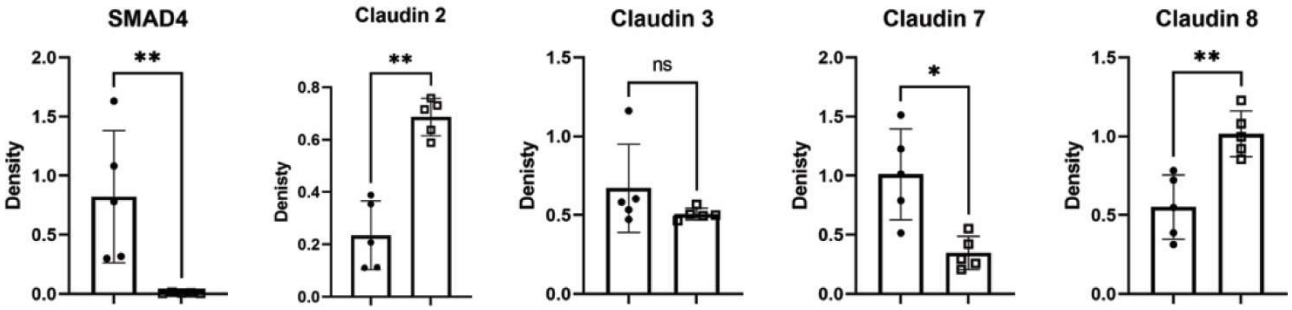
SMAD4
Claudin 2
Claudin 3
Claudin 7
Claudin 8
Density
**
**
ns
*
**

C

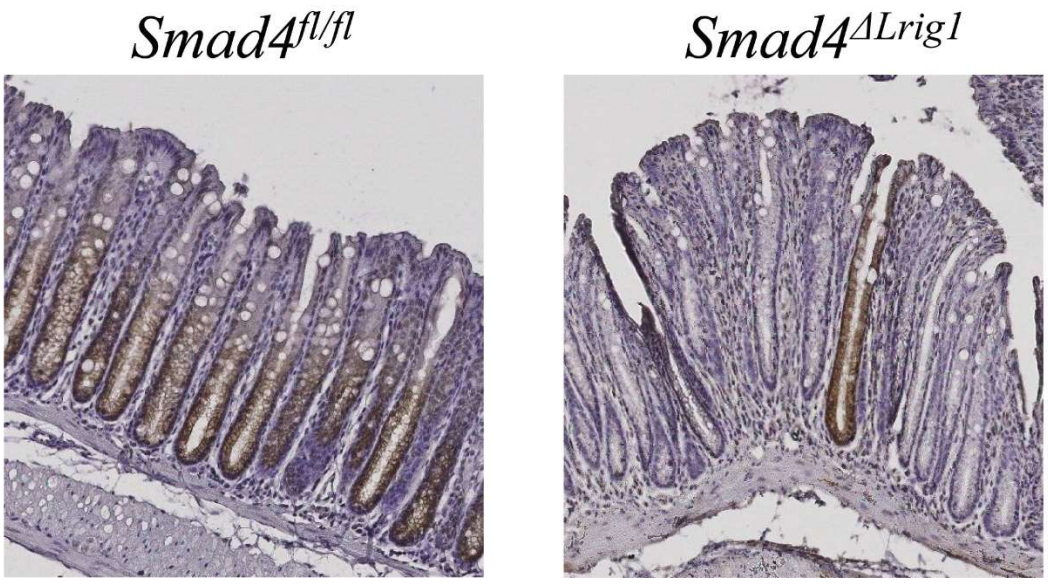
Smad4fl/fl
Smad4ΔLrig1

D
Claudin 2
Yo-Pro-1
Claudin 2/Yo-Pro-1
Smad4f/f
Smad4Δtrig1
35 μm
Claudin 7
Yo-Pro-1
Claudin 7/Yo-Pro-1
Smad4f/f
Smad4Δtrig1
35 μm
Claudin 3
Yo-Pro-1
Claudin 3/Yo-Pro-1
Smad4f/f
Smad4Δtrig1
35 μm
Claudin 8
Yo-Pro-1
Claudin 8/Yo-Pro-1
Smad4f/f
Smad4Δtrig1
35 μm

Figure 4.4 - Loss of intestinal *Smad4* expression is associated with altered levels, but not localization, of several Claudin proteins. (A) Western blots (WB) from protein lysates generated from colon epithelium of five $Smad4^{\Delta Lrig1}$ and five control mice. (B) Quantification of relative protein density by WB. Protein density was compared between mouse genotypes by Mann-Whitney test. (C) Immunohistochemistry for SMAD4 protein (brown) in $Smad4^{fl/fl}$ (SMAD4+) control and $Smad4^{\Delta Lrig1}$ mice. (D) Immunofluorescence staining for indicated Claudin proteins. Claudin proteins in red, nuclei in green.

TGFβ and BMP signaling via SMAD4 regulate Cldn *gene expression in a cell autonomous manner*

To determine if TGFβ signaling is modulating the expression of critical junctional proteins in a cell-autonomous manner, a series of experiments were performed *in vitro*. Wild type colonoids were treated with TGFβ1, BMP2, both, or vehicle for 24 hours and RNA was subsequently isolated for qPCR. Induction of *Smad7* expression served as a control for ligand activity. This largely validated our RNA-seq findings and demonstrated that stimulation of the TGFβ signaling pathway with either TGFβ1, BMP2, or both resulted in differential expression of tight junction-related genes. While *Cldn2* and *Cldn8* expression were significantly decreased with TGFβ pathway stimulation by either TGFβ1, BMP2, or both, *Cldn4* and *Cldn7* expression were significantly increased with TGFβ1, BMP2, or both. Expression levels of *Cldn3*, on the other hand, did not change significantly with TGFβ pathway stimulation by qPCR (**Figure 4.5a**).

Colonoids generated from $Lrig1^{CreERT2}$; $Smad4^{fl/fl}$ mice (that did not receive tamoxifen *in vivo*) were additionally treated with 4OH-tamoxifen or vehicle *in vitro* to generate SMAD4 knockout or SMAD4 positive control colonoids, respectively. Knockout and control colonoids were then stimulated with either TGFβ1/BMP2 co-treatment or vehicle control for 24 hours prior to RNA isolation. This experiment revealed that in the setting of TGFβ pathway stimulation, SMAD4 knockout *in vitro* resulted in increased *Cldn2* and *Cldn8* expression and decreased *Cldn4* and *Cldn7* expression. Additionally, in the absence of SMAD4 expression, TGFβ pathway stimulation failed to elicit significant changes in Claudin gene expression, confirming that the above-described changes in Claudin gene expression due to TGFβ/BMP treatment are dependent on the SMAD-dependent (canonical) signaling pathway rather than the SMAD-independent (non-canonical) TGFβ pathways (**Figure 4.5b**). Of note, gene expression levels of *Cldn3* were not significantly changed with SMAD4 knockout *in vitro*. Collectively, these results suggest that TGFβ signaling via SMAD4 modulates *Cldn2*, *Cldn4*, *Cldn7*, and *Cldn8* gene expression in mouse colon epithelial cells in a cell-autonomous manner, and that the decreased *Cldn3* expression observed with SMAD4 loss *in vivo* may not be due to a cell-intrinsic process.

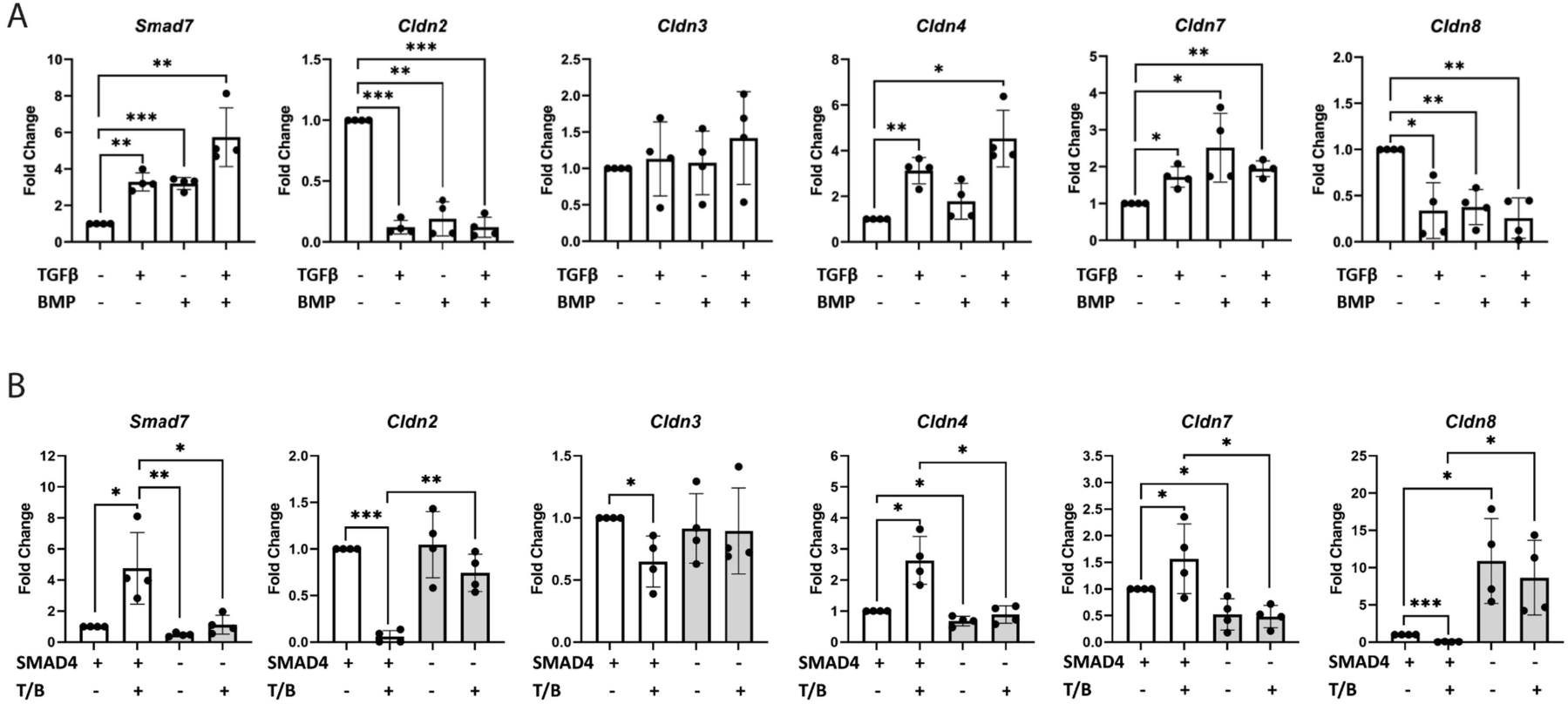
A
Smad7
Cldn2
Cldn3
Cldn4
Cldn7
Cldn8
Fold Change
TGFβ - + - +
BMP - - + +
B
Smad7
Cldn2
Cldn3
Cldn4
Cldn7
Cldn8
Fold Change
SMAD4 + + - -
T/B - + - +

Figure 4.5 - TGFβ/BMP signaling via SMAD4 modulates the expression of *Cldn2*, *Cldn4*, *Cldn7*, and *Cldn8* in a cell-autonomous manner. (A) Wild type colonoids treated with TGFβ1, BMP2, both, or vehicle for 24 hours. (B) SMAD4 knockout and control colonoids treated with TGFβ1/BMP2 (T/B) or vehicle for 24 hours. Fold change indicates the relative level of mRNA compared to vehicle-treated wild type controls for indicated genes. Each data point represents a single biological replicate, with biological replicates treated and harvested on different days. Experimental arms were compared using non-parametric Kruskal-Wallis test with post hoc Welch's *t* test. *Smad7* is used as a positive control to confirm ligand activity.

TGFβ pathway signaling regulates transepithelial resistance (TER) in a cell autonomous manner

To determine if canonical TGFβ signaling has a direct effect on colonocyte barrier function in a cell autonomous manner, SMAD4-null and SMAD4+ control colonoids were plated onto collagen-coated transwells and allowed to polarize. Following polarization (TER ≥500 ohms [Ω]) on days 2-3 after plating (**Figure 4.6a**), ALI was initiated (**Figure 4.6b**). Simultaneous to ALI initiation, transwells were treated with TGFβ/BMP co-treatment or vehicle. TGFβ/BMP co-treatment resulted in a significant increase in TER in SMAD4+ colonoids compared to vehicle-treated controls at both 24- (fold change 1.86 vs 1.31) and 48-hours (fold change 1.95 vs 1.09) ($p<0.001$, **Figure 4.6c**). Importantly, SMAD4-null colonoids were unresponsive to TGFβ pathway stimulation and demonstrated no significant difference in TER compared to vehicle-treated control colonoids at 24- (fold change 1.35 vs 1.26) or 48-hours (fold change 1.22 vs 1.16) ($p=0.641$, **Figure 4.6d**). These data suggest that TGFβ pathway stimulation directly increases TER in mouse colonocytes in a manner dependent on SMAD4.

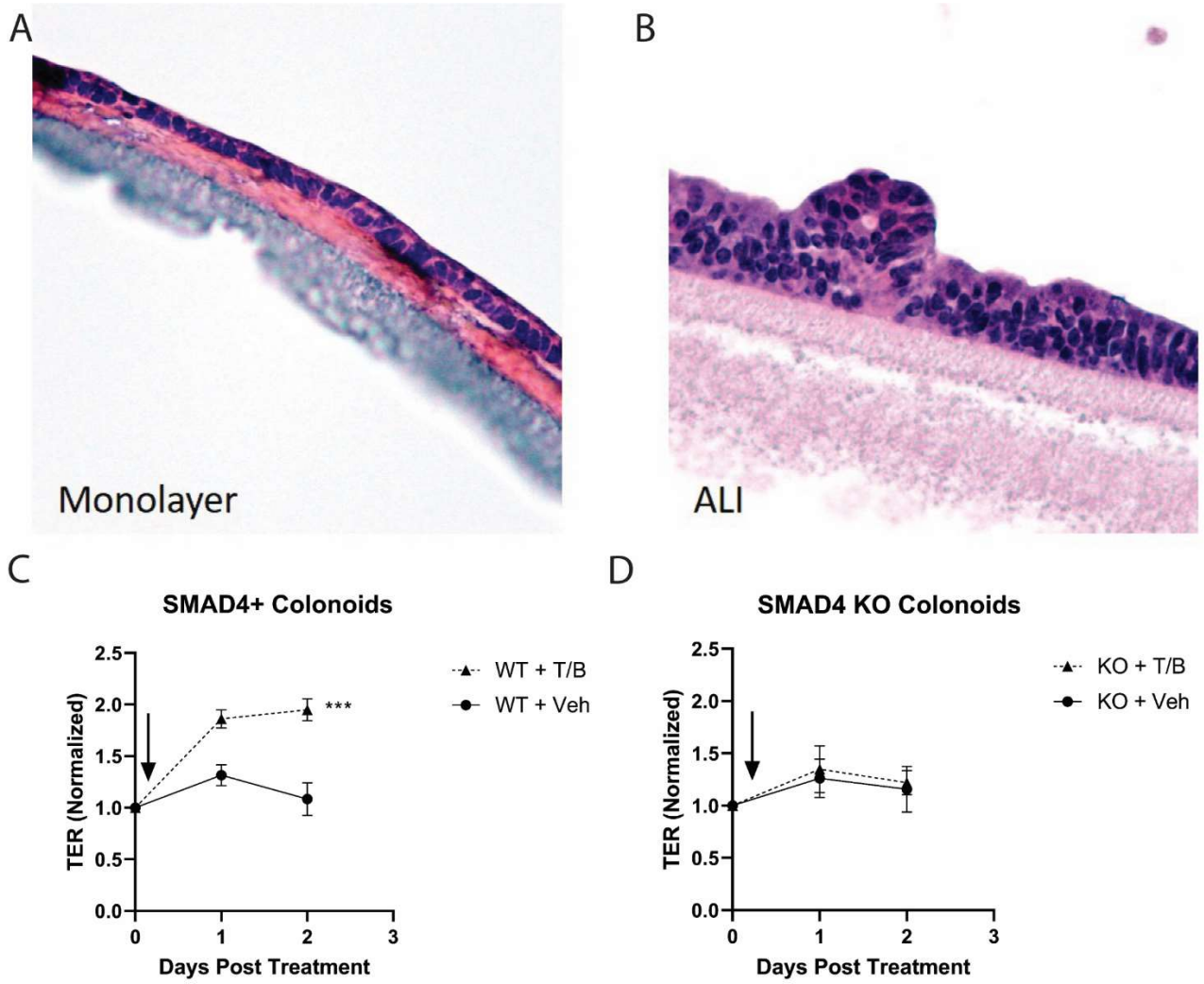

Figure 4.6 - TGFβ/BMP signaling via SMAD4 modulates barrier function/transepithelial resistance in a cell-autonomous manner. Representative images of H&E stain demonstrating polarized monolayers of colon epithelial cells grown on collagen-coated transwell membranes before (A) and after (B) initiation of air-liquid interface (ALI). (C) Normalized TER for wild type (SMAD4+) colonoids on collagen-coated transwells in an ALI system. TGFβ/BMP co-treatment in the basolateral chamber was associated with a significant increase in TER compared to vehicle-treated controls at 24- and 48-hours ($p<0.001$ by repeat measured ANOVA/Mixed effects model). (D) Normalized TER for SMAD4 knockout colonoids grown on collagen-coated transwells in an ALI system. TGFβ/BMP co-treatment in the basolateral chamber failed to elicit a change in TER compared to vehicle-treated controls at 24- or 48-hours. For both (C) and (D), data represents the mean and standard deviation of three biological replicates, with biological replicates being plated, treated, and measured on separate days. Experimental arms were compared using repeat measures ANOVA/Mixed Effects model. TER measurements for each well were normalized to the final pre-treatment TER for that well (Day 0 on the X axis).

TGFβ signaling modulates junctional protein gene expression by disparate mechanisms

To begin to understand the mechanism by which canonical TGFβ signaling pathway is modulating the expression of these critical junctional proteins, a time course experiment was performed. Wild type colonoids underwent vehicle or TGFβ1/BMP2 co-treatment for 0-, 2-, 4-, or 16-hours. TGFβ pathway stimulation significantly decreased the expression of *Cldn2* as early as 4 hours post-treatment with a further decrease in expression at 16 hours post-treatment compared to vehicle-treated control colonoids (**Figure 4.7a**). On the other hand, *Cldn4* and *Cldn8* were not significantly altered at 0-, 2-, or 4-hours post-treatment, but were significantly altered (*Cldn4* increased and *Cldn8* decreased) by 16 hours post-treatment compared to vehicle-treated control colonoids. *Cldn7* expression levels, however, were not significantly changed at 0-, 2-, 4-, or 16-hours although they were significantly changed with TGFβ1/BMP2 co-treatment and SMAD4 knockout at 24 hours in the previously described experiments (Figure 4.5). These data suggest that more than one mechanism may be implicated in the modulation of Claudin gene expression by canonical TGFβ signaling.

TGFβ signaling modulates Cldn2*,* Cldn4*,* Cldn7*, and* Cldn8 *gene expression in a manner that is dependent on nascent RNA transcription*

To determine if changes in *Cldn* gene expression levels were due to altered mRNA stability or to altered transcription, we blocked transcription using Actinomycin D (ActD) (Sobell, 1985) in wild type colonoids with and without TGFβ1/BMP2 stimulation. We found that ActD was 100% lethal to our colonoids by 24 hours but colonoids retained at least 50% viability in the presence of ActD for 6.5 hours. As a positive control, ActD prevented the induction of *Smad7*, a known direct target of SMAD-mediated transcription (Zhao et al., 2000). Treatment of wild type colonoids with TGFβ1/BMP2, +/- ActD, or their respective vehicles for 6.5 hours demonstrated that, for *Cldn2*, *Cldn4*, and *Cldn8*, TGFβ1/BMP2-dependent changes in gene expression levels were blocked by ActD co-treatment, suggesting that TGFβ pathway-dependent changes in *Cldn2, Cldn4,* and *Cldn8* gene expression levels are dependent on a mechanism which includes nascent transcription (**Figure 4.7b**). Because *Cldn7* levels were not significantly changed at 6.5 hours with TGFβ pathway stimulation in the absence of ActD, it is impossible to tell from this experiment if TGFβ-mediated regulation of *Cldn7* requires nascent transcription.

TGFβ signaling modulates the transcription of Cldn4 *and* Cldn8 *genes in a manner that is independent of nascent protein translation*

To determine if these TGFβ-dependent changes in Claudin expression are dependent on novel protein synthesis, we blocked protein translation using cycloheximide (CHX) (Schneider-Poetsch et al., 2010) in wild type colonoids with and without TGFβ1/BMP2 stimulation. Similar to the ActD experiment described above, the 6.5-hour timepoint was used for this experiment as the colonoids retained at least 50% viability in the presence of CHX at 6.5 hours and colonoid viability dropped precipitously after that point. CHX did not alter the ability of TGFβ1/BMP2 to induce *Smad7* expression as expected (**Figure 4.7b**). Similarly, in the setting of CHX, TGFβ1/BMP2 were still able to increase *Cldn4* expression and decrease *Cldn8* expression, suggesting that TGFβ-dependent changes in *Cldn4* and *Cldn8* expression occur in a manner independent of nascent protein translation.

Interestingly, CHX treatment dramatically decreased *Cldn2* levels regardless of the presence or absence of TGFβ pathway stimulation, suggesting that *Cldn2* mRNA expression is dependent on nascent protein synthesis. Given this finding, it is not possible to determine from this experiment whether TGFβ pathway-dependent regulation of *Cldn2* expression relies on nascent protein synthesis. As in the ActD experiment, *Cldn7* levels were not significantly changed at 6.5 hours with TGFβ pathway stimulation even in the absence of CHX, making it impossible to determine if TGFβ-dependent *Cldn7* expression relies on nascent protein production.

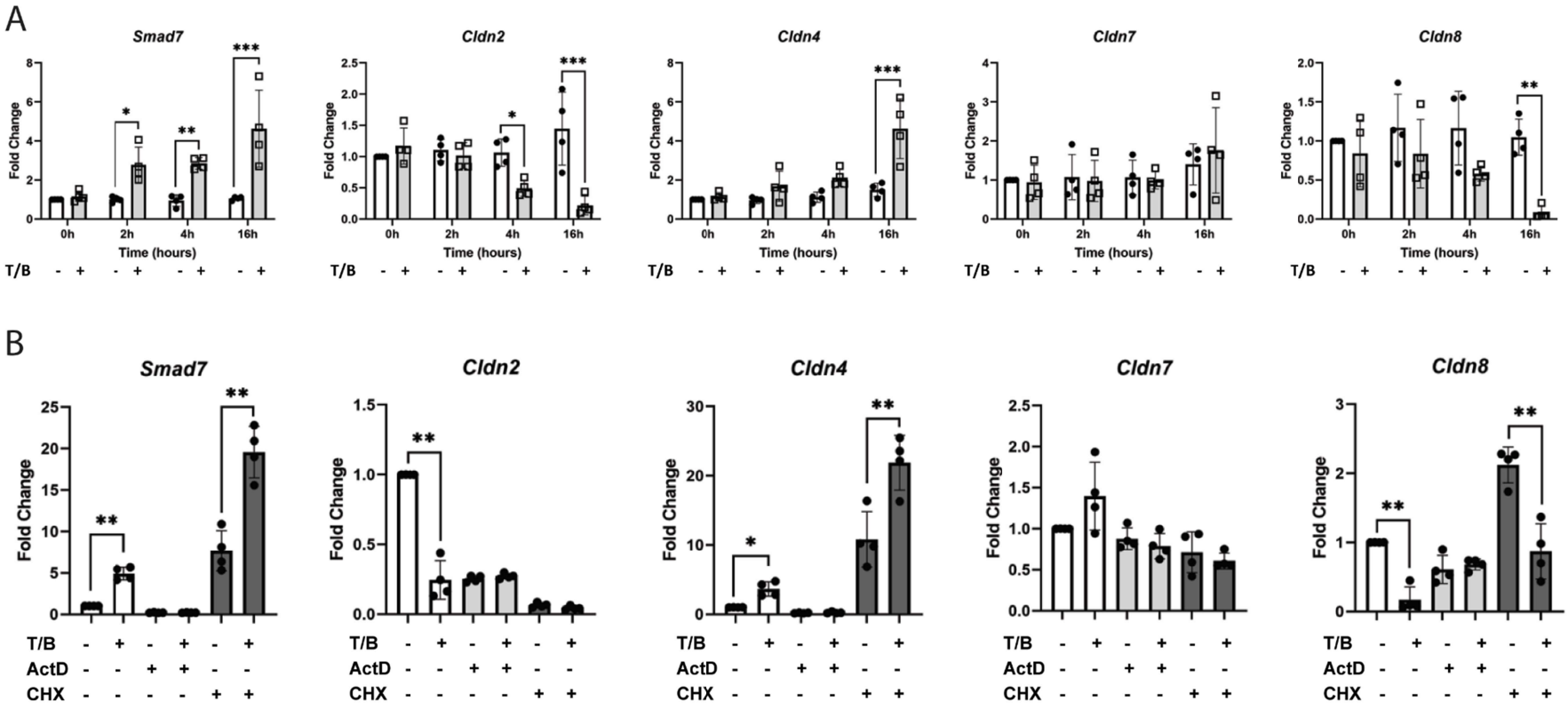
A
Smad7
Cldn2
Cldn4
Cldn7
Cldn8
Fold Change
Time (hours)
0h
2h
4h
16h
T/B
B
Smad7
Cldn2
Cldn4
Cldn7
Cldn8
Fold Change
T/B
ActD
CHX

Figure 4.7 - TGFβ/BMP signaling via SMAD4 modulates the expression of *Cldn* genes by disparate mechanisms. (A) Wild type colonoids treated with TGFβ1/BMP2 (grey bars/open boxes) or vehicle (white bars/closed circles) for the indicated periods of time. (B) Wild type colonoids treated with TGFβ1/BMP2 (T/B) vs. vehicle (white bars, left), T/B vs. vehicle in the presence of Actinomycin D (ActD) (light grey bars, middle), or T/B vs. vehicle in the presence of Cyclohexamide (CHX) (dark gray bars, right) for 6.5 hours. Fold change indicates the relative level of mRNA for indicated genes compared to vehicle-treated control. Each data point represents a single biological replicate, with biological replicates treated and harvested on different days. Experimental arms were compared using non-parametric Kruskal-Wallis test with post hoc Welch's *t* test. *Smad7* is used as a positive control to confirm ligand activity.

Altered expression of SMAD4 and Claudin genes are associated with human IBD and colon cancer

To correlate the above-described findings in mice with human disease, we examined the relationship with TGFβ pathway signaling and *CLDN* expression in human specimens by querying a previously published database consisting of transcriptomic data generated from colonoscopic biopsy samples and analyzed by Microarray (GSE75214) (Vancamelbeke et al., 2017). This database included colon mucosal biopsies from 74 patients with active UC (UCa), 23 patients with inactive UC (UCi), 8 patients with active Crohn's Disease (CDa), and 11 healthy controls (HC). This analysis demonstrated that *SMAD4* expression was significantly decreased in the colon of UCa and CDa specimens compared to HC specimens, similar to previously published reports (Klausen et al., 2018; Means et al., 2018). Additionally, there were significant perturbations in *CLDN* expression in IBD colon specimens compared to HC specimens (**Figure 4.8a**). *CLDN2* expression was significantly increased in UCa specimens compared to HC specimens while *CLDN4, CLDN7,* and *CLDN8* were significantly decreased in UCa specimens compared to HC specimens. These alterations in Claudin gene expression in IBD patient samples are consistent with previously published reports (Lameris et al., 2012; Luettig et al., 2015; Prasad et al., 2005; Randall et al., 2016; Vancamelbeke et al., 2017; Zeissig et al., 2007). Importantly, a significant inverse correlation exists between *SMAD4* expression and *CLDN2* expression, whereas a positive correlation was observed between *CLDN4*, *CLDN7*, and *CLDN8* expression and *SMAD4* expression in the colons of IBD patients (**Figure 4.8b**).

We additionally queried the TCGA database to determine whether this relationship between *SMAD4* and *CLDN* gene expression was observed in sporadic colon cancers in addition to IBD. The TCGA database includes gene expression data generated from RNA-seq analysis of 282 primary colon cancers (CC) and 41 healthy colon controls (HCc) (**Figure 4.8c**). By TCGA analysis, *SMAD4* expression was significantly decreased in CC specimens compared to HCc specimens, consistent with prior reports of decreased *SMAD4* expression in CRC (Means et al., 2018; Wasserman et al., 2018; Yan et al., 2016). Additionally, *CLDN2* expression is significantly increased in CC specimens compared to HCc specimens while expression levels of *CLDN4, CLDN7,* and *CLDN8* are significantly lower in CC specimens compared to HCc. Changes in Claudin gene expression levels observed here by TCGA analysis are largely consistent with prior published reports (Bornholdt et al., 2011; Dhawan et al., 2011; Ueda et al., 2007; V et al., 2017; Xu et al., 2018). Importantly, *CLDN2* and *SMAD4* expression are inversely correlated while *CLDN7* and *CLDN8* expression are both positively correlated with *SMAD4* expression in CC and HCc specimens. Interestingly, *CLDN4* expression is not significantly correlated with *SMAD4* expression in human CC and HCc specimens in the TCGA database (**Figure 4.8d**).

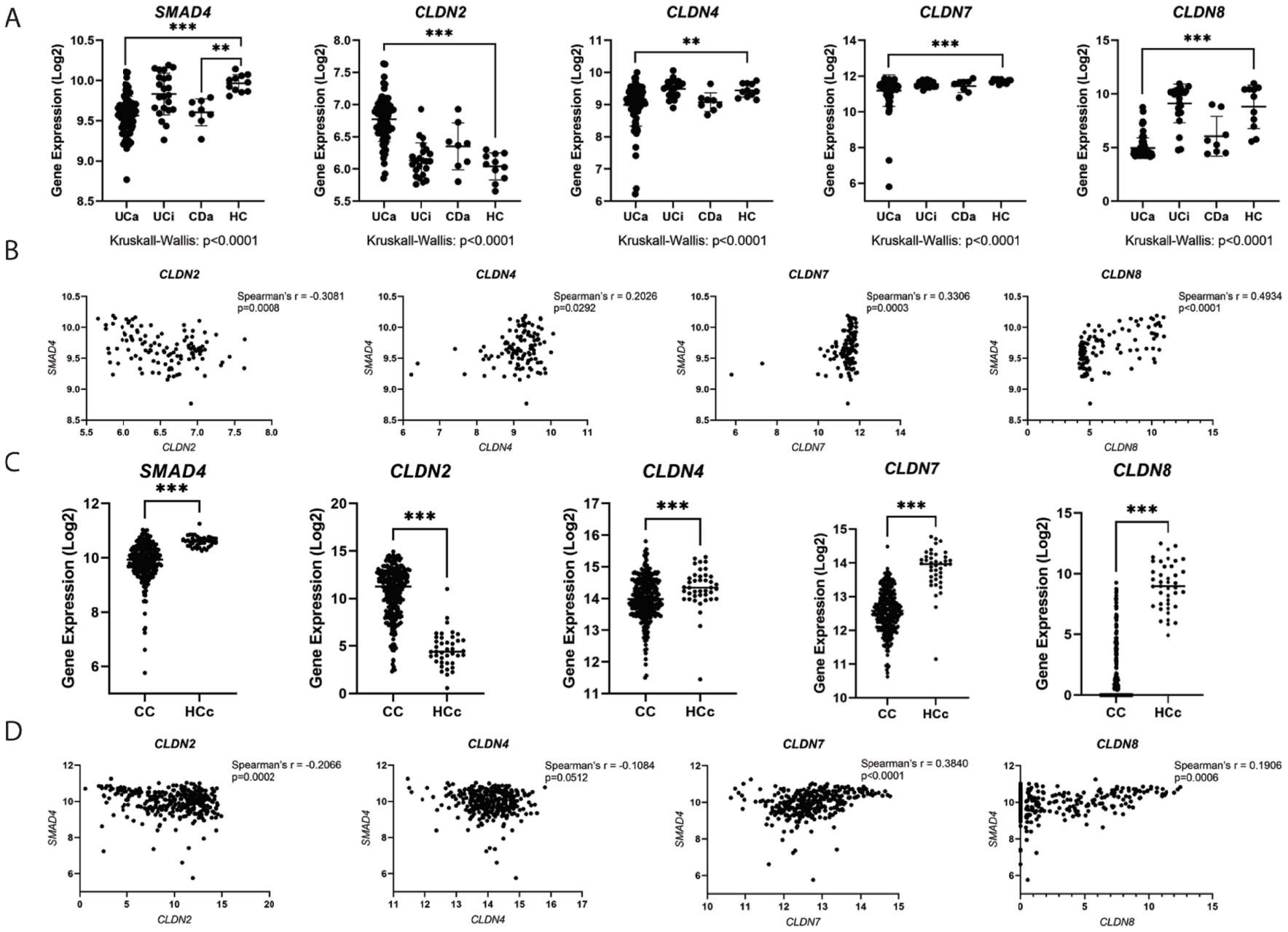
A
SMAD4
CLDN2
CLDN4
CLDN7
CLDN8
Gene Expression (Log2)
UCa UCi CDa HC
Kruskall-Wallis: p<0.0001
B
CLDN2
CLDN4
CLDN7
CLDN8
SMAD4
Spearman's r = -0.3081
p=0.0008
Spearman's r = 0.2026
p=0.0292
Spearman's r = 0.3306
p=0.0003
Spearman's r = 0.4934
p<0.0001
C
CC HCc
D
Spearman's r = -0.2066
p=0.0002
Spearman's r = -0.1084
p=0.0512
Spearman's r = 0.3840
p<0.0001
Spearman's r = 0.1906
p=0.0006

Figure 4.8 - *SMAD4* and *CLDN* genes are dysregulated in human IBD and colon cancer. (A) *In silico* analysis of human microarray database (accession number GSE75214). Samples represent human colon biopsy samples from patients with active Ulcerative Colitis (UCa, n=74), inactive Ulcerative Colitis (UCi, n=23), active Crohn's Disease (CDa, n=8), and healthy controls (HC, n=11). Gene expression in human biopsy samples were compared between groups using the non-parametric Kruskal-Wallis test with post hoc Welch's *t* test. (B) Correlation between *SMAD4* expression and indicated *CLDN* gene expression in human colon biopsy specimens from GSE75214. Spearman's correlation was used to measure correlation between *SMAD4* and *CLDN* gene expression. (C) *In silico* analysis of RNA-sequencing data from The Cancer Genome Atlas (TCGA) database. Samples represent mRNA expression in colon cancer (CC, n=283) or healthy control colon (HCc, n=41) specimens. Non-parametric Mann-Whitney test was used to compare gene expression levels between groups. (D) Correlation between *SMAD4* expression and indicated *CLDN* gene expression in human colon specimens from TCGA. Spearman's correlation was used to measure correlation between *SMAD4* and *CLDN* gene expression. For (A-D), gene expression levels are represented on a Log2 scale.

Discussion:

While the pathophysiology of IBD and CAC is complex with multiple genetic, environmental, and dietary factors likely contributing (Guan, 2019), increased mucosal permeability and impaired barrier function have been observed in first-degree relatives of Crohn's Disease patients (Hollander et al., 1986; Katz et al., 1989) and have also been noted to precede inflammatory symptoms in IBD patients (Wyatt et al., 1993), suggesting that a primary intestinal barrier defect may be a contributing factor in some cases (Martini et al., 2017; McGuckin et al., 2009; Sluis et al., 2006; Söderholm et al., 1999; Vancamelbeke et al., 2017; Wehkamp et al., 2008). At the same time, TGFβ signaling defects have been associated with IBD (Allaire et al., 2011; Babyatsky et al., 1996; Marincola-Smith et al., 2019; Means et al., 2018; Monteleone et al., 2001, 2015; Sedda et al., 2015). However, the relationship between intestinal TGFβ signaling, barrier function, and IBD has not been deeply explored. Both TGFβ signaling in general as well as its regulation of barrier function specifically has been shown to be highly tissue- and context-dependent. While in the pulmonary endothelium and in the esophagus TGFβ signaling profoundly disrupts barrier integrity and decreases TER (Birukova et al., 2005a; Goldberg et al., 2002; Hurst et al., 1999; Nguyen et al., 2018; Pittet et al., 2001), in immortalized two-dimensional jejunal cell lines and in colon cancer cell lines *in vitro*, TGFβ treatment increases TER (Hering et al., 2011; Howe et al., 2005; McKay and Singh, 1997; Planchon et al., 1994, 1999; Roche et al., 2000; Xiao et al., 2017). However, until now, the impact of canonical TGFβ signaling for maintenance of barrier function in non-malignant colon epithelium *in vitro* or in colon epithelium *in vivo* had yet to be explored.

Our data indicate that loss of canonical TGFβ signaling in the intestinal epithelium of mice through conditional and tissue-specific deletion of SMAD4 leads to increased colon mucosal permeability to a 4kD dextran molecule (diameter 28 Å). However, these mice show no gross or histologic evidence of mucosal ulceration or damage, and no increased translocation of luminal bacteria across the colon epithelium, suggesting that the permeability defect due to epithelial SMAD4 loss likely represents a tight junction-dependent "leak" phenotype rather than a more extensive mucosal "damage" phenotype (Shen et al., 2011). While we did observe minor changes in mucin-related gene expression with intestinal SMAD4 loss *in vivo* (including increased expression of *Muc1*, *Muc13*, and *Muc20* and decreased expression of *Muc2*), only *Muc13* was significantly and reciprocally altered with TGFβ pathway stimulation *in vitro.* Additionally, staining for mucin accumulation demonstrated no obvious changes in mucin quantity or distribution, making a primary TGFβ-dependent mucin barrier defect unlikely to be a major driver of barrier dysfunction. While paracellular transport via the tight

junction is mediated by two functionally distinct pathways (the "pore" and "leak" pathways (Shen et al., 2011)), increased permeability to macromolecule 4kD dextran is suggestive of a "leak" pathway dependent process (Anderson and Itallie, 2009; Itallie et al., 2008, 2009; Shen et al., 2011; Weber et al., 2010; Zuo et al., 2020) whereby passage of larger ions and molecules up to 100Å are able to pass without charge selectivity. Additionally, while some statistically significant differences in microbiome composition/diversity were detected by 16S sequencing, the implications for their influence on inflammatory, tumorigenic, or barrier phenotypes seen in *Smad4*$^{\Delta Lrig1}$ mice are unclear.

RNA-seq analysis of *Smad4*$^{\Delta Lrig1}$ mice compared to control revealed alterations in a number of genes related to barrier function. While alterations in any of these genes could contribute to the barrier dysfunction observed here or to the inflammatory phenotype previously described (Means et al., 2018), we chose to focus our attention on five Claudin genes (*Cldn2, Cldn3, Cldn4, Cldn7,* and *Cldn8*) for two main reasons. First, in addition to demonstrating altered expression levels in colon epithelium *in vivo* with SMAD4 loss, these five genes additionally demonstrated reciprocal changes in mouse colonoids with TGFβ pathway stimulation *in vitro*, suggesting that these genes could be directly modulated by TGFβ signaling as opposed to being a downstream effect of other pathways regulated by SMAD4 loss *in vivo* (such as increased inflammation). Second, among the 11 genes that were reciprocally changed with both SMAD4 loss *in vivo* and TGFβ pathway stimulation *in vitro*, these five Claudin genes are known to transcribe proteins with critical roles in tight junction function and are therefore likely to regulate the observed barrier phenotype (Günzel and Yu, 2013; Luettig et al., 2015; Prasad et al., 2005; Raju et al., 2020; Randall et al., 2016; Rosenthal et al., 2010; Tanaka et al., 2015; Tsukita et al., 2018; Xu et al., 2019; Zeissig et al., 2007).

We also demonstrated that at least some of these observed changes in tight junction-related genes observed *in vivo* are the result of colonocyte-intrinsic TGFβ signaling via SMAD4. While TGFβ pathway stimulation resulted in decreased *Cldn2* and *Cldn8* expression and increased *Cldn4* and *Cldn7* expression in wild type colonoids, this TGFβ-responsiveness was lost with SMAD4 deletion *in vitro*, confirming that these Claudin genes are regulated by the SMAD-dependent (canonical) TGFβ signaling pathway in mouse colon epithelium and that this regulation occurs in a cell-autonomous manner. Importantly, we also demonstrated the TGFβ pathway stimulation of wild type colonoids grown on transwell membranes *in vitro* results in increased TER and that this effect is SMAD4-dependent. Collectively, these data suggest an epithelium-intrinsic role for canonical TGFβ signaling in colonic barrier function.

While we have yet to fully understand the mechanism for TGFβ-dependent modulation of Claudin gene expression, our data do allow us to make several conclusions regarding mechanism of action. First, from the *in vitro* SMAD4 knockout experiment described above, we know that *Cldn2, Cldn4, Cldn7,* and *Cldn8* are regulated by TGFβ through the canonical (SMAD dependent) pathway. This differs from what has been published previously with regard to TGFβ regulation of barrier function, the majority of which implicates non-canonical pathways (Birukova et al., 2005a; Clements et al., 2005; Goldberg et al., 2002; Hering et al., 2011; Howe et al., 2002, 2005; Lu et al., 2006a). Second, the impact of TGFβ signaling on the expression of *Cldn2, Cldn4,* and *Cldn8* is blunted with blockade of RNA transcription, demonstrating that TGFβ modulation of *Cldn2, Cldn4,* and *Cldn8* are dependent on nascent RNA transcription. Third, TGFβ pathway regulation of *Cldn4* and *Cldn8* appears to be independent of nascent protein translation, as evidenced by the fact that CHX co-treatment did not abrogate the ability of TGFβ pathway stimulation to alter their expression levels. An additional point of interest is that Qi and colleagues examined SMAD4-DNA binding in small intestinal stem cells through chromatin immunoprecipitation sequencing (ChIP-seq) and reported in their supplemental data that SMAD4 binding sites existed in the promoter/enhancer regions of multiple junctional protein-related genes including *Cldn3*, *Cldn4, Cldn7, Cldn12, Cldn14, Cldn22, Cldn23, and Cldn25* (Qi et al., 2017). Given the tissue- and context-dependent nature of SMAD complex binding and Claudin gene expression, beyond the

scope of this dissertation, similar chromatin-binding experiments will be required to determine whether SMAD binding to the same sites is evident in colon epithelium. Nonetheless, collectively, these data suggest the possibility that the canonical TGFβ signaling pathway modulates the expression of a subset of Claudin genes through direct SMAD complex binding to their respective promoter/enhancer regions.

Importantly, we found that human biopsy specimens from colon cancers and patients with IBD have significantly altered expression levels of *SMAD4* as well as *CLDN2, CLDN4, CLDN7,* and *CLDN8,* consistent with prior reports (Bornholdt et al., 2011; Dhawan et al., 2011; Klausen et al., 2018; Lameris et al., 2012; Luettig et al., 2015; Means et al., 2018; Prasad et al., 2005; Randall et al., 2016; Ueda et al., 2007; V et al., 2017; Vancamelbeke et al., 2017; Wasserman et al., 2018; Xu et al., 2018; Yan et al., 2016). Additionally, we found that *SMAD4* levels are significantly correlated with *CLDN2, CLDN4, CLDN7,* and *CLDN8* levels in human IBD and/or CRC. Interestingly, while *CLDN2, CLDN4,* and *CLDN7* are directionally altered in ways that are consistent with the changes observed with intestinal SMAD4 loss in mice, *CLDN8* expression levels are altered in the opposite direction. While we found *Cldn8* to be significantly decreased in mouse colonoids with TGFβ pathway stimulation *in vitro* and to be significantly increased with SMAD4 loss in mice, *CLDN8* is significantly decreased and positively correlated with *SMAD4* expression in both human IBD and colon cancer specimens. The reason for this disparity between our observations in mice and those observed in human disease are not entirely understood. One possibility is that other important pathways that are frequently altered in human IBD and colon cancers besides the TGFβ pathway (including *APC/WNT*, *KRAS*, *BRAF*, *TP53* pathways and others (Koveitypour et al., 2019)) also regulate *CLDN8* expression, masking the SMAD-dependent effects in these human disease specimens. Alternatively, it is possible that the TGFβ signaling pathway via SMAD4 in humans has a different effect on *CLDN8* expression than it does on the homologous gene in mice. Such a hypothesis is supported by a recent publication by Toyonaga and colleagues, which demonstrated that TGFβ pathway stimulation via the ALK1 receptor increased *CLDN8* expression in cultured human intestinal epithelial cells (Toyonaga et al., 2020). Further studies are required to understand the relationship more fully between canonical TGFβ signaling, *CLDN8* expression, and human IBD and colon cancer.

The implications of our findings are wide ranging. First, TGFβ signaling is known to be frequently disrupted in IBD, CRC, and CAC through TGFβ receptor mutations, loss of SMAD protein expression, and other pathway alterations. Additionally, barrier defects are known to contribute to intestinal inflammation and IBD, and our findings suggest that TGFβ-dependent barrier regulation may be a contributing factor in IBD pathogenesis. Second, Claudin proteins, while best known for roles in governing paracellular permeability, also have additional roles in cell proliferation, transformation, carcinogenesis, and metastasis (Bhat et al., 2015; Dhawan et al., 2005, 2011; Gowrikumar et al., 2019; Pope et al., 2014). The alterations we see in *Cldn2, Cldn4, Cldn7,* and *Cldn8* in these experiments very well could have implications for CRC and CAC development in mouse models and in human cancers beyond their direct role in maintaining barrier function. Third, with the increased prevalence of TGFβ inhibitors in therapeutics and clinical trials (Ciardiello et al., 2020), it is important to understand that these therapies may ultimately have an impact on intestinal barrier function/junctional protein expression which may have clinical implications.

Several elements of the relationship between TGFβ signaling and colon epithelial barrier function remain to be discovered. First, the precise mechanisms by which these Claudin genes are regulated by TGFβ signaling are yet to be resolved. While our data suggest that the TGFβ-dependent regulation of the Claudin genes is dependent on the canonical signaling pathway, is reliant on nascent transcription and, in some cases, is independent of novel protein translation, more work needs to be done to definitively determine whether these genes are regulated by direct SMAD complex binding to promoter/enhancer regions or whether other cell-intrinsic processes are governing these changes. Second, while our data support the idea that TGFβ via SMAD4 signaling directly modulates the expression of critical junctional proteins *in vitro*, whether a primary barrier

defect due to intestinal SMAD4 deletion contributes to the inflammatory and CAC phenotypes that we previously discovered in *Smad4*$^{\Delta Lrig1}$ mice remains unexplored. Future *in vivo* experiments targeting specific junctional protein alterations will help to determine whether abrogating some of the barrier-specific effects of SMAD4 loss can reverse the observed barrier defect and/or inflammatory phenotype previously described. Third, how SMAD4-dependent regulation of inflammation *in vivo* impinges on barrier function remains unexplored. Cytokines, including TNFα and IFNγ, have been previously shown to impact the expression of Claudins in multiple tissue types (Amoozadeh et al., 2015; Capaldo and Nusrat, 2009; Mazzon and Cuzzocrea, 2007; Watson et al., 2005), and intestinal SMAD4 loss has previously been demonstrated to significantly impact inflammatory gene expression and leukocyte recruitment (Means et al., 2018). It is possible, even likely, that in addition to TGFβ-dependent barrier regulation, direct regulation of inflammatory gene expression by SMAD4 may have an additive downstream effect on Claudin gene expression and/or barrier function *in vivo,* and this remains to be explored. Finally, we chose to focus this paper primarily on the tight junction-related genes given the "leak" phenotype observed *in vivo* with intestinal SMAD4 loss, however it is highly possible that some of the other barrier function-related genes (including *Pkp3*, *Gjb3*, *Gja1*, *Ceacam10*, *Ceacam18*, and *Muc13*) are also playing an important role in TGFβ-dependent maintenance of barrier function, and these genes and their protein products deserve closer examination in the future.

In summary, we discovered that loss of epithelial canonical TGFβ signaling via intestine-specific SMAD4 loss is associated with a barrier defect in mouse colon that is consistent with a deficiency in the tight junction-mediated "leak" pathway. Further, we conclude from our observations that the canonical TGFβ signaling pathway regulates the expression of several tight junction-related genes as well as colonic epithelial cell TER in a cell-autonomous manner. Further investigation is necessary to fully understand the mechanism of TGFβ regulation of Claudin gene expression as well as the clinical implications of these findings.

CHAPTER V

TGFβ SIGNALING REGULATES STEMNESS IN COLONIC EPITHELIAL CELLS OF MICE

Abstract:
Background: We have previously demonstrated that mice lacking intestinal *Smad4* expression demonstrate increased colonic inflammation, increased colonic permeability, and increased susceptibility to colitis-associated cancer. As an expanded stem cell compartment could contribute to any or all of these phenotypes, we hypothesized that mice lacking intestinal *Smad4* expression could have an expanded colonic stem cell compartment.
Methods: Transgenic mice with Cre-recombinase expression under the control of an intestine-specific promoter (*Lrig1*) and LoxP sites inserted around critical exons of the *Smad4* gene locus were administered tamoxifen to induce intestine-specific *Smad4* loss ($Smad4^{\Delta Lrig1}$). Four weeks after recombination, mice were dissected, and RNA-sequencing (RNAseq) analysis of their colon epithelium was performed. SMAD4+ and SMAD4 knockout (KO) colon organoids (colonoids) were previously generated from these mice and cultured *in vitro* for qPCR experiments. $Smad4^{\Delta Lrig1}$ and SMAD4+ control mice were additionally subjected to three rounds of Dextran Sulfate Sodium (DSS) in drinking water to initiate chronic inflammation, and then one month following DSS treatment, their colon epithelium was isolated for single cell RNAseq (scRNAseq).
Results: Bulk RNAseq of colon epithelium from $Smad4^{\Delta Lrig1}$ and SMAD4+ control mice demonstrated significant up-regulation of multiple stem cell-related genes with intestinal SMAD4 loss. qPCR experiments on SMAD4 KO and SMAD4+ control colonoids confirmed that TGFβ signaling via SMAD4 regulates the expression of some stem cell-related genes (*Lgr5, Atoh1,* and *Lrig1*) in a cell-autonomous manner. scRNAseq analysis of DSS-treated mice demonstrated an expanded stem cell compartment and lower numbers of Transit Amplifying and Tuft cell populations in $Smad4^{\Delta Lrig1}$ relative to SMAD4+ control mice. $Smad4^{\Delta Lrig1}$ mice additionally demonstrated increased expression of multiple genes related to innate immune response in multiple subpopulations of colon epithelial cells.
Conclusion: We found evidence that loss of intestinal *Smad4* expression is associated with increased stem cell related gene expression as well as an expansion of the stem cell compartment in the colons of mice. Additionally, we find evidence that canonical TGFβ signaling regulates the expression of at least a subset of stem cell-related genes in a cell-autonomous manner. Further work needs to be done to determine how TGFβ signaling via SMAD4 regulates the expression of stem cell-related genes and colon stem cell differentiation, and whether this regulation has a direct effect on the previously observed phenotypes (inflammation, barrier dysfunction, or tumorigenesis) observed in mice lacking intestinal expression of *Smad4*.

Background:

As stated in the preceding chapters, we have found evidence that loss of canonical TGFβ signaling via intestine-specific *Smad4* deletion causes increased colonic inflammation, altered junctional protein expression, increased intestinal permeability, and increased susceptibility to colitis-associated cancer (CAC). In addition, prior unpublished work from our lab suggests that there may be an expanded stem cell compartment in mice lacking intestinal *Smad4* expression. Colonic crypts lacking *Smad4* expression had expanded zones of LRIG1+ and SOX9+ cells suggesting an expansion of the stem cell compartment. Interestingly, the number of Ki67+ proliferating cells was not different between SMAD4+ and SMAD4- crypts, suggesting that SMAD4 regulates the balance of stem and transient amplifying cells rather than increasing both progenitor populations. TGFβ signaling and SMAD4 have also previously been implicated in cell cycle regulation (Dai et al., 1999; Fink et al.,

2001), making alterations in colon stem cell composition and colon epithelial cell composition/differentiation due to *Smad4* loss mechanistically plausible.

Importantly, there are alterations in junctional protein expression along the gastrointestinal tract and along the crypt-villus axis, and different intestinal epithelial cell subsets are known to have distinct junctional protein expression and permeability characteristics (Fihn et al., 2000; Lameris et al., 2012; Pearce et al., 2018). For example, Claudin 2 is a well-known pore forming Claudin, with increased levels of Claudin 2 associated with increased intestinal permeability (Luettig et al., 2015; Randall et al., 2016; Rosenthal et al., 2010). At the same time, Claudin 2 is largely isolated at the crypt base and spared from the differentiated colonocytes (Raju et al., 2020). This data collectively led us to ask whether intestinal-specific deletion of *Smad4* in mice leads to an expanded stem cell compartment, and whether such an alteration in epithelial cell composition could be contributing to the inflammatory, barrier, or tumorigenic phenotypes previously observed in $Smad4^{\Delta Lrig1}$ mice.

Methods:

Mouse model

Animal work was performed with approval from the Vanderbilt University Institutional Animal Care and Use Committee and followed ARRIVE guidelines. Mouse alleles $Lrig1^{CreERT2}$ and $Smad4^{fl/fl}$ have been previously published (Bardeesy et al., 2006; Means et al., 2008, 2018; Powell et al., 2012) and were bred into the C57BL/6J background for at least 10 generations. Controls were sibling littermates and cage mates, and male/female mice were split evenly between experimental arms. Mice were given tamoxifen (2mg in 0.1mL corn oil) intraperitoneally two times on alternating days after 8 weeks of age to ensure that *Smad4* gene deletion occurred during adulthood and not during development. After tamoxifen treatment, bedding was mixed among cages within an experiment once per week.

Mice with $Lrig1^{CreERT2}$ $Smad4^{fl/fl}$ genotype that received tamoxifen injections and who were confirmed by immunohistochemistry (IHC) to have undergone recombination with loss of SMAD4 protein in the intestinal crypts are referred to as $Smad4^{\Delta Lrig1}$. $Smad4^{\Delta Lrig1}$ mice demonstrate loss of SMAD4 protein in 90% or more of colon crypts (Means et al., 2018). SMAD4-expressing control mice (mice with $Smad4^{fl/fl}$ genotype + tamoxifen injection) are referred to as $Smad4^{fl/fl}$, SMAD4+, or simply "control" mice for simplicity.

RNA-Sequencing (RNA-seq) Data Analysis

Previously published RNA-seq data sets generated in our lab (Means et al., 2018) were utilized for *in silico* analysis of differentially expressed stem and differentiation markers. Data files are publicly available on the National Institute of Health Gene Expression Omnibus (GEO) database (Barrett et al., 2013; Edgar et al., 2002), accession number GSE100082.

Colon Organoid ("Colonoid") Experiments

Mouse colonoids were generated and cultured as previously described (Means et al., 2018). Colonoids were suspended and plated in 50-µL beads of Growth Factor Reduced Matrigel (GFR; Corning, Tewksbury, MA). Complete colonoid medium was composed of 40% basal medium (advanced DMEM/F12 [Gibco] supplemented with penicillin/streptomycin [Gibco], N2 [Gibco], B27 [Gibco], Glutamax [Gibco], HEPES [Sigma Aldrich], 50 ng/mL epidermal growth factor [R&D Systems]), 40% Wnt3a-conditioned medium, 10% R-Spondin–conditioned medium, and 10% Noggin-conditioned medium. Colonoids were grown at 37°C in 5% CO_2, media was changed every 2-3 days, and colonoids were passaged every 5-7 days.

After establishing colonoids in culture, colonoids were incubated at 37°C with 20µg/mL 4-OH-Tamoxifen or methanol vehicle control for 24 hours to create a SMAD4 knockout (KO) line or a matched

SMAD4+ control line, respectively. SMAD4 KO and control colonoid lines were maintained in culture under the same conditions.

Colonoids at density of 70-100 per well were treated three days after passage with TGFβ1/BMP2 (3ng/mL and 100ng/mL, respectively) and/or 4mM HCl + 0.1% BSA in PBS vehicle control at designated time points for qPCR experiments. Wells treated with BMP2 had the BMP-inhibitor, Noggin, withheld from the media.

Quantitative Reverse-Transcription Polymerase Chain Reaction (qPCR)

RNA was extracted from colonoids from at least 3 experimental replicates and purified as described (Freeman et al., 2012). Samples were run using a standard SYBR Green qPCR protocol (Green and Sambrook, 2018). All samples were run in triplicate with a negative control on a CFX96 Thermal Cycler (Bio-Rad, Hercules, CA). A well-known TGFβ/SMAD-response gene (Zhao et al., 2000), *Smad7*, was used for a positive control to confirm TGFβ pathway stimulation in all experimental replicates. mRNA levels were normalized to the level of *Pmm1*. All qPCR primer sequences are listed in **Table 5.1**. Each point on each qPCR graph represents a single experimental replicate (each done on a separate day), and each experimental replicate reflects the mean value of three technical replicates.

Antibodies				
Target Protein	**Company**	**Product Number**	**Dilution**	**References**
SMAD4	Abcam	40759	1:1000 (IHC [FFPE])	(Means et al., 2018)
qPCR Primers				
Target Gene	**Forward (5' to 3')**		**Reverse (5' to 3')**	
Lgr5	cttcactcggtgcagtgct		cagccagctaccaaataggtg	
Atoh1	tgcgatctccgagtgagag		tctcttctgcaaggtctgatttt	
Lrig1	actcaagagtctgcgggtct		tcctcgattgtacccgagat	
Alpi	aggatccatctgtcctttggt		cagctgccttcttgttcc	
Chga	cgatccagaaagatgatggtc		cggaagcctctgtctttcc	
Muc3	ttctatgggccacggtgt		actggttactgtcacactcactcc	
Smad7	acccccatcaccttagtcg		gaaaatccattgggtatctgga	
Pmm1 (Reference Gene)	gggtggctctgactactctaagat		acacgtagtcaaacttctcaatgact	

Table 5.1: Antibodies and qPCR primers utilized in Chapter V. IHC = immunohistochemistry. FFPE = Formalin fixed and paraffin embedded.

Single Cell RNA-sequencing (scRNAseq) Analysis

Three *Smad4*$^{\Delta Lrig1}$ and three SMAD4+ control mice were subjected to three rounds of 2.2% Dextran Sulfate Sodium (DSS) in drinking water (five days on, five days off) to induce chronic colitis. Mice were switched back to normal drinking water and allowed to recover in their cages for one month following the final round of DSS treatment. One month following DSS, mice were dissected.

To isolate colon crypts, the colons were removed and cut longitudinally. Colons were then washed in ice cold PBS x3 to remove excess debris/mucus. Tissue was resuspended in 10mL chelation buffer (50mL sterile PBS + 300µL 0.5M EDTA + 25µL 1M Dithiothreitol [DTT]) and placed on a rotator for 75 minutes at 4°C. Chelation buffer was changed at 30 and 60 minutes. Tissue was then moved to a 15mL canonical tube with 10mL ice cold sterile PBS. Tubes were shaken a total of 3 times, each time for 45 seconds, to remove crypts.

The second and third fraction of crypts were washed x3 in sterile PBS (250xg x5min at 4°C), resuspending cells each time with gentle shaking (NO pipetting).

To dissociate crypts into single cells, crypt pellet was resuspended in 1.9 mL of cold protease mixture (Banerjee et al., 2020) (2.5mg/mL DNAse [Sigma DN25-100mg] + 5mg/mL Protease [Sigma P5380-250mg] in ice cold sterile PBS) using a wide bore p1000 pipette tip. The 2 mL tube (with a small air bubble for agitation) was placed on rotator at 4°C x25 minutes, stopping to triturate gently with a wide bore p1000 tip every 10 minutes. Once cells were near 100% dissociated (<5% intact crypts), cells were spun down at 700xg x5 min at 4°C, filtered through a 70µm filter, then washed in ice cold PBS x3. After the final wash, cells were filtered through a 40µm filter and single cells were immediately encapsulated using the inDrop microfluidics system (1CellBio, Watertown, MA) as previously described (Southard-Smith et al., 2020). Encapsulated samples were submitted for sequencing by the VANTAGE core laboratory using paired end 150 base pairs (PE150) reads on the NovaSeq 6000 platform, 100 million reads per sample.

scRNAseq data was analyzed by our expert bioinformatics colleagues, Dr Qi Liu and Dr Jing Yang. DropEst was used to preprocess scRNA-seq reads and to generate gene-by-cell count matrices (Petukhov et al., 2018). Specifically, reads with expected structure was kept and cell barcodes and unique molecular identifier (UMI) were extracted by dropTag. Demultiplexed reads were aligned to the mouse reference transcriptome mm10 using STAR (Dobin et al., 2013). Uniquely mapped reads were quantified into UMI-filtered counts by dropEst. Cells with >10% mitochondrial reads, <500 UMI counts, <200 genes expressed, or >5,000 genes expressed were considered low-quality and were excluded. The gene-by-cell count matrix was normalized to a total of 10,000 UMI counts, and log-transformed after the addition of 1. Top 2000 highly variable genes were selected for principal component (PC) analysis. Cells were clustered by the Louvain method based on the shared nearest neighbor graph built from the top 30 PCs and visualized by UMAP using the Seurat package (Butler et al., 2018; Stuart et al., 2019). Clusters with low UMI reads and insufficient marker genes were considered as low-quality cells or empty droplets and removed from the downstream analysis. Differential expression between SMAD4 KO and WT in each cell type were identified using the Seurat Package.

Ligand-receptor interactions between cell types were predicted by CellChat (Jin et al., 2021). Pathways and upstream regulators were analyzed using IPA software (Qiagen, Inc, https://www.qiagenbioinformatics.com/products/ingenuity-pathway-analysis). Immune cell composition was predicted using ImmuCC software (http://218.4.234.74:3200/immune/) as previously described (Chen et al., 2018).

Statistical Analysis

Results from *in vivo* bulk RNAseq assays were compared as described (Means et al., 2018). *In vitro* colonoid qPCR assays were compared using non-parametric Kruskal-Wallis test and post hoc Welch's *t* test. Results from *in vivo* scRNAseq was analyzed as described in the section above. Statistical analyses were performed using GraphPad Prism 9 Software (San Diego, CA), except as otherwise indicated. Throughout the chapter, statistical significance is designated as: ns ($p \geq 0.05$), * ($p < 0.05$), ** ($p < 0.01$), or *** ($p < 0.001$).

Results:

Loss of intestinal SMAD4 expression is associated with increased expression of multiple stem cell markers in the colon epithelium by bulk RNAseq

Given prior (unpublished) evidence from our laboratory that suggests intestinal SMAD4 loss may be associated with an expanded stem cell compartment and that alterations in epithelial cell composition are associated with alterations in junctional protein expression and barrier function (Fihn et al., 2000; Pearce et al.,

2018), we were interested in determining whether there is a change in epithelial cell composition and/or an increase in the stem cell composition of *Smad4*$^{\Delta Lrig1}$ mice.

In order to investigate this, we referred to previously generated bulk RNAseq data from the colon epithelium of three *Smad4*$^{\Delta Lrig1}$ and three SMAD4+ control mice. Genes that are significantly dysregulated with intestinal SMAD4 loss (FDR <0.05) and are known to transcribe intestinal stem or differentiation-markers are included in **Table 5.2**. This analysis demonstrated several stem- and differentiation-marker related genes that are significantly dysregulated in *Smad4*$^{\Delta Lrig1}$ mice. Several intestinal stem cell markers (including *Lgr5*, *Smoc2, Sox9,* and *Bmi1*) are significantly increased with intestinal SMAD4 loss, while two intestinal stem cell markers are decreased (*HopX* and *Ascl2*). On the other hand, several markers of intestinal epithelial differentiation (including *Muc2, Chga, Dclk1,* and *Alpi*) are significantly decreased in *Smad4*$^{\Delta Lrig1}$ mice relative to SMAD4+ controls. Overall, these data suggest that there is either an expansion of the stem cell compartment in *Smad4*$^{\Delta Lrig1}$ mice, or that the colonic epithelium in these mice is expressing higher levels of stem cell markers and lower levels of differentiation markers while cell composition remains unchanged.

Gene Symbol	Protein Function	Log_2 Fold Change	P-value	FDR	Base Mean
Lgr5	Intestinal stem cell marker, member of *Wnt* signaling pathway	1.39	3.8×10^{-10}	1.0×10^{-8}	13.4
Smoc2	Intestinal stem cell marker, functions in embryogenesis and wound healing	1.08	3.8×10^{-17}	3.9×10^{-15}	55.7
Sox9	Stem cell transcription factor, expressed during proliferation, proto-oncogene	0.49	0.0029	0.010	84.2
Bmi1	Stem cell marker, negatively regulates cell cycle inhibitors, proto-oncogene	0.42	0.0067	0.021	25.2
Muc2	Marker of differentiated goblet cells, encodes a member of mucin protein family	-0.39	0.015	0.041	5181.8
Chga	Marker of differentiated enteroendocrine cells, precursor to several functional peptides that regulate hormone release	-0.63	2.2×10^{-4}	0.0012	31.0
Dclk1	Marker of differentiated tuft cells, involved in tissue regeneration	-0.71	0.0033	0.012	9.3
HopX	Stem cell marker, regulation of proliferation/differentiation	-0.72	2.2×10^{-6}	2.3×10^{-5}	34.9
Alpi	Marker of intestinal cell differentiation, produced in brush border, expressed in TA region and differentiated enterocytes	-1.20	0.0014	0.0056	16.7
Ascl2	Intestinal stem cell marker, transcription factor, *Wnt* target gene	-2.26	7.9×10^{-16}	6.4×10^{-14}	5.7

Table 5.2: Stem and differentiation markers that are significantly altered (FDR <0.05) in the colon epithelium of *Smad4*$^{\Delta Lrig1}$ versus SMAD4+ control mice by bulk RNAseq. Genes listed in descending order of most to least upregulated. FDR = False discovery rate (q-value). TA = Transit Amplifying. Data generated from RNAseq of the colon epithelium of three *Smad4*$^{\Delta Lrig1}$ and three SMAD4+ control mice. Mice were littermates and cage mates. Genotypes were split evenly between sexes.

Canonical TGFβ signaling alters stem cell marker expression in mouse colon epithelial cells in a cell-autonomous manner

In order to determine if changes in stem and differentiation markers are occurring due to intestinal SMAD4 loss in a cell-autonomous manner, we examined the expression of several stem/differentiation marker

genes in mouse colonoids by qPCR. SMAD4 KO and SMAD4+ control colonoids were treated with TGFβ1/BMP2 or vehicle for 24 hours before RNA was collected and qPCR was performed (**Figure 5.1**). This experiment demonstrated that TGFβ pathway of wild type (SMAD4+) colonoids led to a significant reduction in expression of multiple stem cell-related genes including *Lgr5, Atoh1,* and *Lrig1*. For *Lgr5* and *Lrig1*, expression levels were significantly increased with SMAD4 KO compared to SMAD4+ colonoids after 24 hours of TGFβ pathway stimulation. For all three stem cell marker genes examined, SMAD4 KO colonoids did not demonstrate a significant change in gene expression due to TGFβ pathway stimulation. Collectively, these data suggest that TGFβ pathway stimulation negatively regulates the expression of some stem cell-related genes (including *Lgr5, Atoh1,* and *Lrig1*), and that this regulation occurs in a manner dependent on SMAD4 expression.

In this experiment, we similarly examined the impact of TGFβ pathway signaling and SMAD4 expression on differentiation markers. This analysis demonstrated that TGFβ/BMP treatment of SMAD4+ control colonoids resulted in decreased expression of *Chga* and *Muc3*. Interestingly, mRNA expression for both of these genes decreased further with SMAD4 KO relative to vehicle- and/or TGFβ/BMP-treated control colonoids. The explanation for why *Chga* and *Muc3* levels appear to decrease with both TGFβ pathway stimulation and SMAD4 KO of colonoids *in vitro* is not entirely clear. *Alpi* mRNA levels, on the other hand, appeared to increase slightly with TGFβ pathway stimulation of wild type (SMAD4+) control colonoids (although not significantly, p=0.114) and decrease with SMAD4 KO relative to vehicle treated SMAD4+ controls. Collectively, these data suggest that canonical TGFβ signaling is not stimulating the expression of these three differentiation markers (*Alpi, Chga,* and *Muc3*) in a cell-autonomous manner.

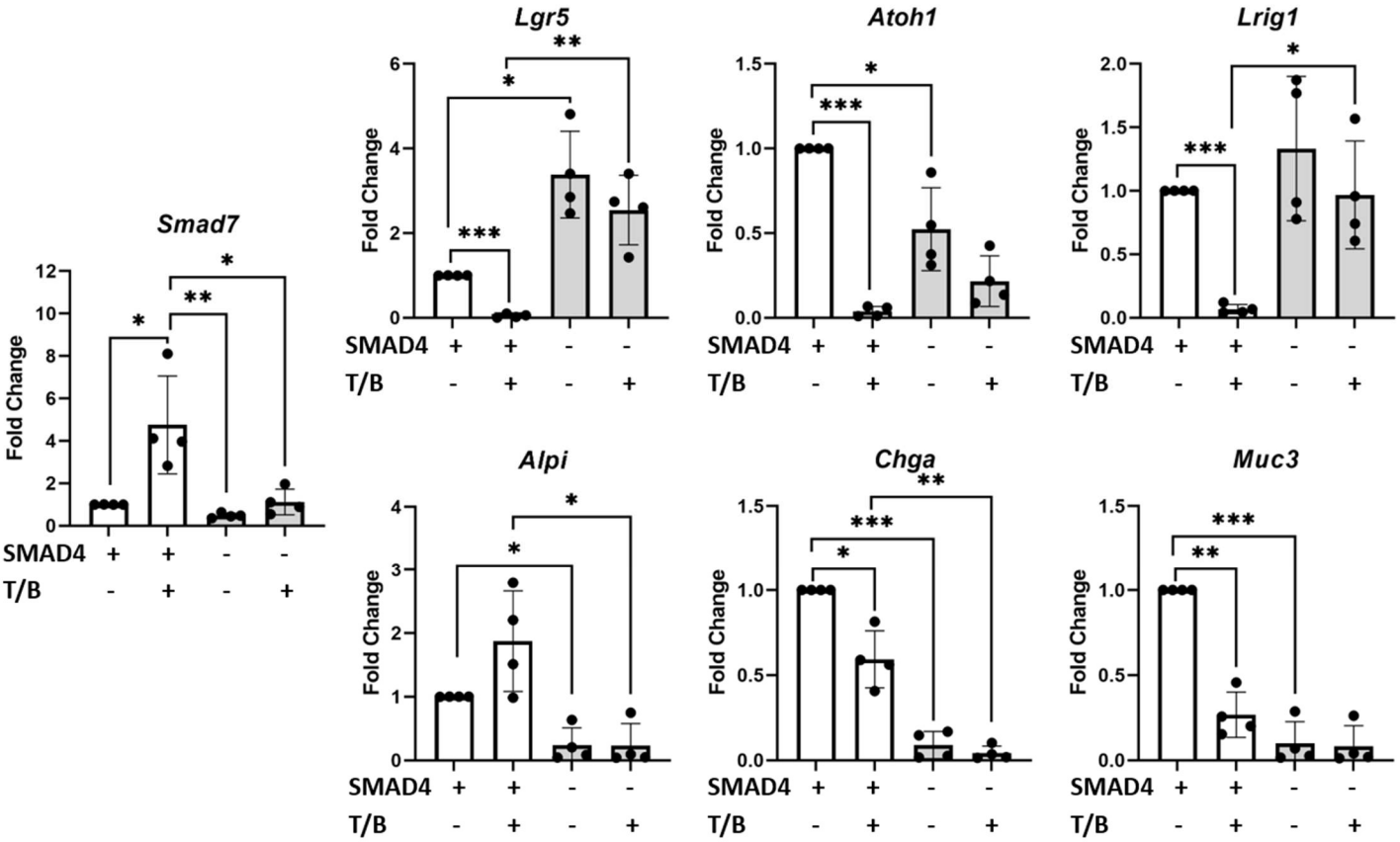

Figure 5.1 – TGFβ signaling via SMAD4 regulates the expression of stem cell markers in a cell-autonomous manner. qPCR of SMAD4 KO (gray bars) and SMAD4+ control (white bars) colonoids with and without TGFβ1/BMP2 stimulation for 24 hours. Fold change indicates the relative level of mRNA relative to vehicle treated SMAD4+ controls for indicated genes. Each data point represents a single biological replicate, with biological replicates treated and harvested on different days. Experimental arms were compared using non-parametric Kruskal-Wallis test with post hoc Welch's *t* test. *Smad7* is used as a positive control to confirm ligand activity.

To begin understanding the mechanism by which canonical TGFβ signaling pathway is modulating the expression of these stem cell markers, a time course experiment was performed. Wild type (SMAD4+) colonoids underwent vehicle or TGFβ1/BMP2 co-treatment for 0-, 2-, 4-, or 16-hours before RNA was harvested and qPCR performed (**Figure 5.2**). For *Lgr5* and *Lrig1*, mRNA expression levels were significantly decreased with TGFβ pathway stimulation at 16 hours post-treatment, but not at 0-, 2-, or 4-hours. For *Atoh1*, on the other hand, mRNA expression level was significantly decreased as early as 4 hours post-treatment and decreased further at 16 hours relative to vehicle-treated controls. These data demonstrates that canonical TGFβ signaling decreases the expression of all three stem cell markers examined (*Lgr5, Atoh1,* and *Lrig1*) by 4-16 hours post-TGFβ pathway stimulation. On the other hand, this time course experiment demonstrated no significant change in mRNA expression levels of differentiation markers *Alpi, Chga,* or *Muc3* at 0-, 2-, 4-, or 16-hours after TGFβ pathway stimulation. This is consistent with the notion that canonical TGFβ signaling is unlikely to be stimulating the expression of these three differentiation markers in a cell-autonomous manner.

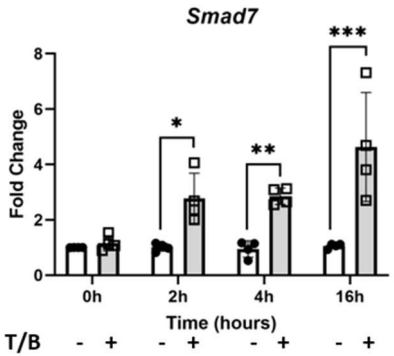
Smad7
Fold Change
0
2
4
6
8
*
**
***
0h
2h
4h
16h
Time (hours)
T/B - + - + - + - +

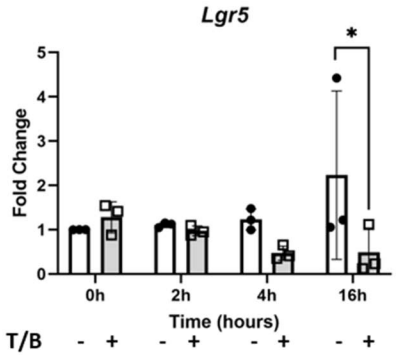
Lgr5
Fold Change
0
1
2
3
4
5
*
0h
2h
4h
16h
Time (hours)
T/B - + - + - + - +

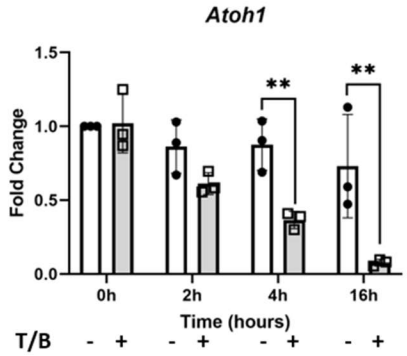
Atoh1
Fold Change
0.0
0.5
1.0
1.5
**
**
0h
2h
4h
16h
Time (hours)
T/B - + - + - + - +

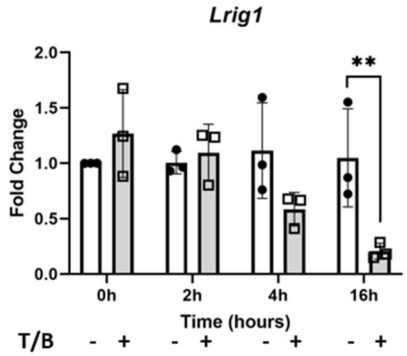
Lrig1
Fold Change
0.0
0.5
1.0
1.5
2.0
**
0h
2h
4h
16h
Time (hours)
T/B - + - + - + - +

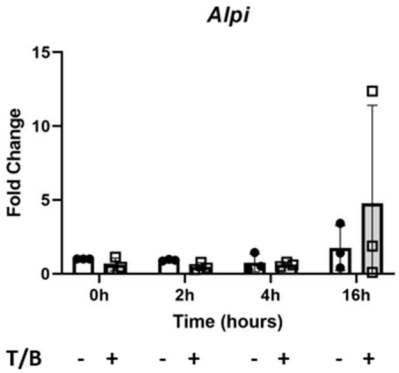
Alpi
Fold Change
0
5
10
15
0h
2h
4h
16h
Time (hours)
T/B - + - + - + - +

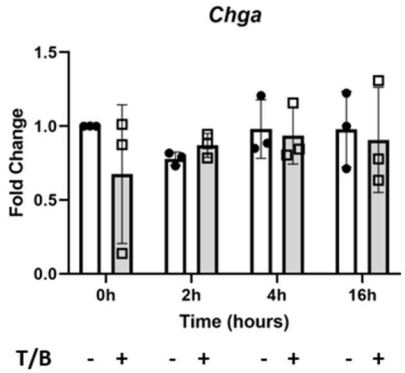
Chga
Fold Change
0.0
0.5
1.0
1.5
0h
2h
4h
16h
Time (hours)
T/B - + - + - + - +

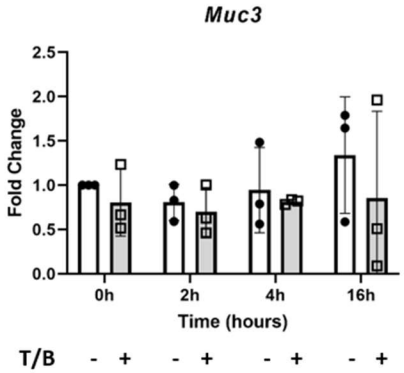
Muc3
Fold Change
0.0
0.5
1.0
1.5
2.0
2.5
0h
2h
4h
16h
Time (hours)
T/B - + - + - + - +

Figure 5.2 – qPCR for stem/differentiation markers from SMAD4+ colonoids treated with TGFβ1/BMP2 (grey bars/open boxes) or vehicle (white bars/closed circles) for 0-, 2-, 4-, and 16-hours. Fold change indicates the relative level of mRNA for indicated genes compared to vehicle-treated control at 0 hours. Each data point represents a single biological replicate, with biological replicates treated and harvested on different days. Experimental arms were compared using non-parametric Kruskal-Wallis test with post hoc Welch's t test. *Smad7* is used as a positive control to confirm ligand activity.

Loss of intestinal SMAD4 expression is associated with alterations in colonic epithelial cell composition following DSS colitis

In order to determine whether the increased stem cell-related gene signature observed with SMAD4 loss *in vivo* and *in vitro* is the result of an expanded stem cell compartment versus increased expression of stem cell-related genes, we performed scRNAseq analysis. Three *Smad4*$^{\Delta Lrig1}$ and three SMAD4+ control mice were subjected to three rounds of DSS in drinking water (5 days on, 5 days off) to induce chronic colitis. One month following completion of DSS, mice were dissected and scRNAseq analysis of their colonic epithelium was performed.

In addition to confirmatory SMAD4 IHC of the residual small bowel, the colonic SMAD4 expression of each of the six samples was confirmed by gene expression analysis. The three *Smad4*$^{\Delta Lrig1}$ had diminished expression of *Smad4* and diminished expression of SMAD-response genes (*Id1, Id2,* and *Id3*) relative to the three SMAD4+ control samples (**Figure 5.3**).

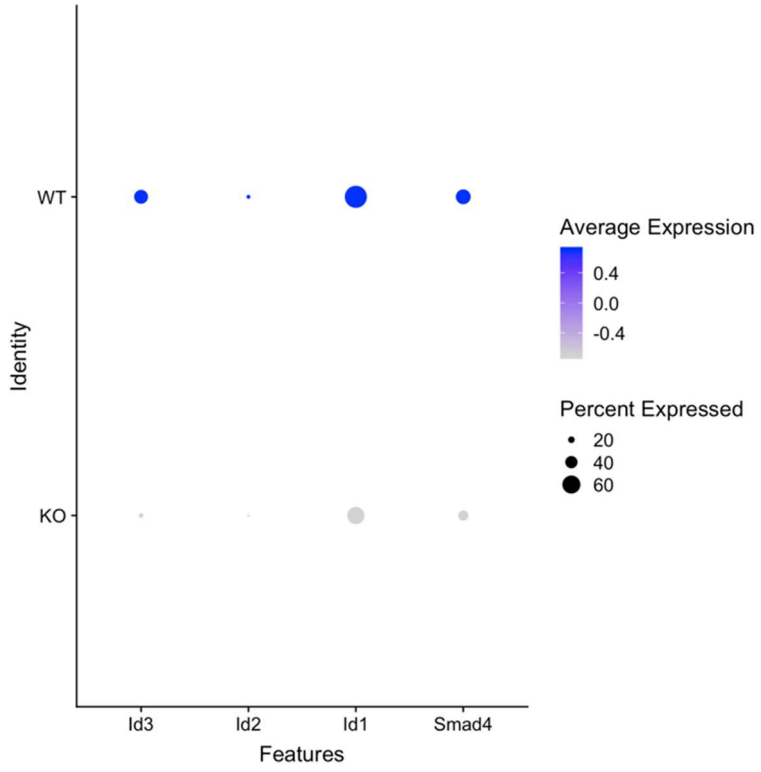

Figure 5.3 – Validation of *Smad4* expression status in mice used for scRNAseq analysis. Six mouse colon samples were analyzed by scRNAseq analysis. Expression levels of *Smad4* and SMAD-response genes (*Id1*, *Id2*, and *Id3*) were compared between mouse types. KO = *Smad4*$^{\Delta Lrig1}$ mice. WT = SMAD4+ control mice. Data represents statistical average of three mice in each group.

By the methods described above, scRNAseq data was analyzed, unsupervised clustering performed, and visualized by UMAP. This method enabled the identification of 11 unique cell populations (**Figure 5.4**). Cell population identity was subsequently assigned by unbiased examination of differentially regulated genes within each cell population and population identities automatically assigned as follows: 0_enterocytes, 1_epithelial cells, 2_epithelial cells, 3_goblet cells, 4_epithelial cells, 5_goblet cells, 6_epithelial cells, 7_T cells, 8_goblet cells, 9_enteroendocrine, and 10_Tuft. Unscaled heatmap visualization demonstrates unique gene expression signatures within each cell population (**Figure 5.5a**) and scaled heatmap visualization demonstrates the relative expression levels of marker genes of interest (**Figure 5.5b**).

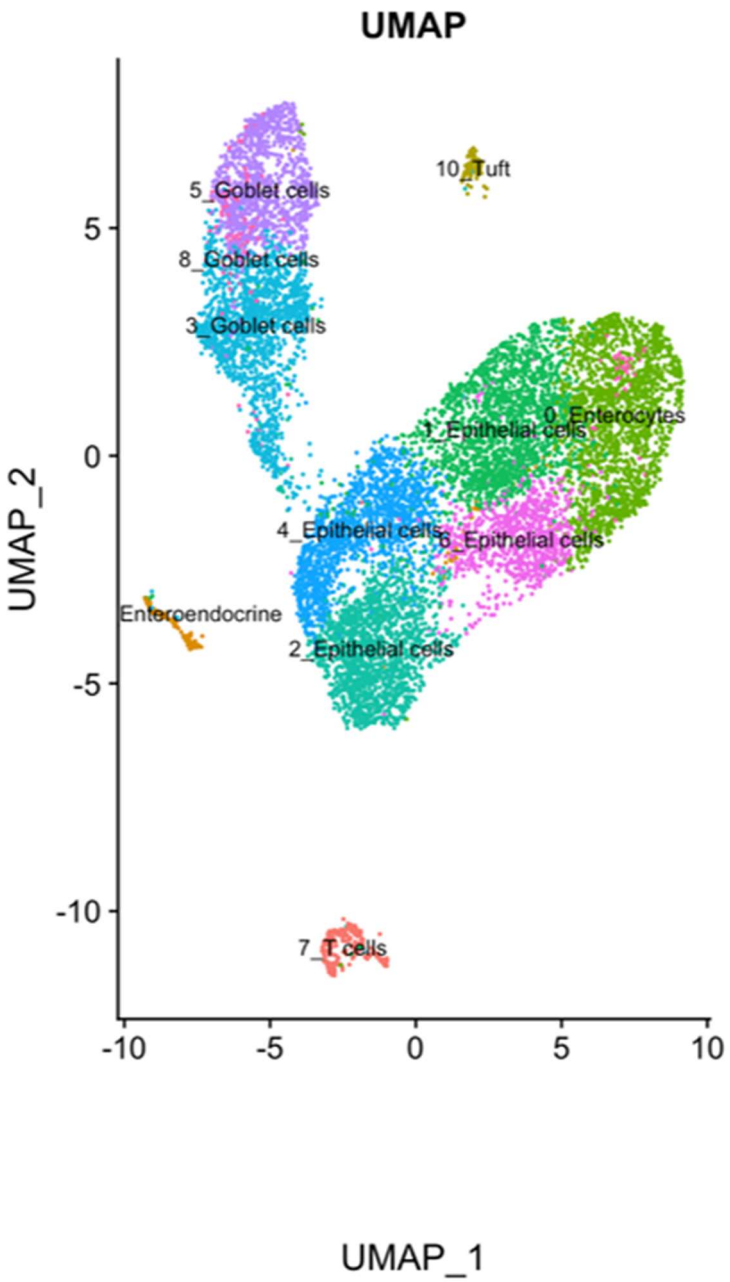

Figure 5.4 – UMAP visualization of scRNAseq analysis of the colon epithelium of three *Smad4*$^{\Delta Lrig1}$ and three SMAD4+ control mice 4 weeks after induction of DSS-induced colitis. Eleven distinct epithelial cell populations were identified by unbiased algorithm-based clustering.

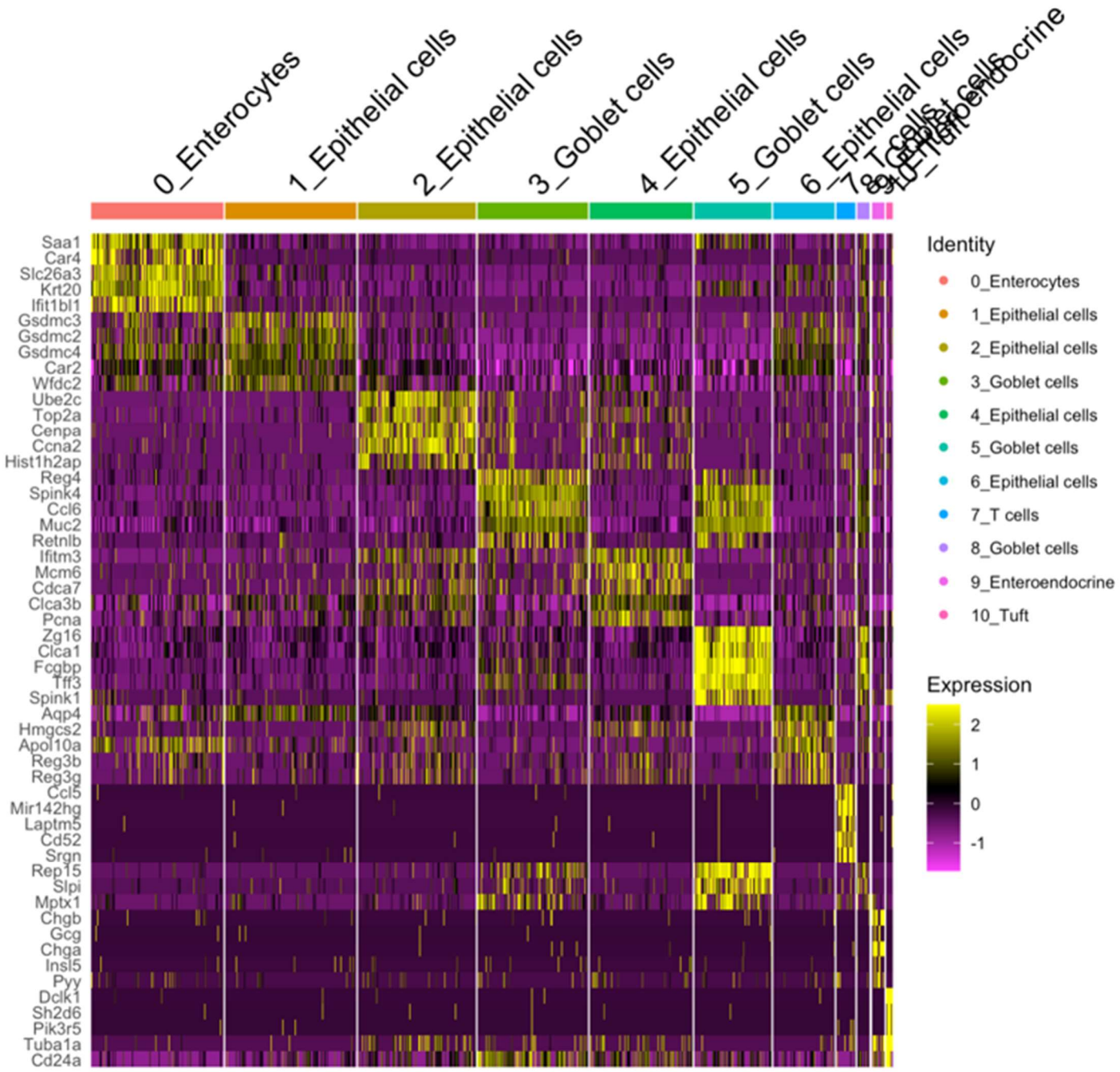

Figure 5.5a – Heatmap of scaled gene expression of the eleven identified cell populations demonstrating a unique gene signature within each population which were identified by unbiased algorithm-based clustering.

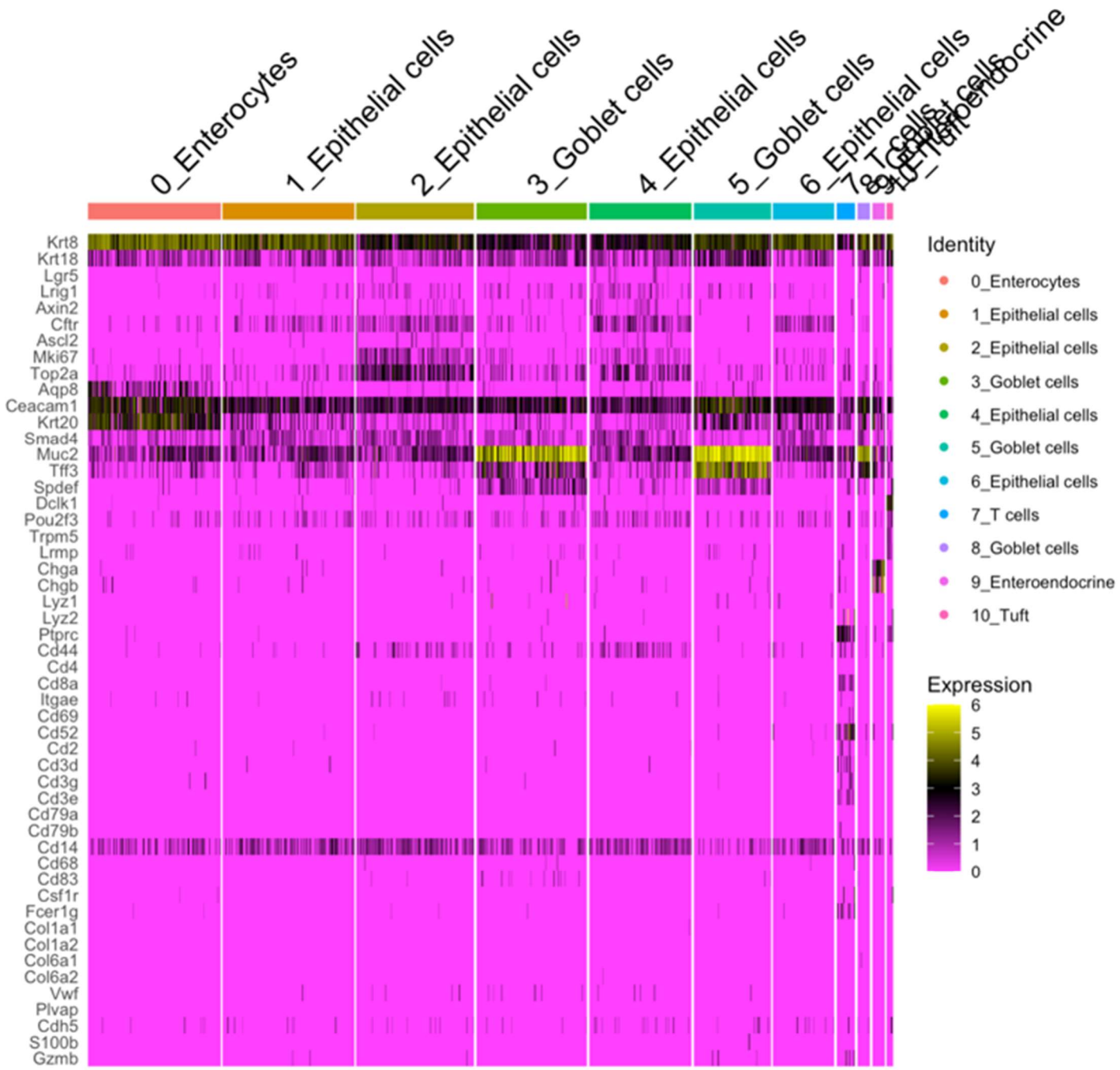

Figure 5.5b - Heatmap of unscaled gene expression of the eleven identified cell populations. Genes of interest were examined for each automatically identified cell population to aid in population identity and naming.

We subsequently assigned each of these eleven cell populations a biologically relevant name based on the expression pattern of specific marker genes. **Table 5.3** lists cell population names along with the gene expression pattern utilized to identify and describe each population. For the remainder of the chapter, we will utilize the biologically relevant cell population names generated by the authors according to Table 5.3.

Abundance of each cell population is quantified and demonstrated in **Figure 5.6**. When *Smad4*$^{\Delta Lrig1}$ ("KO") and SMAD4+ control ("WT") mice are visualized separately by UMAP, we see cell population shift in *Smad4*$^{\Delta Lrig1}$ relative to SMAD4+ control mice (**Figure 5.7**).

		Genes used to assign biologically relevant cell population name	
Automatic, algorithm-assigned name	Biologically relevant name assigned by authors	High expression genes	Low Expression genes
0_enterocytes	Differentiated Colonocytes	*Krt8, Krt 18, Ceamcam1, Krt20*	*Lgr5, Lrig1, Ascl2, Mki67, Dclk1, Chga. Ptprc, Cd3e*
1_Epithelial cells	Epithelial Cells, Unspecified 1	*Krt8, Krt18*	*Lgr5, Axin2, Ascl2, Dclk1, Chga, Ptprc*
2_Epithelial cells	Transient Amplifying (TA) Cells	*Mki67, Top2a*	*Lgr5*
3_Goblet cells	TA-like Cells	*Muc2, Top2a*	*Lgr5, Ascl2, Krt20, Dclk1, Chga, Ptprc*
4_Epithlial cells	Stem Cells	*Lgr5, Lrig1, Axin2*	*Krt20, Tff3, Dclk1, Chga, Ptprc*
5_Goblet cells	Mature Goblet Cells	*Muc2, Tff3*	*Lgr5, Ascl2, Dclk1, Chga, Ptprc*
6_Epithelial cells	Epithelial Cells, Unspecified 2	*Krt8, Krt18*	*Lgr5, Axin2, Ascl2, Dclk1, Chga, Ptprc*
7_T cells	Intraepithelial Lymphocytes	*Ptprc, Cd3e*	*Krt18, Ceacam1*
8_Goblet cells	Mixed Goblet Cell Population	*Krt20, Muc2, Tff3*	*Lgr5, Ascl2, Dclk1, Chga, Ptprc*
9_Enteroendocrine	Enteroendocrine Cells	*Chga, Chgb*	*Krt18, Cd3e*
10_Tuft	Tuft Cells	*Dclk1*	*Lgr5, Lrig1, Krt20, Tff3, Chga, Ptprc*

Table 5.3: Table listing biologically relevant cell population names and the gene expression pattern utilized to identify and describe each population

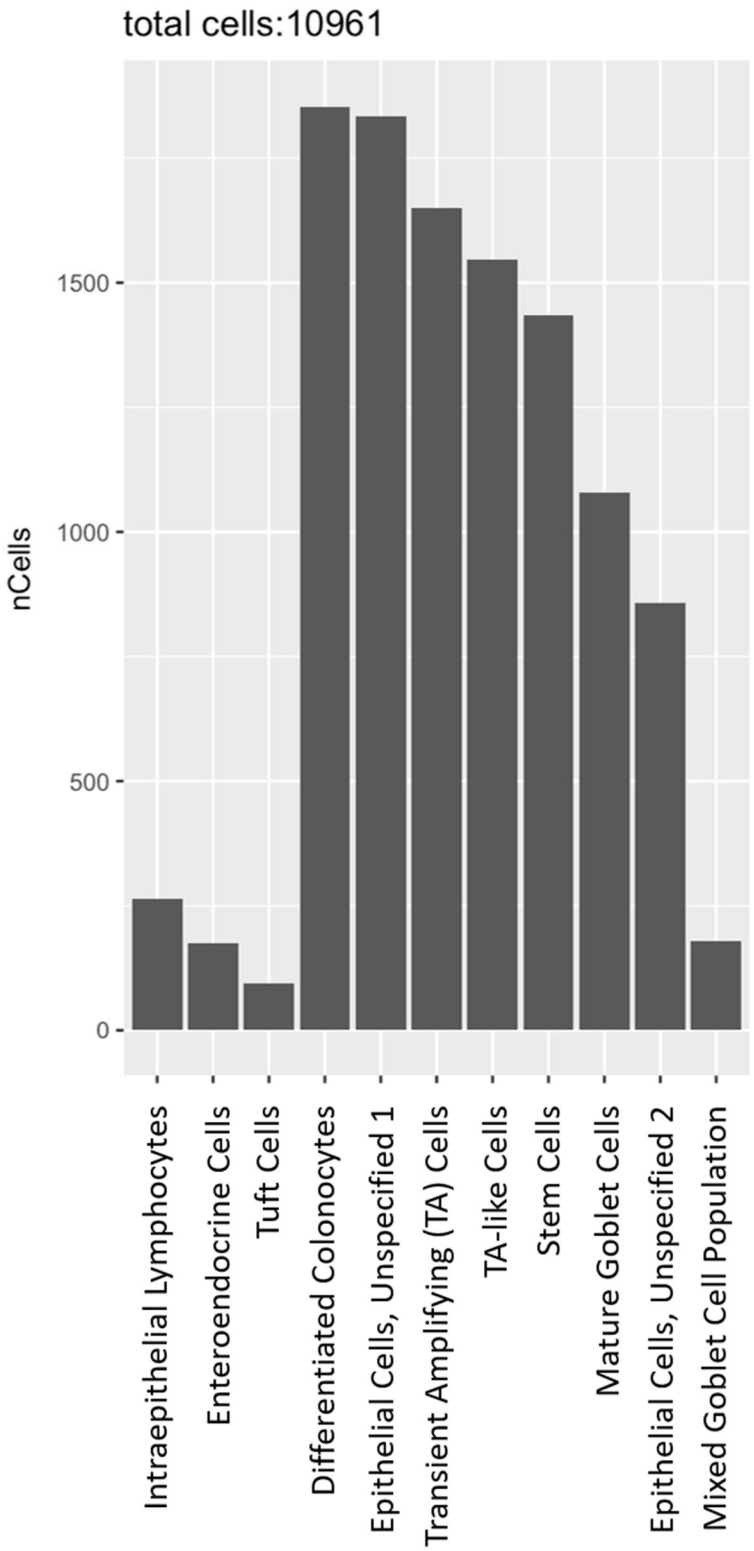

Figure 5.6 – Histogram demonstrating the cell count for each identified cell population/cluster by scRNAseq.

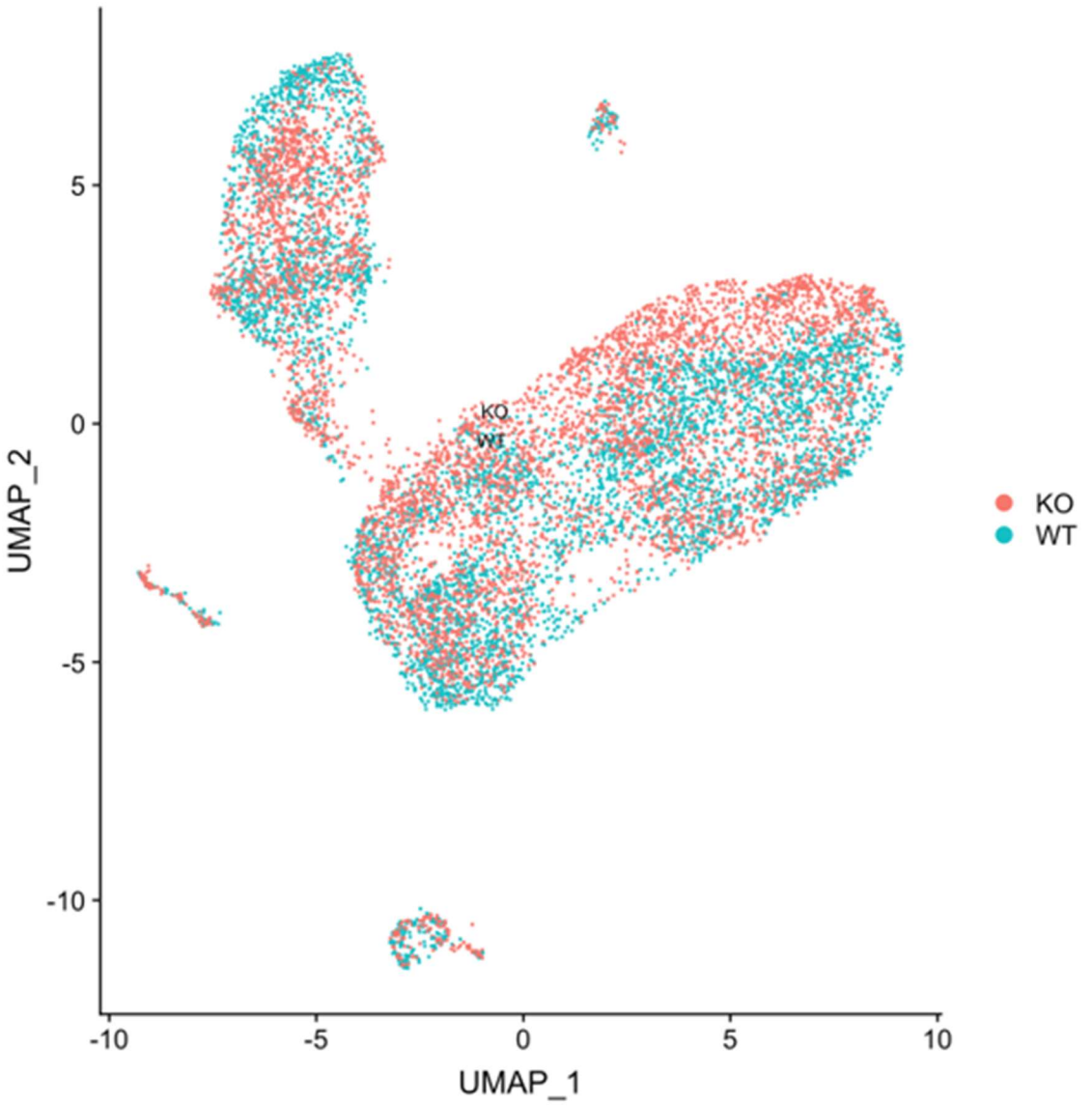

Figure 5.7 – UMAP visualization of scRNAseq analysis of the colon epithelium of three *Smad4*$^{\Delta Lrig1}$ ("KO", red) and three SMAD4+ control ("WT", blue) mice 4 weeks after induction of DSS-induced colitis. Cell population shift is evident in KO versus WT mice.

When relative proportion of epithelial cell subtypes/clusters were compared between *Smad4*$^{\Delta Lrig1}$ ("KO") and SMAD4+ control ("WT") mice, we observed altered proportions of certain epithelial cell subtypes between groups (**Figure 5.8**). *Smad4*$^{\Delta Lrig1}$ ("KO") mice demonstrated a relative increase in proportion of stem cells and a decreased proportion of transit amplifying (TA) cells and tuft cells relative to SMAD4+ control mice, consistent with our prior findings that suggest an expanded stem cell compartment with intestinal SMAD4 loss.

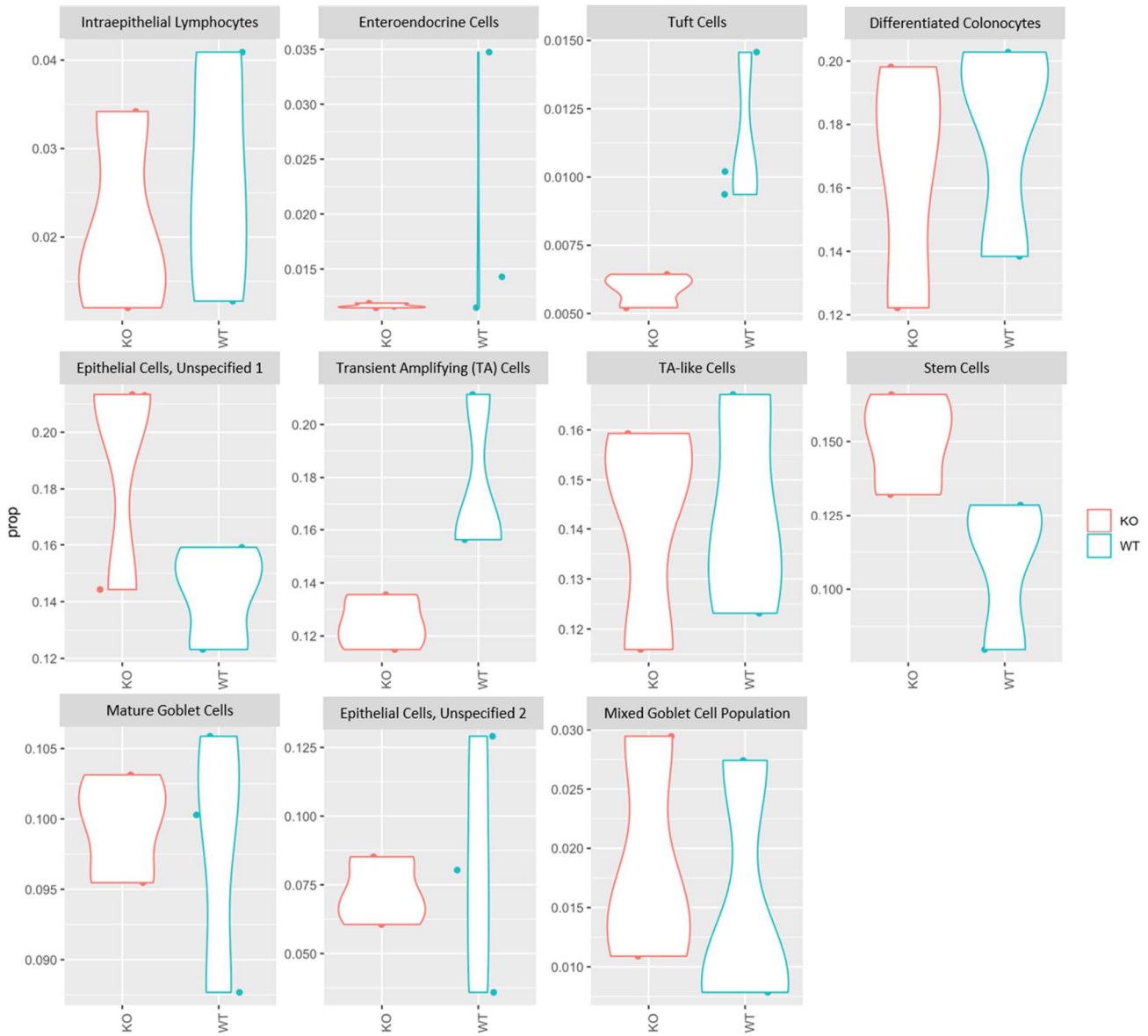

Figure 5.8 – A comparison of the relative abundance of each epithelial cell type/cluster by scRNAseq analysis. Data is aggregate of three *Smad4*$^{\Delta Lrig1}$ ("KO", red) and three SMAD4+ control ("WT", blue) mice. Increased stem cells and decreased TA cells and tuft cells are observed in *Smad4*$^{\Delta Lrig1}$ mice relative to SMAD4+ control mice.

Loss of intestinal SMAD4 expression is associated with altered expression levels of multiple innate immunity-related genes in multiple colon epithelial cell types, including Ccl20

Differential gene expression was manually examined for each of the 11 identified cell types in the above described scRNAseq analysis. The cell type with the most differentially expressed genes (defined as FDR <0.05) was the differentiated colonocytes, with 95 differentially regulated genes between mouse genotypes. Of the 95 differentially regulated genes between the differentiated colonocytes in *Smad4*$^{\Delta Lrig1}$ versus SMAD4+ control mice, 15 genes have a known or suspected function related to the innate immune response. Interestingly, among all the genes differentially regulated in the differentiated colonocytes of *Smad4*$^{\Delta Lrig1}$ mice relative to SMAD4+ control mice, the most significantly up-regulated gene is *Ccl20*, with a Log_2 Fold change of 2.88 (FDR = 2.40 x10^{-10}). *Ccl20* was discussed extensively in Chapter II. Other noteworthy genes significantly increased in the differentiated colonocytes of *Smad4*$^{\Delta Lrig1}$ mice relative to control mice include *Mgst1, Nos2, Lgals3, Steap4, Irf8, Gpx2*, and others.

The other epithelial cell types detected had fewer differentially regulated genes. While several genes known or suspected to relate to the innate immune response were found to be dysregulated in several epithelial cell types, *Ccl20* expression was not significantly altered (increased or decreased) in any other cell type. A complete list of all genes significantly dysregulated in *Smad4*$^{\Delta Lrig1}$ mice relative to SMAD4+ controls that are known or suspected to have functions related to the innate immune response by cell type are listed in **Table 5.4**.

Gene Symbol	Log_2 Fold Change	P-value	FDR	CPM
Differentiated Colonocytes (0_Enterocytes)				
Ccl20	2.88	4.25×10^{-14}	2.40×10^{-10}	74.8
Sgk1	-1.63	1.40×10^{-10}	3.95×10^{-7}	143.2
Mgst1	-1.10	1.00×10^{-8}	9.56×10^{-6}	377.1
AW112010	-1.31	5.66×10^{-8}	2.28×10^{-5}	528.8
Nos2	1.33	5.40×10^{-8}	2.28×10^{-5}	104.3
Lgals3	-0.83	1.45×10^{-7}	5.44×10^{-5}	5746.5
Steap4	1.85	1.12×10^{-6}	3.00×10^{-4}	80.3
Irf8	1.09	4.36×10^{-6}	9.45×10^{-4}	213.8
Gpx2	1.07	2.23×10^{-5}	0.0034	223.8
Clec2d	-1.14	2.99×10^{-5}	0.0043	175.0
Socs1	1.69	3.93×10^{-5}	0.0053	37.5
Tmigd1	-1.25	1.29×10^{-4}	0.013	64.0
Hpgd	-0.73	3.07×10^{-4}	0.023	501.6
Clec14a	-1.26	3.45×10^{-4}	0.025	49.6
Stk10	-1.18	8.06×10^{-4}	0.048	53.1
Epithelial Cells (1_Epithelial Cells)				
Mgst1	-1.25	2.25×10^{-12}	1.11×10^{-8}	561.8
Hpgd	-1.06	1.60×10^{-8}	1.98×10^{-5}	337.2
Gpx2	0.98	8.33×10^{-8}	6.87×10^{-5}	575.0
Lgals3	-0.78	1.52×10^{-7}	1.08×10^{-4}	2409.8
Defb45	2.49	2.74×10^{-7}	1.81×10^{-4}	34.8
Clec2d	-1.07	1.99×10^{-5}	0.0060	106.2
Duox2	1.02	4.18×10^{-5}	0.010	278.5
Psma1	-0.67	1.73×10^{-4}	0.032	381.2
Hspa1a	-0.42	3.0×10^{-4}	0.043	7.0
Cpm	-1.51	3.7×10^{-4}	0.048	23.3
TA Cells (2_Epithelial Cells)				
Retnlb	-1.91	6.13×10^{-10}	2.36×10^{-6}	77.0
Defb45	2.01	3.41×10^{-6}	0.0033	37.5
Ang4	-3.32	5.68×10^{-5}	0.039	12.6
TA-like Cells (3_Goblet Cells)				
Retnlb	-1.73	2.63×10^{-12}	3.79×10^{-9}	2347.7
Cd24a	-0.67	1.27×10^{-4}	0.023	868.9
Ang4	-2.91	4.49×10^{-4}	0.041	199.7
Stem Cells (4_Epithelial Cells)				
Defb45	2.45	4.20×10^{-8}	7.21×10^{-5}	38.5
Mature Goblet Cells (5_Goblet Cells)				
Lgals3	-1.57	7.61×10^{-15}	2.53×10^{-11}	954.1
AW112010	-1.44	2.06×10^{-11}	3.42×10^{-8}	448.6
Retnlb	-3.61	1.48×10^{-9}	1.41×10^{-6}	1626.5
Irf8	1.85	1.29×10^{-8}	9.53×10^{-6}	62.4
Nos2	3.14	9.51×10^{-8}	4.21×10^{-5}	20.7
Ffar2	1.16	4.07×10^{-7}	1.59×10^{-4}	112.3
Rab27b	-0.97	9.96×10^{-6}	0.0019	161.3

Rab27a	-0.74	1.83 x10^{-5}	0.0033	315.7
Steap4	5.05	2.35 x10^{-5}	0.0041	11.96
Rfk	-0.74	5.47 x10^{-5}	0.0081	407.0
Cx3cl1	1.05	5.60 x10^{-5}	0.0081	98.7
Ang4	-4.02	7.12 x10^{-5}	0.0098	861.6
Pdia3	-0.72	2.3 x10^{-4}	0.027	435.4
Igtp	1.29	5.09 x10^{-4}	0.049	78.5
Epithelial Cells (6_Epithelial Cells)				
n/a				
Intraepithelial Lymphocytes (7_T Cells)				
n/a				
Mixed Goblet Cell Population (8_Goblet Cells)				
Lgals3	-1.28	5.14 x10^{-7}	2.1 x10^{-4}	439.4
Gpx2	1.31	6.33 x10^{-5}	0.013	54.8
AW112010	-1.22	9.63 x10^{-5}	0.016	64.5
Retnlb	-2.83	1.01 x10^{-4}	0.016	276.0
Enteroendocrine Cells (9_Enteroendocrine)				
n/a				
Tuft Cells (10_Tuft)				
n/a				

Table 5.4 – Table of differentially regulated genes related to innate immune response in *Smad4*$^{\Delta Lrgi1}$ mice relative to SMAD4+ control mice in the colon epithelium, by cell type. Data generated from scRNAseq analysis. Data represents comparison of three *Smad4*$^{\Delta Lrgi1}$ mice and three SMAD4+ control mice that were littermates and cage mates. Genotypes split evenly between genders. FDR = False Discovery Rate (q-value). CPM = Copies per million.

Loss of intestinal SMAD4 expression is associated with reversed directionality of TNFα signaling in the colon epithelium of mice following induction of experimental colitis

scRNAseq data was analyzed using CellChat software in order to predict ligand-receptor interaction. With this method, it was predicted that the directionality of TNFα signaling within the colon epithelium appeared to be reversed in *Smad4*$^{\Delta Lrig1}$ versus SMAD4+ control mice (**Figure 5.9**). In SMAD4+ control mice, the predominant direction of TNFα signaling was predicted to be from intraepithelial lymphocytes towards epithelial cells (including differentiated colonocytes, TA cells, and stem cells). On the other hand, in *Smad4*$^{\Delta Lrig1}$ mice, the differentiated colonocytes appear to be driving the inflammatory response. For *Smad4*$^{\Delta Lrig1}$ mice, the predominance of TNFα signaling is predicted to be initiating from differentiated colonocytes and targeting other epithelial cell subtypes (including undefined epithelial cell populations, TA cells, stem cells, and goblet cells).

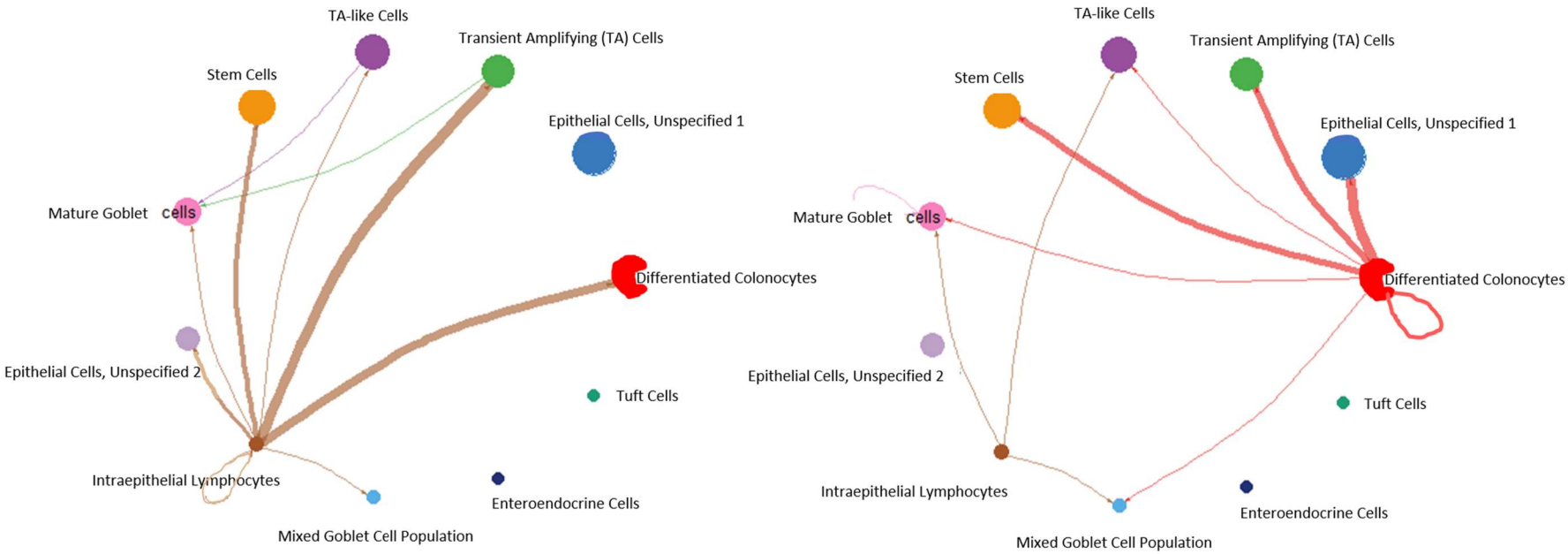
SMAD4+ Control Mice
TA-like Cells
Transient Amplifying (TA) Cells
Stem Cells
Epithelial Cells, Unspecified 1
Mature Goblet cells
Differentiated Colonocytes
Epithelial Cells, Unspecified 2
Tuft Cells
Intraepithelial Lymphocytes
Enteroendocrine Cells
Mixed Goblet Cell Population
Smad4ΔLrig1 Mice
TA-like Cells
Transient Amplifying (TA) Cells
Stem Cells
Epithelial Cells, Unspecified 1
Mature Goblet cells
Differentiated Colonocytes
Epithelial Cells, Unspecified 2
Tuft Cells
Intraepithelial Lymphocytes
Enteroendocrine Cells
Mixed Goblet Cell Population

Figure 5.9 - Reversed directionality of TNFα signaling between *Smad4*$^{\Delta Lrig1}$ and SMAD4+ control mice within the colon epithelium by Ligand-Receptor Interaction analysis using CellChat. In the colon epithelium of SMAD4+ control mice (left), TNFα signaling is predicted to initiate from intraepithelial lymphocytes and effect various epithelial cell subsets. In the colon epithelium of *Smad4*$^{\Delta Lrig1}$ mice, the predominance of the inflammatory response appears to be initiating from the differentiated colonocytes.

Discussion:

Prompted by previously generated (but not yet published) data from our lab which suggested by immunostaining an expanded stem cell compartment in *Smad4*$^{\Delta Lrig1}$ versus SMAD4+ control mice, this chapter explored the changes in epithelial cell composition and stemness due to SMAD4 loss. Here we presented evidence that *Smad4*$^{\Delta Lrig1}$ mice have increased expression of multiple stem cell-related genes (including *Lgr5, Smoc2, Sox9, Bmi1*) and decreased expression of some differentiation markers (including *Muc2*, *Chga*, *Dclk1*, and *Alpi*) in their colon epithelium relative to SMAD4+ control mice. We additionally demonstrated *in vitro* that TGFβ signaling directly modulates the expression of three stem cell-related genes (*Lgr5, Atoh1,* and *Lrig1*) in a manner dependent on SMAD4. Further, we utilized scRNAseq technology to demonstrate that, 1 month following induction of chronic DSS-colitis, *Smad4*$^{\Delta Lrig1}$ mice have an expansion of their stem cell compartment and a reciprocal decrease in TA cell and Tuft cell populations relative to SMAD4+ control mice. These data are consistent with prior immunostaining experiments performed in our lab and collectively demonstrate that loss of intestinal TGFβ signaling via conditional *Smad4* deletion is associated with increased stemness in mouse colon epithelium.

The demonstration that loss of intestinal SMAD4 expression is associated with an expansion of the stem cell compartment is important for several reasons. First, increased stemness (and associated decreased differentiation) in epithelial tissues has been implicated in cancer development and progression (Iacovides et al., 2013; Molchadsky and Rotter, 2017), and this finding in and of itself could have implications for the colitis-associated tumor susceptibility phenotype previously identified in *Smad4*$^{\Delta Lrig1}$ mice. Additionally, there is variability in junctional protein expression and barrier function along the crypt-villus axis, and it is possible that the stem cell niche has higher permeability than more differentiated colonocytes (Fihn et al., 2000; Lameris et al., 2012; Pearce et al., 2018). In support of this, and consistent with what has been previously published (Caron et al., 2021; Darsigny et al., 2009; Garcia-Hernandez et al., 2017; Pearce et al., 2018; Raju et al., 2020; Tsai et al., 2017), we demonstrated in Chapter IV that Claudin 2, a well-known pore-forming Claudin, is expressed exclusively at the crypt base while Claudin 8, a more barrier-forming Claudin is expressed exclusively in more differentiated colonocytes and largely spared from the crypt base.

It is important to note that, however, while it is at least possible that an expanded stem cell compartment is contributing to barrier dysfunction and/or inflammation in *Smad4*$^{\Delta Lrig1}$ mice, it is also possible that it is in fact the other way around. An association between inflammation, infection, and stemness has previously been reported by multiple investigators (Jing et al., 2012; Maitland and Collins, 2008; Reuter et al., 2010), and intestinal proliferation is considered a marker of damage (Nava et al., 2011; Weichselbaum and Klein, 2018). Inflammation is believed to increase stemness and promote epithelial de-differentiation (Krah and Murtaugh, 2016; Rees et al., 2020). The directionality of the relationships between increased stemness, diminished barrier function, and increased inflammatory signaling in mice lacking intestinal SMAD4 expression remains undetermined. However, the ability of TGFβ/BMP signaling to regulate stem cell markers in colonoid cultures suggests that at least some of this regulation is independent of inflammation.

Another important finding in this Chapter is that *Ccl20*, encoding a chemokine significantly upregulated due to SMAD4 loss and one that appears to play an important role in colitis-associated tumor development in *Smad4*$^{\Delta Lrig1}$ mice (see Chapter II for complete discussion on the *Ccl20/Ccr6* axis), was found to be significantly increased in the differentiated colonocytes of *Smad4*$^{\Delta Lrig1}$ mice but not in other epithelial cell types. This finding may be because the inflammatory response in differentiated colonocytes is uniquely upregulated due to loss of SMAD4 expression compared to other colon epithelial cell types, or, alternatively, this could be an artifact of decreased sequencing depth in more rare cell populations (including stem cells, TA cells, enteroendocrine cells, etc). Further, when the scRNAseq data was evaluated using ligand-receptor pair interaction software, it was predicted that the directionality of inflammatory signaling (specifically TNFα signaling) is reversed in *Smad4*$^{\Delta Lrig1}$ mice. SMAD4+ control mice appear to experience TNFα signaling primarily originating in the intraepithelial lymphocytes and targeting the various epithelial cell subsets. *Smad4*$^{\Delta Lrig1}$ mice, on the other hand, are predicted to have a strong TNFα signal originating from the differentiated colonocytes and targeting other epithelial cell populations. Overall, this gives a picture of reversed directionality of inflammatory signaling (and specifically TNFα signaling) in the absence of epithelial SMAD4 expression, implying that it is the differentiated colonocytes that are the major drivers of inflammatory signaling in these *Smad4*$^{\Delta Lrig1}$ mice.

Further investigation is needed to tease out many questions that arise from the data presented in this chapter. First, while we see evidence of increased stemness and an expanded stem cell compartment in mice with intestinal *Smad4* loss, we are not sure of the mechanisms governing these changes. As canonical TGFβ via SMAD4 has well known tumor suppressor functions, it is possible that SMAD4 is responsible for transcriptional regulation of genes directly associated with cell cycle regulation, with dysregulation of these genes directly contributing to expansion of the stem cell compartment. Our lab is currently working on DNA binding assays (including ChIP-sequencing) which may help to determine whether direct binding of the SMAD complex to the promoter/enhancer regions of cell cycle-regulating genes occurs in the colon epithelium of mice. Additionally, whether some of the other phenotypes known to occur in *Smad4*$^{\Delta Lrig1}$ mice (including barrier dysfunction and increased inflammatory signaling) are contributing to stem cell expansion needs to be investigated. *In vitro* assays that focus on the interaction between inflammation and epithelial gene expression are likely to aid in this area.

In conclusion, loss of epithelial TGFβ signaling through conditional deletion of *Smad4* results in increased stemness, expansion of the stem cell compartment with reciprocal decrease in some more differentiated cell populations (Tuft cells and TA cells), and increased inflammatory signaling in some subpopulations (differentiated colonocytes) of the mouse colon. How these changes result from or contribute to the barrier dysfunction, inflammatory, or tumorigenic phenotypes previously discovered in *Smad4*$^{\Delta Lrig1}$ mice remains undetermined.

CHAPTER VI

CONCLUSIONS AND FUTURE DIRECTIONS

Our work, presented in the preceding chapters, supports the notion of canonical TGFβ signaling as a critical mediator of homeostasis in the colon, and establishes the integral role that SMAD4 plays in the modulation of both inflammatory signaling and barrier function. We see evidence that the canonical TGFβ signaling pathway directly modulates the expression of critical inflammatory mediators, such as CCL20, in colonic epithelial cells and that derangements in this chemokine/chemokine receptor axis are likely directly contributing to colitis-associated tumor development in the context of SMAD4 loss (Chapter II). At the same time, we observed that several other chemokines and cytokines dysregulated due to intestinal SMAD4 loss *in vivo* are not directly modulated by canonical TGFβ signaling in mouse colonoids *in vitro*, suggesting that a cell-extrinsic mechanism is likely to be contributing to their dysregulation due to SMAD4 loss *in vivo*. We additionally found evidence that intestinal SMAD4 loss is associated with increased GALT size and an upregulation of genes related to lymphoid trafficking, pathogen recognition, M-cell activity, and mucosal immunity, suggesting increased exposure to luminal antigens may be contributing to the observed inflammatory phenotype. In support of this hypothesis, we subsequently found ample evidence of barrier dysfunction in mice lacking intestinal SMAD4 expression, including increased colonic permeability to fluorescently labeled macromolecules, cell-autonomous dysregulation of critical junctional protein expression due to SMAD4 loss, and direct modulation of TER by TGFβ/BMP in polarized colonocytes (Chapter IV). Collectively, these data demonstrate that TGFβ signaling via SMAD4 directly modulates both inflammatory signaling and barrier function in the mouse colon.

Examining the mechanism of SMAD4-dependent regulation of Ccl20 *expression*

More work needs to be done to fully understand how *Ccl20* is being regulated by SMAD4. Several ongoing experiments in our lab seek to understand these questions, including Chromatin Immunoprecipitation (ChIP-sequencing) and luciferase reporter assays which will enable us to determine the mechanism by which SMAD4 and the TGFβ signaling pathway regulate the expression of inflammatory mediators (including *Ccl20*). These experiments, which are not yet published and that have been performed by other investigators in our lab, so far seem to indicate that SMAD proteins do not bind directly to the *Ccl20* promoter region in response to TGFβ treatment (as evidenced by lack of SMAD2/3 binding on ChIP-sequencing). However, luciferase reporter assays in FET-1 cell lines indicate that TGFβ treatment is able to negatively regulate *Ccl20* promoter activity in response to TNFα stimulation, suggesting that the *Ccl20* promoter region does have a SMAD-response element that does not include direct SMAD protein binding. While we have thus far had difficulty identifying a SMAD4 antibody which works reliably for ChIP-sequencing, an important complementary experiment to the ChIP-sequencing experiment described above (which utilized a SMAD2/3 antibody and TGFβ1 treatment) would be to perform ChIP-sequencing using a SMAD1/5/9 antibody and BMP2 stimulation. This would provide further clarity on whether either side of the canonical TGFβ signaling pathway (either TGFβ- or BMP-mediated signaling) results in SMAD complex binding to the *Ccl20* promoter. Additionally, co-immunoprecipitation experiments that examine the interaction between the SMAD proteins and transcription factors that are known to regulate TNFα response genes (such as C/EBP) may shed light on how the TGFβ signaling pathway is able to negatively regulate *Ccl20* expression in colon epithelial cells. Co-immunoprecipitation and ChIP-sequencing assays could additionally be repeated in $Smad4^{\Delta Lrig1}$ and SMAD4+ control mouse colon samples to investigate whether similar SMAD protein interactions are occurring *in vivo*.

Further examining the role of the CCL20/CCR6 axis on leukocyte trafficking and tumorigenesis

The data presented in this dissertation demonstrate that intestinal SMAD4 loss leads to increased epithelial *Ccl20* expression, increased stromal *Ccr6* expression, and increased CD45+ leukocyte recruitment. However, our data fails to specifically define the differential recruitment of specific leukocyte subsets to SMAD4 null colons. This is largely related to the fact that our initial flow cytometry assay, as currently published (Means et al., 2018) and reported in this dissertation, had only three mice per arm and was likely underpowered to detect subtle changes in specific leukocyte subsets due to intestinal SMAD4 loss. Additionally, the experiment included only general extracellular lineage markers (including CD3, CD4, CD8, CD19, Gr-1, CD11b, CD11c, etc.) and did not include intra-cellular markers that are known to be expressed specifically in CCR6-expressing leukocytes including FoxP3 (Tregs) or IL-17 (Th17 cells). For these reasons, as the data currently stands, we do not know which leukocytes subsets are being preferentially recruited to the SMAD4 null colon. It is for this reason that further immunostaining and immunophenotyping by flow cytometry of $Smad4^{\Delta Lrig1}$ and SMAD4+ control mouse colon would be beneficial. While one could hypothesize from previous literature which leukocyte subsets may be preferentially recruited to the $Smad4^{\Delta Lrig1}$ colon due to increased CCL20 production (including Th17 cells, Treg cells, neutrophils, B cell- and Dendritic cell-subsets, etc. (Comerford et al., 2010)), confirmation by flow cytometry that these cell types are or are not differentially recruited to the $Smad4^{\Delta Lrig1}$ colon may help us to understand why blockade of the CCL20/CCR6 axis with CCR6 knockout significantly blunted the development of colitis-associated tumors due to intestinal SMAD4 loss in these mice. With this information, targeted leukodepletion assays could be performed to determine how the CCL20/CCR6 axis contributes to colitis-associated cancer development in $Smad4^{\Delta Lrig1}$ mice.

In addition to the experiments described above in $Smad4^{\Delta Lrig1}$ and SMAD4+ control mice, it would be helpful to take advantage of the $Ccr6^{EGFP/EGFP}$ mouse colony that we are currently maintaining in our lab. As described in Chapter II, we previously crossed these mice with $Smad4^{\Delta Lrig1}$ mice and determined that blockade of the CCL20/CCR6 chemokine/chemokine receptor axis through CCR6 deletion was sufficient to significantly decrease the formation of colitis-associated cancers due to SMAD4 loss. However, we have as of yet not completed immunostaining or immunophenotyping on these mice to determine how blockade of the CCR6 axis alters leukocyte recruitment to the colon. Such insight would complement the flow cytometry experiments in $Smad4^{\Delta Lrig1}$ and SMAD4+ control mice described, above, and would enable us to confirm that alterations in leukocyte recruitment to the colon in $Smad4^{\Delta Lrig1}$ mice can be attributed to the CCL20/CCR6 axis.

Utilization of the $Ccr6^{EGFP/EGFP}$ mouse colony could additionally enable further targeted gene expression assays. For example, CCR6-expressing heterozygote cells (from $Ccr6^{EGFP/+}$ mice with and without SMAD4 expression) as well as CCR6 knockout cells (from $Ccr6^{EGFP/EGFP}$ mice with and without SMAD4 expression) could be isolated by flow-sorting with an anti-GFP antibody. Flow-sorting for GFP-expressing cells would enable examination of the gene expression patterns (by qPCR or bulk RNA-sequencing) of specific cell types that typically express CCR6 (including Th17 cells, Tregs, B cells subsets, dendritic cell subsets, etc.). This may provide insight into how intestinal SMAD4 loss alters not just the recruitment but also the activity of CCR6+ cell types, and how such activation might contribute to carcinogenesis.

Given that previously published literature associates elevated CCL20/CCR6 levels with human colon cancer and inflammatory bowel disease (Comerford et al., 2010; Frick et al., 2013; Skovdahl et al., 2015), our findings that CCR6 deletion is significantly protective against the development of colitis-associated cancers due to SMAD4 loss in mice suggests heavily that there may be translational implications for CCL20/CCR6 axis blockade in human inflammatory bowel disease. Fortunately, there have been CCL20 neutralizing antibodies (such as GSK3050002) previously developed and published (Bouma et al., 2017), and these antibodies are being actively investigated in human safety trials for other pathologies including plaque psoriasis and psoriatic arthritis (clinicaltrials.gov). With this in mind, it is highly plausible that utilization of a CCL20-neutralizing

antibody such as GSK3050002 could provide benefit to inflammatory bowel disease patients either in treatment of inflammatory symptoms or in preventing high-grade dysplasia or colitis-associated cancers. The first step in investigating the utility of such a strategy would be to determine the antibody's ability to prevent intestinal inflammation or colitis-associated cancer development in *Smad4*$^{\Delta Lrig1}$ versus SMAD4+ control mice. Complementary *in vitro* experiments would then need to be performed using human tissue specimens (including human-derived intestinal organoids) to determine the capacity of CCL20 neutralization to block leukocyte recruitment and inflammatory signaling in the human context.

Examining the mechanism of SMAD4-dependent regulation of Ccl20 *expression*

The data presented in this dissertation provide evidence that the TGFβ canonical signaling pathway is directly regulating the expression of critical tight junction proteins in a cell-autonomous manner. Further, TGFβ-dependent regulation of Claudin gene expression appears to be dependent on SMAD4 and thus the canonical signaling pathway, and at least in some cases, this regulation is dependent on nascent RNA synthesis. Beyond this, however, the mechanism of Claudin gene regulation by the TGFβ signaling pathway in colon epithelium remains undetermined. There are several experiments that would help us to better understand the mechanism by which TGFβ signaling and SMAD4 modulate the expression of these critical tight junction proteins.

First, a ChIP-sequencing assay examining SMAD protein binding to Claudin gene promoter/enhancer regions may be of benefit. Our lab has previously performed a ChIP-sequencing assay using a SMAD2/3 antibody, as described above. This assay did not demonstrate any evidence of SMAD2/3 binding to the promoter/enhancer regions of Claudin gene regulatory elements. While this may indicate that direct SMAD complex binding is not a factor in Claudin gene regulation in mouse colon, one major limitation is that this assay was performed using 2-dimensional immortalized mouse colonocytes (IMCs) which are not known to polarize and do not form normal tight junctions. In fact, a complementary RNA-sequencing experiment perfomed simultaneously on IMCs did not show detectable levels of most of the Claudin genes, although these genes were detected by RNA-sequencing in prior experiments using mouse colonoids. For this reason, it likely not appropriate to make definitive conclusions about SMAD complex binding to the Claudin gene regulatory elements using IMCs. Instead, a future iteration of this experiment could instead utilize either colonic crypts isolated *in vivo* or mouse colonoids that are grown and maintained *in vitro*. Either of these latter experimental systems are more likely to reveal useful information about SMAD complex binding in cells that are known to express tight junctions and Claudin genes. A technical limitation of ChIP-sequencing is that the assay typically requires large numbers of cells due to inherently low signal-to-noise ratio. For this reason, conventional ChIP-sequencing may be difficult to perform utilizing mouse colonoids, which are more challenging and costly to maintain at high densities compared to conventional 2-dimensional cell lines. If insufficient cell numbers prove to be a challenge for ChIP-sequencing of mouse colonoids, a viable alternate option would be to utilize the new CUT&RUN technology (Skene and Henikoff, 2017), which is known to have extremely low background and therefore requires fewer cell numbers.

If a ChIP-sequencing assay is not technically feasible or determines that there is no evidence of direct SMAD complex binding to Claudin gene regulatory elements, there are alternate approaches that may prove efficacious in determining the mechanism of TGFβ/SMAD4 regulation of Claudin genes. For example, transcription factors SP1 and CDX2 are two of the most well-known regulators of Claudin gene expression (Khan and Asif, 2015). Both of these proteins have been demonstrated to interact with SMAD proteins and/or the TGFβ/BMP signaling pathways previously (Barros et al., 2008; Docagne et al., 2004; Pardali et al., 2000), suggesting a possible mechanism of regulation. Experiments that selectively target SP1 or CDX2 *in vitro* may be fruitful in determining whether TGFβ/SMAD-dependent regulation of Claudin gene expression is dependent

on these transcription factors. Further, co-immunoprecipitation assays would enable direct examination of SMAD-SP1 or SMAD-CDX2 interaction, which could shed light on the mechanism of TGFβ-dependent regulation of Claudin gene expression.

Examining the relationship between inflammatory and barrier phenotypes in SMAD4 null mice

While we have provided evidence that dysregulation of the *Ccl20/Ccr6* signaling axis due to intestinal SMAD4 loss directly contributes to colitis-associated tumorigenesis, we do not yet know what the implications of SMAD4-dependent junctional protein dysregulation and barrier dysfunction are in *Smad4*$^{\Delta Lrig1}$ mice (**Figure 6.1**). We have several reasons to hypothesize that SMAD4-dependent barrier dysfunction contributes to the observed intestinal inflammation, including: 1) we demonstrated that TGFβ-dependent regulation of colonic junctional protein gene expression and barrier function occurs in a cell-autonomous manner, 2) we observed that decreased expression levels of *SMAD4* and altered expression levels of critical Claudin genes are significantly correlated in human colon cancer and IBD specimens, 3) we see evidence of increased GALT size and stromal RNAseq data from *Smad4*$^{\Delta Lrig1}$ mice are consistent with an upregulation of gene expression related to luminal antigen exposure, and 4) there is ample evidence from other groups in both mice and humans that barrier dysfunction and Claudin protein dysregulation precede or directly contribute to intestinal inflammation (Katz et al., 1989; Lameris et al., 2012; Luettig et al., 2015; Martini et al., 2017; McGuckin et al., 2009; Munkholm et al., 1994; Söderholm et al., 1999; Tanaka et al., 2015; Vancamelbeke et al., 2017; Xu et al., 2019; Zeissig et al., 2007; Zhu et al., 2019). These data suggest the possibility that SMAD4-dependent barrier dysregulation could directly contribute to the intestinal inflammation observed in our *Smad4*$^{\Delta Lrig1}$ mice. However, the experiments necessary to prove this causal effect have yet to be completed. One such experiment would be to cross *Smad4*$^{\Delta Lrig1}$ mice with Claudin transgenic mice (such as the Claudin 2 knockout mouse published by Turner and colleagues (Raju et al., 2020)). Using these dual-knockout mice, we would be able to examine the role of Claudin 2 in the observed barrier and tumorigenic phenotypes under both homeostatic and DSS-treated conditions. Such an experiment would determine whether SMAD4-dependent regulation of specific Claudin proteins is directly contributing to the inflammatory and/or tumorigenic phenotypes observed in *Smad4*$^{\Delta Lrig1}$ mice.

Alternatively, an experiment focused on the contribution of luminal microbes and antigens could answer a separate, but related, question: whether or not susceptibility to colitis-associated tumorigenesis due to SMAD4 loss is dependent on contributions from luminal antigens. A simple way to perform this experiment would be to subject *Smad4*$^{\Delta Lrig1}$ and SMAD4+ control mice to broad-spectrum antibiotics (or vehicle control) in drinking water before, during, or after induction of experimental colitis and determining whether a significant reduction in intestinal bacterial load has a corresponding effect on inflammatory signaling or colitis-associated tumor development due to intestinal SMAD4 loss. One or both of these experiments would provide insight into whether barrier dysfunction/luminal antigen exposure are playing a significant role in the inflammatory and/or tumorigenic phenotypes observed due to intestinal SMAD4 loss in mice.

It is also important to note, of course, that altered inflammatory signaling and immune cell infiltration/activation due to intestinal SMAD4 loss could also be negatively regulating barrier function. Ample evidence exists that pro-inflammatory cytokines (such as TNFα and IFNγ) alter epithelial junctional protein expression and lead to diminished TER and barrier breakdown (Hering et al., 2011; McKay and Singh, 1997; Planchon et al., 1994, 1999). As there is evidence tying dysregulated *CCL20*/CCL20 levels to IBD (Guan, 2019; Skovdahl et al., 2015; Zhang et al., 2012), and as we do have direct evidence that intestinal SMAD4 loss leads to altered *Ccl20* expression in a cell-autonomous manner, it is possible that the direct effects of the CCL20/CCR6 signaling axis leads to barrier dysfunction either directly or via altered immune cell recruitment. One could explore this question by utilizing our new *Ccr6*$^{EGFP/EGFP}$ mice (described in Chapter II). While we

know that crossing these mice with our *Smad4*$^{\Delta Lrig1}$ mice greatly reduces susceptibility to colitis-associated tumorigenesis, we have yet to explore whether loss of CCL20/CCR6 signaling effects barrier dysfunction or junctional protein dysregulation due to SMAD4 loss. Repeating the permeability assays and RNAseq experiments in mice with and without *Ccr6* expression could help us to determine the causality of this relationship.

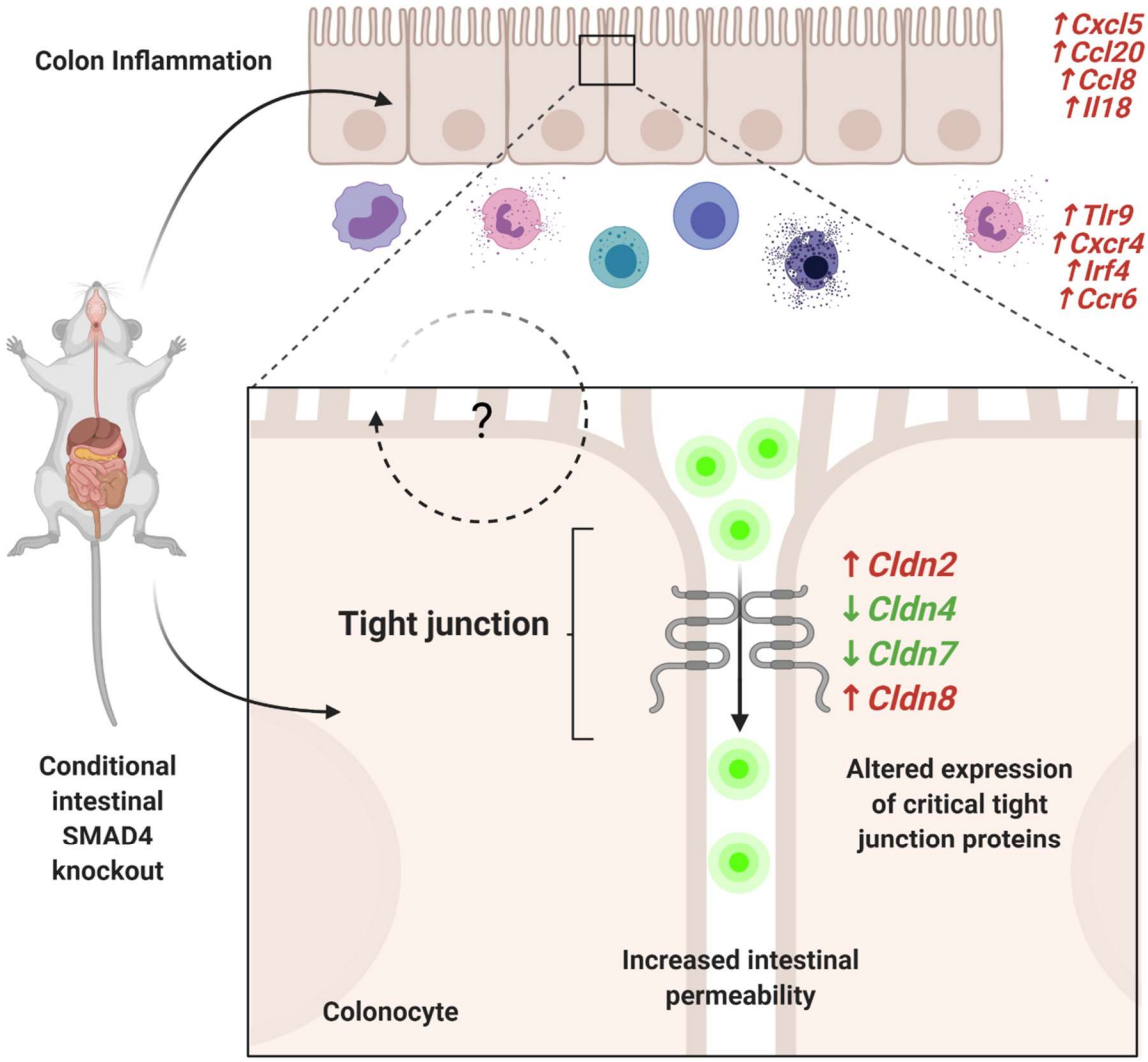

Figure 6.1 – Summary Figure. Intestinal SMAD4 loss leads to increased inflammatory signaling/immune cell recruitment as well as dysregulation of critical junctional protein expression/diminished barrier function. How these factors impinge upon one another, and how they contribute to tumorigenesis in SMAD4 null mice, remains undetermined. Figure adapted from Marincola Smith, et al. *American Journal of Physiology – Gastrointestinal and Liver Physiology*, 2021.

A complimentary *in vitro* approach could take advantage of our previously generated mouse colonoids. Co-culturing mouse colonoids (with and without SMAD4 expression) with murine-derived immune cells would enable observation of leukocyte migration as well as leukocyte-mediated gene expression changes in the epithelium and alterations in epithelial TER. Adding in CCL20/CCR6 blockade (through either siRNA for *Ccl20/Ccr6* or utilizing a previously published anti-CCL20 monoclonal antibody (Heo et al., 2020; Liao et al., 2020)) would enable us to determine whether immune cell recruitment and activation due to the CCL20/CCR6 axis is playing a critical role in the SMAD4-dependent barrier regulation observed *in vivo*. If it is determined that SMAD4-dependent leukocyte trafficking is significantly modulating epithelial barrier function (or junctional protein expression), follow-up experiments could focus on specific leukocyte-derived effector molecules (such as TNFα or IFNγ) that could be directly responsible for the inflammation-related barrier changes observed (Hering et al., 2011; McKay and Singh, 1997; Planchon et al., 1994, 1999).

Examining SMAD4-dependent regulation of colon epithelial differentiation

It is also important to note that we now have several pieces of evidence pointing towards an expanded stem cell compartment in *Smad4*$^{\Delta Lrig1}$ mice. Other members of our group have previously performed immunostaining on mice with intestinal *Smad4* loss which demonstrated increased LRIG1+ and SOX9+ cells with *Smad4* loss. We additionally provided evidence in Chapter V of increased expression of multiple stem cell-related genes in the colon epithelium of *Smad4*$^{\Delta Lrig1}$ mice relative to SMAD4+ control mice *in vivo* as well as direct regulation of stem cell-related genes by TGFβ/BMP *in vitro*. Also, by scRNAseq, we see a significantly higher proportion of stem cells and a significantly lower proportion of transient amplifying cells and tuft cells in the colon epithelium of *Smad4*$^{\Delta Lrig1}$ relative to SMAD4+ control mice 1 month following DSS-induced colitis. Collectively, these data suggest heavily that mice lacking intestinal *Smad4* expression have an expanded colon epithelial stem cell compartment. Further, the colitis-associated tumors we observe in *Smad4*$^{\Delta Lrig1}$ mice seem to originate from the crypt bases (the stem cell compartment) and invade downward (similar to what is observed in human colitis-associated cancers) rather than from apical polyps, as is frequently observed in sporadic colon cancers. Collectively, these data suggest that SMAD4-dependent regulation of differentiation and stemness may be playing an important role in colitis-associate tumor development due to intestinal SMAD4 loss. The mechanism of such a relationship, however, remains unclear.

Interestingly, it has been previously demonstrated that there is variability in junctional protein expression and barrier function along the crypt-villus axis, and that the stem cell niche may have higher levels of permeability than more differentiated colonocytes (Fihn et al., 2000; Pearce et al., 2018). In this context, it is possible that an expansion of the stem cell compartment due to loss of *Smad4* expression could be directly contributing to our observed barrier and/or inflammatory phenotypes in *Smad4*$^{\Delta Lrig1}$ mice. Conversely, it is possible that primary barrier dysfunction and/or inflammation could be promoting stemness through inflammation-driven de-differentiation, tissue re-programming, or promotion of epithelial plasticity and replication (Michael et al., 2016; Nava et al., 2011).

There are several experiments that might help us to better understand the relationship between SMAD4-dependent regulation of epithelial differentiation and tumorigenesis. First, the scRNAseq experiment described in Chapter V was performed at one timepoint only (1 month following DSS-induced injury). Repeating this experiment under homeostatic conditions (without DSS treatment), after acute DSS-induced injury, and at 2 months following DSS-induced chronic injury (which is roughly the time we begin to observe tumors develop in *Smad4*$^{\Delta Lrig1}$ mice) would allow us to associate the timing of the stem cell compartment changes detected with other factors (including epithelial injury and tumor development). Additionally, while a powerful tool for understanding global gene expression changes within cell clusters and cell-cell interaction, inherit limitations of the scRNAseq technology makes it fundamentally difficult to examine alterations in rare mRNAs, especially in

relatively rare cell populations (such as stem cells). With this in mind, we are currently working on flow-sorting specific subsets of colon epithelium (including stem cells, transient amplifying cells, tuft cells, differentiated colonocytes, etc.) from *Smad4*$^{\Delta Lrig1}$ and SMAD4+ control mice, similarly to what has been previously described (Habowski et al., 2020; Wang et al., 2013). This will enable us to ask specific questions with regard to gene regulation and expression in specific cell subsets. For instance, flow-sorting for stem cells in *Smad4*$^{\Delta Lrig1}$ and SMAD4+ control mice and then isolating RNA from this population would allow us to perform bulk RNA-sequencing on the epithelial stem cells specifically. This would increase our sequencing depth (compared to that which we could achieve with scRNAseq) and improve our ability to detect significant gene expression changes due to SMAD4 loss specifically within this relatively rare epithelial cell sub-population. In particular, we are interested in determining whether significant changes in cell cycle regulation, differentiation, and inflammation exist in SMAD4 null stem cells, and such discovery would enable us to pursue stem cell-specific regulation as a major contributing factor to colitis-associated tumorigenesis (or inflammation) in *Smad4*$^{\Delta Lrig1}$ mice.

Conclusion

In summary, loss of intestinal SMAD4 expression is associated with increased epithelial inflammatory signaling (including *Ccl20* expression), increased immune cell recruitment, dysregulation of junctional protein expression, barrier dysfunction, and expanded stem cell compartment in the mouse colon. How these phenotypes are contributing to one another, and how they may or may not contribute to colitis-associated tumor development in mice, remain undetermined, and further understanding of these relationships, their mechanisms, and causality will shed light on critical mechanisms of IBD, CRC, and CAC development in humans.

REFERENCES

Aigner, K., Dampier, B., Descovich, L., Mikula, M., Sultan, A., Schreiber, M., Mikulits, W., Brabletz, T., Strand, D., Obrist, P., et al. (2007). The transcription factor ZEB1 (δEF1) promotes tumour cell dedifferentiation by repressing master regulators of epithelial polarity. Oncogene *26*, 6979–6988.

Aitchison, A.A., Veerakumarasivam, A., Vias, M., Kumar, R., Hamdy, F.C., Neal, D.E., and Mills, I.G. (2008). Promoter methylation correlates with reduced Smad4 expression in advanced prostate cancer. Prostate *68*, 661–674.

Alazzouzi, H., Alhopuro, P., Salovaara, R., Sammalkorpi, H., Jarvinen, H., Mecklin, J.-P., Hemminki, A., Schwartz, S., Aaltonen, L.A., and Arango, D. (2005). SMAD4 As a Prognostic Marker in Colorectal Cancer. Clinical Cancer Research *11*, 2606–2611.

Allaire, J.M., Darsigny, M., Marcoux, S.S., Roy, S.A.B., Schmouth, J.-F., Umans, L., Zwijsen, A., Boudreau, F., and Perreault, N. (2011). Loss of Smad5 leads to the disassembly of the apical junctional complex and increased susceptibility to experimental colitis. Am J Physiol-Gastr L *300*, G586–G597.

Aloysius, A., DasGupta, R., and Dhawan, J. (2018). The transcription factor Lef1 switches partners from β-catenin to Smad3 during muscle stem cell quiescence. Sci Signal *11*, eaan3000.

Amoozadeh, Y., Dan, Q., Xiao, J., Waheed, F., and Szászi, K. (2015). Tumor necrosis factor-α induces a biphasic change in claudin-2 expression in tubular epithelial cells: role in barrier functions. Am J Physiol-Cell Ph *309*, C38–C50.

Anderson, J.M., and Itallie, C.M.V. (2009). Physiology and Function of the Tight Junction. Csh Perspect Biol *1*, a002584.

Arthur, J., Perez-Chanona, E., Muhlbauer, M., Tomkovich, S., Uronis, J., Fan, T.-J., Campbell, B., Abujamel, T., Dogan, B., Rogers, A., et al. (2012). Intestinal Inflammation Targets Cancer-Inducing Activity of the Microbiota. Science *338*, 120–123.

Ashikari, D., Takayama, K., Obinata, D., Takahashi, S., and Inoue, S. (2017). CLDN8, an androgen-regulated gene, promotes prostate cancer cell proliferation and migration. Cancer Sci *108*, 1386–1393.

Aytac, E., Sulu, B., Heald, B., O'Malley, M., LaGuardia, L., Remzi, F.H., Kalady, M.F., Burke, C.A., and Church, J.M. (2015). Genotype-defined cancer risk in juvenile polyposis syndrome. Brit J Surg *102*, 114–118.

Babyatsky, M.W., Rossiter, G., and Podolsky, D.K. (1996). Expression of Transforming Growth Factors alpha and beta in Colonic Mucosa in Inflammatory Bowel Disease. Gastroenterology *110*, 975–984.

Bakin, A.V., Tomlinson, A.K., Bhowmick, N.A., Moses, H.L., and Arteaga, C.L. (2000). Phosphatidylinositol-3 Kinase Function is Required for TGFß-mediated Epithelial to Mesenchymal Transition and Cell Migration. J Biol Chem *275*, 36803–36810.

Balda, M.S., and Matter, K. (2014). Tight junctions in health and disease. Semin Cell Dev Biol *36*, 147–148.

Banerjee, A., Herring, C.A., Chen, B., Kim, H., Simmons, A.J., Southard-Smith, A.N., Allaman, M.M., White, J.R., Macedonia, M.C., Mckinley, E.T., et al. (2020). Succinate Produced by Intestinal Microbes Promotes Specification of Tuft Cells to Suppress Ileal Inflammation. Gastroenterology *159*, 2101-2115.e5.

Bardeesy, N., Cheng, K., Berger, J.H., Chu, G.C., Pahler, J., Olson, P., Hezel, A.F., Horner, J., Lauwers, G.Y., Hanahan, D., et al. (2006). Smad4 is dispensable for normal pancreas development yet critical in progression and tumor biology of pancreas cancer. Gene Dev *20*, 3130–3146.

Barrett, T., Wilhite, S.E., Ledoux, P., Evangelista, C., Kim, I.F., Tomashevsky, M., Marshall, K.A., Phillippy, K.H., Sherman, P.M., Holko, M., et al. (2013). NCBI GEO: archive for functional genomics data sets—update. Nucleic Acids Res *41*, D991–D995.

Barros, R., Pereira, B., Duluc, I., Azevedo, M., Mendes, N., Camilo, V., Jacobs, R., Paulo, P., Santos-Silva, F., Seuningen, I. van, et al. (2008). Key elements of the BMP/SMAD pathway co-localize with CDX2 in intestinal metaplasia and regulate CDX2 expression in human gastric cell lines. J Pathology *215*, 411–420.

Batlle, E., Sancho, E., Francí, C., Domínguez, D., Monfar, M., Baulida, J., and Herreros, A.G. de (2000). The transcription factor Snail is a repressor of E-cadherin gene expression in epithelial tumour cells. Nat Cell Biol *2*, 84–89.

Bazzoni, G., and Dejana, E. (2004). Endothelial Cell-to-Cell Junctions: Molecular Organization and Role in Vascular Homeostasis. Physiol Rev *84*, 869–901.

Behzadian, M., Wang, X.-L., Windsor, L., Ghaly, N., and Caldwell, R. (2001). TGF-beta increases retinal endothelial cell permeability by increasing MMP-9: possible role of glial cells in endothelial barrier function. IOVS *42*, 853–859.

Bhat, A.A., Pope, J.L., Smith, J.J., Ahmad, R., Chen, X., Washington, M.K., Beauchamp, R.D., Singh, A.B., and Dhawan, P. (2015). Claudin-7 expression induces mesenchymal to epithelial transformation (MET) to inhibit colon tumorigenesis. Oncogene *34*, 4570–4580.

Bhat, A.A., Uppada, S., Achkar, I.W., Hashem, S., Yadav, S.K., Shanmugakonar, M., Al-Naemi, H.A., Haris, M., and Uddin, S. (2019). Tight Junction Proteins and Signaling Pathways in Cancer and Inflammation: A Functional Crosstalk. Front Physiol *9*, 1942.

Bhowmick, N.A., Zent, R., Ghiassi, M., McDonnell, M., and Moses, H.L. (2001a). Integrin β1 Signaling Is Necessary for Transforming Growth Factor-β Activation of p38MAPK and Epithelial Plasticity. J Biol Chem *276*, 46707–46713.

Bhowmick, N.A., Ghiassi, M., Bakin, A., Aakre, M., Lundquist, C.A., Engel, M.E., Arteaga, C.L., and Moses, H.L. (2001b). Transforming Growth Factor-beta1 Mediates Epithelial to Mesenchymal Transdifferentiation through a RhoA- dependent Mechanism. Molecular Biology of the Cell *12*, 27–36.

Bierie, B., and Moses, H.L. (2010). Transforming growth factor beta (TGF-β) and inflammation in cancer. Cytokine Growth F R *21*, 49–59.

Bierie, B., Chung, C.H., Parker, J.S., Stover, D.G., Cheng, N., Chytil, A., Aakre, M., Shyr, Y., and Moses, H.L. (2009). Abrogation of TGF-β signaling enhances chemokine production and correlates with prognosis in human breast cancer. J Clin Invest *119*, 1571–1582.

Birukova, A.A., Birukov, K.G., Adyshev, D., Usatyuk, P., Natarajan, V., Garcia, J.G.N., and Verin, A.D. (2005a). Involvement of microtubules and Rho pathway in TGF-β1-induced lung vascular barrier dysfunction. J Cell Physiol *204*, 934–947.

Birukova, A.A., Adyshev, D., Gorshkov, B., Birukov, K.G., and Verin, A.D. (2005b). ALK5 and Smad4 are involved in TGF-β1-induced pulmonary endothelial permeability. Febs Lett *579*, 4031–4037.

Biswas, S., Chytil, A., Washington, K., Romero-Gallo, J., Gorska, A.E., Wirth, P.S., Gautam, S., Moses, H.L., and Grady, W.M. (2004). Transforming Growth Factor Beta Receptor Type II Inactivation Promotes the Establishment and Progression of Colon Cancer. Cancer Research *64*, 4687–4692.

Blaine, S.A., Ray, K.C., Anunobi, R., Gannon, M.A., Washington, M.K., and Means, A.L. (2010). Adult pancreatic acinar cells give rise to ducts but not endocrine cells in response to growth factor signaling. Development *137*, 2289–2296.

Bornholdt, J., Friis, S., Godiksen, S., Poulsen, S.S., Santoni-Rugiu, E., Bisgaard, H.C., Lothe, I.M., Ikdahl, T., Tveit, K.M., Johnson, E., et al. (2011). The level of claudin-7 is reduced as an early event in colorectal carcinogenesis. Bmc Cancer *11*, 65.

Bornstein, S., White, R., Malkoski, S., Oka, M., Han, G., Cleaver, T., Reh, D., Andersen, P., Gross, N., Olson, S., et al. (2009). Smad4 loss in mice causes spontaneous head and neck cancer with increased genomic instability and inflammation. J Clin Invest *119*, 3408–3419.

Bouma, G., Zamuner, S., Hicks, K., Want, A., Oliveira, J., Choudhury, A., Brett, S., Robertson, D., Felton, L., Norris, V., et al. (2017). CCL20 neutralization by a monoclonal antibody in healthy subjects selectively inhibits recruitment of CCR6+ cells in an experimental suction blister. Brit J Clin Pharmaco *83*, 1976–1990.

Brandes, M.E., Mai, U.E.H., Ohura, K., and Wahl, S.M. (1991). Type I transforming growth factor-beta receptors on neutrophils mediate chemotaxis to transforming growth factor-beta. The Journal of Immunology *147*, 1600–1606.

Broermann, A., Winderlich, M., Block, H., Frye, M., Rossaint, J., Zarbock, A., Cagna, G., Linnepe, R., Schulte, D., Nottebaum, A.F., et al. (2011). Dissociation of VE-PTP from VE-cadherin is required for leukocyte extravasation and for VEGF-induced vascular permeability in vivo. J Exp Medicine *208*, 2393–2401.

Butler, A., Hoffman, P., Smibert, P., Papalexi, E., and Satija, R. (2018). Integrating single-cell transcriptomic data across different conditions, technologies, and species. Nat Biotechnol *36*, 411–420.

Callahan, B.J., McMurdie, P.J., Rosen, M.J., Han, A.W., Johnson, A.J.A., and Holmes, S.P. (2016). DADA2: High-resolution sample inference from Illumina amplicon data. Nat Methods *13*, 581–583.

Cano, A., Pérez-Moreno, M.A., Rodrigo, I., Locascio, A., Blanco, M.J., Barrio, M.G. del, Portillo, F., and Nieto, M.A. (2000). The transcription factor Snail controls epithelial–mesenchymal transitions by repressing E-cadherin expression. Nat Cell Biol *2*, 76–83.

Capaldo, C.T., and Nusrat, A. (2009). Cytokine regulation of tight junctions. Biochimica Et Biophysica Acta Bba - Biomembr *1788*, 864–871.

Caporaso, J.G., Kuczynski, J., Stombaugh, J., Bittinger, K., Bushman, F.D., Costello, E.K., Fierer, N., Peña, A.G., Goodrich, J.K., Gordon, J.I., et al. (2010). QIIME allows analysis of high-throughput community sequencing data. Nat Methods *7*, 335–336.

Caron, T.J., Scott, K.E., Sinha, N., Muthupalani, S., Baqai, M., Ang, L.-H., Li, Y., Turner, J.R., Fox, J.G., and Hagen, S.J. (2021). Claudin-18 Loss Alters Transcellular Chloride Flux but not Tight Junction Ion Selectivity in Gastric Epithelial Cells. Cell Mol Gastroenterology Hepatology *11*, 783–801.

Chen, J.-J., Sun, Y., and Nabel, G.J. (1998). Regulation of the Proinflammatory Effects of Fas Ligand (CD95L). Science *282*, 1714–1717.

Chen, Z., Quan, L., Huang, A., Zhao, Q., Yuan, Y., Yuan, X., Shen, Q., Shang, J., Ben, Y., Qin, F.X.-F., et al. (2018). seq-ImmuCC: Cell-Centric View of Tissue Transcriptome Measuring Cellular Compositions of Immune Microenvironment From Mouse RNA-Seq Data. Front Immunol *9*, 1286.

Cheng, B., Rong, A., Zhou, Q., and Li, W. (2019). CLDN8 promotes colorectal cancer cell proliferation, migration, and invasion by activating MAPK/ERK signaling. Cancer Management Res *11*, 3741–3751.

Choksi, Y.A., Reddy, V.K., Singh, K., Barrett, C.W., Short, S.P., Parang, B., Keating, C.E., Thompson, J.J., Verriere, T.G., Brown, R.E., et al. (2018). BVES is required for maintenance of colonic epithelial integrity in experimental colitis by modifying intestinal permeability. Mucosal Immunol *11*, 1363–1374.

Ciardiello, D., Elez, E., Tabernero, J., and Seoane, J. (2020). Clinical development of therapies targeting TGFβ: current knowledge and future perspectives. Ann Oncol *31*, 1336–1349.

Clements, R.T., Minnear, F.L., Singer, H.A., Keller, R.S., and Vincent, P.A. (2005). RhoA and Rho-kinase dependent and independent signals mediate TGF-β-induced pulmonary endothelial cytoskeletal reorganization and permeability. Am J Physiol-Lung C *288*, L294–L306.

Comerford, I., Bunting, M., Fenix, K., Haylock-Jacobs, S., Litchfield, W., Harata-Lee, Y., Turvey, M., Brazzatti, J., Gregor, C., Nguyen, P., et al. (2010). An immune paradox: How can the same chemokine axis regulate both immune tolerance and activation? Bioessays *32*, 1067–1076.

Corada, M., Mariotti, M., Thurston, G., Smith, K., Kunkel, R., Brockhaus, M., Lampugnani, M., Martin-Padura, I., Stoppacciaro, A., Ruco, L., et al. (1999). Vascular endothelial-cadherin is an important determinant of microvascular integrity in vivo. PNAS *96*, 9815–9820.

Corbet, C., Bastien, E., Jesus, J.P.S. de, Dierge, E., Martherus, R., Linden, C.V., Doix, B., Degavre, C., Guilbaud, C., Petit, L., et al. (2020). TGFβ2-induced formation of lipid droplets supports acidosis-driven EMT and the metastatic spreading of cancer cells. Nat Commun *11*, 454.

Dai, J.L., Bansal, R.K., and Kern, S.E. (1999). G1 cell cycle arrest and apoptosis induction by nuclear Smad4/Dpc4: Phenotypes reversed by a tumorigenic mutation. Proc National Acad Sci *96*, 1427–1432.

Darsigny, M., Babeu, J.-P., Dupuis, A.-A., Furth, E.E., Seidman, E.G., Lévy, É., Verdu, E.F., Gendron, F.-P., and Boudreau, F. (2009). Loss of Hepatocyte-Nuclear-Factor-4α Affects Colonic Ion Transport and Causes Chronic Inflammation Resembling Inflammatory Bowel Disease in Mice. Plos One *4*, e7609.

Dhasarathy, A., Phadke, D., Mav, D., Shah, R.R., and Wade, P.A. (2011). The Transcription Factors Snail and Slug Activate the Transforming Growth Factor-Beta Signaling Pathway in Breast Cancer. Plos One *6*, e26514.

Dhawan, P., Singh, A.B., Deane, N.G., No, Y., Shiou, S.-R., Schmidt, C., Neff, J., Washington, M.K., and Beauchamp, R.D. (2005). Claudin-1 regulates cellular transformation and metastatic behavior in colon cancer. J Clin Invest *115*, 1765–1776.

Dhawan, P., Ahmad, R., Chaturvedi, R., Smith, J.J., Midha, R., Mittal, M.K., Krishnan, M., Chen, X., Eschrich, S., Yeatman, T.J., et al. (2011). Claudin-2 expression increases tumorigenicity of colon cancer cells: role of epidermal growth factor receptor activation. Oncogene *30*, 3234–3247.

Dieleman, L., Palmen, M., Akol, H., Bloemena, E., Pena, A., and Meuwissen, S. (1988). Chronic experimental colitis induced by dextran sulphate sodium (DSS) is characterized by Th1 and Th2 cytokines. Clin Exp Immunol *114*, 385–391.

Dignass, A., and Podolsky, D. (1993). Cytokine modulation of intestinal epithelial cell restitution: Cell role o transforming growth factor beta. Gastro *105*, 1323–1332.

Dobin, A., Davis, C.A., Schlesinger, F., Drenkow, J., Zaleski, C., Jha, S., Batut, P., Chaisson, M., and Gingeras, T.R. (2013). STAR: ultrafast universal RNA-seq aligner. Bioinformatics *29*, 15–21.

Docagne, F., Gabriel, C., Lebeurrier, N., Lesne, S., Hommet, Y., Plawinski, L., MacKenzie, E., and Viven, D. (2004). Sp1 and Smad transcription factors co-operate to mediate TGF-beta-dependent activation of amyloid-beta precursor protein gene transcription. Biochem J *383*, 393–399.

Dongre, A., and Weinberg, R.A. (2019). New insights into the mechanisms of epithelial–mesenchymal transition and implications for cancer. Nat Rev Mol Cell Bio *20*, 69–84.

Edgar, R., Domrachev, M., and Lash, A.E. (2002). Gene Expression Omnibus: NCBI gene expression and hybridization array data repository. Nucleic Acids Res *30*, 207–210.

Elinav, E., Nowarski, R., Thaiss, C.A., Hu, B., Jin, C., and Flavell, R.A. (2013). Inflammation-induced cancer: crosstalk between tumours, immune cells and microorganisms. Nat Rev Cancer *13*, 759–771.

Engel, M.E., McDonnell, M.A., Law, B.K., and Moses, H.L. (1999). Interdependent SMAD and JNK Signaling in Transforming Growth Factor-beta-mediated Transcription. The Journal of Biological Chemistry *274*, 37413–37420.

Fahy, R.J., Lichtenberger, F., McKeegan, C.B., Nuovo, G.J., Marsh, C.B., and Wewers, M.D. (2003). The Acute Respiratory Distress Syndrome. Am J Resp Cell Mol *28*, 499–503.

Farkas, A.E., Capaldo, C.T., and Nusrat, A. (2012). Regulation of epithelial proliferation by tight junction proteins. Ann Ny Acad Sci *1258*, 115–124.

Fihn, B., Sjöqvist, A., and Jodal, M. (2000). Permeability of the rat small intestinal epithelium along the villus-crypt axis: Effects of glucose transport. Gastroenterology *119*, 1029–1036.

Fink, S., Swinler, S., Lutterbaugh, J., Massague, J., Thiagalingam, S., Kinzler, K., Vogelstein, B., Willson, J., and Markowitz, S. (2001). Transforming growth factor-beta-induced growth inhibition in a Smad4 mutant colon adenoma cell line. Cancer Research *61*, 256–260.

France, M.M., and Turner, J.R. (2017). The mucosal barrier at a glance. J Cell Sci *130*, jcs.193482.

Freeman, T.J., Smith, J.J., Chen, X., Washington, M.K., Roland, J.T., Means, A.L., Eschrich, S.A., Yeatman, T.J., Deane, N.G., and Beauchamp, R.D. (2012). Smad4-Mediated Signaling Inhibits Intestinal Neoplasia by Inhibiting Expression of β-Catenin. Gastroenterology *142*, 562-571.e2.

Frick, V.O., .Rubie, C., Kölsch, K., Wagner, M., Ghadjar, P., Graeber, S., and Glanemann, M. (2013). CCR6/CCL20 Chemokine Expression Profile in Distinct Colorectal Malignancies. Scand J Immunol *78*, 298–305.

Fridlender, Z.G., Sun, J., Kim, S., Kapoor, V., Cheng, G., Ling, L., Worthen, G.S., and Albelda, S.M. (2009). Polarization of Tumor-Associated Neutrophil Phenotype by TGF-β: "N1" versus "N2" TAN. Cancer Cell *16*, 183–194.

Fries, W., renda, M., Presti, M., Raso, A., Orlando, A., Oliva, L., Giofre, M., Maggio, A., Mattaliano, A., Macaluso, A., et al. (2005). Intestinal permeability and genetic determinants in patients, first-degree relatives, and controls in a high-incidence area of Crohn's Disease in Southern Italy. American Journal of Gastroenterology *100*, 2730–2736.

Fukata, M., Chen, A., Vamadevan, A.S., Cohen, J., Breglio, K., Krishnareddy, S., Hsu, D., Xu, R., Harpaz, N., Dannenberg, A.J., et al. (2007). Toll-Like Receptor-4 Promotes the Development of Colitis-Associated Colorectal Tumors. Gastroenterology *133*, 1869-1869.e14.

Garcia-Hernandez, V., Quiros, M., and Nusrat, A. (2017). Intestinal epithelial claudins: expression and regulation in homeostasis and inflammation. Ann Ny Acad Sci *1397*, 66–79.

Garrod, D., and Chidgey, M. (2008). Desmosome structure, composition and function. Biochimica Et Biophysica Acta Bba - Biomembr *1778*, 572–587.

Ginzberg, H.H., Shannon, P.T., Suzuki, T., Hong, O., Vachon, E., Moraes, T., Abreu, M.T.H., Cherepanov, V., Wang, X., Chow, C.-W., et al. (2004). Leukocyte elastase induces epithelial apoptosis: role of mitochondial permeability changes and Akt. Am J Physiol-Gastr L *287*, G286–G298.

Glassner, K.L., Abraham, B.P., and Quigley, E.M.M. (2020). The microbiome and inflammatory bowel disease. J Allergy Clin Immun *145*, 16–27.

Goldberg, P.L., MacNaughtten, D.E., Clements, R.T., Minnear, F.L., and Vincent, P.A. (2002). p38 MAPK activation by TGF-b1 increases MLC phosphorylation and endothelial monolayer permeability. American Journal of Physiology-Lung Cellular and Molecular Physiology *282*, L146-54.

Gorelik, L., and Flavell, R.A. (2000). Abrogation of TGFβ Signaling in T Cells Leads to Spontaneous T Cell Differentiation and Autoimmune Disease. Immunity *12*, 171–181.

Gorelik, L., and Flavell, R.R. (2002). Transforming Growth Factor-β In T-Cell Biology. Nature Reviews Immunology *2*, 46–53.

Gottfried, Y., Rotem, A., Lotan, R., Steller, H., and Larisch, S. (2004). The mitochondrial ARTS protein promotes apoptosis through targeting XIAP. Embo J *23*, 1627–1635.

Gowrikumar, S., Ahmad, R., Uppada, S.B., Washington, M.K., Shi, C., Singh, A.B., and Dhawan, P. (2019). Upregulated claudin-1 expression promotes colitis-associated cancer by promoting β-catenin phosphorylation and activation in Notch/p-AKT-dependent manner. Oncogene *38*, 5321–5337.

Grady, W.M., Myeroff, L.L., Swinker, S.E., Rajput, A., Thiagalingam, S., Lutterbaugh, J.D., Neumann, A., Brattain, M.G., Chang, J., Kim, S.-J., et al. (1999). Mutational Inactivation of Transforming Growth Factor Beta Receptor Type II in Microsatellite Stable Colon Cancers. Cancer Research *59*, 320–324.

Grande, M.T., Sánchez-Laorden, B., López-Blau, C., Frutos, C.A.D., Boutet, A., Arévalo, M., Rowe, R.G., Weiss, S.J., López-Novoa, J.M., and Nieto, M.A. (2015). Snail1-induced partial epithelial-to-mesenchymal transition drives renal fibrosis in mice and can be targeted to reverse established disease. Nat Med *21*, 989–997.

Green, M.R., and Sambrook, J. (2018). Quantification of RNA by Real-Time Reverse Transcription-Polymerase Chain Reaction (RT-PCR). Cold Spring Harb Protoc *10*, 847–856.

Grelet, S., Link, L.A., Howley, B., Obellianne, C., Palanisamy, V., Gangaraju, V.K., Diehl, J.A., and Howe, P.H. (2017a). A regulated PNUTS mRNA to lncRNA splice switch mediates EMT and tumour progression. Nat Cell Biol *19*, 1105–1115.

Grelet, S., McShane, A., Geslain, R., and Howe, P.H. (2017b). Pleiotropic Roles of Non-Coding RNAs in TGF-β-Mediated Epithelial-Mesenchymal Transition and Their Functions in Tumor Progression. Cancers *9*, 75.

Grivennikov, S.I., Wang, K., Mucida, D., Stewart, C.A., Schnabl, B., Jauch, D., Taniguchi, K., Yu, G.-Y., Österreicher, C.H., Hung, K.E., et al. (2012). Adenoma-linked barrier defects and microbial products drive IL-23/IL-17-mediated tumour growth. Nature *491*, 254–258.

Guan, Q. (2019). A Comprehensive Review and Update on the Pathogenesis of Inflammatory Bowel Disease. J Immunol Res *2019*, 1–16.

Gudey, S.K., Sundar, R., Heldin, C.-H., Bergh, A., and Landström, M. (2017). Pro-invasive properties of Snail1 are regulated by sumoylation in response to TGFβ stimulation in cancer. Oncotarget *8*, 97703–97726.

Guinney, J., Dienstmann, R., Wang, X., Reyniès, A. de, Schlicker, A., Soneson, C., Marisa, L., Roepman, P., Nyamundanda, G., Angelino, P., et al. (2015). The consensus molecular subtypes of colorectal cancer. Nat Med *21*, 1350–1356.

Günzel, D., and Yu, A.S.L. (2013). Claudins and the Modulation of Tight Junction Permeability. Physiol Rev *93*, 525–569.

Habowski, A.N., Bates, J.M., Flesher, J.L., Edwards, R.A., and Waterman, M.L. (2020). Isolation of murine large intestinal crypt cell populations with flow sorting. Research Square 1–16.

Hahm, K.-B., Im, Y.-H., Parks, T.W., Park, S.-H., Markowitz, S., Jung, H.-Y., Green, J., and Kim, S.-J. (2001). Loss of transforming growth factor β signalling in the intestine contributes to tissue injury in inflammatory bowel disease. Gut *49*, 190.

Hanafusa, H., Ninomiya-Tsuji, J., Masuyama, N., Nishita, M., Fujisawa, J., Shibuya, H., Matsumoto, K., and Nishida, E. (1999). Involvement of the p38 Mitogen-activated Protein Kinase Pathway in Transforming Growth Factor-beta-induced Gene Expression. The Journal of Biological Chemistry *274*, 27161–27167.

Harris, T.J.C., and Tepass, U. (2010). Adherens junctions: from molecules to morphogenesis. Nat Rev Mol Cell Bio *11*, 502–514.

Hayashi, H., Abdollah, S., Qiu, Y., Cai, J., Xu, Y.-Y., Grinnell, B.W., Richardson, M.A., Topper, J.N., Gimbrone, M.A., Wrana, J.L., et al. (1997). The MAD-Related Protein Smad7 Associates with the TGFbeta Receptor and Functions as an Antagonist of TGFbeta Signaling. Cell *89*, 1165–1173.

Healing, E., Charlier, C.F., Meira, L.B., and Elliott, R.M. (2019). A panel of colorimetric assays to measure enzymatic activity in the base excision DNA repair pathway. Nucleic Acids Res *47*, gkz171-.

Heino, J., Ignotz, R., Hemler, M., Crouse, C., and Massague, J. (1989). Regulation of Cell Adhesion Receptors by Transforming Growth Factor-beta. J Biol Chem *264*, 380–388.

Heo, Y.J., Choi, S.-E., Lee, N., Jeon, J.Y., Han, S.J., Kim, D.J., Kang, Y., Lee, K.W., and Kim, H.J. (2020). CCL20 induced by visfatin in macrophages via the NF-κB and MKK3/6-p38 signaling pathways contributes to hepatic stellate cell activation. Mol Biol Rep *47*, 4285–4293.

Hering, N.A., Andres, S., Fromm, A., Tol, E.A. van, Amasheh, M., Mankertz, J., Fromm, M., and Schulzke, J.D. (2011). Transforming Growth Factor-β, a Whey Protein Component, Strengthens the Intestinal Barrier by Upregulating Claudin-4 in HT-29/B6 Cells. J Nutrition *141*, 783–789.

Hernandez, N.M., Casselbrant, A., Joshi, M., Johansson, B.R., and Sumitran-Holgersson, S. (2012). Antibodies to kidney endothelial cells contribute to a “leaky” glomerular barrier in patients with chronic kidney diseases. Am J Physiol-Renal *302*, F884–F894.

Hinshelwood, R.A., Huschtscha, L.I., Melki, J., Stirzaker, C., Abdipranoto, A., Vissel, B., Ravasi, T., Wells, C.A., Hume, D.A., Reddel, R.R., et al. (2007). Concordant Epigenetic Silencing of Transforming Growth Factor-β Signaling Pathway Genes Occurs Early in Breast Carcinogenesis. Cancer Res *67*, 11517–11527.

Hocevar, B.A., Brown, T.L., and Howe, P.H. (1999). TGF-β induces fibronectin synthesis through a c-Jun N-terminal kinase-dependent, Smad4-independent pathway. The EMBO Journal *18*, 1345–1356.

Höfler, P., Wehrle, I., and Bauer, G. (1993). TGF-β induces an inhibitory effect of normal cells directed against transformed cells. Int J Cancer *54*, 125–130.

Hofmann, T.G., Stollberg, N., Schmitz, M.L., and Will, H. (2003). HIPK2 Regulates Transforming Growth Factor-beta-Induced c-Jun NH2-Terminal Kinase Activation and Apoptosis in Human Hepatoma Cells. Cancer Research *63*, 8271–8277.

Hollander, D., Vadheim, C., Brittholz, E., Petersen, G., Delahunty, T., and Rotter, J. (1986). Increased Intestinal Permeability in Patients with Crohn’s Disease and Their Relatives. A Possible Etiologic Factor. Annals of Internal Medicine *105*, 883–885.

Howe, K., Gauldie, J., and McKay, D.M. (2002). TGF-β effects on epithelial ion transport and barrier: reduced Cl− secretion blocked by a p38 MAPK inhibitor. Am J Physiol-Cell Ph *283*, C1667–C1674.

Howe, K.L., Reardon, C., Wang, A., Nazli, A., and McKay, D.M. (2005). Transforming Growth Factor-β Regulation of Epithelial Tight Junction Proteins Enhances Barrier Function and Blocks Enterohemorrhagic Escherichia coli O157:H7-Induced Increased Permeability. Am J Pathology *167*, 1587–1597.

Huppert, L., Matthay, M., and Ware, L. (2019). Pathogenesis of Acute Respiratory Distress Syndrome. Semin Resp Crit Care *40*, 031–039.

Hurst, V., Goldberg, P.L., Minnear, F.L., Hiemark, R.L., and Vincent, P.A. (1999). Rearrangement of adherens junctions by transforming growth factor-beta1: role of contraction. American Journal of Physiology-Lung Cellular and Molecular Physiology *276*, L582-95.

Iacovides, D., Michael, S., Achilleos, C., and Strati, K. (2013). Shared mechanisms in stemness and carcinogenesis: lessons from oncogenic viruses. Front Cell Infect Mi *3*, 66.

Ignotz, R., and Massague, J. (1986). Transforming Growth Factor-beta Stimulates the Expresion of Fibronectin and Collagen and Their Incorporation into the Extracellular Matrix. J Biol Chem *261*, 4337–4345.

Ikushima, H., and Miyazono, K. (2010). TGFβ signalling: a complex web in cancer progression. Nat Rev Cancer *10*, 415–424.

Inamoto, S., Itatani, Y., Yamamoto, T., Minamiguchi, S., Hirai, H., Iwamoto, M., Hasegawa, S., Taketo, M.M., Sakai, Y., and Kawada, K. (2016). Loss of SMAD4 Promotes Colorectal Cancer Progression by Accumulation of Myeloid-Derived Suppressor Cells through the CCL15–CCR1 Chemokine Axis. Clin Cancer Res *22*, 492–501.

Irvine, E.J., and Marshall, J.K. (2000). Increased intestinal permeability precedes the onset of Crohn's disease in a subject with familial risk. Gastroenterology *119*, 1740–1744.

Itallie, C.M.V., Holmes, J., Bridges, A., Gookin, J.L., Coccaro, M.R., Proctor, W., Colegio, O.R., and Anderson, J.M. (2008). The density of small tight junction pores varies among cell types and is increased by expression of claudin-2. J Cell Sci *121*, 298–305.

Itallie, C.V., Fanning, A., Bridges, A., and Anderson, J. (2009). ZO-1 Stabilizes the Tight Junction Solute Barrier through Coupling to the Perijunctional Cytoskeleton. Molecular Biology of the Cell *20*, 3930–3940.

Itatani, Y., Kawada, K., Fujishita, T., Kakizaki, F., Hirai, H., Matsumoto, T., Iwamoto, M., Inamoto, S., Hatano, E., Hasegawa, suguru, et al. (2013). Loss of SMAD4 From Colorectal Cancer Cells Promotes CCL15 Expression to Recruit CCR1D Myeloid Cells and Facilitate Liver Metastasis. Gastroenterology *145*, 1064–1075.

Izeradjene, K., Combs, C., Best, M., Gopinathan, A., Wagner, A., Grady, W.M., Deng, C.-X., Hruban, R.H., Adsay, N.V., Tuveson, D.A., et al. (2007). KrasG12D and Smad4/Dpc4 Haploinsufficiency Cooperate to Induce Mucinous Cystic Neoplasms and Invasive Adenocarcinoma of the Pancreas. Cancer Cell *11*, 229–243.

Jin, S., Guerrero-Juarez, C.F., Zhang, L., Chang, I., Ramos, R., Kuan, C.-H., Myung, P., Plikus, M.V., and Nie, Q. (2021). Inference and analysis of cell-cell communication using CellChat. Nat Commun *12*, 1088.

Jing, Y., Han, Z., Liu, Y., Sun, K., Zhang, S., Jiang, G., Li, R., Gao, L., Zhao, X., Wu, D., et al. (2012). Mesenchymal Stem Cells in Inflammation Microenvironment Accelerates Hepatocellular Carcinoma Metastasis by Inducing Epithelial-Mesenchymal Transition. Plos One *7*, e43272.

Johnson, J.L., Najor, N.A., and Green, K.J. (2014). Desmosomes: Regulators of Cellular Signaling and Adhesion in Epidermal Health and Disease. Csh Perspect Med *4*, a015297.

Kaminski, N., Allard, J., Pittet, J., Zuo, F., Griffiths, M., Morris, D., Huang, X., Sheppard, D., and Heller, R. (2000). Global analysis of gene expression in pulmonary fibrosis reveals distinct programs regulating lung inflammation and fibrosis. PNAS *97*, 1778–1783.

Katz, K.D., Hollander, D., Vadheim, C.M., McElree, C., Delahunty, T., Dadufalza, V.D., Krugliak, P., and Rotter, J.I. (1989). Intestinal permeability in patients with Crohn's disease and their healthy relatives. Gastroenterology *97*, 927–931.

Khan, N., and Asif, A.R. (2015). Transcriptional Regulators of Claudins in Epithelial Tight Junctions. Mediat Inflamm *2015*, 1–6.

Khor, B., Gardet, A., and Xavier, R.J. (2011). Genetics and pathogenesis of inflammatory bowel disease. Nature *474*, 307–317.

Kim, Y., Volpert, G., Shin, K., Kim, S., Shin, S., Lee, Y., Sung, S.H., Lee, Y., Ahn, J., Pewzner-Jung, Y., et al. (2017). Ablation of ceramide synthase 2 exacerbates dextran sodium sulphate-induced colitis in mice due to increased intestinal permeability. J Cell Mol Med *21*, 3565–3578.

Kitamura, T., Kometani, K., Hashida, H., Matsunaga, A., Miyoshi, H., Hosogi, H., Aoki, M., Oshima, M., Hattori, M., Takabayashi, A., et al. (2007). SMAD4-deficient intestinal tumors recruit CCR1+ myeloid cells that promote invasion. Nat Genet *39*, 467–475.

Klausen, P., Karstensen, J.G., Coskun, M., Săftoiu, A., Vilmann, P., Cowland, J.B., and Riis, L.B. (2018). SMAD4 Protein Expression Is Downregulated in Ileal Epithelial Cells from Patients with Crohn's Disease with Significant Inverse Correlation to Disease Activity. Gastroent Res Pract *2018*, 1–8.

Kojima, T., Takano, K., Yamamoto, T., Murata, M., Son, S., Imamura, M., Yamaguchi, H., Osanai, M., Chiba, H., Himi, T., et al. (2007). Transforming growth factor-β induces epithelial to mesenchymal transition by down-regulation of claudin-1 expression and the fence function in adult rat hepatocytes. Liver Int *28*, 534–545.

Kolb, M., Margetts, P.J., Anthony, D.C., Pitossi, F., and Gauldie, J. (2001). Transient expression of IL-1β induces acute lung injury and chronic repair leading to pulmonary fibrosis. J Clin Invest *107*, 1529–1536.

Komarova, Y.A., Kruse, K., Mehta, D., and Malik, A.B. (2017). Protein Interactions at Endothelial Junctions and Signaling Mechanisms Regulating Endothelial Permeability. Circ Res *120*, 179–206.

Kontani, K., Kajino, K., Huangi, C.-L., Fujino, S., Taguchi, O., Yamauchi, A., Yokomise, H., and Ogasawara, K. (2006). Spontaneous elicitation of potent antitumor immunity and eradication of established tumors by administration of DNA encoding soluble transforming growth factor-β II receptor without active antigen-sensitization. Cancer Immunol Immunother *55*, 579–587.

Koveitypour, Z., Panahi, F., Vakilian, M., Peymani, M., Forootan, F.S., Esfahani, M.H.N., and Ghaedi, K. (2019). Signaling pathways involved in colorectal cancer progression. Cell Biosci *9*, 97.

Krah, N.M., and Murtaugh, L.C. (2016). Differentiation and Inflammation: 'Best Enemies' in Gastrointestinal Carcinogenesis. Trends Cancer *2*, 723–735.

Krug, S.M., Schulzke, J.D., and Fromm, M. (2014). Tight junction, selective permeability, and related diseases. Semin Cell Dev Biol *36*, 166–176.

Kucharzik, T., Hudson, J.T., Waikel, R.L., Martin, W.D., and Williams, I.R. (2002). CCR6 expression distinguishes mouse myeloid and lymphoid dendritic cell subsets: demonstration using a CCR6 EGFP knock-in mouse. Eur J Immunol *32*, 104–112.

Kurose, M., Kojima, T., Koizumi, J., Kamekura, R., Ninomiya, T., Murata, M., Ichimiya, S., Osanai, M., Chiba, H., Himi, T., et al. (2007). Induction of claudins in passaged hTERT-transfected human nasal epithelial cells with an extended life span. Cell Tissue Res *330*, 63–74.

Lameris, A.L., Huybers, S., Kaukinen, K., Mäkelä, T.H., Bindels, R.J., Hoenderop, J.G., and Nevalainen, P.I. (2012). Expression profiling of claudins in the human gastrointestinal tract in health and during inflammatory bowel disease. Scand J Gastroentero *48*, 58–69.

Laukoetter, M.G., Nava, P., Lee, W.Y., Severson, E.A., Capaldo, C.T., Babbin, B.A., Williams, I.R., Koval, M., Peatman, E., Campbell, J.A., et al. (2007). JAM-A regulates permeability and inflammation in the intestine in vivo. J Exp Medicine *204*, 3067–3076.

Laun, R., Schroder, O., Schoppnies, M., Roher, H.-D., Ekkernkamp, A., and Schulte, K.-M. (2003). Transforming growth factor-beta1 and major trauma: time-dependent association with hepatic and renal insufficiency. Shock *19*, 16–23.

Leclerc, V.B., Roy, O., Santerre, K., and Proulx, S. (2018). TGF-β1 promotes cell barrier function upon maturation of corneal endothelial cells. Sci Rep-Uk *8*, 4438.

Levy, L., and Hill, C.S. (2006). Alterations in components of the TGF-β superfamily signaling pathways in human cancer. Cytokine Growth F R *17*, 41–58.

Li, M.O., Wan, Y.Y., Sanjabi, S., Robertson, A.-K.L., and Flavell, R.A. (2006). TRANSFORMING GROWTH FACTOR-β REGULATION OF IMMUNE RESPONSES. Immunology *24*, 99–146.

Li, W., Qiao, W., Chen, L., Xu, X., Yang, X., Li, D., Li, C., Brodie, S.G., Meguid, M.M., Hennighausen, L., et al. (2003). Squamous cell carcinoma and mammary abscess formation through squamous metaplasia in Smad4/Dpc4 conditional knockout mice. Development *130*, 6143–6153.

Liao, L., Zhang, M.-W., Gu, Y.-J., and Sun, X.-C. (2020). Targeting CCL20 inhibits subarachnoid hemorrhage-related neuroinflammation in mice. Aging *12*, 14849–14862.

Liao, R.-Y., Mao, C., Qiu, L.-X., Ding, H., Chen, Q., and Pan, H.-F. (2010). TGFBR1*6A/9A polymorphism and cancer risk: a meta-analysis of 13,662 cases and 14,147 controls. Mol Biol Rep *37*, 3227–3232.

Lu, Q., Harrington, E.O., Jackson, H., Morin, N., Shannon, C., and Rounds, S. (2006a). Transforming growth factor-β1-induced endothelial barrier dysfunction involves Smad2-dependent p38 activation and subsequent RhoA activation. J Appl Physiol *101*, 375–384.

Lu, S.-L., Herrington, H., Reh, D., Weber, S., Bornstein, S., Wang, D., Li, A.G., Tang, C.-F., Siddiqui, Y., Nord, J., et al. (2006b). Loss of transforming growth factor-β type II receptor promotes metastatic head-and-neck squamous cell carcinoma. Gene Dev *20*, 1331–1342.

Luettig, J., Rosenthal, R., Barmeyer, C., and Schulzke, J. (2015). Claudin-2 as a mediator of leaky gut barrier during intestinal inflammation. Tissue Barriers *3*, e977176.

Lügering, A., Ross, M., Sieker, M., Heidemann, J., Williams, I.R., Domschke, W., and Kucharzik, T. (2010). CCR6 identifies lymphoid tissue inducer cells within cryptopatches. Clin Exp Immunol *160*, 440–449.

Macedonia, M.C., Drewes, J.L., Markham, N.O., Simmons, A.J., Roland, J.T., Vega, P.N., Scurrah, C.R., Coffey, R.J., Shrubsole, M.J., Sears, C.L., et al. (2020). Clinically adaptable polymer enables simultaneous spatial analysis of colonic tissues and biofilms. Npj Biofilms Microbiomes *6*, 33.

Maitland, N.J., and Collins, A.T. (2008). Inflammation as the primary aetiological agent of human prostate cancer: A stem cell connection? J Cell Biochem *105*, 931–939.

Marincola-Smith, P., Means, A.L., and Beauchamp, R.D. (2019). Immunomodulatory Effects of TGF-β Family Signaling within Intestinal Epithelial Cells and Carcinomas. Gastrointest Disord *1*, 290–300.

Markowitz, S., Wang, J., Myeroff, L., Parsons, R., Sun, L., and Lutterbaugh, J. (1995). Inactivation of the type II TGF-Beta receptor in colon cancer cells with microsatellite instability. Science *268*, 1336–1338.

Martini, E., Krug, S.M., Siegmund, B., Neurath, M.F., and Becker, C. (2017). Mend Your Fences The Epithelial Barrier and its Relationship With Mucosal Immunity in Inflammatory Bowel Disease. Cell Mol Gastroenterology Hepatology *4*, 33–46.

Massagué, J. (2012). TGFβ signalling in context. Nat Rev Mol Cell Bio *13*, 616–630.

Matthay, M.A., Zemans, R.L., Zimmerman, G.A., Arabi, Y.M., Beitler, J.R., Mercat, A., Herridge, M., Randolph, A.G., and Calfee, C.S. (2019). Acute respiratory distress syndrome. Nat Rev Dis Primers *5*, 18.

May, G., Sutherland, L., and Meddings, J. (1993). Is small intestinal permeability really increased in relatives of patients with Crohn's disease? Gastro *104*, 1627–1632.

Mazzon, E., and Cuzzocrea, S. (2007). Role of TNF-α in lung tight junction alteration in mouse model of acute lung inflammation. Respir Res *8*, 75.

McClintock, S.D., Attili, D., Dame, M.K., Richter, A., Silvestri, S.S., Berner, M.M., Bohm, M.S., Karpoff, K., McCarthy, C.L., Spence, J.R., et al. (2020). Differentiation of human colon tissue in culture: Effects of calcium on trans-epithelial electrical resistance and tissue cohesive properties. Plos One *15*, e0222058.

McEwen, A.E., Escobar, D.E., and Gottardi, C.J. (2012). Adherens Junctions: from Molecular Mechanisms to Tissue Development and Disease. Subcell Biochem *60*, 171–196.

McGuckin, M.A., Eri, R., Simms, L.A., Florin, T.H.J., and Radford-Smith, G. (2009). Intestinal barrier dysfunction in inflammatory bowel diseases. Inflamm Bowel Dis *15*, 100–113.

McKay, D., and Singh, P. (1997). Superantigen activation of immune cells evokes epithelial (T84) transport and barrier abnormalities via IFN-gamma and TNF-alpha: inhibition of increased permeability, but not diminished secretory responses, by TGF-beta2. The Journal of Immunology *159*, 2382–2390.

McLean, M.H., Murray, G.I., Stewart, K.N., Norrie, G., Mayer, C., Hold, G.L., Thomson, J., Fyfe, N., Hope, M., Mowat, N.A.G., et al. (2011). The Inflammatory Microenvironment in Colorectal Neoplasia. Plos One *6*, e15366–e15368.

McNicholas, B.A., Rooney, G.M., and Laffey, J.G. (2018). Lessons to learn from epidemiologic studies in ARDS. Curr Opin Crit Care *24*, 41–48.

Means, A.L., Ray, K.C., Singh, A.B., Washington, M.K., Whitehead, R.H., Harris, R.C., Wright, C.V.E., Coffey, R.J., and Leach, S.D. (2003). Overexpression of heparin-binding EGF-like growth factor in mouse pancreas results in fibrosis and epithelial metaplasia. Gastroenterology *124*, 1020–1036.

Means, A.L., Xu, Y., Zhao, A., Ray, K.C., and Gu, G. (2008). A CK19CreERT knockin mouse line allows for conditional DNA recombination in epithelial cells in multiple endodermal organs. Genesis *46*, 318–323.

Means, A.L., Freeman, T.J., Zhu, J., Woodbury, L.G., Marincola-Smith, P., Wu, C., Meyer, A.R., Weaver, C.J., Padmanabhan, C., An, H., et al. (2018). Epithelial Smad4 deletion upregulates inflammation and promotes inflammation-associated cancer. Cell Mol Gastroenterology Hepatology *6*, 257–276.

Meng, X.-M., Chung, A.C.K., and Lan, H.Y. (2013). Role of the TGF-β/BMP-7/Smad pathways in renal diseases. Clin Sci *124*, 243–254.

Michael, S., Achilleos, C., Panayiotou, T., and Strati, K. (2016). Inflammation Shapes Stem Cells and Stemness during Infection and Beyond. Frontiers Cell Dev Biology *4*, 118.

Miyazono, K., Ehata, S., and Koinuma, D. (2011). Tumor-promoting functions of transforming growth factor-β in progression of cancer. Upsala J Med Sci *117*, 143–152.

Molchadsky, A., and Rotter, V. (2017). p53 and its mutants on the slippery road from stemness to carcinogenesis. Carcinogenesis *38*, 347–358.

Monteleone, G., Kumberova, A., Croft, N.M., McKenzie, C., Steer, H.W., and MacDonald, T.T. (2001). Blocking Smad7 restores TGF-β1 signaling in chronic inflammatory bowel disease. J Clin Invest *108*, 601–609.

Monteleone, G., Blanco, G.D.V., Monteleone, I., Fina, D., Caruso, R., Gioia, V., Ballerini, S., Federici, G., Bernardini, S., Pallone, F., et al. (2005). Post-transcriptional Regulation of Smad7 in the Gut of Patients With Inflammatory Bowel Disease. Gastroenterology *129*, 1420–1429.

Monteleone, G., Fantini, M.C., Onali, S., Zorzi, F., Sancesario, G., Bernardini, S., Calabrese, E., Viti, F., Monteleone, I., Biancone, L., et al. (2012a). Phase I Clinical Trial of Smad7 Knockdown Using Antisense Oligonucleotide in Patients With Active Crohn's Disease. Mol Ther *20*, 870–876.

Monteleone, G., Caruso, R., and Pallone, F. (2012b). Role of Smad7 in inflammatory bowel diseases. World J Gastroentero *18*, 5664–5668.

Monteleone, G., Neurath, M.F., Ardizzone, S., Sabatino, A.D., Fantini, M.C., Castiglione, F., Scribano, M.L., Armuzzi, A., Caprioli, F., Sturniolo, G.C., et al. (2015). Mongersen, an Oral SMAD7 Antisense Oligonucleotide, and Crohn's Disease. New Engl J Medicine *372*, 1104–1113.

Mörbe, U.M., Jørgensen, P.B., Fenton, T.M., Burg, N. von, Riis, L.B., Spencer, J., and Agace, W.W. (2021). Human gut-associated lymphoid tissues (GALT); diversity, structure, and function. Mucosal Immunol 1–10.

Morikawa, M., Koinuma, D., Miyazono, K., and Heldin, C.-H. (2013). Genome-wide mechanisms of Smad binding. Oncogene *32*, 1609–1615.

Morita, K., Sasaki, H., Furuse, M., and Tsukita, S. (1999). Endothelial Claudin. J Cell Biology *147*, 185–194.

Moses, H.L., and Serra, R. (1996). Regulation of differentiation by TGF-beta. Current Opinion in Genetics & Development *6*, 581–586.

Moustakas, A., and Heldin, C.-H. (2005). Non-Smad TGF-β signals. J Cell Sci *118*, 3573–3584.

Munkholm, P., Langholz, E., Hollander, D., Thornberg, K., Orholm, M., Katz, K.D., and Binder, V. (1994). Intestinal permeability in patients with Crohn's disease and ulcerative colitis and their first degree relatives. Gut *35*, 68.

Myers, R.B., Fredenburgh, J.L., and Grizzle, W.E. (2018). Carbohydrates. In Theory and Practice of Histological Techniques (Sixth Edition), K. Suvarna, C. Layton, and J. Bancroft, eds. (Elsevier), pp. 161–186.

Nava, P., Capaldo, C.T., Koch, S., Kolegraff, K., Rankin, C.R., Farkas, A.E., Feasel, M.E., Li, L., Addis, C., Parkos, C.A., et al. (2011). JAM-A regulates epithelial proliferation through Akt/β-catenin signalling. Embo Rep *12*, 314–320.

Nguyen, N., Fernando, S.D., Biette, K.A., Hammer, J.A., Capocelli, K.E., Kitzenberg, D.A., Glover, L.E., Colgan, S.P., Furuta, G.T., and Masterson, J.C. (2018). TGF-β1 alters esophageal epithelial barrier function by attenuation of claudin-7 in eosinophilic esophagitis. Mucosal Immunol *11*, 415–426.

Okayasu, I., Yamada, M., Mikami, T., Yoshida, T., Kanno, J., and Ohkusa, T. (2002). Dysplasia and carcinoma development in experimental colitis. Journal of Gastroenterology and Hepatology *17*, 1078–1083.

Otani, T., Nguyen, T.P., Tokuda, S., Sugihara, K., Sugawara, T., Furuse, K., Miura, T., Ebnet, K., and Furuse, M. (2019). Claudins and JAM-A coordinately regulate tight junction formation and epithelial polarityClaudins and JAM-A in tight junction formation. J Cell Biology *218*, 3372–3396.

Otegbeye, F., Ojo, E., Moreton, S., Mackowski, N., Lee, D.A., Lima, M. de, and Wald, D.N. (2018). Inhibiting TGF-beta signaling preserves the function of highly activated, in vitro expanded natural killer cells in AML and colon cancer models. Plos One *13*, e0191358.

Overgaard, C.E., Mitchell, L.A., and Koval, M. (2012). Roles for claudins in alveolar epithelial barrier function. Ann Ny Acad Sci *1257*, 167–174.

Panpetch, W., Chancharoenthana, W., Bootdee, K., Nilgate, S., Finkelman, M., Tumwasorn, S., and Leelahavanichkul, A. (2018). Lactobacillus rhamnosus L34 Attenuates Gut Translocation-Induced Bacterial Sepsis in Murine Models of Leaky Gut. Infect Immun *86*, e00700-17.

Pardali, K., Kurisaki, A., Morén, A., Dijke, P. ten, Kardassis, D., and Moustakas, A. (2000). Role of Smad Proteins and Transcription Factor Sp1 in p21Waf1/Cip1 Regulation by Transforming Growth Factor-β*. J Biol Chem *275*, 29244–29256.

Parsons, R., Myeroff, L.L., Liu, B., Willson, J.K., Markowitz, S.D., Kinzler, K.W., and Vogelstein, B. (1995). Microsatellite Instability and Mutations of the Transforming Growth Factor Beta Type II Receptor Gene in Colorectal Cancer. Cancer Research *55*, 5548–5550.

Pasche, B., Kolachana, P., Nafa, K., Satagopan, J., Chen, Y.-G., Lo, R.S., Brener, D., Yang, D., Kirstein, L., Oddoux, C., et al. (1999). TbR-I(6A) Is a Candidate Tumor Susceptibility Allele. Cancer Research *59*, 5678–5682.

Pasche, B., Kaklamani, V., Hou, N., Young, T., Rademaker, A., Peterlongo, P., Ellis, N., Offit, K., Caldes, T., Reiss, M., et al. (2004). TGFBR1*6A and Cancer: A Meta-Analysis of 12 Case-Control Studies. Journal of Clinical Oncology *22*, 756–758.

Pearce, S.C., Al-Jawadi, A., Kishida, K., Yu, S., Hu, M., Fritzky, L.F., Edelblum, K.L., Gao, N., and Ferraris, R.P. (2018). Marked differences in tight junction composition and macromolecular permeability among different intestinal cell types. Bmc Biol *16*, 19.

Peeters, M., Geypens, B., Claus, D., Nevens, H., Ghoos, Y., Verbeke, G., Baert, F., Vermeire, S., Vlietinck, R., and Rutgeerts, P. (1997). Clustering of increased small intestinal permeability in families with Crohn's Disease. Gastro *113*, 802–807.

Petukhov, V., Guo, J., Baryawno, N., Severe, N., Scadden, D.T., Samsonova, M.G., and Kharchenko, P.V. (2018). dropEst: pipeline for accurate estimation of molecular counts in droplet-based single-cell RNA-seq experiments. Genome Biol *19*, 78.

Pierucci-Alves, F., Yi, S., and Schultz, B.D. (2012). Transforming Growth Factor Beta 1 Induces Tight Junction Disruptions and Loss of Transepithelial Resistance Across Porcine Vas Deferens Epithelial Cells. Biol Reprod *86*, Article 36, 1-8.

Pittet, J.-F., Griffiths, M.J.D., Geiser, T., Kaminski, N., Dalton, S.L., Huang, X., Brown, L.A.S., Gotwals, P.J., Koteliansky, V.E., Matthay, M.A., et al. (2001). TGF-β is a critical mediator of acute lung injury. J Clin Invest *107*, 1537–1544.

Planchon, S., Martins, C., Guerrant, R., and Roche, J. (1994). Regulation of intestinal epithelial barrier function by TGF-beta1. Evidence for its role in abrogating the effect of a T cell cytokine. The Journal of Immunology *153*, 5730–5739.

Planchon, S., Fiocchi, C., Takafuji, V., and Roche, J.K. (1999). Transforming Growth Factor-b1 Preserves Epithelial Barrier Function: Identification of Receptors, Biochemical Intermediates, and Cytokine Antagonists. Journal of Cellular Physiology *181*, 55–66.

Pope, J.L., Ahmad, R., Bhat, A.A., Washington, M.K., Singh, A.B., and Dhawan, P. (2014). Claudin-1 overexpression in intestinal epithelial cells enhances susceptibility to adenamatous polyposis coli-mediated colon tumorigenesis. Mol Cancer *13*, 167.

Powell, A.E., Wang, Y., Li, Y., Poulin, E.J., Means, A.L., Washington, M.K., Higginbotham, J.N., Juchheim, A., Prasad, N., Levy, S.E., et al. (2012). The Pan-ErbB Negative Regulator Lrig1 Is an Intestinal Stem Cell Marker that Functions as a Tumor Suppressor. Cell *149*, 146–158.

Prasad, S., Mingrino, R., Kaukinen, K., Hayes, K.L., Powell, R.M., MacDonald, T.T., and Collins, J.E. (2005). Inflammatory processes have differential effects on claudins 2, 3 and 4 in colonic epithelial cells. Lab Invest *85*, 1139–1162.

Principe, D.R., Doll, J.A., Bauer, J., Jung, B., Munshi, H.G., Bartholin, L., Pasche, B., Lee, C., and Grippo, P.J. (2014). TGF-β: Duality of Function Between Tumor Prevention and Carcinogenesis. Jnci J National Cancer Inst *106*, djt369–djt369.

Principe, D.R., DeCant, B., Staudacher, J., Vitello, D., Mangan, R.J., Wayne, E.A., Mascarinas, E., Diaz, A.M., Bauer, J., McKinney, R.D., et al. (2017). Loss of TGFβ signaling promotes colon cancer progression and tumor-associated inflammation. Oncotarget *8*, 3826–3839.

Qi, Z., Li, Y., Zhao, B., Xu, C., Liu, Y., Li, H., Zhang, B., Wang, X., Yang, X., Xie, W., et al. (2017). BMP restricts stemness of intestinal Lgr5+ stem cells by directly suppressing their signature genes. Nat Commun *8*, 13824.

Qiao, W., Li, A.G., Owens, P., Xu, X., Wang, X.-J., and Deng, C.-X. (2006). Hair follicle defects and squamous cell carcinoma formation in Smad4 conditional knockout mouse skin. Oncogene *25*, 207–217.

Qin, J., Li, R., Raes, J., Arumugam, M., Burgdorf, K.S., Manichanh, C., Nielsen, T., Pons, N., Levenez, F., Yamada, T., et al. (2010). A human gut microbial gene catalogue established by metagenomic sequencing. Nature *464*, 59–65.

Raju, P., Shashikanth, N., Tsai, P.-Y., Pongkorpsakol, P., Chanez-Parades, S., Steinhagen, P.R., Kuo, W.-T., Singh, G., Tsukita, S., and Turner, J.R. (2020). Inactivation of paracellular cation-selective claudin-2 channels attenuates immune-mediated experimental colitis in mice. J Clin Invest *130*, 5197–5208.

Rakoff-Nahoum, S., and Medzhitov, R. (2007). Regulation of Spontaneous Intestinal Tumorigenesis Through the Adaptor Protein MyD88. Science *317*, 124–127.

Randall, K., Henderson, N., Reens, J., Eckersley, S., Nyström, A.-C., South, M.C., Balendran, C.A., Böttcher, G., Hughes, G., and Price, S.A. (2016). Claudin-2 Expression Levels in Ulcerative Colitis: Development and Validation of an In-Situ Hybridisation Assay for Therapeutic Studies. Plos One *11*, e0162076.

Ray, K.C., Moss, M.E., Franklin, J.L., Weaver, C.J., Higginbotham, J., Song, Y., Revetta, F.L., Blaine, S.A., Bridges, L.R., Guess, K.E., et al. (2014). Heparin-binding epidermal growth factor-like growth factor eliminates constraints on activated Kras to promote rapid onset of pancreatic neoplasia. Oncogene *33*, 823–831.

Rees, W.D., Tandun, R., Yau, E., Zachos, N.C., and Steiner, T.S. (2020). Regenerative Intestinal Stem Cells Induced by Acute and Chronic Injury: The Saving Grace of the Epithelium? Frontiers Cell Dev Biology *8*, 583919.

Reuter, S., Gupta, S.C., Chaturvedi, M.M., and Aggarwal, B.B. (2010). Oxidative stress, inflammation, and cancer: How are they linked? Free Radical Bio Med *49*, 1603–1616.

Rhee, K.-J., Jasper, P.J., Sethupathi, P., Shanmugam, M., Lanning, D., and Knight, K.L. (2005). Positive selection of the peripheral B cell repertoire in gut-associated lymphoid tissues. J Exp Medicine *201*, 55–62.

Ribatti, D., Tamma, R., and Annese, T. (2020). Epithelial-Mesenchymal Transition in Cancer: A Historical Overview. Transl Oncol *13*, 100773.

Richards, E.J., Zhang, G., Li, Z.-P., Permuth-Wey, J., Challa, S., Li, Y., Kong, W., Dan, S., Bui, M.M., Coppola, D., et al. (2015). Long Non-coding RNAs (LncRNA) Regulated by Transforming Growth Factor (TGF) β LncRNA-HIT-MEDIATED TGFβ-INDUCED EPITHELIAL TO MESENCHYMAL TRANSITION IN MAMMARY EPITHELIA*. J Biol Chem *290*, 6857–6867.

Roberts, A.B., and Wakefield, L.M. (2003). The two faces of transforming growth factor beta in carcinogenesis. PNAS *100*, 8621–8623.

Roche, J.K., Martins, C.A.P., Cosme, R., Fayer, R., and Guerrant, R.L. (2000). Transforming Growth Factor β1 Ameliorates Intestinal Epithelial Barrier Disruption by Cryptosporidium parvum In Vitro in the Absence of Mucosal T Lymphocytes. Infect Immun *68*, 5635–5644.

Rosenthal, R., Milatz, S., Krug, S.M., Oelrich, B., Schulzke, J.-D., Amasheh, S., Günzel, D., and Fromm, M. (2010). Claudin-2, a component of the tight junction, forms a paracellular water channel. J Cell Sci *123*, 1913–1921.

Roth, A.D., Delorenzi, M., Tejpar, S., Yan, P., Klingbiel, D., Fiocca, R., d'Ario, G., Cisar, L., Labianca, R., Cunningham, D., et al. (2012). Integrated Analysis of Molecular and Clinical Prognostic Factors in Stage II/III Colon Cancer. Jnci J National Cancer Inst *104*, 1635–1646.

Samanta, D., and Datta, P.K. (2012). Alterations in Smad pathway in human cancers. Frontiers in Bioscience *17*, 1281–1293.

Sánchez-Tilló, E., Lázaro, A., Torrent, R., Cuatrecasas, M., Vaquero, E.C., Castells, A., Engel, P., and Postigo, A. (2010). ZEB1 represses E-cadherin and induces an EMT by recruiting the SWI/SNF chromatin-remodeling protein BRG1. Oncogene *29*, 3490–3500.

Sands, B.E., Feagan, B.G., Sandborn, W.J., Schreiber, S., Peyrin-Biroulet, L., Colombel, J.F., Rossiter, G., Usiskin, K., Ather, S., Zhan, X., et al. (2020). Mongersen (GED-0301) for Active Crohn's Disease: Results of a Phase 3 Study. Am J Gastroenterol *115*, 738–745.

Schmitz, S.U., Grote, P., and Herrmann, B.G. (2016). Mechanisms of long noncoding RNA function in development and disease. Cell Mol Life Sci *73*, 2491–2509.

Schneider, C.A., Rasband, W.S., and Eliceiri, K.W. (2012). NIH Image to ImageJ: 25 years of image analysis. Nat Methods *9*, 671–675.

Schneider-Poetsch, T., Ju, J., Eyler, D.E., Dang, Y., Bhat, S., Merrick, W.C., Green, R., Shen, B., and Liu, J.O. (2010). Inhibition of eukaryotic translation elongation by cycloheximide and lactimidomycin. Nat Chem Biol *6*, 209–217.

Schulte, D., Küppers, V., Dartsch, N., Broermann, A., Li, H., Zarbock, A., Kamenyeva, O., Kiefer, F., Khandoga, A., Massberg, S., et al. (2011). Stabilizing the VE-cadherin–catenin complex blocks leukocyte extravasation and vascular permeability. Embo J *30*, 4157–4170.

Sedda, S., Marafini, I., Dinallo, vincenzo, Fusco, D.D., and Monteleone, G. (2015). The TGF-beta/Smad System in IBD Pathogenesis. Inflammatory Bowel Disease *21*, 2921–2925.

Shen, L., Weber, C.R., Raleigh, D.R., Yu, D., and Turner, J.R. (2011). Tight Junction Pore and Leak Pathways: A Dynamic Duo. Annu Rev Physiol *73*, 283–309.

Shi, Y., and Massagué, J. (2003). Mechanisms of TGF-β Signaling from Cell Membrane to the Nucleus. Cell *113*, 685–700.

Shin, I., Bakin, A.V., Rodeck, U., Brunet, A., and Arteaga, C.L. (2001). Transforming Growth Factor β Enhances Epithelial Cell Survival via Akt-dependent Regulation of FKHRL1. Mol Biol Cell *12*, 3328–3339.

Shiou, S.-R., Datta, P.K., Dhawan, P., Law, B.K., Yingling, J.M., Dixon, D.A., and Beauchamp, R.D. (2006). Smad4-dependent Regulation of Urokinase Plasminogen Activator Secretion and RNA Stability Associated with Invasiveness by Autocrine and Paracrine Transforming Growth Factor-β. J Biol Chem *281*, 33971–33981.

Simpson, E.H. (1949). Measurement of Diversity. Nature *163*, 688–688.

Singh, A.B., Sharma, A., and Dhawan, P. (2010). Claudin Family of Proteins and Cancer: An Overview. J Oncol *2010*, 541957.

Singh, A.B., Uppada, S.B., and Dhawan, P. (2017). Claudin proteins, outside-in signaling, and carcinogenesis. European J Physiology *469*, 69–75.

Skene, P.J., and Henikoff, S. (2017). An efficient targeted nuclease strategy for high-resolution mapping of DNA binding sites. Elife *6*, e21856.

Skovdahl, H.K., Granlund, A. van B., Østvik, A.E., Bruland, T., Bakke, I., Torp, S.H., Damås, J.K., and Sandvik, A.K. (2015). Expression of CCL20 and Its Corresponding Receptor CCR6 Is Enhanced in Active Inflammatory Bowel Disease, and TLR3 Mediates CCL20 Expression in Colonic Epithelial Cells. Plos One *10*, e0141710.

Sluis, M.V. der, Koning, B.A.E.D., Bruijn, A.C.J.M.D., Velcich, A., Meijerink, J.P.P., Goudoever, J.B.V., Büller, H.A., Dekker, J., Seuningen, I.V., Renes, I.B., et al. (2006). Muc2-Deficient Mice Spontaneously Develop Colitis, Indicating That MUC2 Is Critical for Colonic Protection. Gastroenterology *131*, 117–129.

Sobell, H.M. (1985). Actinomycin and DNA Transcription. PNAS *82*, 5328–5331.

Söderholm, J.D., Olaison, G., Lindberg, E., Hannestad, U., Vindels, A., Tysk, C., Järnerot, G., and Sjödahl, R. (1999). Different intestinal permeability patterns in relatives and spouses of patients with Crohn's disease: an inherited defect in mucosal defence? Gut *44*, 96.

Sofia, E., Landstrom, M., Heldin, C.-H., and Aspenstrom, P. (2002). Transforming Growth Factor-Beta–induced Mobilization of Actin Cytoskeleton Requires Signaling by Small GTPases Cdc42 and RhoA. Molecular Biology of the Cell *13*, 902–914.

Song, M., Chan, A.T., and Sun, J. (2019). Influence of the Gut Microbiome, Diet, and Environment on Risk of Colorectal Cancer. Gastroenterology *158*, 322–340.

Southard-Smith, A.N., Simmons, A.J., Chen, B., Jones, A.L., Solano, M.A.R., Vega, P.N., Scurrah, C.R., Zhao, Y., Brenan, M.J., Xuan, J., et al. (2020). Dual indexed library design enables compatibility of in-Drop single-cell RNA-sequencing with exAMP chemistry sequencing platforms. Bmc Genomics *21*, 456.

Spaderna, S., Schmalhofer, O., Wahlbuhl, M., Dimmler, A., Bauer, K., Sultan, A., Hlubek, F., Jung, A., Strand, D., Eger, A., et al. (2008). The Transcriptional Repressor ZEB1 Promotes Metastasis and Loss of Cell Polarity in Cancer. Cancer Res *68*, 537–544.

Stuart, T., Butler, A., Hoffman, P., Hafemeister, C., Papalexi, E., Mauck, W.M., Hao, Y., Stoeckius, M., Smibert, P., and Satija, R. (2019). Comprehensive Integration of Single-Cell Data. Cell *177*, 1888-1902.e21.

Sukriti, S., Tauseef, M., Yazbeck, P., and Mehta, D. (2014). Mechanisms Regulating Endothelial Permeability. Pulm Circ *4*, 535–551.

Takaku, K., Oshima, M., Miyoshi, H., Matsui, M., Seldin, M.F., and Taketo, M.M. (1998). Intestinal Tumorigenesis in Compound Mutant Mice of both Dpc4(Smad4) and Apc Genes. Cell *92*, 645–656.

Tanaka, H., Takechi, M., Kiyonari, H., Shioi, G., Tamura, A., and Tsukita, S. (2015). Intestinal deletion of Claudin-7 enhances paracellular organic solute flux and initiates colonic inflammation in mice. Gut *64*, 1529.

Tauriello, D.V.F., Palomo-Ponce, S., Stork, D., Berenguer-Llergo, A., Badia-Ramentol, J., Iglesias, M., Sevillano, M., Ibiza, S., Cañellas, A., Hernando-Momblona, X., et al. (2018). TGFβ drives immune evasion in genetically reconstituted colon cancer metastasis. Nature *554*, 538–543.

Teng, Y., Sun, A.-N., Pan, X.-C., Yang, G., Yang, L.-L., Wang, M.-R., and Yang, X. (2006). Synergistic Function of Smad4 and PTEN in Suppressing Forestomach Squamous Cell Carcinoma in the Mouse. Cancer Res *66*, 6972–6981.

Thomas, D.A., and Massagué, J. (2005). TGF-β directly targets cytotoxic T cell functions during tumor evasion of immune surveillance. Cancer Cell *8*, 369–380.

Thompson, B.T., Chambers, R.C., and Liu, K.D. (2017). Acute Respiratory Distress Syndrome. New Engl J Medicine *377*, 562–572.

Toyonaga, T., Steinbach, E.C., Keith, B.P., Barrow, J.B., Schaner, M.R., Wolber, E.A., Beasley, C., Huling, J., Wang, Y., Allbritton, N.L., et al. (2020). Decreased Colonic Activin Receptor-Like Kinase 1 Disrupts Epithelial Barrier Integrity in Patients with Crohn's disease. Cell Mol Gastroenterology Hepatology *10*, 779–796.

Tsai, P.-Y., Zhang, B., He, W.-Q., Zha, J.-M., Odenwald, M.A., Singh, G., Tamura, A., Shen, L., Sailer, A., Yeruva, S., et al. (2017). IL-22 Upregulates Epithelial Claudin-2 to Drive Diarrhea and Enteric Pathogen Clearance. Cell Host Microbe *21*, 671-681.e4.

Tsukita, S., Tanaka, H., and Tamura, A. (2018). The Claudins: From Tight Junctions to Biological Systems. Trends Biochem Sci *44*, 141–152.

Ueda, J., Semba, S., Chiba, H., Sawada, N., Seo, Y., Kasuga, M., and Yokozaki, H. (2007). Heterogeneous Expression of Claudin-4 in Human Colorectal Cancer: Decreased Claudin-4 Expression at the Invasive Front Correlates Cancer Invasion and Metastasis. Pathobiology *74*, 32–41.

V, H.-S., V, Ahmad, A., Befekadu, R., and Nilsson, T. (2017). Expression of claudin 1, claudin 4, and claudin 7 in colorectal cancer and its relation with CLDN DNA methylation patterns. Tumor Biology *2017*, 1–10.

Vancamelbeke, M., Vanuytsel, T., Farré, R., Verstockt, S., Ferrante, M., Assche, G.V., Rutgeerts, P., Schuit, F., Vermeire, S., Arijs, I., et al. (2017). Genetic and Transcriptomic Bases of Intestinal Epithelial Barrier Dysfunction in Inflammatory Bowel Disease. Inflamm Bowel Dis *23*, 1718–1729.

Vestweber, D. (2007). VE-Cadherin. Arteriosclerosis Thrombosis Vasc Biology *28*, 223–232.

Viel, S., Marçais, A., Guimaraes, F.S.-F., Loftus, R., Rabilloud, J., Grau, M., Degouve, S., Djebali, S., Sanlaville, A., Charrier, E., et al. (2016). TGF-β inhibits the activation and functions of NK cells by repressing the mTOR pathway. Sci Signal *9*, ra19–ra19.

Vivinus-Nébot, M., Frin-Mathy, G., Bzioueche, H., Dainese, R., Bernard, G., Anty, R., Filippi, J., Saint-Paul, M.C., Tulic, M.K., Verhasselt, V., et al. (2014). Functional bowel symptoms in quiescent inflammatory bowel diseases: role of epithelial barrier disruption and low-grade inflammation. Gut *63*, 744.

Volynets, V., Reichold, A., Bárdos, G., Rings, A., Bleich, A., and Bischoff, S.C. (2016). Assessment of the Intestinal Barrier with Five Different Permeability Tests in Healthy C57BL/6J and BALB/cJ Mice. Digest Dis Sci *61*, 737–746.

Walshe, T.E., Saint-Geniez, M., Maharaj, A.S.R., Sekiyama, E., Maldonado, A.E., and D'Amore, P.A. (2009). TGF-β Is Required for Vascular Barrier Function, Endothelial Survival and Homeostasis of the Adult Microvasculature. Plos One *4*, e5149.

Wang, F., Scoville, D., He, X.C., Mahe, M.M., Box, A., Perry, J.M., Smith, N.R., Lei, N.Y., Davies, P.S., Fuller, M.K., et al. (2013). Isolation and Characterization of Intestinal Stem Cells Based on Surface Marker Combinations and Colony-Formation Assay. Gastroenterology *145*, 383-395.e21.

Wang, L., Liu, Q., Sun, Q., Zhang, C., Chen, T., and Cao, X. (2008). TLR4 signaling in cancer cells promotes chemoattraction of immature dendritic cells via autocrine CCL20. Biochem Bioph Res Co *366*, 852–856.

Wasserman, I., Lee, L.H., Ogino, S., Marco, M.R., Wu, C., Chen, X., Datta, J., Sadot, E., Szeglin, B., Guillem, J., et al. (2018). SMAD4 loss in colorectal cancer patients correlates with recurrence, loss of immune infiltrate, and chemoresistance. Clin Cancer Res *25*, clincanres.1726.2018.

Watson, C.J., Hoare, C.J., Garrod, D.R., Carlson, G.L., and Warhurst, G. (2005). Interferon-γ selectively increases epithelial permeability to large molecules by activating different populations of paracellular pores. J Cell Sci *118*, 5221–5230.

Weber, C.R., Raleigh, D.R., Su, L., Shen, L., Sullivan, E.A., Wang, Y., and Turner, J.R. (2010). Epithelial Myosin Light Chain Kinase Activation Induces Mucosal Interleukin-13 Expression to Alter Tight Junction Ion Selectivity. J Biol Chem *285*, 12037–12046.

Wehkamp, J., Koslowski, M., Wang, G., and Stange, E.F. (2008). Barrier dysfunction due to distinct defensin deficiencies in small intestinal and colonic Crohn's disease. Mucosal Immunol *1*, S67–S74.

Weichselbaum, L., and Klein, O.D. (2018). The intestinal epithelial response to damage. Sci China Life Sci *61*, 1205–1211.

Weiss, A., and Attisano, L. (2013). The TGFbeta Superfamily Signaling Pathway. Wiley Interdiscip Rev Dev Biology *2*, 47–63.

Wilkes, M.C., Mitchell, H., Penheiter, S.G., Doré, J.J., Suzuki, K., Edens, M., Sharma, D.K., Pagano, R.E., and Leof, E.B. (2005). Transforming Growth Factor-β Activation of Phosphatidylinositol 3-Kinase Is Independent of Smad2 and Smad3 and Regulates Fibroblast Responses via p21-Activated Kinase-2. Cancer Res *65*, 10431–10440.

Wrzesinski, S.H., Wan, Y.Y., and Flavell, R.A. (2007). Transforming Growth Factor-β and the Immune Response: Implications for Anticancer Therapy. Clin Cancer Res *13*, 5262–5270.

Wyatt, J., Vogelsang, H., Hubl, W., Waldhoer, T., and Lochs, H. (1993). Intestinal permeability and the prediction of relapse in Crohn's Disease. Lancet *341*, 1437–1439.

Xiao, K., Song, Z.-H., Jiao, L.-F., Ke, Y.-L., and Hu, C.-H. (2014). Developmental Changes of TGF-β1 and Smads Signaling Pathway in Intestinal Adaption of Weaned Pigs. Plos One *9*, e104589.

Xiao, K., Cao, S.T., Jiao, L.F., Lin, F.H., Wang, L., and Hu, C.H. (2016). Anemonin improves intestinal barrier restoration and influences TGF-β1 and EGFR signaling pathways in LPS-challenged piglets. Innate Immun *22*, 344–352.

Xiao, K., Cao, S., Jiao, L., Song, Z., Lu, J., and Hu, C. (2017). TGF-β1 protects intestinal integrity and influences Smads and MAPK signal pathways in IPEC-J2 after TNF-α challenge. Innate Immun *23*, 276–284.

Xu, C., Wang, X., Li, W., Wang, K., and Ding, L. (2018). Expression and Clinical Significance of Claudin-7 in Patients With Colorectal Cancer. Technol Cancer Res T *17*, 1–10.

Xu, C., Wang, K., Ding, Y.-H., Li, W.-J., and Ding, L. (2019). Claudin-7 gene knockout causes destruction of intestinal structure and animal death in mice. World J Gastroentero *25*, 584–599.

Xu, J., Lamouille, S., and Derynck, R. (2009). TGF-β-induced epithelial to mesenchymal transition. Cell Res *19*, 156–172.

Xu, X., Brodie, S.G., Yang, X., Im, Y.-H., Parks, W.T., Chen, L., Zhou, Y.-X., Weinstein, M., Kim, S.-J., and Deng, C.-X. (2000). Haploid loss of the tumor suppressor Smad4/Dpc4 initiates gastric polyposis and cancer in mice. Oncogene *19*, 1868–1874.

Xu, X., Kobayashi, S., Qiao, W., Li, C., Xiao, C., Radaeva, S., Stiles, B., Wang, R.-H., Ohara, N., Yoshino, T., et al. (2006). Induction of intrahepatic cholangiocellular carcinoma by liver-specific disruption of Smad4 and Pten in mice. J Clin Invest *116*, 1843–1852.

Yan, M., Rerko, R.M., Platzer, P., Dawson, D., Willis, J., Tong, M., Lawrence, E., Lutterbaugh, J., Lu, S., Willson, J.K., et al. (2004). 15-Hydroxyprostaglandin dehydrgenase, a COX-2 oncogene antagonist, is a TGF-beta-induced suppressor of human gastrointestinal cancers. PNAS.

Yan, P., Klingbiel, D., Saridaki, Z., Ceppa, P., Curto, M., McKee, T.A., Roth, A., Tejpar, S., Delorenzi, M., Bosman, F.T., et al. (2016). Reduced Expression of SMAD4 Is Associated with Poor Survival in Colon Cancer. Clin Cancer Res *22*, 3037–3047.

Yang, L., Mao, C., Teng, Y., Li, W., Zhang, J., Cheng, X., Li, X., Han, X., Xia, Z., Deng, H., et al. (2005). Targeted Disruption of Smad4 in Mouse Epidermis Results in Failure of Hair Follicle Cycling and Formation of Skin Tumors. Cancer Res *65*, 8671–8678.

Yang, L., Huang, J., Ren, X., Gorska, A.E., Chytil, A., Aakre, M., Carbone, D.P., Matrisian, L.M., Richmond, A., Lin, P.C., et al. (2008). Abrogation of TGFβ Signaling in Mammary Carcinomas Recruits Gr-1+CD11b+ Myeloid Cells that Promote Metastasis. Cancer Cell *13*, 23–35.

Yang, L., Pang, Y., and Moses, H.L. (2010a). TGF-β and immune cells: an important regulatory axis in the tumor microenvironment and progression. Trends Immunol *31*, 220–227.

Yang, M.-H., Hsu, D.S.-S., Wang, H.-W., Wang, H.-J., Lan, H.-Y., Yang, W.-H., Huang, C.-H., Kao, S.-Y., Tzeng, C.-H., Tai, S.-K., et al. (2010b). Bmi1 is essential in Twist1-induced epithelial–mesenchymal transition. Nat Cell Biol *12*, 982–992.

Ye, X., and Weinberg, R. (2017). The SUMO guards for SNAIL. Oncotarget *8*, 97701–97702.

Yi, J.Y., Shin, I., and Arteaga, C.L. (2005). Type I Transforming Growth Factor β Receptor Binds to and Activates Phosphatidylinositol 3-Kinase. J Biol Chem *280*, 10870–10876.

Zeisel, M.B., Dhawan, P., and Baumert, T.F. (2019). Tight junction proteins in gastrointestinal and liver disease. Gut *68*, 547.

Zeissig, S., Bürgel, N., Günzel, D., Richter, J., Mankertz, J., Wahnschaffe, U., Kroesen, A.J., Zeitz, M., Fromm, M., and Schulzke, J.-D. (2007). Changes in expression and distribution of claudin 2, 5 and 8 lead to discontinuous tight junctions and barrier dysfunction in active Crohn's disease. Gut *56*, 61.

Zemans, R.L., and Matthay, M.A. (2004). Bench-to-bedside review: The role of the alveolar epithelium in the resolution of pulmonary edema in acute lung injury. Crit Care *8*, 469.

Zhang, Y.E. (2009). Non-Smad pathways in TGF-β signaling. Cell Res *19*, 128–139.

Zhang, Y.-Z., and Li, Y.-Y. (2014). Inflammatory bowel disease: Pathogenesis. World J Gastroentero *20*, 91–99.

Zhang, F., Wang, H., Wang, X., Jiang, G., Liu, H., Zhang, G., Wang, H., Fang, R., Bu, X., Cai, S., et al. (2015). TGF-beta induces M2-like macrophage polarization via SNAIL-mediated suppression of a pro-inflammatory phenotype. Oncotarget *7*, 52294–52306.

Zhang, H., Zhong, W., Zhou, G., Ding, X., and Chen, H. (2012). Expression of chemokine CCL20 in ulcerative colitis. Mol Med Rep *6*, 1255–1260.

Zhao, J., Crowe, D., Castillo, C., Wuenschell, C., Chai, Y., and Warburton, D. (2000). Smad7 is a TGF-beta-inducible attenuator of Smad2/3-mediated inhibition of embryonic lung morphogenesis. Mechanisms of Development *93*, 71–81.

Zhao, M., Mishra, L., and Deng, C.-X. (2018). The role of TGF-β/SMAD4 signaling in cancer. Int J Biol Sci *14*, 111–123.

Zhou, S., Piao, X., wang, C., Wang, R., and Song, Z. (2019). Identification of claudin-1, -3, -7 and -8 as prognostic markers in human laryngeal carcinoma. Molecular Medicine Reports *20*, 393–400.

Zhu, L., Han, J., Li, L., Wang, Y., Li, Y., and Zhang, S. (2019). Claudin Family Participates in the Pathogenesis of Inflammatory Bowel Diseases and Colitis-Associated Colorectal Cancer. Front Immunol *10*, 1441.

Zihni, C., Balda, M.S., and Matter, K. (2014). Signalling at tight junctions during epithelial differentiation and microbial pathogenesis. J Cell Sci *127*, 3401–3413.

Zuo, L., Kuo, W.-T., and Turner, J.R. (2020). Tight junctions as targets and effectors of mucosal immune homeostasis. Cell Mol Gastroenterology Hepatology *10*, 327–340.